AD739197

Contract No. F33657-71-C-0859
Report No. IITRI-C6239-A005-1

SUBMICRON SEPARATION AND DATA

AFTAC TD/4
Alexandria, Virginia

Attention: Major R. N. Park

Prepared by

R. Davies
D. Werle
W. Wnek

IIT Research Institute
10 West 35th Street
Chicago, Illinois 60616

31 October 1971

Report for Period April 16-October 31, 1971
Task 1 - Literature Survey

IIT RESEARCH INSTITUTE

UNCLASSIFIED

Security Classification

DOCUMENT CONTROL DATA - R & D

(Security classification of title, body of abstract and indexing annotation must be entered when the overall report is classified)

1. ORIGINATING ACTIVITY (Corporate author)
IIT Research Institute
10 West 35th St.
Chicago, Ill. 60616

2a. REPORT SECURITY CLASSIFICATION
Unclassified

2b. GROUP

3. REPORT TITLE
Submicron Separation and Data

4. DESCRIPTIVE NOTES (Type of report and inclusive dates)
Task 1, Literature Survey April 16 to October 31, 1971

5. AUTHOR(S) (First name, middle initial, last name)
Reg Davies
Don K. Werle
Walter J. Wnek

6. REPORT DATE
October 31, 1971

7a. TOTAL NO. OF PAGES
334

7b. NO. OF REFS
1162

8a. CONTRACT OR GRANT NO
F33657-71-C-0859

b. PROJECT NO VT/1414/RDE/ASD
ARPA order No. 1702

c.
Program Code No. 1F10

d.

8b. ORIGINATOR'S REPORT NUMBER(S)
IITRI-C6239-A005-1

9b. OTHER REPORT NO(S) (Any other numbers that may be assigned this report)

DISTRIBUTION STATEMENT A
Approved for public release;
Distribution Unlimited

10. DISTRIBUTION STATEMENT This document is subject to special export controls and each transmittal to foreign governments or foreign nationals may be made only with prior approval of AFTAC.

11. SUPPLEMENTARY NOTES

12. SPONSORING MILITARY ACTIVITY
AFTAC TD/4
Alexandria, Va.

13. ABSTRACT

The science involved in the separation of submicron particles from a collected sample of atmospheric aerosol was found to be very complex. It involved many facets of the basic sciences, each of which had an equally important role in the separation process. To separate two or more particles in contact on a surface, one had to first supply energy to overcome the forces that bound them together and then devise means to keep them apart until they could be analyzed. The binding force was shown to be a function of many parameters, all of which were related to the nature and properties of the particles and surface. As this program was concerned with particles collected from atmospheric aerosols, the study began by an attempt to classify the nature of such particles.

DD FORM 1 NOV 68 1473

UNCLASSIFIED

Security Classification

14. KEY WORDS	LINK A		LINK B		LINK C	
	ROLE	WT	ROLE	WT	ROLE	WT
adhesion						
agglomeration						
submicron particulates						
Van der Waals forces						
aerosols						
suspensions						
dispersion						
size distribution						
zeta potential						
contact angles						
surface energy						
floculation						
conglomeration						
adsorption						
chemi-sorption						
electrical forces						
coulombic forces						
capillary forces						
valency forces						
powders						

FOREWORD

This report was prepared for the Air Force Technical Applications Center (AFTAC), and it represents the results of the work performed under Item 1, Increment 1, Task 1 of IITRI Project C6239, entitled "Submicron Separation and Data."

The objective of Project C6239 is to develop the methods, procedures, and equipment required to isolate individual submicron particles from an agglomerated matrix for analysis by various techniques. The particles of prime interest are those submicron particles found in the atmosphere as a result of industrial air pollution.

The objective of Task 1 of this program was to perform a literature survey of previous work in fields related to submicron atmospheric-particle separation. The references reviewed under this task numbered between 50,000 and 100,000 and over 2000 abstracts were reviewed. Over 500 documents were processed by the information science and technical staff, many of which were in French, German and Russian. Translation of these documents has been slow and even now, at the conclusion of this task, many good references have yet to be received from the translators. In consequence, this document was prepared as the report of Task 1-Literature Survey in compliance with the contract specifications, but it is felt that a supplementary document should be issued at a later date to include those references from foreign sources still under translation that are pertinent to the program. At this point, we would like to acknowledge the assistance of the particle technology group at the Institüt für Mechanische Verfahrenstechnik, University of Karlsruhe, West Germany, for their complete cooperation in providing their literature survey on the subject of adhesion. This enabled very rapid initial progress to be made in the program. In addition to this, their cooperation during personal discussions was extremely useful and greatly appreciated. We

would also like to acknowledge the cooperation and assistance of the National Center for Atmospheric Research in Boulder, Colorado, during discussions on atmospheric aerosols. Once again their assistance was invaluable in obtaining the information contained in Section 2 of this report.

Respectfully submitted,

IIT RESEARCH INSTITUTE

R Davies

R. Davies
Research Physicist
Fine Particles Research

Approved by:

J. Stockham

J. Stockham
Manger
Fine Particles Research

SUMMARY

SUBMICRON SEPARATION AND DATA

The science involved in the separation of submicron particles from a collected sample of atmospheric aerosol was found to be very complex. It involved many facets of the basic sciences each of which had an equally important role in the separation process. To separate two or more particles in contact on a surface, one had to first supply energy to overcome the forces that bound them together and then devise means to keep them apart until they could be analyzed. The binding force was shown to be a function of many parameters, all of which were related to the nature and properties of the particles and surface. As this program was concerned with particles collected from atmospheric aerosols, the study began by an attempt to classify the nature of such particles.

It was found that aerosols present in the atmsophere were composed of a wide variety of constituents from many sources, both natural and anthropogenic. On a worldwide production basis, it was estimated that 1.6 billion tons of particles below 5 μ in diameter were put into the atmosphere annually, one-third of which were converted sulfates, with lesser amounts of converted nitrates, hydrocarbons, and sooty combustion products, and only a small proportion was man-made. A large part came from mineral and organic particles raised by the wind, from ocean spray and wave crests, and from photochemical and chemical reactions. Lesser amounts of natural aerosols came from forest fires, volcanic dust, and meteoritic dust. Vegetation contributed considerable quantities of both reactive gases and cellular particulates to the atmosphere.

In the northern hemisphere, industrial sources accounted for about one-third of the aerosol components, and localized urban pollution by man inundated the natural background aerosol. Despite the complex nature of atmospheric aerosols, it was noted

that the chemical profile of a region was highly individualistic, depending upon the input of all sources, and several investigators were able to relate trace element composition to specific industries in the region, differentiating between industrial and natural aerosols by elemental ratios for different size fractions.

The modeling of atmospheric agglomerates appeared to be a formidable task in view of the somewhat catholic yet individualistic nature of particulates and adsorbed gases present throughout the world. However, useful models could be devised to test experimental separation procedures using such components as carbon black, ferric oxide, ammonium sulphate and sodium chloride powders.

The types of forces and bonds that were found to cause adhesion or separation of particles to and from surfaces, or to each other, were mechanical, Van der Waals, electrical, electrostatic, capillary, electrical double layer, covalent, ionic, metallic, and hydrogen.

In air, the force of adhesion depended on the interaction of these forces which in turn depended on the prevailing experimental conditions. In dry air, mechanical molecular, electrical and electrostatic forces were important, but in moist air with humidity >65%, the capillary forces of the liquid far outweighed any other. Such factors as surface hardness, surface roughness, particle shape, particle size and temperature affected the magnitude of the force. When suspended in liquids, many of these forces disappeared or were reduced, and, in fact, forces of repulsion could be induced to facilitate separation. Adsorption of specific surfactants onto the particle and substrate surfaces at temperatures of 60°C caused particle separation with a minimum of energy, and the additional factors that affected the magnitude of the force in air were minimized in the liquid medium. For the most effective separation, it was important that liquids and surfactant be chosen which caused

the greatest difference in wettability between surfaces and particles. Ideally, a surface had to be made hydrophobic and a particle hydrophilic for good separation. In aqueous suspensions, this could be done by selective phosphate and silicate treatments, while in non-aqueous liquids it could be done by varying the hydrogen bonding demand of the solvent. Particle adhesion forces could then be measured by several techniques, but for submicron particles, a centrifugal system appeared to be the best approach. However, vibrational methods including ultrasonics, and methods of high shear in specially made roller mills had to be tried. Preliminary analysis of the degree of separation could be made using turbidity and particle size analysis.

However, before analysis could be performed, particles had to be sampled and collected. For particles in air, it was found that extreme care has to be taken in sampling them, as diffusion and electrostatic charge caused serious losses to the walls of sampling tubes and collecting instrument inlets. Submicron particles from 0.01-1 μ could be collected very easily using high speed centrifugal spectrometers, in which the size spectrum was deposited in a manner suitable for analysis. In liquid media, the method of sampling was not critical for submicron particles provided that the suspension was stable, and they could be readily collected using a supercentrifuge of the type developed by Hausner and Lynn.

To test the degree of separation that had been attained in the separation method, the collected particles from air or liquid were best analyzed statically by interfacing an electron microscope with a Quantmet 720 automatic microscope, so that particle size distributions interparticle distance and degree of agglomeration could be quickly measured on the collector surface.

For preliminary testing of the dispersing system, a dynamic analytical method could be used. For this purpose, the Whitby Aerosol Analyzer was best for particles in air, and the Micromeritics X-Ray Analyzer or Kaye Disc Centrifuge for particles in liquid.

Finally, to relate the experimental data taken during the separation, collection and analytical phases with the theoretical degree of separation possible from the model system, a knowledge of the previous mathematical models employed to describe the many forces of adhesion was considered essential. A study of these theoretical models was conducted and it was found that for many cases the force acting between colloidal particles consisted of an attractive part due to London-Van der Waals forces and a repulsive part due to the interaction of the electrical double layers of the particles. Equations were put forward for the purpose of determining these forces. These allowed the stability of a colloidal system to be described by means of a calculated potential energy of interaction curve. The result was that the stability of a system could be qualitatively assessed by the magnitude of the curve's maximum value. The larger this value, the more stable was the system. The theory was able to explain most of the experimentally observed phenomena of colloidal systems. However, the one important thing that it could not do was to predict how long a system would be stable. In order to accomplish this, the collision rate of particles had to be investigated. The analysis yielded an integro-differential equation to be solved. This equation could only be solved analytically for situations that were not likely to occur in practice while in all other cases a computer had to be used. Current numerical techniques demanded the simultaneous solution of hundreds of differential equations which required excessive computer time. Also, in the cases investigated in this way, only simple systems were considered where there were no interaction forces between the

particles. However, in these cases the theory was in agreement with data. It should be noted that mainly spherical particles were treated and to a very slight extent particles of other shapes.

In addition to this work, equations were presented to describe the tensile strength of powders, the force between a particle in contact with plate, and bodies bonded together by capillary forces. These equations were in general agreement with data, but it should be kept in mind that their purpose was more to give an order of magnitude rather than exact values.

TABLE OF CONTENTS

		Page
1.	INTRODUCTION	1
1.1	Basic Concepts of Submicron Separation	2
1.2	Discrete Particles and Particulate Systems	3
1.3	Particle Size and Particle Size Distribution	5
1.4	Particle Shape	5
1.5	Surface Area and Surface Structure	6
1.6	Surface Energy and the Adsorption of Film	8
1.7	Multilayer Adsorption and Effect of Free Liquid	10
1.8	Plastic Deformation, Melting and Sintering	12
1.9	Summary	14
2.	ATMOSPHERIC AEROSOLS	16
2.1	Definitions	16
2.2	Basic Properties of Aerosols	18
2.3	Sources of Aerosols in the Atmosphere	22
2.4	Nature of Aerosols Close to Ground Level	28
2.4.1	General References	28
2.4.2	Soil Derived Aerosols	31
2.4.3	Sulfur Derived Aerosols	33
2.4.4	Other Inorganic Components	38
2.4.5	Organic and Biological Components	42
2.4.6	Radioactive Aerosols in the Atmosphere	46
2.5	Nature of Aerosols in the Upper Atmosphere	47
2.6	Size and Shape of Atmospheric Particulates	49
2.7	Summary	53
3.	ADHESION OF ATMOSPHERIC PARTICLES	55
3.1	Types of Forces	55
3.1.1	Summary	60
3.2	Magnitude of Surface Forces in Air	60
3.3	Magnitude of Forces in Liquid	69
3.4	Mechanism and Methods of Measuring Adhesion and Separation Forces	73

TABLE OF CONTENTS (cont.)

		Page
3.4.1	Microbalance Methods	77
3.4.2	Pendulum Method	78
3.4.3	Varying the Slope of Surfaces	78
3.4.4	Vibration Methods	79
3.4.5	The Centrifugal Method	81
3.4.6	Aerodynamic Method	83
3.4.7	Vibration Methods	86
3.4.8	Turbulence and Shear	87
3.5	Methods of Modifying Forces of Adhesion	90
3.6	Indexes of Dispersion	103
3.6.1	Suspension Turbidity and Mean Particle Size	106
3.6.2	Sedimentation Volume	107
3.6.3	Change in Mean Size and Size Distribution with Time	108
3.6.4	Zeta Potential	108
3.6.5	pH and Electrical Conductivity	109
3.6.6	Surface Active Agent Nature, Purity and Critical Concentration	109
3.7	Summary	110
4.	MATHEMATICAL MODELS OF ADHESION AND AGGLOMERATION	112
4.1	London-Van der Waals Force of Attraction	112
4.2	Retardation of London-Van der Waals Forces	117
4.3	Attraction Between Macroscopic Bodies	119
4.4	Two Spherical Particles	119
4.5	Flat Surface and a Spherical Particle	126
4.6	Other Configurations	126
4.7	Effect of Adsorbed Layers	127
4.8	Repulsion Forces Due to the Electrical Double Layer	129
4.9	The Poisson-Boltzmann Equation	132

TABLE OF CONTENTS (cont.)

		Page
4.10	Single Flat Double Layer	133
4.11	Free Energy of the Double Layer	136
4.12	Single Spherical Double Layer	137
4.13	Two Flat Double Layers	138
4.14	Two Spherical Double Layers	146
4.15	Total Potential Energy	149
4.16	Corrections to the Poisson-Boltzmann Equation.	151
	4.16.1 Stern's Correction	151
4.17	Ionic Volume Correction	155
4.18	Dielectric Saturation	157
4.19	Ion Polarization	159
4.20	The Self-Atmosphere Effect of the Ions	159
4.21	The Combined Effect of the Corrections	160
4.22	The Statistical Mechanics Approach to the Electrical Double Layer	161
4.23	APPENDIX I - Derivation of Poisson's Equation.	165
4.24	APPENDIX II - Derivation of the Boltzmann Distribution	166
4.25	Constant Surface Potential vs. Constant Surface Charge	168
4.26	The Relationship Between the Surface Potential and the Zeta Potential	170
4.27	The Rate of Agglomeration	178
4.28	The Collision Rate	178
4.29	The Kinetic Equation	184
4.30	Methods of Solving the General Kinetic Equation	187
4.31	Mean Free Path Effect	194
4.32	Effect of Hydrodynamic Interaction	197
4.33	Other Mechanisms of Agglomeration	198
4.34	Agglomeration of Charged Particles in a Non-Aqueous Medium	199
4.35	Agglomeration of Non-Spherical Particles	200
4.36	The Strength of Agglomerates	203
4.37	Adhesion of Small Particles to a Flat Plate	206

TABLE OF CONTENTS (cont.)

	Page
4.38 Adhesion Due to Capillary Condensation	208
4.39 Summary	209
5. METHODS OF SAMPLING, COLLECTING AND ANALYZING SUBMICRON PARTICLES	211
5.1 Particles in Air	211
5.1.1 Sampling	211
5.1.2 Collection	217
5.1.3 Centrifugal Systems	217
5.1.4 Cyclones	217
5.1.5 Classifiers	219
5.1.6 Aerosol Spectrometers	220
5.1.7 Thermal Precipitation	225
5.1.8 Electrostatic Precipitation	229
5.1.9 Analysis	234
5.2 Particles in Liquid	236
5.2.1 Sampling	236
5.2.2 Collection	236
5.2.3 Centrifuges	237
5.2.4 Analysis	246
5.2.5 Dynamic Methods	246
5.2.6 Static Method	248
5.3 Summary	249
6. CONCLUSIONS	250
REFERENCES	252
INTRODUCTION	252
ATMOSPHERIC AEROSOLS	257
ADHESION OF ATMOSPHERIC PARTICLES	294
METHODS OF SAMPLING, COLLECTING AND ANALYZING SUBMICRON PARTICLES	317
GLOSSARY	336

LIST OF TABLES

Table		Page
1	Relative Hardness Scale-Relative to Mohs	13
2	Estimated Sources of Primary Particle Production	25
3	Annual Worldwide Hydrocarbon Emission Estimate ..	26
4	Some Important Sources of Atmospheric Aerosols ..	27
5	Adhesive Force of Particles Determined by Various Methods for Various Air Humidities ...	65
6	Forces to Remove 98% of 50 μ Diameter Particles .	66
7	Accelerations Required to Dislodge Adhering Particles of Atmospheric Dust, Fly Ash and Glass Beads	85
8	Bulk Air Velocity Required to Dislodge Adhering Particles of Atmospheric Dust, Fly Ash, and Glass Beads	86
9	Liquids Suitable for the Dispersion of Specific Powders	102
10	ν^d and A in Water for Various Substances at 20°C	115
11	Illustrating the Difference Between the Approximation and the Theory of Muller for Spherical Particles	138
12	Comparison of Linear Approximation with the Tabulated Function of Devereux and De Bruyn	147
13	Values for $[1 + 1/2\ f(\kappa a)]$ in the Henry Equation for a Range of Ka Values	174
14	Values of Correction Terms in Equations 122 and 123	175
15	Particle Mobilities in μ/Sec per Volt/cm as a function of the Zeta Potential atVarious Values of a a for Particles Suspended in Aqueous Solution at 25°C Containing Only 1:1 Electrolyte with Ionic Mobilities Corresponding to $\lambda = 70\ \text{ohm}^{-1}\ \text{cm}^{-2}\ \text{eq}^{-1}$	177

LIST OF FIGURES

Figure		Page
1	Particle Nomenclature	17
2	Size Distribution of Aerosols in the Atmosphere	21
3	Force of Mechanical Adhesion	55
4	Effect of Adsorbed Liquid on Adhesion	59
5	The Spheres Under Gravitational Force	61
6	Particle-Size and Agglomerate-Strength Regions in Which Various Binding Mechanisms Predominate	62
7	Effect of Moisture on Cohesion	63
8	Effect of Surface Roughness on Adhesion	67
9	Removal Results, Glass Powder Bed Experiments	70
10	Adhesion of Gold Spheres, 3 μm Diameter, to Cellulose	72
11	Adhesion of Gold Spheres, 3 μm Diameter, to Polyester	72
12	Adhesion of Spherical Fe Particles of 4 μm Diameter to Fe Substrate at Room Temperature in Air as a Function of Applied Force	76
13	Sloping Table Measure of Adhesion	79
14	Kimax Tube for Sedimentation Volume Measurement	107
15	Particles P in Medium M	116
16	Correction Factor Due to Retardation for the Contribution of One Excited State to the Usual London Energy	113
17	Coordinate System Between a Sphere and a Point	120
18	Coordinate System Between Two Spheres	122
19	Attraction Potential at Varying Distances of Separation Between the Particle Surface, Using the Hamaker Equation for Particles of 0.04, 0.1, 0.2, 0.4, 1.0 and 2.0 Microns Diameter $A_p = 1.1 \times 10^{-12}$ erg, $A_M = 5 \times 10^{-13}$ erg	123

Figure		Page
20	Retardation Correction Factor to the London Attraction Between Two Equal Spherical Particles. The Radii of the Particles are Resp. 0.6, 3 and 30 Times $\lambda/2$ where λ is the London-Wavelength. The Abscissa is the Shortest Distance Between the Two Spheres Again Expressed in Multiples of $\lambda/2\pi$	125
21	Attraction Potential Between Particles of 0.2 and 1.0 Microns Diameter Using the Vold Equation, With Varying Thicknesses of Adsorbed Layer, (a) nil (b) 25Å (c) 50Å (d) 75Å (e) 100Å, A_p = 1.1×10^{-13} erg, $A_S = 7 \times 10^{-13}$ erg	130
22	Attraction Potential With Adsorbed Layers of Medium 50 Angstroms Thick, at Varying Distances of Separation Between the Outer Surfaces of the Adsorbed Layers, Using the Vold Equation, for Particles of 0.04, 0.1, 0.2, 0.4, 1.0 and 2.0 Microns Diameter, $A_p = 1.1 \times 10^{-12}$ erg, $A_S = 7 \times 10^{-13}$ erg	131
23	Electric Potential in the Double Layer. The Curves Marked 1, 2, 4, 8 are Drawn According to the Exact Equation for $\frac{Ze\psi_o}{kT}$ = 1, 2, 4 and 8 Resp. The Dotted Lines Follow the Approximate Equation	135
24	Schematic Respresentation of the Electric Potential Between Two Plates, in Comparison With That for a Single Double Layer	139
25	Potential (ψd) Half-Way Between the Plates as a Function of the Plate Distance (2d) for Different Values of the Surface Potential (ψ_o). In the Figure the Values of $U = \frac{ze\psi d}{kT}$, $Z = \frac{ze\psi_o}{kT}$ and κd are Given	141
26	Repulsive Potential as a Function of κd, for Strong Interaction (Small κd)	143

LIST OF FIGURES (cont.)

Figure		Page
27	Geometrical Construction Used in the Calculation of the Interaction Between Two Dissimilar Spherical Particles, Radii a_1 and a_2 From the Interaction of Two Infinite Flat Platex	148
28	The Repulsive Potential V_R Between Two Spherical Particles, When the Exact Expression for High Potentials is Applied. Dotted Lines = Repulsive Potential According to the Approximated Equation	150
29	Total Potential Energy (V_T) Diagram for Two Colloidal Particles	150
30	Showing the Influence of the Concentration of Electrolyte (κ) on the Total Potential Energy of Interaction of Two Spherical Particles $a = 10^{-5}$ cm; $A = 10^{-12}$ ergs; $\psi_o = \frac{kT}{e} = 25.6$ mV	152
31	Showing the Influence of the Surface Potential (ψ_o) on the Total Potential Energy of Interaction of Two Spherical Particles $a = 10^{-5}$ cm; $A = 10^{-12}$ ergs; $\kappa = 10^{6}$ cm^{-1}	153
32	Schematic Representation of the Double Layer According to the Theory of Stern	154
33	Charge vs. Potential Curve I According to Boltzmann Distribution; Curve II According to Ionic Volume Correction	157
34	Forces Acting on an Element of Liquid in an Electrical Field	171
35	Electrophoretic Mobility in Symmetrical Electrolytes (Eq. 122). Values of $e\zeta/kT$ and 1, 2, and 4 or ζ About 25, 50 and 100 mv., Respectively. The line Marked 0 Forms the Limit for Very small Values of the Zeta Potential. Full Lines for Monovalent and Broken Lines for Bivalent Electrolytes	176

LIST OF FIGURES (cont.)

Figure		Page
36	Electrophoretic Mobility in Unsymmetrical Electrolytes (Eq. 123). For All Curves $e\zeta/kT$ Values Equal 2 or ζ About 50 mv.	176
37	Possible Liquid Distributions in Particle Piles	203
38	Theoretical Tensile Strength of Agglomerates: Curve 1, Fluid Bridges; Curve 2, Completely Filled Void Volume. 2a Uniformly Size, 2b RRS Distribution, n = 0.8; 2c RRS Distribution, n = 1.4	205
39	Model of Particle Adhesion	206
40	Capillary Condensation Associated with the Contact of Two Particles (a) and of a Particle with a Surface (b,c). a,b) Without any Intermediate Layer; c) With an Intermediate Layer in the Contact Zone	209
41	Effect of Particle Diameter on Deposition Velocity	213
42	Goetz Spectrometer	221
43	Hochrainer and Brown Cylindrical Centrifuge	223
44	Hochrainer and Brown Conical Centrifuge	223
45	Conifuge	224
46	Stöber and Flachbart Ring Slit Conifuge	224
47	Hochrainer Centrifuge	226
48	Donohue and Bostock Centrifuge	239
49	Diagrammatic Section of the Hauser Lynn Centrifuge	241
50	Sharples Supercentrifuge	242
51	Operation of the Reorienting Gradient Zonal Rotors	244

SUBMICRON SEPARATION AND DATA

1. INTRODUCTION

The quality of atmospheric air has received much attention during the last decade. The presence and concentration of gases, liquids and solids at all levels of the atmosphere has been studied with the intention of relating experimental measurements to the deterioration of the environment. One part of this nationwide study is focused on the effect that particulate matter has on both plant and animal life. Particles appear in the atmosphere as a result of many processes, and in experimental studies, they are sampled, collected and analyzed for various reasons. The fact that they appear suspended in air at all, indicates that in most circumstances their size is small. Yet when they are collected and observed, the collected sample often contains few independent or discrete particles, but rather it is seen in the form of large groups or agglomerates of many particles in contact. Isolation of any one discrete particle from this matrix proves difficult particularly when its size is classed as submicron or less than 1×10^{-4} cm. In many studies, specific particles do need to be separated from this matrix, recollected and subjected to independent analysis. To do this, one has to involve several basic operations. First of all, one has to overcome the forces that hold the matrix together, then separate the particles of interest, and finally collect them in a manner acceptable to the analyst.

The purpose of this study is to devise a method whereby this operation can be successfully carried out on matrices from any ambient air or ground level sampling point. The study demands a knowledge of the types and structures of atmospheric aerosols under the current sampling conditions and it necessitates an understanding of the factors involved in their sampling, collection and ultimate separation. To do this,

the forces that bind matrices together have to be studied and measured, so that separation mechanisms can be prescribed. This has to involve a study of the mathematical models used to represent matrix agglomeration, from which a model can be devised and compared with experimental data to inform the analyst of his degree of success in the physical separation process. The most suitable types and applications of energy, fluids and surface active agents required to perform this task have to be tabulated, and ideally methods devised to collect the separated particles in the same degree of dispersion and chemical composition as they had in the atmosphere. As much work has been done in this general field of interest, the first task of such a program is to determine the state of the art in particle separation processes. As this involves a wide series of subjects, a basic knowledge of the concepts involved in submicron separation has to be first developed.

1.1 Basic Concepts of Submicron Separation

The science involved in the separation of submicron particles from an agglomerated matrix is very complex. It incorporates many facets of the basic sciences, each of which has an equally important role in the separation process. To understand the mechanism and energy involved in this process, one has to first appreciate the role played by each of the separate entities and then the way in which they interact.

To separate two particles in contact, one has to supply energy to overcome the forces that bind them together, and once this has been achieved, one has to devise means to keep them apart. The binding force between two particles can be shown to be a function of such parameters as the particle size, the particle size distribution, the particle macroshape and rugosity, the total and external surface area, the nature and structure of the surface, the energy at the surface, the area of contact between the particles and their hardness and melting points. Once they have parted, the two particles can

be kept apart by collecting them on a surface in such a way that either the interparticle distance is greater than that over which coagulation forces act, or adsorb ions onto their surfaces so that they repel each other, or change the rheology of the fluid in which they are suspended, so that they are mechanically held apart.

With this complex framework of interacting variables, it appears logical to introduce this literature survey by briefly discussing the importance and mode of interaction of each of the variables independently. The way in which they interact with one another can then be developed, so that at the conclusion of this introductory section, the reader has a basic knowledge of particulate systems onto which the more specific and detailed parts of this literature survey can be built.

1.2 Discrete Particles and Particulate Systems

A "discrete particle" can be usefully described as a single unit of matter which can change in "size" only by the breakdown or fracture of chemical bonds within its structure. It may or may not be of uniform "density" throughout its mass, and its "shape" will be dependent on the method by which it is made. In other branches of science the word particle has a completely different meaning, but it is only to be above definition, that reference will be given in the current research. The discrete particle can consist of a solid, a liquid or a gas, depending on the phase in which it is suspended. Powders, dusts and slurries are examples of discrete solid particles, emulsions, sprays and mists are examples of discrete liquid particles and foams and bubbles, present as "porosity", in ceramic and steel compacts are examples of discrete gaseous particles. In the research conducted in this program, only the first category is of importance, i.e., the category involving discrete solid particles.

*Words marked thus " ", are defined in a glossary of terms in Appendix 1.

In the collection of discrete solid particles, we utilize a property of the particle which causes it to stick to plane surfaces. The process of the sticking of particles or in fact liquids or films to a plane surface by purely physical bonding is terms "adhesion" (1). In some cases the term "adherence" is used synonymously with "adhesion", but in this program we will use the latter. This property is not restricted to the sticking to plane surfaces. Discrete particles stick to each other irrespective of chemical composition, and this process is generally termed "cohesion". When chemically identical particles stick together the process can be termed "agglomeration". when chemically different particles stick together it can be termed "conglomeration". From both of these processes, a new particulate unit evolves. It is usually in the form of grouping of individual or discrete particles bound together by physical bonds. This unit can exist permanently in a fluid and behave as if it was a discrete particle of size similar to that of the unit itself. If the discrete particles are of the same chemical composition, the unit can be termed an "agglomerate", if they are of different composition it can be termed a "conglomerate". When the bonding between particles is not physical in nature, for example in chemical reactions or sintering the particulate unit can be termed as "aggregate". In this unit, the bonding is chemical, there is no point of contact and the particles are joined by necks of the same structural form as the particles themselves.

In future sections of this report, the terms agglomerate, conglomerate and aggregate will be used as defined here. For simplicity, the adjective "discrete" will be omitted from the term "discrete particle" and the term particle will generally apply to all discrete systems. Its use up to this stage was simply to enable the definitions of multiparticle units to be clearly understood.

1.3 Particle Size and Particle Size Distribution

For many practical purposes, the particle has to be characterized by its size, shape and "surface". For most solid particles, size is non-unique (2). It depends entirely on the method by which it is measured, the experimental conditions prevailing at the time, and the instrument which is used to make the measurement. This is often operator dependent, and hence any unqualified statements indicating size are meaningless. The units of particle size can be centimeters, millimeters, microns or angstroms. In most branches of particle technology, the term micron is used in which 1 micron (μ) is 10^{-4} cm. The angstrom (Å) is also encountered and here 1 angstrom is 10^{-4} micron. As most molecules exist in the range 10-100 Å, the range of particles of interest in this program are generally from 1 μ, i.e., 10^{4} Å to 0.01 μ, i.e., 10^{2} Å. Within any system involving discrete particles, a distribution of sizes is always present. "Particle size distributions" are usually measured, and data reported in terms of frequency, surface, volume or mass distributions. The mean values of these distributions will all be different, so care has to be taken in interpreting any data from particle size distribution measurements (3-6).

1.4 Particle Shape

In a similar way particle "shape" cannot be described without difficulty. In general, shape can be subdivided into two categroies, "macro and micro shape". Macro shape is a measure of the particle form, i.e., whether it is spherical, cuboidal, conical, etc., while micro shape or "rugosity" is a measure of surface roughness. Both of these parameters can be measured experimentally (7-48), but again, qualification of the method employed to measure them, has to be provided with shape measurement data if it is to be meaningful. For the purpose of this research, the measurement of microshape or rugosity is most important. This is because the adhesion

between particles and a plane surface and the cohesion between particles themselves depends upon the area of contact between the bodies, which in turn depends upon the particle surface roughness. This fact leads to the most important particle characteristic involved in adhesion studies, the particle surface.

1.5 Surface Area and Surface Structure

The surface of a particle in a fluid is the boundary or interface between the two phases. The extent of this surface is a function of particle size and surface roughness. For a given weight of solid matter, the lower the particle size, and the rougher the particle surface the greater the surface area. This "factor" is usually subdivided into two categories. These are the "external surface area" which is equivalent to the surface of all prominences on the particle plus the area of all indentations which are wider than they are deep, and the "internal surface area" which is that part of the surface contained in indentations deeper than they are wide (49). At all points over the total surface, i.e., external and internal, there are unsatisfied bonds which give rise to a field of force around the particle. This property is a specific feature of a surface which no other part of the particle exhibits In order to appreciate how a surface attains this property, one has to understand some of the features involved in the structure of solids.

Solids can be subdivided into crystalline and noncrystalline substances. The former have a high degree of order in their molecular structure, in which the crystal is built up in a pattern or space lattice. In contrast, a noncrystalline solid has complete disorder within its structure. Four different kinds of lattice exist in a crystalline solid and these are termed "ionic", "homopolar", "molecular", and "metallic" (49). In ionic lattices the constituent entities are ions, and the structure is held together by the attraction of unlike

charges or "electrical forces" (50). Examples are Sodium Chloride, Potassium Bromide, etc. In homopolar lattices, the entities are neutral atoms, and the structure is held together by ordinary chemical valences. An example is diamond. In a metallic lattice (51), all electrons can be regarded as making up an assembly in which chemical valency bonds are formed between each atom and its neighbors in the lattice. In a molecular lattice, the entities are molecules which are held together by physical or "Van der Waals forces". These arise from the interaction between electrons and adjacent molecules. An example is stearic acid (49). In all cases, the forces holding lattices together are attractive, and their strengths increase in the order Van der Waals, electrostatic and valency forces, respectively. For the case of a perfect lattice, the forces can be calculated, and at the surface where unlinked bonds predominate, an estimate of the attractive force can be found. Unfortunately, perfect lattices are rare, and imperfect lattices are the general rule. Stone (52) and Gray (53) discuss lattice defects and define two distinct kinds termed interstitial ion and ion vacancy defects. This means that at some point in the crystal, more ions are present than should be there (if interstitial ion defects are present), and alternatively less ions are present than should be there (if ion vacancy defects are present). This gives rise to localized areas of high and low attraction at the surface of the particle. These kind of defects give rise to the property of semiconductivity in solids (54). Stone (52) discusses a third defect due to non-stoichiometry in the lattice, which he categorizes into excess metal with anion vacancies, excess metal with interstitial cations, excess electronegative constituents with interstitial anions, and excess electronegative constituents with cation vacancies. The problem is complicated even further when the ion deficiencies are filled with ions of a different kind, i e., when impurity ions are present in the lattice. This has a detrimental effect, if the impurity ion has a different valency,

when the lattice structure is subjected to strain. Cottrell (55) and Reid (56) discuss the effect of lattice strain particularly for the cases when solids are deformed or dislocated. An analogy to this effect is faulting and folding of geological strata in the earth's crust. Differences in the size and nature of the ions are responsible for the degree of deformation, and it has been shown to be greater for anions than cations and to increase with the radius of the ion. One effect of deformation is the polarization of the structure, which is reflected in a change in the bond strength between the ions (57). Thus, in some cases, a highly deformed ionic bond can behave like an unsymmetrical homopolar one (49). On these grounds, it is very difficult in practice to predict the strength and nature of the bond at the surface of any non-perfect lattice. However, irrespective of whether the strength of the surface bonds are predictable or not, some field of force will exist as a result of their presence. Thus, when a second particle is brought close to the first one in such a way that their fields of force overlap, attraction and eventual adhesion takes place.

1.6 Surface Energy and the Adsorption of Films

The force of adhesion will depend on the force of the field around the solid, and a measure of this is the "surface energy". This is defined as the isothermal reversible work which requires to be done in creating $1cm^2$ of new surface. This, if a solid particle in the form of a 1 cm cube was pulled apart to make two equal halves, with plane forces and the operation was performed in a vacuum, the surface energy would be twice the free energy associated with each surface. If these two halves were placed in contact once again perfect adhesion would take place, with a gain in energy of the same magnitude. If the operation was performed in air or in the presence of a vapor, this would not occur. Instead, the unsatisfied surface bonds would attract molecules of moisture or vapor to the surfaces, and when the two halves were placed

in contact once again, the gain in energy would be less (58). In this case, the force of attraction between the two surfaces of the clean solid has been replaced by the force of attraction between two adsorbed layers. In general, these have lower values of Van der Waals forces than the solid itself. Thus, the adsorption of surface films reduce the force of adhesion between two perfect surfaces.

If the experiment was now repeated in such a way the 1 cm cube was torn apart with a highly irregular interface between the two halves, each interface would be the perfect mate to the other, but the energy involved would be greatly different, as the surface area of the rough interface would be greater than 1 cm^2. With an irregular interface in a vacuum, it is possible that lattice distortion could then occur due to attraction between unsatisfied bonds in narrow cracks in the surface which could result in a change in the microshape. In this way, the surface could be modified and it would no longer be the perfect mate for the other interface. In addition, in air or a vapor, the adsorption of films would be different in cracks than on prominences due to capillary condensation, and so when the two interfaces were brought together, the energy involved in the adhesion would be much lower than predicted. This introduces much uncertainty into the estimation of adhesion forces on nonplane surfaces, and even more uncertainty is introduced when one considers the effect of the surface defects and impurities discussed previously. It was shown that areas of high and low attraction could be present even on plane surfaces, so that they certainly can be present, and influence the uniformity of adsorption of surface films on irregular surfaces. In this way, surface roughness, surface energy, surface purity, and surface structure cause the force of adhesion to vary from point to point over a single particle surface, and the force between any two particles will depend on the specific surface location where contact will be made, and the actual contact area between the particles in question.

1.7 Multilayer Adsorption and Effect of Free Liquid

So far in this discussion, the adsorption of moisture or vapor onto surfaces has been restricted to surface films or monomolecular layers. In the presence of high humidity, multilayer adsorption can occur (59-63), and in the ultimate case, free water can form a "pendular bond" between particles. In this case, new forces are introduced termed "capillary forces" which bind the particles together strongly. If the pendular bond is an organic vapor or volatile component which has a low melting point, condensation can be followed by partial solidification and the pendular bond then acts like a cement or binder. In this case, the adhesive properties of the binder are added to those of the particles which, of course, is the prime objective with a wide range of adhesives manufactured by the chemical industries. In this case, the particles are cemented together into an aggregate-type structure, which is almost inseparable by physical dispersive techniques. However, considering only the case for water at the present time, additional increases in concentration leads to a complete coverage of the particles by a layer of water, which may or may not "wet" the surface. If the forces of attraction at the solid surface are greater for the liquid than for the solid itself, wetting will occur spontaneously. In contrast, if the forces of attraction at the surface of the solid particle are greater for another solid particle than for the liquid, then the liquid will not wet the particles, but agglomeration will be observed. This behavior is related to a parameter termed the "contact angle," i.e., the angle between the liquid interface and the solid surface. If the angle is 0°, complete wetting occurs while if the angle is 180°, no wetting takes place. Hence, by using a liquid whose affinity for the solid is greater than the solids affinity for itself, i.e., a liquid whose contact angle with the solid is 0°, one can replace the adhesion between particles, by the adhesion between a particle and a liquid. In this way, particles can

be separated or dispersed with a relatively low amount of energy (64). This can be facilitated by proper selection of a pure liquid or by adding a "surface active substance" to the liquid itself. This substance has a high affinity for the surface, and is adsorbed there from solution. The interface or surface of the solid with the liquid is now converted to an interface of surfactant with the liquid, which leads to yet a further force involved in particle-particle interactions. It has been shown that at a particle surface, there is a field of force due to the presence of unsatisfied bonds, which, depending on the ion, can lead to a surface charge. If this surface is placed in contact with a liquid containing positive and negative ions, a "double layer" is developed between the ions localized in the surface of the solid, and those in the region extending into the solution (64-69). When the particle is in motion, shear is developed between the double layer and the bulk solution. The potential difference between any point in the bulk solution and this shear plane is termed the "zeta potential" (70). This parameter can be used as a measure of the stabilizing potential of the double layer. Compression of this layer, leads to a reduction in zeta potential and loss of stability, i.e., coagulation and flocculation take place. In other words, loss of stability means the nett force acting between the particles is now attractive, whereas in stable systems, when the zeta potential is high, the nett force is repulsive. In this way "double layer forces" are very important in particle separation phenomena in a liquid medium.

Liquid layers have yet another significant effect in adhesion between surfaces, which arises as a result of capillary condensation. With any two rough surfaces, the adhesion between them is a function of the areas of the surface in contact. With highly irregular surfaces, perhaps contact occurs at only one point, such as at the tip of a prominence in the surface. If it occurred at the tips of two prominences, the contact area would be radically changed if the valley between them was filled

completely with liquid. In this case, contact would be made at the tips of the prominences and over the area of the liquid film. Thus, the overall contact area would be increased. A similar effect is obtained due to plastic deformation or surface melting.

1.8 Plastic Deformation, Melting and Sintering

When two surfaces are brought into contact under conditions of known pressure, the extent of deformation of the solids at the point of contact depends on the area of the initial contact and the elasticity of the surfaces (49,71,72,73,74). In general, the lower the value of Young's mondulus of elasticity, the softer the material, the greater the deformation and, consequently, the greater the adhesion. The hardness of materials was conveniently tabulated by Moh who developed a scale of hardness by which most chemical substances can be relatively compared. This is shown in Table 1. In addition to elasticity, the deformation of a solid is a function of the applied pressure, and many materials can be made to adhere purely by the application of high pressures (73). Examples can be found in the manufacture of cold welded compacts, in which scrupulously clean metal surfaces such as aluminum can be pressed together to form metal parts (49). Scrupulously clean means freedom from oxide films, liquid films and dust, which adhere to the surface bonds and lower the adhesional energy of the surfaces. Welding is usually accomplished by the use of heat, which acts as a surface softener and promotes rapid deformability. Adhesion at high temperatures is termed "sintering" and in this process surface melting and subsequent deformability lead to surface bonding. However, sintering does begin below the melting point of most solids, and there is an actual temperature termed the "Tamman" temperature which is approximately half the value of the solid melting point in °K. At this temperature, the rate of sintering rapidly increases (70,73,74). It is probable that at this temperature, the lattice defects, discussed earlier, are no longer rigidly

Table 1

RELATIVE HARDNESS SCALE - RELATIVE TO MOHS

Solid	Mohs Scale	Relative Linear Scale	Solid	Mohs Scale	Relative Linear Scale
Wax(OC)	0.02	0.006	Iron	4-5	0.25-0.6
Graphite	0.5-1	0.02	Zinc Oxide	4.5	0.4
*Talc	1	0.03	Glass	4.5-6.5	0.4-1
(a) Diat. Earth	1-1.5	0.035	*Apatite	5	0.6
Asphalt	1.5	0.04	Carbon Black	5	0.6
Lead	1.5	0.04	Asbestos	5	0.6
*Gypsum	2	0.05	Steel	5-8.5	0.6-2.3
Fingernail	2	0.05	Knife Blade	5.2	0.65
Organic Crysts	2	0.05	Window Glass	5.2	0.65
Soda Ash	2	0.05	(a) Chromite	5.5	0.7
Hyd. Lime	2-3	0.05-0.2	*Orthoclase	6	0.8
Sulfur	2	0.05	Iron Oxide	6	0.8
Salt	2	0.05	Pumice	6	0.8
Tin	2	0.05	File	6.3	0.9
Zinc	2	0.05	Mag. Oxide	5-6.5	0.6-1
Anthracite	2.2	0.08	Pyrites	6.5	1.0
Silver	2.5	0.13	Tit. Dioxide	6.5	1.0
Borax	2.5	0.13	*Quartz(Silica)	7	1.25
(a) Kaolin	2.5	0.13	Sand (Silica)	1.25	1.25
Litharge	2.5	0.13	Zirconia	7+	1.6
Bicarb. Soda	2.5	0.13	Beryllia	7+	1.8
Copper (coin)	2.5	0.13	Emery	7-9	1.2-2.5
Aluminum	2-3	0.13	*Topaz	8	2.0
*Calcite	3	0.2	Garnet	8.2	2.1
(a) Limestone	3-4	0.23	*Corundum	9	2.5
(a) Bauxite	3	0.2	Alundum	9+	2.5+
(a) Mica	3	0.2	Tungsten Carb	9.2	2.7
Plastics(many)	3	0.2	Alumina	9.25	2.9
Barite	3.3	0.21	Tantalum Carb	9.3	3.0
Brass	3-4	0.23	Titanium Carb	9.4	3.5
(a) Quicklime	3-4	0.05-0.25	Silicon Carb	9.4	3.5
(a) Dolomite	3.5-4	0.24	Boron Carbide	9.5	4.0
*Fluorite	4	0.25	*Diamond	10	10

* Minerals used as standard in Mohs Scale
(a) Can also have more abrasive impurities present

bound in the lattice, and ion migration takes place at the surface. Thus, the structure and properties of the surface are modified by the release of impurities and defects, and this is usually demonstrated by an increase in the force of adhesion (49). Deformability of this kind can also be induced by friction. As the areas of contact between particles are usually very small, very high local temperatures can be induced by the rubbing of one particle surface against another (73). When this occurs, the very high pressures and temperatures induced at the points of contact result in the localized plastic flow of the softened surface. This continues until the total area of contact is such that the local pressure has fallen to the characteristic yield pressure of the softened material, and the temperature has fallen below the Tamman value (73). Friction deformability can be reduced by the presence of adsorbed films between surfaces which, of course, is the principal mechanism involved in lubrication (73,74). It should be noted that the multiparticle structures arising from the sintering of particles are aggregates and these cannot be separated by normal dispersion techniques. If the energy is increased in order to separate such structures, one runs the risk of fracturing the discrete particles themselves.

1.9 Summary

In this introduction, the many variables that play a role in the adhesion process, have been generally introduced. This information has been found in standard books on the subject and is lacking in specific detail. What this introduction has done is provide a base onto which specific literature can now be built. In the following sections of this report, literature has been assembled which details information found in recent work in all these aspects of adhesion. As adhesion has been shown to be a function of the chemical and physical nature, structure and purity of the particles involved, it seemed logical to begin the specific search by a study of atmospheric

aerosols, so that the important properties of the particles likely to be involved in the study can be defined.

2. ATMOSPHERIC AEROSOLS

2.1 Definitions

Nowhere on earth is there air which is completely free of particles. There are areas such as the polar regions which contain very low particle concentrations compared to polluted urban air; and visible pollution above cities decreases with altitude as any air traveler can observe. However, even in the stratosphere one can find particles of terrestrial and extraterrestrial origin. Aerosol particles to be found in the atmosphere can range from briefly airborne soil derived dust such as grains of sand carried aloft in a sand storm to molecular aggregates produced by cosmic radiation or natural radioactivity. Between these extremes which range from angstrom to millimeters in size, atmospheric aerosols are to be found wherever there is atmospheric air to transport them. Particles in the air can be categorized as dusts, smokes, and mists.

Dusts consist of solid particles suspended in air as the result of mechanical disintegration or aerodynamic dispersal of previously disintegrated bulk particulates. Dusts generally have a very broad size distribution and as a result tend to settle rapidly under the influence of gravity, although the size distribution can extend into the sub-micron region. Smokes usually refer to more stable suspensions of particles which are formed by volatilization and condensation, chemical reaction, and pulverization. Smokes generally have particles less than 5 μ in size. Mists result from the condensation of vapor and consist of droplets usually larger than 5 μ in size. Cloud and fog droplets are examples of a mist and these droplets very often carry dissolved components as well as insoluble particles. Snow and rain forming in and descending through the atmosphere inevitably collect atmospheric aerosols and vapors before reaching the earth's surface.

Nuclei are particles typically submicron in size, with condensation nuclei larger than about 0.2 μ in diameter and Aitken nuclei less than 0.2 μ in diameter. All natural cloud droplets start by vapor condensation on nuclei particles.

The terms haze and smog refer to combinations of the above types of aerosol particles and are often used to describe combinations of natural and anthropogenic aerosols.

Aerosol size and property parameters are depicted in Figure 1 and show size ranges important for ions, light scattering, cloud physics, air chemistry, and routine air pollution measurements (75).

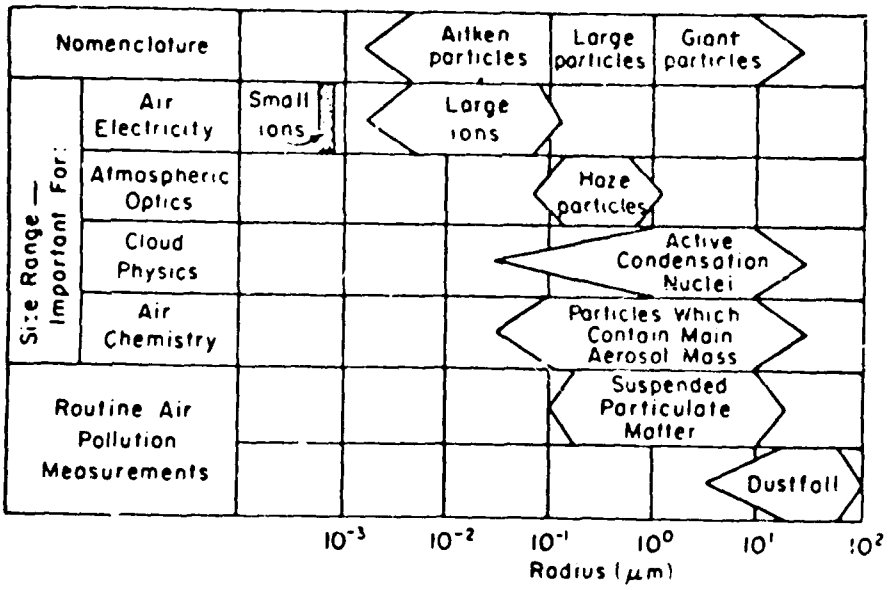

Figure 1

PARTICLE NOMENCLATURE (Ref. 75)

2.2 Basic Properties of Aerosols

Aerosol suspensions are fundamentally unstable and cannot persist unless continuously or periodically reinforced to replace particles being removed by natural forces. Gravity continuously acts on aerosols and results in sedimentation which increases as the particle size increases. Particles larger than about 1 μ have terminal velocities of fall which exceed brownian motion displacements. The reverse is true for submicron particles, and they would have exceedingly long airborne lifetimes except for other factors.

Particles in suspension also tend to agglomerate, and the rate of coagulation increases with increasing particle concentration. Since the number concentration of atmospheric aerosols reaches a maximum in the submicron range, growth of these small aerosol particles by coagulation is an ever present mechanism which would result in a decreasing number concentration except for a continual replenishment of submicron particles. Thus, as the submicron particles collide with and attach to other particles, whether submicron or larger, they eventually become either attached to an agglomerate of sufficient size to fall to the surface of the earth, or be scavenged by snow, rain, or hail. Electrostatic charges on aerosol particles unless unipolar, will enhance coagulation. Positive and negative ions produced by ionizing radiation in the air attach themselves to nearby particles to produce charged particles.

Thermal gradients in the air can result in particle migration (thermophoresis) toward a colder collecting surface, e.g., an evaporating droplet or a snowflake descending through warm air. Vapor pressure gradients can result in particle migration (diffusiophoresis) in the direction of low vapor concentration. Thus vapor condensing on a drop will tend to transport particles to the drop surface unless balanced by a repelling thermophoretic force.

Air suspended particles illuminated by sunlight can move in complex paths depending upon the light intensity, color, pressure of the air, particle size, shape, material and on additional fields such as electric and magnetic. Such motions induced by illumination are known as photophoresis. At sea level, particles below 0.1 μ will be very photophoretic. Also, ferromagnetic particles will show magnetophotophoretic motion in the direction of the magnetic field of the earth. The photophoretic or magnetophotophoretic velocity in sunlight at sea level is of the order of 10^{-2} cm/sec and can even result in particles rising against gravity in the atmosphere under certain conditions.

Falling particulates and hydrometeors will accumulate additional particles during their descent through impaction and interception. The sampling of hydrometeors such as snow or rain can be an effective means of sampling particulates from the volume of air through which the snow falls. Examination of particulates removed through the centuries by accumulated polar snows has revealed much information concerning atmospheric aerosols in ages past.

Atmospheric aerosols also interact with gases and vapors. Condensation nuclei tend to be hygroscopic such that a rise in humidity will cause particle growth. Condensation can start on hygroscopic nuclei at comparatively low humidities as indicated by Houghton (76). Hygroscopic gases such as SO_3 and NH_3 will also react with water vapor to produce droplets at low humidities. Vapors also adsorb on particle surfaces through physical adsorption, and reactions can be promoted or catalyzed by particles which contain active components. The inevitable presence of adsorbed or absorbed moisture on atmospheric particles leads to solution of soluble components and can result in recrystallization and mechanical binding of agglomerates through interparticle crystallization. Even in the absence of soluble components, adsorbed moisture will hold particles together through surface tension effects. Even

moisture condensed from a particle free atmospheric air parcel will extract surface active gaseous components which will not revert completely to a gas on subsequent evaporation of the droplet (77).

The presence of soil derived aerosols containing transition elements also provides catalytic surfaces which could promote chemical reactions. These reactions could result in a still more tightly bound agglomerate. It has become evident as well that many other reactions in the atmosphere, including the Los Angeles smog, occur preferentially on the surface of particles already in suspension, often coating them with a heavy layer of added material (78).

Particle concentrations in the atmospheric air can range from a few particles cm^{-3} in the polar regions to 200-300 cm^{-3} over some parts of the ocean to as high as 10^5 cm^{-3} in highly polluted atmospheres. Concentrations by weight can range from a few micrograms $meter^{-3}$ in very clean to as high as nearly 1000 micrograns $meter^{-3}$ during heavy smogs in London. It is not unusual to find concentrations in cities as low as 60 micrograms $meter^{-3}$, and measurements far from civilization in the rain forests of Panama showed occasional concentrations in excess of 40 micrograms $meter^{-3}$.

The smaller the particle in the atmosphere, the greater is its number concentration down to some lower limit. Junge (79) first characterized atmospheric particulate size distributions into the submicron region and showed that for each 10-fold decrease in particle size, there is about a 1000-fold increase in particle number. Therefore, the mass of particles, for example, between 0.8 and 0.9 μ will equal the mass of particles between 8 and 9 μ. Figure 2 shows some size distributions of aerosols at various stations in Germany as determined by Junge.

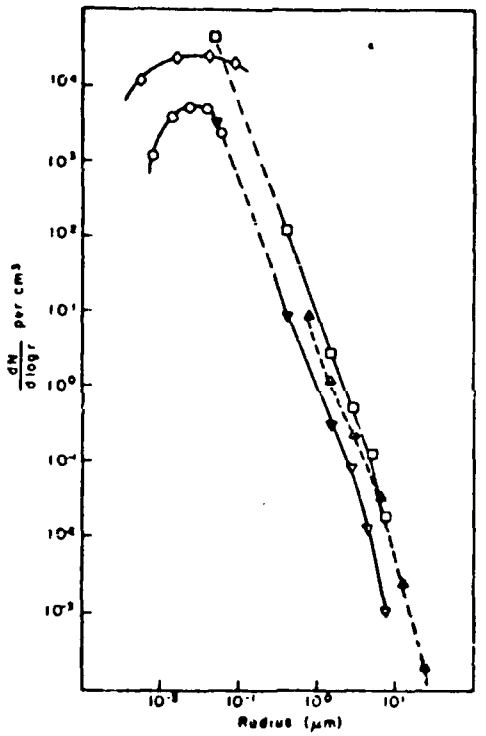

Complete size distribution of aerosols at various stations in Germany. Individual curves are based on average data of many measurements and are not entirely based on simultaneous sampling. The dashed curves between 8×10^{-3} and 4×10^{-1} μm are interpolated. The points ◇ and ○ are based on ion mobility measurements at Frankfurt and the Zugspitze, respectively. Other points are based on impactor measurements or nuclei count. ▽ Zugspitze, □ Frankfurt, △ Zugspitze sedimentation data (C. E. Junge, p. 117, 1963).

Figure 2

SIZE DISTRIBUTION OF AEROSOLS IN THE ATMOSPHERE

2.3 Sources of Aerosols in the Atmosphere

Green and Lane (80) have summarized that continental aerosols have three main components in the size range above 0.1 μ. The first is sea salt, which is the predominant constituent of nuclei greater than 1 μ in diameter. The second is a sulfate component, which may be present either as sulfuric acid, or combined as a salt, perhaps ammonium sulfate, and which predominates in nuclei between 0.1 and 1 μ in diameter. Other hygroscopic materials may be present. The third component consists of insoluble particles largely derived from the soil, and its concentration depends upon the soil conditions, terrain, and ground wind. The relative influence of these three components will clearly depend upon the previous exposure of the air parcel.

In a recent 3-week study and seminar at Stockholm, Sweden (81), Dr. Christian Junge, of Max-Planck Institut für Chemie, Mainz, West Germany, estimated that man-made particles account for 10 to 50% of the atmosphere's total particles. Natural injection of particles into the atmosphere totals 773 million to 2.2 billion metric tons annually. Man-made emissions total 185 million to 415 million metric tons per year. All but 10 million to 90 million metric tons of the man-made annual total comes from chemical precursors, such as sulfur dioxide from combustion of fuels and nitrogen oxides from industrial emissions. Gaseous oxides convert in the atmosphere to sulfate and nitrate particles. Man-made sulfate particles attain about the same level as natural species (130 million to 200 million metric tons annually) and are the largest single man-made contribution of particles. Dust and smoke emissions account for 10 million to 90 million metric tons of the man-made annual total, nitrate for 30 to 35 million metric tons, and hydrocarbons for 15 to 20 million metric tons. Natural sources of sulfur yield 130 to 200 million metric tons annually of sulfate particles, ammonia and nitrogen oxides

give 140 to 700 million metric tons of nitrate, and hydrocarbons form 75 to 200 million metric tons annually of particles in the atmosphere. Sea salt, soil, volcanic ash, and forest fires account for the remaining 438 million to 1.1 billion metric tons annually of natural particles.

Diamant (82) has indicated that globally the annual input of particles below 5 μ diameter into the atmosphere amounts to 1,600 million tons, of which 560 million tons are converted sulfates, 35 million tons are converted nitrates, 15 million tons are converted hydrocarbons, while 40 million tons could be described as soot from combustion. Critchlow (83) points out that of the below 5 μ particles in the lower atmosphere, only a small proportion is man-made. The majority are derived from natural processes and tend to be permanently present in the air with minor fluctuations. Hans (84) reports that a large part comes from combustion, from mineral and organic particles raised by the wind, from ocean spray and wave crests, and from chemical reactions, with a minor component of cosmic dust. Chovin (85) presents a systematic general review of the origin and nature of chemical pollutants of the atmosphere with reference to France, England, and the U.S.

Georgii (86) indicates that in the northern hemisphere, industrial sources account for 30% of the aerosol components. Salt nuclei from the sea account for 20-25% of the nuclei which are active in cloud formation. Also, the number of giant maritime nuclei exceeds that of giant terrestrial nuclei; their concentration in the troposphere decreases exponentially with altitude. In central Europe the otherwise natural background aerosol of other uninhabited areas has been obliterated by numerous anthropogenic sources. Beyond a height of 700 meters, local aerosol differences disappear. Corn (87) says that the chemical profile of an air basin is highly individualistic, dependent on the input of aerosols from natural, industrial, domestic and mobile sources of pollution in the region. Nitrogen

dioxide is the dominant photochemical reactant in the lower atmosphere according to Johnston (88). He also discusses photochemical reactions and resultant products including aerosols. Knop (89) enumerates major sources of hazardous and annoying industrial dusts and gases; quarries, cement factories, the ceramic industry, the asphalt industry, iron ore sintering plants, blast furnaces, and foundries are large contributors of dusts and gaseous emissions. Estimates were made for the year 1966-1967 of nationwide emissions of air pollutants including particulates, and information is broken down by source category (90). More recently, Hidy (91) has estimated worldwide production of primary particles from industry and by nature, and includes secondary chemical aerosols produced by reactions in the atmosphere. Hidy's tabulations are shown in Tables 2 to 4. Ivliev (92) discusses aerosol distribution as related to sources.

Vandegrift (93) conducted a study to identify, characterize and quantify the natural particulate air pollution problem from stationary sources in the U.S. Emissions were determined from data on emission factors, grain loadings, and material balances. These particulate emissions currently total 18 million tons per year. The major stationary sources of particulates include power plants, crushed stone, agriculture and related operations, cement, iron and steel, and forest products. Dreisbach (94) indicates the major types of air pollutants in the San Francisco Bay area, and their sources and effects. Crouse (95) has also conducted a source inventory of the San Francisco Bay area which shows transportation, incineration, chemical, metallurgical, and combustion pollutants as 87% of the industrial particulates in 1965. Maps have been prepared by Selezneva (96) which show the distribution of condensation nuclei over Russia and their sources are identified. The material covered by Selezneva is Russian in origin with some reference to non-Russian work.

Table 2

ESTIMATED SOURCES OF PRIMARY PARTICLE PRODUCTION

	tons yr^{-1}	Emission Factor	Production Rate (tons day^{-1})
A. Combustion of Fuel & Waste			
1. Coal	2.9×10^9	15#/ton	6×10^4
2. Liquid Hydrocarbons	1.3×10^9	14#/1000 gal.	0.3×10^4
*3. Natural Gas	$1.9 \times 10^7 ft^3$		10^{-4}
*4. Incinerators	12×10^6	14.8#/ton	2.5×10^2
B. Industry*			
1. Steel	1.3×10^8	10#/ton	0.18×10^4
2. Iron	9.1×10^7	17#/ton	0.21×10^4
3. Smelting (Cu, Pb, Zn)	2×10^4		10^2
4. Petroleum Refineries	11.3×10^6 bbl.	1 ton/10^5 bbl. day	$.3 \times 10^2$
5.	-	-	$< 10^3$ (?)
6. Pulp Mills	25.7×10^6	260#/ton	0.9×10^4
7. Portland Cement	3.08×10^7 bbl.	38#/ton	3.2×10^4
8. Bitumens Cement	1.11×10^6 bbl.	0.2#/ton	10^1
9. Food and Feed	-	-	$< 10^2$ (?)
			$\sim 1 - 3 \times 10^5$ **

*U.S. Only

**Range for projection of extrapolation to world industry.

Table 3

ANNUAL WORLDWIDE HYDROCARBON EMISSION ESTIMATE
(From Robinson and Robbins)

Source	Source Quantity tons ($\times 10^6$)	Emission Factor lb/ton	Percent Reactive, %	Total Emission tons ($\times 10^6$)	Reactive Emission, tons ($\times 10^4$)
Coal					
Power	1,219	0.2	15	0.2	3
Industrial	1,369	1.0	15	0.7	10.5
Domestic & Commercial	404	10	15	2.0	30
Petroleum					
Refineries	11,317 bbl.	56 tons/ 10,000 bbl.	14	6.3	88
Gasoline	379	180	44	34	1500
Kerosene	100	0.6	18	< 0.1	1
Fuel Oil	287	1.0	18	0.1	1.8
Residual Oil	507	0.9	18	0.2	3.6
Evaporation & Transfer Loss	379	41	20	7.8	156
Other					
Solvent Use	3	30 lb/yr/ person	15	10	150
Incinerators	500	100	30	25	750
Wood Fuel	466	3	15	0.7	10.5
Forest Fires	324	7	21	1.2	25
				88.3	2,729.4

Table 4

SOME IMPORTANT SOURCES OF ATMOSPHERIC AEROSOLS
(Production Rate in Tons Day^{-1} on a Worldwide Basis)

Source	Estimated Production Rate	Max. % by Wt. of Total
1. Primary		
Dust rise by wind	$2 \times 10^4 - 10^6$	9.3
Sea Spray	3×10^6	28.
Extraterrestrial (Meteoritic Dust)	50 - 550	
Volcanic Dust (Intermittent)	10^4	0.09
Forest Fires (Intermittent)	4×10^5	3.8
2. Secondary		
Vegetation	$5 \times 10^5 - 3 \times 10^6$	28.
Sulfur Cycle (oxidation of $H_2S \rightarrow SO_4^{=}$)	$10^5 - 10^6$	9.3
Nitrogen Cycle		
Ammonia	7×10^5	6.5
$NO_x \rightarrow NO_3^-$	10^6	8.3
Volcanoes (volatiles SO_2 & H_2S) - Intermittent	$\sim 10^3$	0.009
Sub-Total	10.1×10^6	94.

Internal combustion engine aerosols consist of (a) mists of partly cracked and partly oxidized hydrocarbons emitted as crankcase blowby; (b) mists of partly cracked and partly oxidized hydrocarbons from the exhaust during choked operation; (c) mists of partly cracked and partly oxidized lubricating oil from the exhaust during over-run of worn engines; (d) black smoke during prolonged operation with the choke closed; and dispersion of lead salts (97). The exhaust particulates amount to about 5% by weight of the amount of hydrocarbon emission, and the non-volatile reaction products include free acids, high molecular weight olefins, and carbonyl compounds (98).

Marchesani (99) estimates pollutant sources often overlooked which include aerosol spray cans, ground dust, leaf burning, cosmic dust, perfumes, smoking, marsh gas, tire tread wear, shoe wear, pavement wear, and other sources. Windom (100) indicates that the mineral talc which is used as a carrier and diluent for pesticides has been detected at levels as high as a percent by weight and is traced to agricultural crop dusting activity. Parkin (101) sampled dust across the temperate North Atlantic and noted that in the greater than 3 μ fraction anthropropogenic combustion-derived carbon and fly ash spherules were as high as 60% of the sample near land, while in mid-ocean there are usually about 5% spherules. Talc, especially abundant in January, was present in all samples. Using spherules as a tracer, it was noted that a pollution stream increases in width fivefold in moving from Newfoundland to Ireland. Close to the West African coast, near Dakar, the concentration of red-brown dusts is 10 $\mu g\ m^{-3}$ with 0.1% larger than 23 μ. At Barbados there was much less quartz and the corresponding size was 0.1% larger than 11 μ.

2.4 Nature of Aerosols Close to Ground Level

2.4.1 General References

Vohra (102,103) discusses aerosol formation by chemical reactions in the atmosphere, and says the processes of oxidation,

nitration, chloride formation, hydrolysis, hydration, and recombination of specific oppositely charged species forming inorganic acids are some of the basic aerosol forming reactions. Nuclei formation in the dark in filtered air is due at least partly to the recombination of certain ionic species by natural ionization. The role of solar radiations, electric discharges and ozone in the formation of acids is also considered. Mohnen (104) presents anomalous data on aerosol formation from gases. Mosher, et al. (105), analyzed Los Angeles smog data and found that frequent surface inversions in winter resulted in gaseous and particulate concentrations more than twice as high as comparable summer time concentrations. Goldsmith (106) notes that the Los Angeles smog which is photochemical in nature differs from the dominant air pollution in England by occurring more in hot, dry weather than in cold wet weather, being oxidizing rather than reducing and being related to vehicle exhaust rather than household heating.

Reviews on chemical analysis of air pollution including suspended particulate matter and inorganic and organic constituents have been presented by Altshuller (107) and later by Mueller (108) who complements Altshuller's review. A review of atmospheric haze by Germogenova (109) includes chemical composition of hazes over oceans and land masses and indicates trends in haze research. A comprehensive literature survey (110) on transport, dispersion, and depletion processes in the atmosphere contains 2,112 references largely from 1940-1969. The influence of turbulent interchange on aerosol concentration in the lower atmosphere was studied by Lomaya (111) who derived an empirical formula for this effect.

On examining particulate patterns over 1957 to 1966, Spirtas and Levin (112,113) find that while a considerable margin still exists, the gap in particulate levels between urban and non-urban sites is narrowing, and the relatively pure air of rural areas will be a vanishing phenomenon if the

trend persists. Electrical conductivity measurements of the atmosphere indicate a 5% decrease between 1929 and 1962; this implies a worldwide increase in fine particle pollution over this period (114). Porch, et al. (115), present atmospheric light scattering measurements which suggest the existence of a background level of atmospheric aerosol which is augmented locally by pollution sources. Atmospheric aerosols are discussed by Dufour (116,117) and McCaldin, et al. (118). McCrone (119) describes the use of morphological microscopic examination to identify atmospheric particulates and estimate composition.

A collaborative study (120) of smog aerosols in Los Angeles during the summer of 1969 involved size determinations over the range of 0.003 to 6 μ, chemical analysis of impactor and gas samples, measurement of optical properties, nuclei, coagulation, humidity effects, and single particle chemical analysis. Harris (121) presented a paper on a study of Los Angeles aerosols. Suspended Los Angeles particulates were also reported on by MacPhee and Bokian (122). Similar studies of aerosols in Delhi (123), Milan (124), Finland (125), and New York (126) were reported. The latter study showed increased vanadium and nickel particulates during the heating season. Pollution by metal foundries in Osaka including measuring the concentration of heavy metals in particulates was investigated by Yagi, et al. (127).

Junge (128) has studied the chemistry of unpolluted atmospheres. Other aerosol studies in areas of low pollution were conducted in the Alps (129), in Pacific air masses (130), and in the Antarctic (131). Air samples from Amazonia, Brazil (132) show low concentration and relatively small, uniform particle size, which suggests domination by local sources. These sources are in turn dominated by particle formation in the air through condensation and reaction. The particle size data are similar to those of Panama except for

the inorganic size ranges. There are many biological particles not seen in Panama. Sodium chloride particles tend to be small relative to those characterizing oceanic air, and are of a size compatible with long residence times in air. Particles were classified on the basis of morphological identification.

Schaefer (133) conducted experiments with relatively clean country air in Arizona to which he added turpentine vapor and found very large increases in Aitken nuclei independent of illumination. He concludes that the molecular or ion clusters that agglomerate to nuclei appear to be always present in pollution free air. The effects of humidity on atmospheric aerosols and hygroscopic particles has been examined recently by several investigators (134,135,136,137), and Morachevsky (138) has examined the structure of the adsorption layers of atmospheric aerosols.

Properties of atmospheric aerosols from optical measurements have been reported (139,140,141), and Hanel (142) has determined the mean density and refractive index of atmospheric aerosol particles.

2.4.2 Soil Derived Aerosols

Soil derived aerosols, often referred to as dust, have historical considerations. Analysis of the deposited dusts accumulated over the centuries gives invaluable information on climatic implications, dust storms, and archeological data. Sears (143) discusses the varieties and types of dust and origins or sources as related to dust deposits in the past.

Flanigan and DeLong (144) examined seventy soil samples from locations around the world to determine their compositions and spectral characteristics. There were 5 major components which selectively absorb radiation in the 700-1300 cm^{-1} region: three clay minerals, silica, and calcium carbonate. Spectra of soil samples are given. Hoidale, et al. (145) examined the absorption spectra of airborne dust collected on the top of a

mountain in New Mexico over a wider wavelength range of 250-4000 cm^{-1} and found absorption bands for silicate clays, ammonium sulfate, and carbonates. Variation in silicate to carbonate ratios was attributed to advection of fresh soil particles from the Great Plains and aged soil particles from the overlying free atmosphere. Dust deposition was monitored in the Kansas-Colorado-Oklahoma-Texas region by Smith and Twiss (146) who found deposition over a number of months ranging from a maximum of 46 lb $acre^{-1}$ at Hays, Kansas (grassy with no evidence of soil blowing), to a minimum of 20 lb $acre^{-1}$ at Manhattan, Kansas, with no noticeable dust in the air. Dispersion with Calgon indicated 16-65% clay with median silt plus sand diameters between 7-30 μ with some particles greater than 100 μ.

Dustfall sampled 400 miles southwest of the Canary Islands in the Atlantic (February 1962) consisted of one-third aggregate particles consisting of quartz, mica, and a clay mineral (147). Organic matter was abundant. More than 80% of the dust particles had diameters between 5 μ and 30 μ. The Spanish Sahara was believed to be the origin of the dust. Continental dusts in the Pacific have been examined by Prospero and Bonatti (148) and by Ferguson, et al. (149). The Ferguson group collected airborne dust samples between California and Alaska and found illite to be the most dominant clay mineral. Other minerals found were montmorillonite, chlorite, kaolinite, mica, plagiodase and quartz. It was deduced that the probable source was from the arid areas of Europe and Asia. The dust content during the sampling period, probably low due to frequent rains, was 0.5 to 1.0 micrograms $meter^{-3}$.

Kashina (150) measured dust content of the air in Central Asia and found variations with location, with high concentrations in desert zones. During dust storms, dust concentrations varied exponentially with height. Andreyev and Lavrinenko (151) also sampled Central Asia aerosols larger than 0.5 μ and discuss relations between soil compositions and aerosols, with respect

to ionic components, particle size, acidity, molecular species, and height of sampling.

The particle size of Saharan dust which settled on Britain in July 1968 was reported by Pitty (152). Prospero and co-workers (153) were able to trace dust in the Caribbean air to an African dust storm of unusual energy which transported dust across the Atlantic in five days at 40 km hr^{-1}, and resulted in a concentration of 2.2 micrograms $meter^{-3}$ in Barbados. Air sampled off the West African coast in the spring of 1969 averaged less than 10 micrograms $meter^{-3}$, and the minor mineral characteristics of the north-east trade dusts were significantly different than those of dusts collected in the boundary region with the westerly winds (154). Junge (155) examined size-distribution data on atmospheric dusts and noted that distributions fall within a relatively narrow band of a rather uniform slope, and differs from that of the background aerosols. The Barbados data also showed that sea salt particles contained dust originating from northern Africa.

Ground dusts in Kyoto, Japan, were observed to constitute from 1/3 to 1/2 of the total of suspended particles with combustion related aerosols contributing to most of the balance over a 2-year period (156). Sakabe, et al. (157) found as much as 34 micrograms $meter^{-3}$ of quartz, feldspar, cristobalite, mica, and kaolin minerals in Tokyo air. Hoidale (158) used dispersion staining and infrared absorption to determine concentrations of quartz, kaolinite, illite, gypsum, carbonate, mirabilite, and dolomite in microgram samples of airborne dust in New Mexico over an eight-month period.

2.4.3 Sulfur Derived Aerosols

Friend (159) discusses the global sulfur cycle and indicates the uncertainty concerning production of H_2S and SO_2 by natural processes. Volcanic sources, though 1% of other sources, produce large increases in stratospheric sulfate aerosol amounts.

One-third of the sulfur reaching the atmosphere comes from anthropogenic sources according to Robinson and Robbins (160). They indicate that natural sources produce 142 x 10^6 tons $year^{-1}$, mainly as H_2S and sulfate sea spray. More than two-thirds of the total sulfur emissions occur in the northern hemisphere. Cadle and Allen (161) give a detailed review of photochemical reactions in the troposphere, stratophere, and mesophere and note the existence in the stratosphere of a worldwide layer having high levels of particulate sulfates and persulfates, at about 18-KM altitude, in which conentrations increase after major volcanic eruptions. A bibliography on sulfur oxides and other compounds is available from the U.S. Government Printing Office (162). Urone and Schroeder (163) have reviewed the literature on atmospheric SO_2 reactions. A series of eight papers on sulfur reactions in the atmosphere and the formation of acid smogs was presented in Germany in 1967 (164).

Heard and Wiffen (165) describe the use of the electron microscope to identify natural aerosols and particulate ammonium sulfate as sampled from the atmosphere. Lodge and Frank (166) have also identified particulates in the Aitken nucleus size range taken in a variety of environments free of local influence and all have shown that sulfuric acid admixed with ammonium sulfate is the predominant single class of particles in this submicron size range. The individual particles observed in the electron microscope have a dry size near 0.1 μ and they are collected as aqueous drops several times that size.

Good and Thynne (167) find that sulfur dioxide-oxygen reactions with hydrocarbon radicals tend to form RSO_2 and RO_2 radicals, and expect that reactions in the atmosphere at low SO_2 concentrations will occur rapidly. The formation of particles from the photochemical oxidation of SO_2 in air was examined by Quon, et al. (168). McKay (169) investigated the kinetics of the conversion of ammonia and sulfur dioxide to ammonium-sulfate in water droplets in the atmosphere and concluded that

appreciable amounts may be formed in a few minutes. Cox and Penkett (170) found a rapid reaction between SO_2 and unsaturated hydrocarbons even at concentrations below 1 ppm, and they give rates of aerosol formation for four different olefins. Okita (171) noted that while sulfate in cloud and fog at a rural site in Japan was mainly calcium sulfate, ammonium sulfate and sulfuric acid predominated at a mountain site. Hill (172) has demonstrated that SO_2 can react with amines to give solid particles.

A number of workers have shown that the presence of particulate matter greatly accelerates adsorption and H_2SO_4 production from SO_2 in the atmosphere (173,174,175). Urone, et al. (176) found that SO_2 in the presence of oxides of aluminum, calcium, chromium, iron, lead, and vanadium reacted within minutes even without ultraviolet radiation. Bowen (177) indicates that due to the relatively rapid oxidation of SO_2, such pollution by industry is mainly a local problem.

Lodge and Pate (178) found sulfuric acid droplets at all sampling sites in Panama despite the apparent availability of free ammonia in the atmosphere. Total sulfate remained fairly constant, but showed a progression from ammonium sulfate to sulfuric acid with greater distance inland and greater altitude. Carribbean aerosols were characterized by the presence of ammonium sulfate and the virtual absence of sulfuric acid, suggesting that the Atlantic is an ammonia source. Particle concentrations in the Antarctica (179) are quite low and usually is less than 1 cm^{-3} on impactor samples (0.2 to 2 μ diameter). Measurements indicate that the range of particles from nearly pure sulfuric acid to nearly pure ammonium sulfate accounts for more than 50% of all particles. Less than 10% may consist of sodium chloride. There is an indication of some mineral content; probably calcium aluminum silicates, particularly around McMurdo Station, which is built on lava and has a fair amount of vehicular traffic. Concentrations of sulfur

dioxide and nitrogen dioxide in the antarctic atmosphere were near the estimation limit of roughly 0.5 ppb, clearly less than the values found in Panama of 2 ppb for each of these gases (180). Traces of aldehydes, sulfur dioxide, and nitrogen dioxide appeared to occur at some times and places in Antarctica despite a nearly total absence of the biotic conditions which might be expected to constitute a major source of these gases. Samples of impactor collected particles in the antarctic atmosphere contained much higher concentrations of sulfur than similar samples collected in most parts of the world (181). Most sulfur was present as sulfate but some persulfate was detected. Cations were largely NH_4^+ and H^+. For most samples more than 50% of all particles collected ranged from nearly pure sulfuric acid to nearly pure ammonium sulfate. The concentrations in the air of collected particles varied from 0.1 to 1 cm^{-3}.

Buffaloni (182) has presented a review of the reactions of sulfur dioxide in polluted atmospheres. Reactions of sulfur dioxide in the presence of foreign particles and reactions with metal salt solutions are also included. Heterogeneous reactions, formation and chemical identity of aerosols, and the effect of nucleating particles on photochemical aerosol formation are discussed. Little work has been done on determining the chemical identity of SO_2 derived aerosols. Some of the chemicals which have been identified are H_2SO_4, a copolymer of 2-pentene and SO_2, a cyclohexene-copolymer, aldehydes, ketones, organic acids, ammonium sulfate, and turpene derived copolymers.

Wagman, et al. (183) found average sulfate mass median diameters (MMD) in Cincinnati, Chicago, and Fairfax (Ohio) were nearly the same (0.42 μ) despite large differences in sulfate concentration and heterodispersity. Sulfate MMD generally increased with increasing relative humidity. Garland (184) has calculated the size of ammonium sulfate nuclei as a function of relative humidity. During 1965, the fumes from the main vent of Kilauea volcano in Hawaii was sampled with a staged

impactor and the 3 μ and 5 μ MMD stages collected the bulk of the particles (185). Particles were present as agglomerated droplets that remained liquid at 30% RH, and consisted of supersaturated solutions of ammonium sulfate. Elemental sulfur was absent. It is likely that fuming volcanoes at times emit enormous amounts of ammonium sulfate into the atmosphere.

Junge (186) sampled air in London and three German cities and noted that the acid content was higher by titration than by the pH method, indicating the presence of either weak acids, or strong acids buffered by weak bases. Sulfuric acid accounted for the measured sulfur content. Particles smaller than 0.2 μ contain preferentially the water soluble part of the aerosol particles, particularly the acid content. Most of the total mass of the aerosol was in particles larger than 0.2 μ diameter. DeBary (187) has prepared maps which show the mean concentration of sulfur and chlorine in air and precipitation over north western Europe in summer and winter. Eggleton (188) has determined that the Tees area (England) aerosol during June to October 1967 contained large concentrations of ammonium sulfate with measured concentrations as high as 130 micrograms meter^{-3} over a 24-hour period. These concentrations were similar to those at AERE, suggesting that non-industrial sources are significant and perhaps dominant. Kapoor (189) investigated sulfate aerosols in Delhi and Okita, et al. (190) noted that the SO_4 to SO_2 ratio in Tokyo increased with an increase in humidity and a decrease in wind speed. Ammonia concentrations were higher in Tokyo than in other cities. In West Germany, Georgii (191) found only a small vertical decrease in sulfate concentrations, and the vertical sulfate distribution was fairly independent of the prevailing stability of atmospheric layers. The SO_2-NH_3 water reaction is considered the primary contributor of sulfate in the atmosphere.

2.4.4 Other Inorganic Components

Iron, lead and zinc were found to be the most abundant metals in the atmosphere at various urban and nonurban areas (192). Except for copper, urban fractions are typically twice those found at nonurban locations. Lead, vanadium, and nickel showed increased levels in larger cities. Maienthal (193) used polarographic techniques to determine iron, copper, lead and cadmium in aerosols sampled in residential and rural areas. Schroeder (194) noted that the frequency of cadmium, lead, and tin in the lungs of people from every country but Africa suggests industrial contamination as the source. Covert, et al. (195) have studied the relation of aerosol chemical composition and humidity with light scattering.

Lead concentrations as high as 45 micrograms meter^{-3} or more have been measured in cities (194) and Chow and Earl (196) show how the concentration of lead aerosols in the atmosphere has been increasing in recent times. Atkins (197) noted that lead concentrations in Palo Alto were nearly proportional to traffic flow, and that a large amount of lead is removed from the atmosphere by dry sedimentation. Marine air sampled over the north and central Pacific Ocean showed a lead concentration in the range of 0.0003 to 0.0015 micrograms meter^{-3} (198). Lead concentrations in north polar ice sheets have increased from less than 0.001 gamma kg^{-1} ice in 800 B.C. to more than 0.200 gamma kg^{-1} ice, the sharpest rise occurring after 1940 (199). Seasonal variations in lead, sea salts, and silicate dust were noted. Daines, et al. (200) found that over 65% of the lead in the air from 30 to 1750 ft from a well traveled highway consists of particles under 2 μ, with over 85% consisting of particles under 4 μ in diameter. In Yokohama, the concentrations of lead in air decreased with the distance from the road as far as 100 meters, but became constant further from that point (201).

Fluorine containg compounds in the atmosphere have been examined by several investigators (202,203,204) who indicate concentrations typically below 0.05 micrograms F meter^{-3}. Mercury concentrations in the San Francisco Bay area vary from 0 to 100 nanograms meter^{-3} (205). Mercury plumes were detected coming from power plants, chemical plants, pesticide plants, junkyards and landfill sites in concentrations as high as 4000 nanograms meter^{-3}. Much higher natural emissions were measured at The Geysers. Kothny (206) says most mercury enters the air by evaporation from drying soil, and subsequently is removed from air by adsorption on particulate matter. Coal and petroleum used as fuels contain ppm levels of selenium, and release about 8 million pounds of selenium to the air annually in the U.S. (207). Selenium concentrations in Cambridge (1964-1965) averaged 0.2 micrograms liter^{-1} of precipitation or per 200 meter^3 of air (208). Sullivan (209) reviewed pollution by nickel and its compounds and noted that in 1964 the national average atmospheric concentration was 0.032 micrograms meter^{-3} while the maximum was 0.69 micrograms meter^{-3}. Sources of vanadium which dominate in cities appear to be the combustion of coal and oil and industrial emissions (210).

Robinson and Robbins (211) estimated that 2.7 x 10^8 tons year^{-1} of NH_3 discharged into the atmosphere produces aerosols which deposit on the earth, 80% by precipitation and 20% by dry deposition. Estimated background levels are 1.0 microgram meter^{-3} of NH_4 (compound) and 0.2 microgram meter^{-3} of NO_3 (salt aerosol). Ammonia levels in West Berlin were measured and compared with measurements in American and Soviet cities (212). The process by which ammonium salts are destroyed in the atmosphere was studied and the authors concluded that the formation and photolysis of ammonium and ammonium nitrate are strongly dependent on the geographical location of a land mass (213).

Chemical composition of atmospheric precipitation and clouds in the Soviet Union is reported by several investigators (214,215,216). Relative concentrations and probable sources are discussed (215). The concentrations of 19 elements measured in rainwater at Quillayute, Washington, were compared to concentrations in seawater and the earth's crust to establish the origin of each element (217). The sodium, chlorine and bromine are primarily of marine origin; the scandium, cobalt, manganese, potassium, chromium, rubidium and cesium could come from continental dust. The silver, selenium, antimony, arsenic, zinc, and possibly copper appear to have origins independent of the marine aerosol or continental dust. Lazrus, et al. (218) have also analyzed atmospheric precipitation in the U.S. and suggest that human activity is the primary source of lead, zinc, copper, iron, manganese, and nickel.

McMullen, et al. (219) analyzed nonurban suspended particulates and found nickel, iron, manganese, ammonium ion and nitrate ion present at constant percentages in the remote and intermediate regions, indicating these constituents are pervasive. Copper and sulfate ion appear to be present in relatively constant amounts in the urban and near urban regions, suggesting that these substances are invading the rural areas from urban air. Pate, et al. (220) sampled air in the remote forests of Brazil and found NH_3, SO_2, NO, NO_2 and RCHO concentrations comparable to those found in the forests of Panama, despite the influence of oceanic air in Panama. Strackee (221) sampled airborne dust in the Netherlands and observed paramagnetic iron with lesser amounts of paramagnetic Mn and Cu present. It was concluded that the iron is in the form of a ferric oxide hydrate complex. The chemical composition of particulates in marine aerosols (222,223,224) and oceanic cloud water (225) have been reported. Analysis of particulates sampled from a ship between California and Hawaii show elemental ratios for Cu, V and Al which indicate a non-marine source (226). Al and V probably come from the weathering of continental crustal material. The

source for Cu may be augmented by human activities. Wilkniss, et al. (227) noted a continental origin in the Ce, Sc, Co, Eu, Al and Mn content of marine aerosols.

Matveev (228) presents data on the chemical composition of soluble substances which entered a water reservoir in USSR from dust particles and atmospheric precipitation falling onto the surface. Egorov, et al. (229) measured concentrations of 11 metals in air over locations within the USSR and in maritime regions. Tables of trace element concentration, location and monthly variation are given. Selezneva, et al. (230) conducted a compositional survey of natural aerosols over the western USSR and give data for sulfate, chloride, bicarbonate, nitrate, ammonium, sodium, potassium, magnesium and calcium ions.

Volcanic aerosols can put enormous amounts of inorganic particulates into the air (185,231,232). On the other hand, extraterrestrial particles apparently contribute but a small amount toward the atmospheric burden. Bigg, et al. (233) shows electron micrographs of extraterrestrial particles. Rosinski (234) analyzed magnetic extraterrestrial spherules collected in air samples throughout the world. The spherules generally ranged from 2 to 30 μ in diameter and concentrations were typically from 1-200 meter^{-3} from August 18 to October 15, 1967. Composition was either pure magnetite or stony with Al, Si, Ca, Ti and Fe in different proportions.

Lininger, et al. (235) determined halogens and lead in aerosols in Cambridge, Massachusetts. Thompson (236) has reported on atmospheric trace metal analysis. In an air quality survey in Clinton, Tennessee, airborne cadmium was traced to a nearby industry (237). Rahn, et al. (238) determined diurnal concentrations of 15 atmospheric trace elements in Livermore, California. Aerosols in Northwest Indiana were analyzed for 30 trace elements by neutron activation (239,240). Some elements such as Na, K, Ti, Al, Sm and Eu showed only minor concentration variations over the area while others, such as Cu, W, Cr, Zn,

Sb, Ga, Br, Ag, Fe and Ce show large variations, indicative of important local sources. In aerosols at Newton, Massachusetts, Fe, Sc and Ce were soil related, Co and Se were found in oil soot, and Sb and Br were traced to automative exhaust (241). Neutron activation analysis on Chicago area aerosols for up to 33 elements showed the following elements in decreasing order of concentration: Fe, Cl, Al, Zn, Mn, Na, Br, V, Cr, Sb, Hg, Se, Ce, Ag, Co, La, Sc, Ce and Eu (242,243,244). Lindsey (245) has reported on 22 elements detected in an urban atomosphere in England and includes a bibliography. Kneip, et al. (126) report on airborne metals in New York City, and attempt to account for the sources. In Hamburg, Hettche (246) found titanium, molybdenum and beryllium in addition to the more common aerosol components. Aleksandrov, et al. (247) used spark emission analyses to detect airborne metals in Russia including chromium, beryllium, barium and strontium. Masek (248) determined grain size, surface area, and chemical and x-ray analyses of dusts collected in the industrial area of Ostrava in Czechoslovakia. A significant arsenic content was measured.

Trace metals in suspended particulates were measured in Osaka (249,250). Vanadium was abundant near oil combustion areas and iron and manganese proliferated around cupola furnaces. Most lead particulates were below 2 μ in size. The chemical composition of suspended dusts in urban and industrial areas in Japan have been reported by Kiyoura, et al. (251,252), Himi (253), Iki (254,255), Oya (256), and Sato (257).

2.4.5 Organic and Biological Components

As noted previously, Smith, et al. (77) were able to condense gaseous surface-active materials in filtered air. The condensed materials, probably organic, did not completely evaporate when the humidity was lowered, and served as condensation nuclei for subsequent cycles. Went (258) estimates that 10^9 tons $year^{-1}$ of volatile organic substances are released by vegetation throughout the world. Many of these organics react in the

atmosphere to form peroxides, ozonides, or free radicals that lead to submicron particles. Anthropogenic combustion processes and forest or brush fires lead to a wide variety of organic effluents including potentially carcinogenic polycyclic aromatic hydrocarbons (PAH) (259). Particulate matter from air filtration plants has been analyzed for PAH and the yearly average expressed as a percentage of the total air solids were 0.012 for the seven PAH compounds, while the soluble organic matter amounted to 4.5% (260). Other investigators who have examined PAH in air include Sawicki (?61,262,263), Saringer (264), Clemo (265), Fujie (266), Barrett (267), Gilbert and Lindsey (268), and Bosco and Grella (269).

Semenov, et al. found free amino acids, urea, reducing sugars, polysaccharides, aldehydes, and acetic acid, as well as butyric, valeric, and caproic acids in rain and snow samples throughout the USSR (270). Rain scavenged as much as 24 mg $liter^{-1}$ and snow to 7.2 mg $liter^{-1}$ of organic carbon. Fujie (271) determined sugars and glycolic derivatives in airborne particles in Osaka, Japan. Atmospheric levels of pesticides have been reported by Tabor (272), and Stanley, et al. (273). The latter investigators detected DDT at all localities sampled in the U.S., but urban levels were much lower. The mass spectra of fatty acids from airborne particles in an urban atmosphere show 16 to 21 carbon atoms with palmitic and stearic acids dominating (274). These are the most common fatty acids in animal and vegetable fats. Tabor and Fair (275) examined the NASN data on the fraction of benzene soluble organic matter and found no significant difference in the mean values between coastal and inland stations, suggesting nonurban organic matter may be highly diluted urban pollution.

Keng (276) has shown that some organic gaseous pollutants, such as methyl amine, increase the dewpoint temperature and promote condensation on hygroscopic particles. Nix (277) postulated that an organic film which hindered water droplet

evaporation could explain the odd behavior of city air in a novel condensation chamber. Levy (278) has predicted large formaldehyde concentrations due to oxidation of methane in the atmosphere.

Peroxyacetyl nitrates (PAN) form in the atmosphere in the presence of light, oxygen, nitric oxide, and hydrocarbon, leading to oxidation of nitric oxide to nitrogen dioxide with concomitant consumption of hydrocarbons (279,280). Even though the most reactive hydrocarbons are olefins, some aromatic hydrocarbons are more reactive than some olefins, and some paraffins are more reactive than some aromatics (281). Stephens and Price (282) have examined the infrared spectra of photochemical smog aerosol and workers at the National Bureau of Standards (283) examined the photochemical changes of aromatic air pollutants adsorbed on soil particulates.

Went (284,285) discusses photochemical aerosol formation derived from plant generated hydrocarbons and estimates a world production of 5×10^8 tons $year^{-1}$ of submicroscopic particulate organic matter, more than the total steel or cement production. Fish (286) has postulated that microscopic elongated wax fingers observed on pine needles is due to an electrical brush discharge which melts and aerosolizes some of the wax, perhaps augmenting or supplanting the photochemical route postulated by Went.

It is acknowledged that organic compounds containing unsaturated bonds exhibit a general tendency to polymerize to linear thermoplastics by addition in the presence of heat, light, or catalyst (287). Peroxides and other highly oxygenated compounds catalyze polymerization because they readily form free radicals. Olefinic oxides in the presence of water can also polymerize by ring scission. Many of these species are present in the atmosphere, often adsorbed at particle-to-particle contacts where catalytic polymerization is certainly a possibility, and Cukor (288) has found that much of the 66% of the organic particulate matter present in the oxygenated

fractions of atmospheric particulates contain polymerized oxidized hydrocarbon ketones, aldehydes, acids and esters. Molecular weights observed ranged from 110 to 2,300 with an average of 310 to 350, and two to three double bonds per molecule based on the normalized empirical compound $C_{32}H_{61}$ were found. Reactions between SO_2 and olefins were studied by Hunt and Marvel (289), and Staudinger (290) who noted that the propylene derivative is insoluble in organic solvents but soluble in aqueous alkalies. Staudinger (290) also noted that the comparable high polymer butadiene sulfones, which developed rapidly, were also insoluble in organic solvents but were soluble in concentrated sulfuric acid. Jellinek (291) reported on cross linking of polymers by small concentrations of SO_2 and NO_2 in illuminated air. The presence of formaldehyde (180,220, 292) and amines, including urea (270), in the atmosphere also opens the possibility of amine-aldehyde condensation polymers forming at agglomerate particle contacts, perhaps enhancing agglomerate binding forces.

Uncontaminated arctic air in Alaska has been found to contain methane, butane, acetone and n-butanol (293). Sheesley, et al. (294) found a total atmospheric hydrocarbon content of 3 ppm in remote forests of Brazil and noted high concentrations of isobutane and methanol at the river sites. Garrett (295,296) and Blanchard (297) found ocean derived organic matter including fatty acids to be an important constituent of marine aerosols.

Junge (298) discusses the tropospheric distribution of microorganisms which are typically larger than 1 μ, soil derived, and usually attached to other inorganic particles. Ackermann (299) reviews 95 articles dealing with air fungi and notes a vegetation origin for fungi rather than soil since concentrations are low during the cold season. Helmut (300) surveys biological aerosols in the atmosphere and concludes that at least 50% of the natural aerosol is of biological origin. Pollen and fungus spores in the air throughout the

year show well marked seasonal and diurnal changes (301,302). Russian investigators have identified 784 strains of airborne intestinal bacteria (303), and Seisaburo, et al. (304) noted a correlation of airborne bacterial counts in Toyonaka, Japan, with human activity in the area. Shlichting (305) sampled airborne algae and protozoa in Texas (0-8 cells ft^{-3}) and Michigan (0-1.8 cells ft^{-3}). Wright, et al. (306) noted that regardless of altitude (to 500 ft), molds constituted approximately 70% of the total viable population, bacteria between 19 and 26%, and yeasts and actinomycetes the remainder in the air of the industrial area of the Twin Cities, Minnesota, between May and November 1967. Mean viable counts were 58 ft^{-3} at grade level to 22 ft^{-3} at 500 ft. The viable population was associated principally with particles in the 3-5 μ range regardless of month, altitude, or meteorological factors. Microbial clouds were sampled over the North Sea from aircraft by Gregory (307) who observed discrete spore clouds.

Laseter (308) solvent extracted airborne urediospores (produced by a common rust fungus) and found free fatty acids (C_{14} to C_{24}), alkanes (C_{18} to C_{35}), high molecular weight ketones, esters, and a variety of aromatic compounds. The presence of an 18 carbon epoxy acid was confirmed. Since a significant amount of the atmospheric particulate matter contains fungal spores, a portion of the organic film on agglomerates may be derived from such spores.

2.4.6 Radioactive Aerosols in the Atmosphere

Junge (309) has written a book on air chemistry and radioactivity, and Stewart (310) more recently has reviewed atmospheric radioactive contaminants and their characteristics. McEachern, et al. (311) noted that average uranium concentrations in surface air within New York State ranged from 0.10 to 1.47 ng/m^3, with each area indicating that a significant correlation exists between the uranium concentration and the density of total suspended particulates. Present levels of uranium

in the air are attributed primarily to naturally occurring uranium sources and nonnuclear industrial activity. In the immediate vicinity of a nuclear fuel processing plant, a slight excess uranium has been detected by observing the degree of U^{235} enrichment. Breslin and Glauberman (312) measured radioactive dust dispersed by the wind from exposed U-tailing piles. Jones and Pond (313) determined resuspension factors for plutonium-239 deposited in the form of powdered plutonium oxide and plutonium nitrate on different types of floor surfaces. Madelaine (314) demonstrated the atmospheric existence of neutral particles of thorium B which have dimensions comparable to those of small ions. Kozlova, et al. (315) sampled air in Moscow in 1965 and measured long duration beta activity in the dust. Volchok (316) and Chen and Kuroda (317) have recently reported on the spatial and temporal distribution of fallout particles and aerosols from nuclear explosions. Machta, et al. (318) suggest the use of naturally occurring cosmogenic radionuclides such as beryllium-7 and argon-37 to provide data on large scale precipitation scavenging in the atmosphere.

2.5 Nature of Aerosols in the Upper Atmosphere

An international symposium on atmospheric trace constituents and atmospheric circulation covered upper atmosphere constituents and chemical composition of aerosol air (319,320). Cadle has written a book on atmospheric particles with emphasis on meteorological aspects of aerosols (321). Cole has written a chapter on precipitation, clouds and aerosols (322). Bibliographies on cloud nuclei are given in Meteorological Abstracts, and they date back to 1955 (323,324,325). Rosinski and associates (326) report that hailstones collected in Colorado can contain as high as 10^6 particle ml^{-1} of vegetative debris and soil particles lifted by the wind. Severe convective storms have ingested as much as 1.5 grams of soil $meter^{-3}$ in the Colorado-Nebraska region (327). Hidy, et al. (328) noted that relatively heavy pollution from great distances could persist

at higher altitudes as indicated in samples of aged aerosols that originated far from Colorado. The nature and composition of cloud and Aitken condensation nuclei have been reported by Went (329), Bricard, et al. (330) and Radke and Hobbs (331). Cadle, et al. (332) report on trace constituents near jet streams and Ludwig and Robinson (333) observed aerosols in California stratus clouds. Jiusto (334) reports on aerosol and cloud measurements over Hawaii.

Cowan, et al. (335) used aircraft sampling to track and characterize 12 different types of isolated aerosol sources. Some 30 elements were detected by neutron activation analysis to fingerprint elemental composition even when mixed with other aerosols. SEM examination is being developed to further identify these particles by their morphological characteristics, size distributions, and chemistry.

Kishko (336) quantitatively sampled viable bacterial microorganisms in the air and found the greatest number in the first 500 meters of altitude. The concentration dropped to 12% at 3,000 meters and to 1% at 7,000 meters. Clouds included large quantities of microorganisms.

Vertical distributions and concentrations of dust have been determined using optical techniques (337,338,339,340). Measurements confirmed the existence of a stratopheric dust layer at around 20 KM.

Blifford and Ringer (341) and Potzl (342) have reported on the elemental composition and chemical analysis of aerosols in the troposphere. Other investigations of tropospheric aerosols include those of Rosen (343), Kelley (344), and Blifford (345). Gillette and Blifford (346) used x-ray techniques to analyze aerosol samples collected with a three-stage impactor at altitudes to 10 KM in the western hemisphere and the central Pacific Ocean. The soil component of the aerosol believed to be indicated by uniform mass ratios of Ti/Si, K/Si, and Ca/Si was quite constant with respect to altitude and

location. Most average mass concentrations of the elements Cl, S, K, Ca, and Ti decreased rapidly from the ground to about half or less the ground concentration at 1 KM and then maintained more or less constant values up to 10 KM. Low Cl concentrations compared to the ocean surface suggest a small sea salt contribution at the higher altitudes. Mass median diameters smaller than 0.3 μ were typical for most of the determined elements at the altitudes samples.

The literature contains several reports on stratospheric aerosols: volcanic dust (347,348), radioactive aerosols (349), meteoric dust (350), optical properties (351), chemical composition (352), and general observations (353-363).

Bigg, et al. (364) impacted particles on EM grids at altitudes between 20 and 37 KM. They consisted of sulfuric acid with varying degrees of ammoniation (less at the lower levels). Many particles at the higher levels had liquid or semi-liquid coatings, with probably micrometeoric inclusions. Equivalent sphere diameters were estimated at 0.1 to 0.4 μ at concentrations of 2 to 8 particles cm^{-3} (corrected to sea level air density and temperature). In the region between 6.2 miles and 15.5 miles, the particulates have been found to be composed almost exclusively of sulfuric acid (365).

2.6 Size and Shape of Atmospheric Particulates

C. E. Junge, a pioneer in the evaluation of atmospheric size distributions, has shown that the continental and maritime components of NH_4, Na, Cl, SO_4, and NO_3 can be separated for two different size ranges, large particles (0.16 to 1.6 μ diameter) and giant particles (1.6 μ to 16 μ diameter) (366). A pronounced difference between the two aerosols was noted, and the continental influence on aerosols extends far into the ocean. While theory predicts an upper size limit of about 30 μ for atmospheric aerosols, actual measurements showed no upper limit to 150 μ and no dependence on locality, altitude,

or elevation (to 3570 meters in the Alps) (367). The distribution of the larger particles is a smooth continuation of the distribution of the sizes between 0.1 and 10 μ. Not only are aerosol size distributions typically log-normal, but concentrations about a point source are usually nearly log-normally distributed (368). Twomey, et al. (369) reports on the aerosol sizes below 0.1 μ which typically outnumber (370) larger particles. Many investigators have explored the theory and utility of a self-preserving size distribution for the dynamic atmospheric aerosol which is continually reinforced with particles even as it ages and particles are removed by natural processes (371-379).

The size and number distributions of natural and anthropogenic aerosols has also received much attention (380-392) and Noll (393) recently reviewed the state of the art which indicates two mass peaks: one in the 0.1 to 1 μ region and the other is the 10 to 100 μ region, with a count distribution peak in the 0.01 to 0.1 μ size. Ocean air has a larger peak size since coagulation controls, but continental air has many fresh sources. Sholtes (394) indicates an increase in size in locally polluted air, however. The size distribution of giant atmospheric particles is reported by Noll (395). The charge equilibrium on submicron atmospheric particles in the atmosphere was investigated by Sekikawa (396). Size data obtained on the NASN cascade impactor network show particles in urban air are predominantly submicron, and curves for individual and composite samples were approximately log-normal (397).

Whitby and Liu (398) summarize urban aerosol size data obtained with the Minnesota aerosol analyzing system (MAAS). Waller, et al. (399) observed aerosol aggregates and lung tissue particulates in the electron microcope. When removed from lung tissue, these aggregates were found to be extremely stable, unaffected by the severe chemical treatment needed to isolate them from human tissue. Airborne aggregates, however,

were generally fragile and were either lost or disturbed in the EM. Shalmon (400) discusses the sizing of atmospheric aerosols by light and electron microscopy. Byers, et al. (401) used a computerized SEM to characterize atmospheric aerosols. They measured number mean diameters in urban areas from 0.008 to 0.015 μ. Noll (402) used a simple technique with one instrument to get the complete size distribution of atmospheric aerosols. He noted a larger-size secondary peak concentration when maritime air was advected into the area. Rain and showers had little effect on 0.01 to 2.0 μ particles. Horvath (403) used a Goetz spectrometer to sample air in town and in the mountains and found the size frequency curves for the two types of aerosols had the same general shape.

The effect of humidity on the size distribution of atmospheric aerosols (404,405) has been examined. Investigations of the optical properties of atmospheric aerosols show that size information including distributions can be inferred (406-410).

Gladney, et al. (411) collected aerosols in Massachusetts with a six stage cascade impactor and analyzed the various size fractions by neutron activation. Vanadium is concentrated on the smallest particles as is Br, Zn, and Sb; Al, Fe and Sc on the larger ones; and La and Co are rather uniformly distributed, slightly favoring the small particles. Lundgren (412) found high concentrations of 0.5-2 μ NH_4NO_3 particles on days of high smog levels in Los Angeles. Lee, et al. (413) and Nifong, et al. (414,415,416) determined the size distribution of urban air metal components in the Midwest and noted that lead was mostly submicron. Nifong (415) noted that trace element aerosols fall into distinct particle size distribution groups which to some extent permitted industry source identification. Rahn, et al. (417,418) has tabulated particle size distributions of 18 elements and notes diurnal variations in concentrations. Friedlander (419) relates the size and chemical composition of aerosols. The size distribution of aerosols in automobile (420)

and jet engine (421) exhausts was investigated. Robinson and Ludwig (422) made 59 lead aerosol size determinations for localities across the U.S. and found an average mass median equivalent diameter of 0.25 μ and lower and upper quartile points of 0.16 μ and 0.43 μ, respectively. The size distributions of atmospheric sulfates (423), sulfur containing aerosols (424), nitrate and calcium particles (425), and phosphate, nitrate, chloride, and ammonium particulate (426) have been measured. Hoidale and Blanco (427) examined giant and large particles using infrared spectroscopy to identify components.

The size distributions of aerosols in Russia (428), Germany (429), Japan (430,431), Italy (432), Czeckoslovakia (433), and Hungary (434,435) are given. Aerosols distant from pollution sources have been size characterized for a desert (436), ocean air (437-439), and the polar region (440,441).

Rosen (442) notes that the relative humidity, dust concentration and size distribution appear to be correlated in the first 10,000 ft of altitude over the Twin City area. Others who have determined size distributions as a function of altitude include Carnuth (443) and Ivlev (444). Junge, et al. (445) reported on the interrelationship of aerosol size, composition, and cloud nuclei properties. A listing of the publications of various authors on the size of aerosols at various altitudes in the troposphere and the stratosphere is included (446-463).

The size spectrum of natural radioactive dust particles in Russia and elsewhere is reviewed (464). Radioactive fallout in Vienna was sampled and β-activity was found to be mainly attached to particles smaller than about 0.7 μ Stokes diameter (465). Relatively little activity was attached to particles of 0.7 to 1.0 μ. Junge (466) determined the size distribution of radioactive aerosols in the upper troposphere and noted that except after fresh injections of nuclear debris in the stratosphere, particles of global stratospheric radioactive fallout reaching the tropopause and entering the troposphere have

diameters between 0.1 and 0.6 μ. As they descend through the atmosphere they coagulate with natural aerosols and undergo considerable changes in size distribution.

Vittori (467) and Nagamoto (468) determined the size distribution of extraterrestrial magnetic spheroids in the atmosphere and observed spherules as small as 0.1 μ (smooth) and 0.5 μ (rough). It was concluded that the yearly flux of magnetic particles to the earth's surface could not be estimated from data obtained at one location over a short period of time due to concentration variations in time and place. Concentrations as high as 50,000 meter^{-3} were noted at Boulder, Colorado, on 5-23 January 1970 (468).

Corn analyzed suspended urban particulate matter for particle shape, surface area and density, and chemical composition of size segregated aggregates (469,470,471,472). The large variation in particle shape suggests that modeling of the urban aerosol by using average particle shape, as is done for certain quartz and coal dusts, is not feasible (469). Pittsburgh air particulates had surface areas of 1.9 to 3.0 meter^2 gram^{-1} and densities of 1.8 to 2.1 gram cm^{-3} (471).

2.7 Summary

From the foregoing it is apparent that aerosols found in the atmosphere are composed of a wide variety of constituents from many sources, both natural and anthropogenic. On a worldwide production basis, it has been estimated that 1.6 billion tons of particles below 5 μ in diameter are put into the atmosphere annually, one-third of which are converted sulfates, with lesser amounts of converted nitrates, hydrocarbons, and sooty combustion products, and only a small proportion is man-made. A large part comes from mineral and organic particles raised by the wind, from ocean spray and wave crests, and from photochemical and chemical reactions. Lesser amounts of natural aerosols come from forest fires, volcanic dust, and meteoritic

dust. Vegetation contributes considerable quantities of both reactive gases and cellular particulates to the atmosphere.

In the northern hemisphere, industrial sources account for about one-third of the aerosol components, and localized urban pollution by man can inundate the natural background aerosol. Despite the complex nature of atmospheric aerosols, it has been noted that the chemical profile of a region is highly individualistic, depending upon the input of all sources, and several investigators have been able to relate trace element composition to specific industries in the region, differentiating between industrial and natural aerosols by elemental ratios for different size fractions.

The modeling of atmospheric agglomerates appears to be a formidable task in view of the somewhat catholic yet individualistic nature of particulates and adsorbed gases present throughout the world. Nonetheless, the good probability of extracting useful information on trends and techniques in submicron particle separation makes modeling a challenging and potentially fruitful technique.

3. ADHESION OF ATMOSPHERIC PARTICLES

3.1 Types of Forces

There are many types of forces that act to bind solid particles together. Some of them predominate under dry conditions, some predominate under conditions of humidity, and others predominate when the particles are suspended in a liquid. The force of adhesion that either binds a particle to a surface or to another particle, depends on both the experimental conditions under which the particles and surfaces are studied, and the way in which the various forces interact. The "force of adhesion" has been defined by Krupp (472) as "that force applied perpendicular to the center of gravity of the particle necessary to remove the particle from the substrate in a fixed period of time".

Considering the case of a single particle on a flat substrate, the simplest force that can be described is the "force of mechanical adhesion". In Figure 3(a) a sphere resting on a smooth surface has negligible mechanical adhesion, while a dendritic particle on a very rough surface can have high mechanical adhesion. In Figure 3(b) the same effect can apply to particles: This force is orientation dependent, and can vary widely for the same particle. Salomon

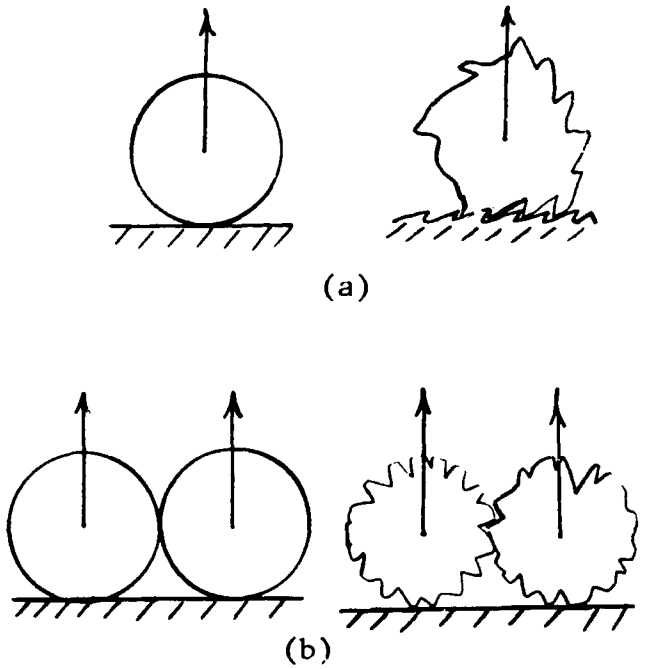

Figure 3

FORCE OF MECHANICAL ADHESION

and Houwink gave an example of rubber adhering to textile fibers by mechanical adhesion (474). The second type of force which is sometimes termed a physical force, a molecular force,or a secondary force is more commonly termed the Van der Waals force (473,747). This force comprises of three parts, each of which subscribe a donation to the total force (475). These parts are termed dispersion, induction and orientation forces respectively. The induction force arises from the interaction between a permanent dipole e.g. CH_2Cl and an induced dipole e.g. in C_6H_5-. It decreases with X^{-6} where X is the distance between the particles. Orientation forces arise from interaction between rigidly held dipoles on a surface. Here the interaction decreases more slowly i.e. according to X^{-3}. Dispersion forces are based on electric interactions: they are due to the interaction of dipoles within the particles themselves, and these may be the permanent dipoles of polar particles or the dipoles induced in the non-polar particles which are polarizable. The interaction between dipoles is electromagnetic in character and it can be readily shown that this force is attractive and additive. A molecule (a) can induce periodic dipoles in a neighboring molecule (b) and the induced dipoles are then attracted to (a). In this way the energy of attraction between the two bodies can be regarded as the sum of the energies of attraction between the corresponding pairs of molecules forming the bodies in question (475). Zimon (475) points out that the first two contributors are negligible in contrast to the dispersion forces. In consequence, this is often the only term used to describe this force and it gives rise to the common term London-Van der Waals forces of physical adhesion. These molecular forces are long range, relatively weak and are considered non-directional. However, this molecular component of adhesive force manifests itself before direct contact takes place between the particles and the surface; it is due to the specific properties of the bodies coming into contact and depends on

the particle radius r and also on the true contact area. By changing one of these factors (by modifying the surface, changing the particle size, altering the surface roughness, etc.) we may change the molecular forces and thus also the forces of adhesion. A special type of dipole interaction due to the sharing of a proton by two electronegative atoms, mostly oxygen, is termed a "hydrogen bond." The range of this force is farther than that of Van der Waals and its strength can be of the order of a weak chemical bond. When particles come into contact with the surface and there is a contact potential difference between them, "electrical forces" arise.

These forces are proportional to the area of contact, which in turn is proportional to $r^{2/3}$. The presence of moisture in the gap between the contiguous surfaces eliminates the possibility of electrical forces appearing.

"Coulomb forces" (image interaction) appear when the particles are charged in advance by a high-voltage field. Coulomb forces exceed molecular forces and the electrical forces associated with contact potential differences in value, and determine the adhesion of the particles. These forces cause interaction between charged particles and a surface when there is a definite gap between the contiguous bodies, and are inversely proportional to the square of the particle radius, i.e., $1/r^2$; they appear at the first instant of contact between the particle and the surface. The conductivity of the particle material and the contact zone, as well as moisture, cause charge leakage and lead to a reduction in the Coulomb forces, and hence the adhesion.

When two particles charge each other by electro transfer, the interaction is sometimes called an "electrostatic double layer force (473-475)".

In contrast to these long range, non-directional physical forces, there exist short range directional chemical forces that are very much stronger.

Sometimes these are termed primary or valence forces.

Examples of these are homopolar or covalent bonds in which there is an exchange of electrons between atoms. The interaction takes place between a very small number of atoms and this makes the bond highly direction. The metallic bond is partly covalent and shor range, but it differs from covalency by the great mobility of the conducting electrons. Ionic or electrostatic bonds are formed by interactions between ions in a crystal, and are short range directional bonds.

In addition to these adhesional forces, some authors reference additional categories such as deformational, diffusional and magnetic forces. When solids deform, the adhesion between their surfaces increases due to an increase in the area of contact. Usually the force of adhesion is due to Van der Waals or physical origin. Examples of deformational systems include welding, brazing, soldering and gluing. However, when electrons diffuse across this contact surface and non-physical bonds arise, the adhesion is sometimes termed diffusional. Voyutsku (476) pointed out that this is very rare and takes place only for a very narrow range of compounds. Magnetic adhesion is a special case and occurs due to the field forces of the solid and not to surface interactions.

When the particles and surface are exposed to humidity, additional forces come into play. Adsorbed layers give rise to their own forces, many of which are repulsive in nature. For low viscosity liquids, Orr stated that as the liquid phase increases around the particles, the condition shown in Figure 4(a) eventually occurs (477). Liquid bridges or pendular bonds (479) are formed between the particles and in these bridges a negative capillary pressure is created. This pulls particles together by a capillary force. As the liquid concentration rises a funicular state (b) is reached where the liquid now forms a network which contains free air plugs. When the liquid does not extend to the edges of the particles and concave surfaces of liquid persist, (c), the condition is

termed the capillary state. In cases (b) and (c), the capillary force is still exerted. When the particles are surrounded by liquid in a convex drop (d) or in a suspension, etc., interfacial tension state persists and no capillary force is exerted.

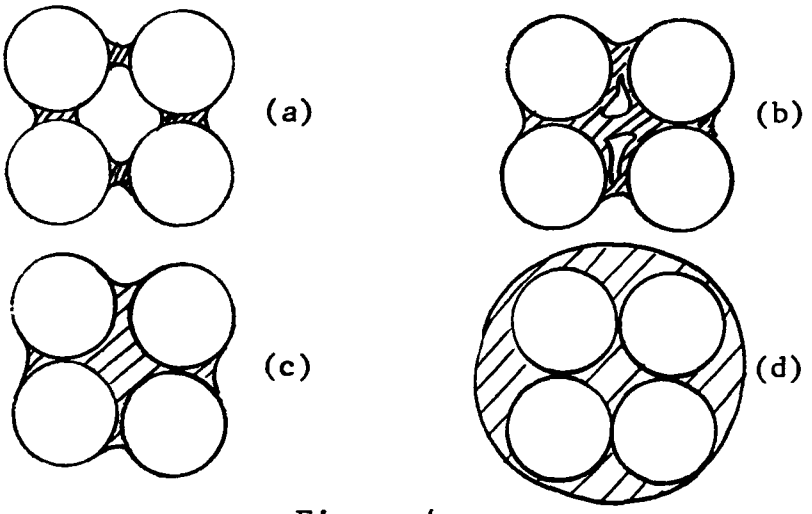

Figure 4

EFFECT OF ADSORBED LIQUID ON ADHESION

Capillary forces arise in the presence of a liquid meniscus in the space between the particle and the surface and for a relative air humidity exceeding 65%. Capillary forces (with or without making allowance for the disjoining effect of the liquid interlayer) depend on the particle dimensions.

Capillary forces may be reduced by hydrophobization of the surface, thus reducing the adhesion of the particles. This is discussed later. With high viscosity liquids, similar bridging occurs, but here the liquid is termed a binder. The properties of a good binder demand that the adhesional strength of the binder to the solid has to greater than the cohesion of the binder itself. Examples are sugars, glue, gelatin, dextrin, gum, starch, molasses, shellac, wax and lacquer. These are used in many industries particular for granulation and tabletting processes. Solid bridging also occurs as a result of

fusion at the points of contact. This occurs by the already mentioned diffusion and chemical bonding. It occurs during sintering, and when liquid bridges set or harden, e.g., silicates and cement. It also occurs when pendular bonds of water evaporate leaving crystal bridges of dissolved solids.

3.1.1 Summary

From this discussion, it is seen that many forces exist and, in fact, in any one adhesional study many of them interact so that the adhesional force is a complex resultant of them all. The conditions of the experiment determine their contributors to this resultant force, and so suitable conditions should be chosen to minimize them. In air, with varying humidity, Van der Waals, coulombic, and capillary forces can all exist, and they all are attractive. In liquid the latter two are eliminated (478), the Van der Waals forces between the adherents are partly shielded so adhesion is reduced. If the liquid contains an electrolyte, in particular a surfactant, electrolytic double layers are built up adjacent to the contact area of the adherents. These exert a repulsive force on the adherents and with detergents in particular, strong specific adsorption and entropy effects may contribute to the repulsive forces. By these means, the forces of adhesion should be reduced and separation facilitated. It now remains to investigate the magnitude of the various adhesive forces and to reveal the experimental advantages of attempting to separate collected submicron particles in air or liquid medium.

3.2 Magnitude of Surface Forces in Air

When two 50 μ solid quartz particles, a and b, are brought together under ambient conditions, by Newton's law of gravitation, the force of gravitational attraction is 2×10^{-16} dynes. If the pair are held vertically by the top particle (a) so that they lie in the gravitational field of the earth, Figure 5, the gravitational force on the lower particle (b) is 2×10^{-2} dynes. Usually, this particle would not fall from the firmly

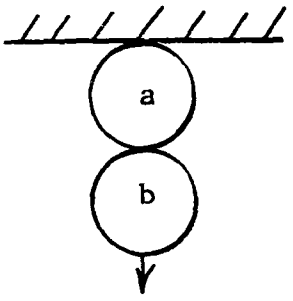

Figure 5

THE SPHERES UNDER GRAVITATIONAL FORCE

held one (a) due to force of adhesion in excess of 2×10^{-2} dynes. If the force is actually measured, it may be of the order of 0.5 dynes. If the two particles were bonded by chemical bonds through an area of 1 sq μ, the force required to overcome the molecular attraction would be 10 dynes, which corresponds to the mechanical strength of the material quartz itself (480). The forces of adhesion between (a & b) then usually would fall between these values for that contact area. If the contact area increases, the force of adhesion would increase also. The presence of an electrostatic charge or coulombic force can drastically alter the strength of a bond, as shown by Oweberg and Brunetz (481), Deryaguin and Zimon (482), Penney and Klinger (483), Donald (484), and Kunkel (485,486). Forces of adhesion can be increased by a factor of two when the net number of unit charges per 50 μ particle increases from 700 to 2500 (487). When the electrical force is due to fluctuations within the particle structure only and not due to the presence of surface electrostatic forces, Kunkel calculated that the electronic force was 1000 times less than Van der Waals. Morgan (488) reported that Van der Waals was between 10 and 10^{-3} dynes for separation distances of 0.1-1 μ between cleaved mica plates. To give some estimation of the differences between Van der Waals, electrostatic double layer, hydrogen bond, covalent bond and ionic bond energies, Krupp (493) reported that Van der Waals and electronic fluctuation forces had energies of approximately 0.1 eV, hydrogen bond and double layer forces had energies of 0.1-1 eV and covalent and ionic bond forces had energies of 1-10 eV. Similar ratios of forces of adhesion were reported by Houwink and Saloman (474) in which

values of Van der Waals having energies of 2 Kcals/mole and covalent bonds having energies of +100 Kcals/mole were reported. Priesing (489) reported ionic bonds having energies from 50-200 Kcals/mole; which was said could never be broken or made by coagulation processes. When free moisture was present, Orr, Burson and Linoya (487) reported that for a 200 μ particle, the capillary force was in the order of 20 dynes. Thus when free liquid was present, the force of adhesion was almost all controlled by the capillary forces. For a further indication of the relative differences between the forces, the Figure 6 reported by Rumpf (490) is useful. Here the relation between the tensile strengths of agglomerates is related to the particle diameter, and the magnitudes of the more important forces listed.

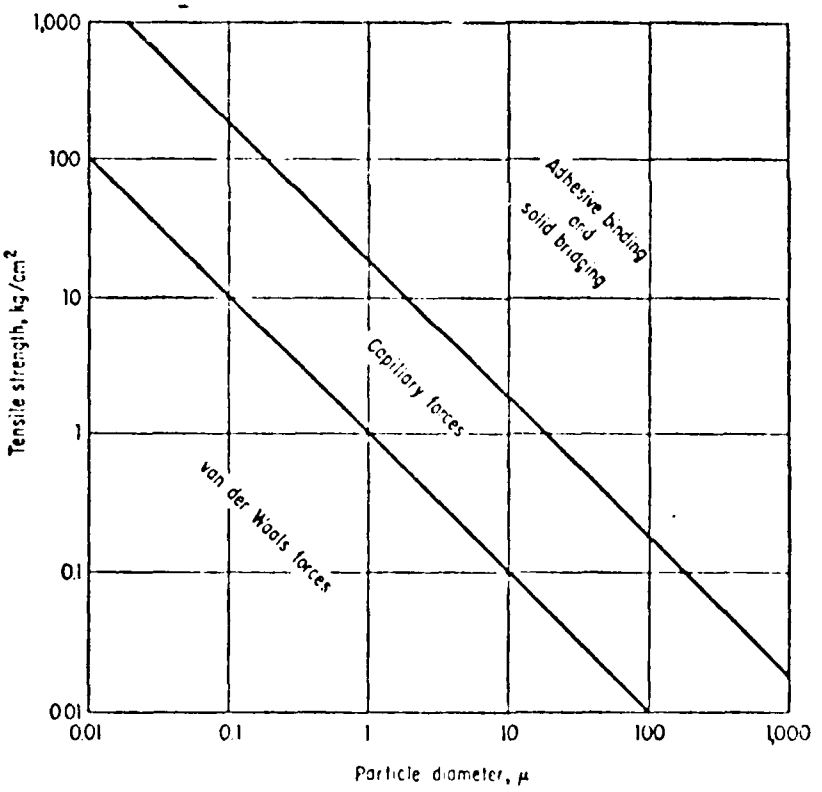

Figure 6

PARTICLE-SIZE AND AGGLOMERATE-STRENGTH REGIONS IN WHICH VARIOUS BINDING MECHANISMS PREDOMINATE

[After H. Rumpf, "The Strength of Granules and Agglomerates," in W. A. Knepper (ed.), *Agglomeration* (New York: Wiley, 1962), p. 399.]

Several studies have been undertaken to investigate the role of relative humidity in adhesion. The magnitude of some of tnese forces is shown in Figure 7 by Rumpf (490). Very low humidity air would be expected to produce relatively low adhesion. Reduced hunidity, however, removes the adsorbed vapor layer between the particle and substrate. This leads to closer approach and hence the formation of stronger bonds between the two materials. Since the electrostatic charge on the particle or substrate is less mobile or less shielded at low humidity, it may be a major reason for increased adhesion at low relative humidities.

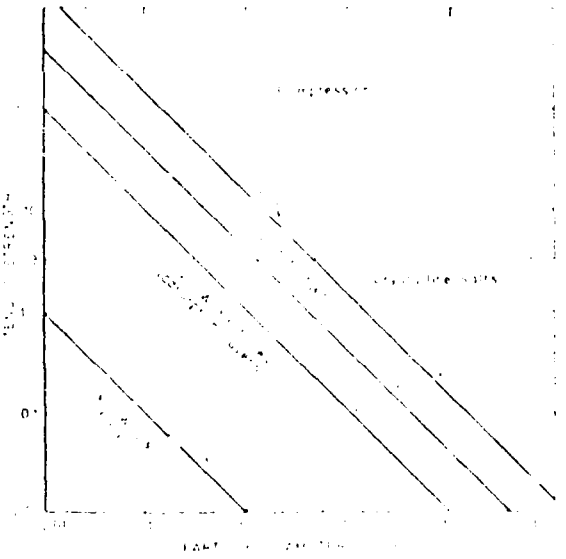

Figure 7

EFFECT OF MOISTURE ON COHESION

Effects of capillary condensation which depend upon exposure time of the interface to the vapor, require about one hour to approach the full effect. For particles 20-30 and 40-60 μ the effect of relative humidity can be considered negligible under 65% relative humidity. Capillary condensation and capillary forces act when the relative humidity > 65% (491, 492). Values for the adhesive force under different conditions of relative humidity and determined by different methods are shown in Table 5 (475), and Table 6 (492). Different values for the adhesive force will therefore be found as the humidity varies between 65 and 100% R.H. Similar results were reported by Corn (493). In addition to this parameter, several others influence the force of adhesion. Zimon (475) reports that the elasticity of the particle and surface change the force of adhesion, and gives values for adhesion to different surfaces. Particle shape also affects the force of adhesion, the minimum force occurring for particles of isometric shape, i.e., a sphere or regular polygon.

Spherical particles have lower forces of adhesion than plane particles, i.e., particles with their lengths and widths much greater than their thickness, e.g., Kaolin bentonite mica graphite gypsum (494).

Fibrous or accular particles, e.g., prisms needles which have one dimension greatly exceeding all others have even higher forces of adhesion. The effects of particle roughness were studied by Reumuth (495), Meldau (494), and Nishivaki (496), and surface roughness by Zimon and Volkova (497), Böhme, et al. (498) and Corn (499,500).

When ideally smooth surfaces are encountered, adhesion is a maximum (Figure 8a). When the heights of the projections or asperities are an order of magnitude smaller than the particle diameter, the force of the adhesion falls (Figure 8b). However, when the height of the asperities is greater or equal

Table 5
(Ref. 475)

ADHESIVE FORCE OF PARTICLES DETERMINED BY VARIOUS METHODS FOR VARIOUS AIR HUMIDITIES*

Substrate material	Particle Material	D_p, μm	Fa, dynes for air humidity 50-60%	90%
Pyrex	Detachment of individual particles			
	Quartz (fused ends of filaments)	25	0.28	0.37
		36	0.3	0.55
		63	0.6	0.76
		88	0.88	1.38
Glass	Glass	400	22	-
		800	30	-
	Centrifuging for γ_F= 2%			
Glass	Glass	50	0.37	1 83
	Sand	50	0.76	0.06
	Coal	50	0.55	0.94
Plexiglas	Glass	50	1.44	1.97
Teflon	Sand	50	0.65	1.28
Brass	Coal	50	0.90	2.85
	Centrifuging for γ_F= 50%			
Starch	Starch	7-9	0.2	-
		13-15	0.2	-
		18-21	0.2	-
Gold	Gold	4	0.07	-
		5-6	0.09	-
		7	0.1	-
		8	0.16	-
	Vibration method for γ_F= 2%			
Steel	Glass	40-60	1.64	-
	Vibration method for γ_F= 50%			
Steel	Glass	5-10	$1.33 \cdot 10^{-2}$	-
		10-20	$6.12 \cdot 10^{-3}$	-
		20-30	$2.15 \cdot 10^{-3}$	-
		40-60	$2.13 \cdot 10^{-4}$	-

Table 6
(Ref. 492)

FORCES TO REMOVE 98% of 50 μ DIAMETER PARTICLES

Identification of materials		Force required to remove 98% of particles at		
Particle	Solid surface	90% Relative humidity (dynes)	50% Relative humidity (dynes)	10% Relative humidity (dynes)
Glass*	Aluminium	0·50	1·35	1·06
Glass*	Brass	2·85	0·90	—
Glass*	Brick	1·59	—	—
Glass*	Copper	—	4·18	—
Glass*	Enamel (paint brushed)	3·63	6·26	—
Glass*	Enamel (paint sprayed)	—	2·23	2·80
Glass*	Glass	1·83	0·37	0·15
Glass*	Micarta	—	0·65	0·96
Glass*	Plexiglass	1·97	1·44	—
Glass*	Teflon	—	—	0·62†
Glass*	Teflon	1·28	0·65	4·15
Sand‡	Aluminium	6·60	—	1·37
Sand‡	Brass	0·45	—	—
Sand‡	Enamel (paint brushed)	6·34	—	—
Sand‡	Glass	0·06	0·76	1·21
Sand‡	Holly leaf	5·67	—	—
Sand‡	Micarta	7·77	—	3·29
Sand‡	Plexiglass	2·78	—	—
Sand‡	Wood	12·56	—	—
Charcoals	Aluminium	0·97	—	—
Charcoals	Brass	0·32	—	—
Charcoals	Enamel (paint brushed)	2·30	—	—
Charcoals	Glass	0·94	0·55	1·19
Charcoals	Plexiglass	0·70	—	—
Charcoals	Teflon	0·34	—	—
Rubber*	Glass	0·81	—	—
Rubber*	Plexiglass	1·93	—	—

to the particle diameter, the adhesion rises again (Figure 8c). This is always the case for submicron particles. Zimon had grave doubts about the validity of the previously published studies on the effect of surface roughness, because in most cases the surfaces were not characterized well enough.

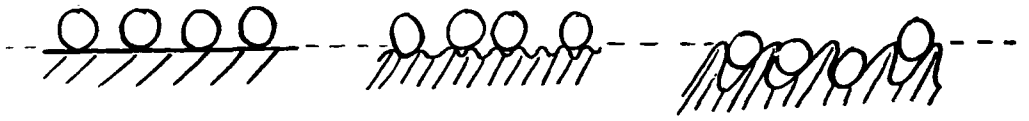

(a) (b) (c)

Figure 8

EFFECT OF SURFACE ROUGHNESS ON ADHESION

The cleanliness of the surface was also shown to be important by Akhnatov (501,502), Fuks (503), Deryagin (504), Stone (505), McFarland and Tabor (506), Bradley (507,508), and Howe, et al. (509). The method of cleaning the surface affected the adhesion, and the way the particles were deposited did likewise. The effect of particle size was studied by Malkina (510), Bradley (507,508), Corn (499-500), Deryagin and Zimon (504), Kordecki and Orr (492), Morgan (488) and Böhme (498). Generally, for macroscopic bodies, size has little effect. In some cases for smaller particles the forces of adhesion were found to be inversely proportional to the size of the particle but in some cases size again had no effect at all. No work was reported on submicron particles. To summarize the effect of size, Zimon (475) reported that, quote: "Each of the components of the adhesive forces depends on the particle size in the following way:

Component of adhesive force...

	Coulomb	Electric	Molecular	Capillary
Dependence on dust-particle radius.....	$1/r^2$	$r^{2/3}$	r	$r(1-1^{x-1})$

The adhesion is only proportional to the particle dimensions when the molecular forces prevail. If electrical, capillary, and Coulomb forces have to be overcome in addition to these in order to effect detachment, the total adhesive force may then not be proportional to particle size.

The thermodynamic Deryagin theory of adhesion considers adhesion as an equilibrium and reversible process and the adhesive force as a function of the gap separating the contiguous surfaces. When this gap equals zero, the adhesive force is proportional to the dimensions of the bodies in contact.

However, the adhesion process is not in fact reversible, since before the particle comes into contact with the surface some forces (Coulomb and partly molecular) are acting, while after contact others (molecular, electric, capillary, and Coulomb) have to be overcome in order to achieve detachment. The interaction of the particles with the surface resulting from forces other than molecular means that the process disobeys the conditions for which the Deryagin theory is valid. The adhesive force -- particle size relationship may thus well differ from direct proportionality.

We see from the results presented that adhesion varies with particle size in different ways. It may be directly proportional, or even inversely proportional, to the particle diameter, or alternatively, it may be independent of particle size.

The particle material also has an effect on the adhesive force. Thus, for particles 50 μ in diameter made of different materials (glass, sand, coal) the adhesive force relative to a glass surface fluctuates from 0.06 to 1.83 dyn.

Results obtained by different methods of adhesion measurement (with the same materials and under the same conditions) are similar. Thus, the adhesive forces for glass particles sticking to a metal surface (brass and steel) are approximately

the same, despite differences in the method of detachment (vibration and centrifuging); the adhesive forces measured with a relative air humidity of 50-60%, using the centrifuge method to remove the glass particles, are the same as those obtained by the method of detaching individual particles." (Zimon, 475)

3.3 Magnitude of Forces in Liquid

When the particles on surfaces are immersed in liquid, Zimon (475) reported that the force of adhesion is at least one-half that in air, and the energy expended to detach particles from surfaces in water is 1/10th of that in air. Zimon and Petunin (511) and Zimon and Deryagin (512) reported that for 5-10 μ particles, the forces required to separate glass from steel was 10^{-2} dynes in air and 10^{-6} dynes in water. However, Fuks, et al. (513) and Fuks (514) pointed out that this was dependent on the wettability of the surface. When the wettability of one component, e.g., the surface, was different to that of the other, e.g., particles, adhesion between them was usually at a minimum. When the liquid around the particle was an electrolyte, different results were obtained. Buzagh (515-526), Fuks (513,514,527) and Zimon (512-528) showed that the adhesion was related to the elecrolyte concentration and to the valency of the cation. For the same values of zeta potential, univalent cations created higher values of adhesion than divalent cations which in turn gave higher values than tertiary or quadrivalent cations. Generally, at the maximum zeta potential the adhesion force was a minimum. The pH was also found to be effective. In alkaline media the particles had still lower adhesive forces than in neutral or acid solutions. With surfactants, Buzagh (515), Fuks (529), and Zimon (528) reported that there was an optimum concentration of surface active substance for which there was a maximum reduction on the adhesive force. Taylor and Wood (530) showed that polyphosphates collected at a surface and reduced adhesion. This was, however, time dependent, as time had to be allowed for the buildup of

the double layer. Smith (621) reported theoretical and experimental work which investigated the spontaneous removal of carbon black particles from glass surfaces by varying the concentration of two surfactants sodium dodecyl sulphate and undecane 3-sulphate. He found that optimum conditions of both surfactant and electrolytic concentration existed at which the removal efficiencies were very high and at this point no mechanical action was required in the dispersion. His results are shown in Figure 9 for carbon black adhering to glass particles in a packed bed. It is seen that the removal efficiency was dependent on the surfactant, and he suggested the reason for this was differences in molecular concentration of the adsorbed surfactant on the surface. In contrast to the adhesion in air,

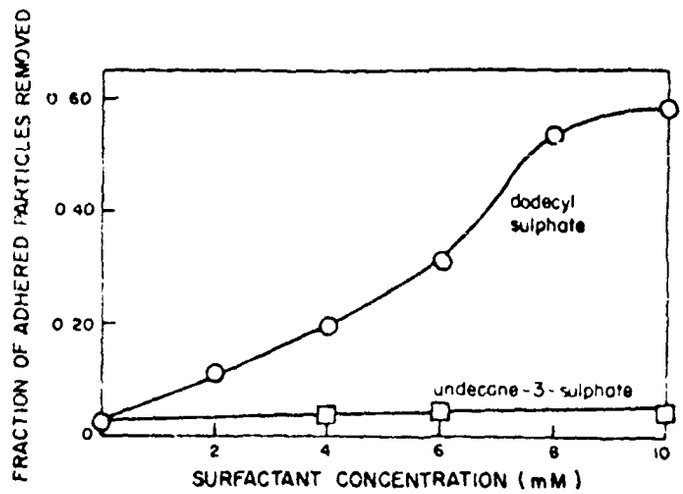

Figure 9

REMOVAL RESULTS, GLASS POWDER BED EXPERIMENTS

particle roughness and surface roughness were found to be less important in liquid media than in air (497). With increase in temperature, adhesion in liquids and electrolytes increased (510, 530). This was also true in air (510,530). The reason for this was that temperature increased the molecular activity of a solid increasing the Van der Waals forces. Therefore, in air, liquid and electrolyte separation was facilitated at 0-20°C. The converse was true for surfactant solutions where adhesion was at a minimum at 60°C. A most useful example of these effects was given by Krupp (478) who measured the forces of adhesion of gold spheres, 3 μ diameter on cellulose and polyester. Krupp stated that quote:

"The experimental results are summarized in Figures 10 and 11. The percentage of adhering particles is plotted against the force (centrifugal acceleration times particle mass) applied. For comparison, data obtained in earlier experiments on the adhesion in the dry state have been entered into Figures 10 and 11.

A significant width of distribution of the adhesion forces is observed in the ensemble of particles used. A measure of this distribution is the deviation of the curves of Figures 10 and 11 from a step function.

Immersion in water and in the above solutions significantly reduced adhesion compared with that in the dry state. In the immersed state the adhesion to the polyester substrate is larger by a factor of about 2 than to the cellulose.

With the dodecyl sulfate solution the adhesive force is reduced by about 7 millidynes to about half that when immersed in water. The alkaline salts cause an analogous shift of the adhesion curves to the left. As the adhesive forces on polyester are higher, the relative decrease in adhesive force is less in the system polyester-gold than in the system cellulose-gold.

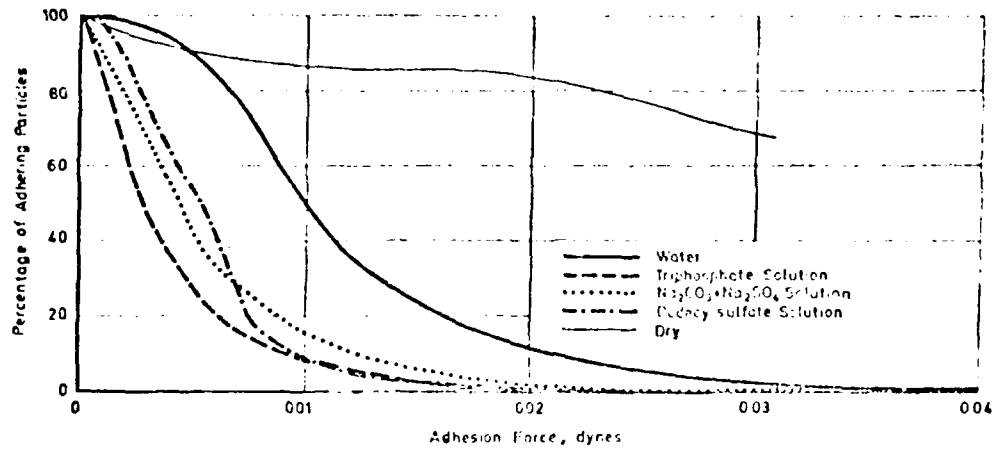

Figure 10

ADHESION OF GOLD SPHERES, 3 μm DIAMETER, TO CELLULOSE

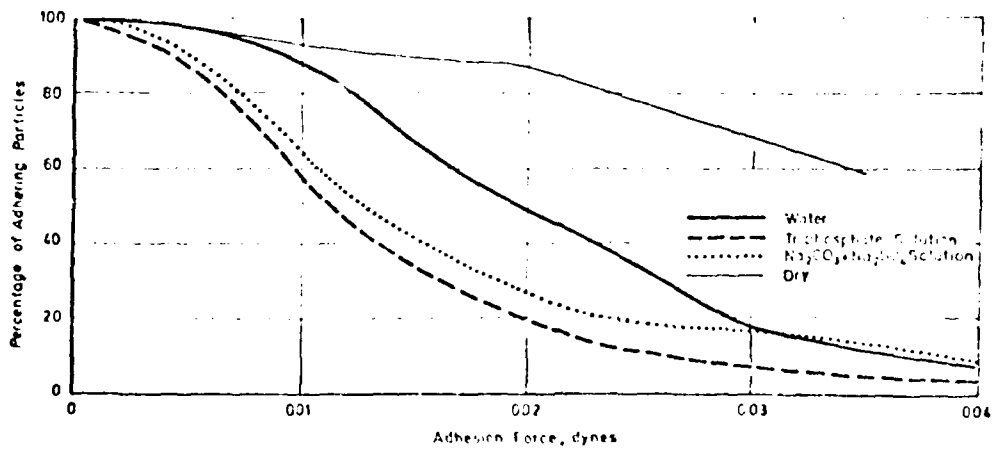

Figure 11

ADHESION OF GOLD SPHERES, 3 μm DIAMETER, TO POLYESTER

(Reference 478)

The action of the surfactant may be explained on the basis of formation of electrolytic double layer and in terms of entropy effects.

Double-layer repulsion will be the only active mechanism in the case of the alkaline salts. Adsorption of the polyvalent anions in addition to the OH^--ions from the triphosphate solution seems to be the reason for the slightly stronger repulsive action of the triphosphate solution.

The difference between the strength of adhesion of gold to cellulose on the one hand and to polyester on the other cannot yet be explained on the grounds of the present adhesion theory."

3.4 Mechanisms and Methods of Measuring Adhesion and Separation Forces

Krupp (473) suggested that the mechanism of particle adhesion proceeded as follows:

1. At first, particle and substrate come into contact at one point by a contact area of atomic dimensions.
2. By long range attractive forces between the two, the particle is subject to a moment of force so that several contacts are made between non-perfectly smooth adherents.
3. By interaction forces the area at these contacts increases until the attractive forces and the forces resisting further deformation at the interface are in equilibrium. An adhesive area of finite size is formed between the adherents.
4. The effectiveness of contact depends on the magnitude of force acting on the particle at the instant of contact, i.e., kinetic energy given up by the particle through its stopping distance or by pressure on given force applied by particle to the substrate.

From this, substrate separation then takes place as follows:

1. The external forces of separation excited on the particle cause a partial and complete recovery of the deformation at the interface.
2. Generally, the center of attack of the separating force will not be symmetrical to the location and strength of the individual contact sites so that a particle is subject to a moment of force, and individual contacts may become broken separately. Finally, the last contacts are separated, the particle is set free.
   The adhesive area is the area of one common interface between the adherent collection during the last step.

Several methods have been employed to separate particles from substrates, some of which have been applied to measure the force of adhesion.

In air the following experimental methods have been used to measure the adhesion force of single particles on surfaces.

a) Varying the slope of a surface
b) Microbalance technique
c) Pendulum method
d) Centrifuge method
e) Aerodynamic method
f) Vibration method

The following discussions relate the adhesive forces determined by each of the several methods. A modification of the microbalance technique was used by Beischer (545) who allowed coagulating threads of individual Fe_2O_3 particles of 0.5 μm diameter to break under their own weight. The force required was estimated from the size of the separated fragment. His work indicated that for submicron particles the adhesive force was of the order of 0.5×10^{-4} dynes. Before each method is discussed, of particular importance in this section, is the

realization that the removal of identical particles from a surface is based on probability.

If several identical particles are dispersed separately upon a substrate, the force required to remove each one will not be the same. Application of a fixed force will remove but a fraction of the particles. Complete separation of all particles may require a significant increase in the force field. The probabilistic nature of this phenomenon is presented in Figure 12 in which the relative number of particles adhering is plotted against the adherence force. It is very common, then, to relate adhesion to the rates of the number of particles detached under the influence of a specific force to the initial number on a substrate. A value termed the adhesion number is expressed as the ratio of the number of particles remaining on a surface to number initially here after the application of force. The adhesion number is usually related to the forces holding particles to the dust surface by integral curves as shown in Figure 12. In some cases, however, detachment occurs in layers of particles and this is discussed in detail by Zimon (475). Sometimes adhesion is expressed in the form of the number of rotations of a centrifuge, the frequency of oscillation of a vibrating plate or the angle of rotation of a dusty plate. In estimating the force, we realize the existence of a minimum force under which the first few particles are removed and a maximum force under which the majority are removed. Orr and Kordecki (492) and Zimon (475) show that it is better to estimate the force as being that value at which 50% by number are removed under the specific conditions and measuring method used in the experiment. This is now accepted as being the better method of relating adhesion measurements but it is not without error (475).

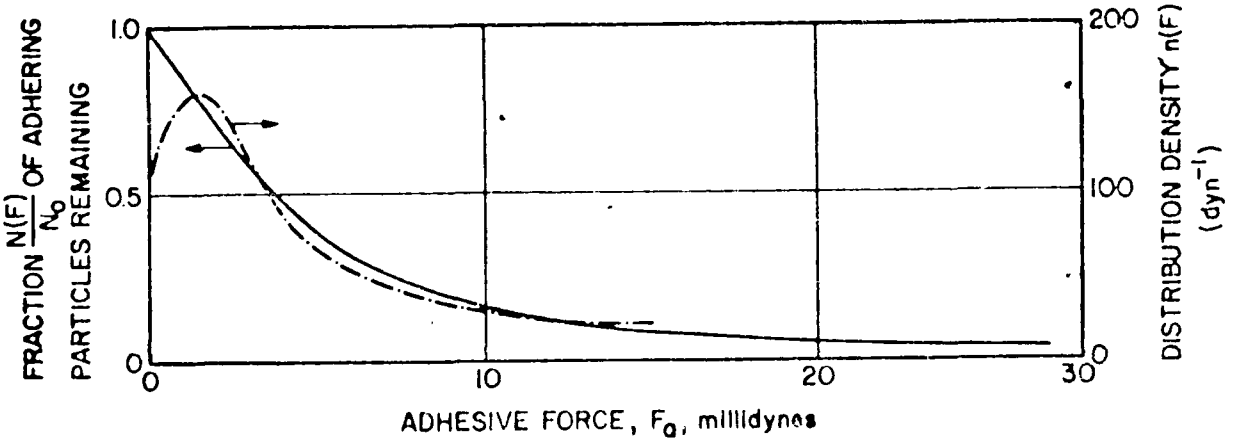

Figure 12

ADHESION OF SPHERICAL FE PARTICLES OF 4 .m DIAMETER
TO FE SUBSTRATE AT ROOM TEMPERATURE IN AIR
AS A FUNCTION OF APPLIED FORCE
(from Böhme, et al., Ref. 498)

Several methods that have been used to measure particles were devised purely for macroscopic particles. Zimon (475) and Corn (493) reviewed these very well. The first methods given are those used mainly in air.

3.4.1 Microbalance Methods

Separation in Air

Corn reported that, quote: "Microbalances are usually based on the use of quartz fibres which can take the form of a cantilever, helical spring, or torsion balance, depending on the manner in which the applied force acts on the quartz fibre, spring, or beam (532). Electromicrobalances sensitive to 0.1 μg are commercially available (533). Microbalance techniques were used by Hamaker (534), Stone (536), Tomlinson (537, 538), Howe, et al. (509), Bradley (535), and Overbeek and Sparnaay (539) to study the force of adhesion in air or vacuum between quartz fibres or spheres, and to relate these measurements to the Van der Waals force. More recently, electronic microbalances with precise feedback control have been used to determine the Van der Waals force (540,541,542). The adhesion between 5-90 μ glass particles and solid surfaces was measured by Corn (543) using a microbalance of the cantilever type. Further work was reported by McFarlane and Tabor (544) and Beischer (545).

Microbalance techniques require that a single particle, preferably less than 50 μ in size, be attached to the balance spring or beam. This is a very difficult operation. Because the adhesion of particles is dependent on the microscopic particle and substrate contacts, a range of forces can be measured for repeated contacts of the same particle and substrate. The determination of the range of adhesive forces possible with particles of different sizes becomes a very time-consuming and tedious task.

An interesting variation of these techniques is that reported by Beischer (545). The weight of a chain of charged or magnetized particles attracted to a charged or polarized microbalance caused rupture of the chain after the field was turned off. The adhesive force could be estimated from the diameter and length of the chain at breakage.

3.4.2 Pendulum Method

In this method, the gravitational force acting on the particle causes disruption of the adhesive bond between particle and substrate. Initially, the particle is suspended on a vertical fibre in contact with the substrate. The substrate is then raised and the angle between fibre and the vertical plane is recorded at the moment of breakage of the particle-surface bond. The method was used by McFarlane and Tabor (544) and Howe, et al. (509), and is applicable to relatively large particles having sufficient weight to overcome the force of adhesion."

For smaller particles, other types of approaches have been made.

3.4.3 Varying the Slope of Surfaces

Zimon (475) reviewed this method and pointed out that it was first used by Buzagh (515) who dusted particles on a surface at the bottom of a vessel and rotated the surface through a specific angle. Fuks (513,529) modified this technique by constructing a special cuvette mounted on a microscope. This was used extensively to measure the adhesion of particle layers by Cremer (547), Bakel (548), Patat and Schmid (549) Pecht (551), and Zimon (550). For particles less than 20 μ this was of no value. The method can be used to measure the force between particles - the tensile strength by mounting the powder in a vessel as shown in Figure 13. The vessel is tilted in the horizontal position with powder under known compression and

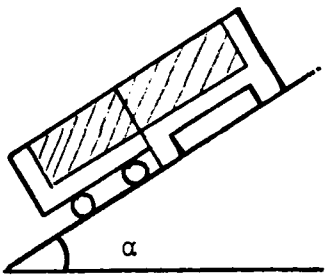

atmospheric conditions. The table is then tilted and the angle at which the bed separates is measured. The effect of adsorbed layers and capillary forces were measured on a similar device by Schubert and Wibowo (546).

Figure 13

SLOPING TABLE MEASURE OF ADHESION

3.4.4 Vibration Methods

Zimon (475) stated that, quote: "The vibration method was first used for determining the adhesion of films (552). Later, Larsen (553) determined the adhesive forces of spherical particles to fibers vibrating at a frequency of the order of tens of cycles. This method was improved and extended (482) by using sonic and ultrasonic vibrations.

The vibration method is only used for determining the adhesive force of dust in air. For this purpose either low-frequency (20-30 cps) or high-frequency (hundreds or thousands of cps) vibrations are used.

With the high-frequency system, the sound vibrations, previously amplified, set in motion a dynamic diffuser to which the dust-laden plate is attached. The frequency of the oscillations is usually no greater than 2 kcs and the value of the detaching force reaches 2500 g.

By varying the frequency of the vibrations, one may vary the detaching force over a wide range. In order to increase the range of detaching forces, one may use an ultrasonic system generating oscillations at a frequency of 10-20 kcs (482). Here the value of the detaching force will be $(10\text{-}24)\cdot 10^4$ g.

For relatively small forces of detachment, a greater number of particles are detached in the vibrational than in the centrifugal method. The difference becomes less marked as the applied detaching force becomes greater. The detachment of firmly held particles takes place more intensively in the centrifugal than in the vibration method.

The vibration method may be accomplished by simultaneous measurement of the electric charges arising from the detachment of the particles, these being required in order to calculate the electric component of the adhesive forces. For this purpose one may use an apparatus (553) differing from those employed earlier (of the electrometer type (482,554)), using electronic and loop oscillographs. This obviates the dependence on visual measurements and photographically records the electrical processes taking place.

A variation on the vibration method is the pulse method, which is used to determine adhesion in vacuum and in the vapor of various liquids.

The dust-laden test surface was placed under a vacuum bell-jar and the required vapor concentration was created by evaporating the liquid released by a dropping funnel in the jar. The space under the jar could be filled with any gas. Detachment of the particles was effected by means of a blow from an arm on the dust-laden surface. The elasticity of the substrate and the force of the blow from the impinging arm were the same in all the experiments; this ensured a constant value of the detaching force and made it possible to compare experimental results.

One variant of the impulse method was proposed by Deryagin and co-workers (555). The detachment of the dust particles was effected by shooting pellets at the dust-laden surface from an air gun.

In order to detach dust particles in liquid media, the loading method may be employed (528). The dust-laden surface is immersed in the test solution for a specified time interval. The conditions of immersion and extraction of the samples from the solutions should be exactly the same.

For removing particles from a dust-laden surface, the latter may be subjected to an air blast (487). Here, even for particles of a single size, the value of the detaching force is not susceptible to exact calculation, while for powder of many particle sizes the calculation is still more difficult. In order to create identical conditions for detaching the particles, the rate of air flow and the direction of the flow relative to the dust-laden surface must be exactly the same."

The discussion of the use of ultrasonics is given in the section dealing with liquids.

3.4.5 The Centrifugal Method

Kordecki, et al. (556,492) used a centrifuge in studies of the adhesion of particles to a flat surface. Determinations were made of the size distribution of the particles initially sprinkled on a slide and of the size distributions of those remaining after subjection in discrete steps to successively higher fields of force. The maximum acceleration applied was in excess of 8 g. At maximum acceleration, nearly all of the largest particles and a significant fraction of the smallest particles were removed.

Böhme, Krupp, et al. (478,557-563) also have used the ultracentrifuge, one of them capable of producing forces in excess of 10^6 g. Because they used a very narrow size range of particles, they plotted their results differently. They compared the per cent of particles adhering versus the applied force (dynes) and found that the variation of force with particle size was small. Apparently the larger acceleration required for small particles is a consequence of their small

mass. Also, these authors have gathered some data on the influence of surface composition and texture on the adhesion of particles to the surface.

Deryagin, et al. (564) have used centrifugal fields providing up to 300,000 g. They did not succeed in removing all 5 μ diameter glass particles from a polished steel rotor.

On comparing the various possible errors, Zimon (475) concluded that, quote: "the main error in the centrifugal method is due to the different sizes of the particles in a specified fraction.

In order to avoid errors associated with the rate of rotation, one must increase (or reduce) the revolutions of the centrifuge smoothly in order to eliminate the effects of inertial forces, holding the specified number of revolutions for several seconds. Further increasing the time of centrifuging has no effect on the detachment of dust particles in air. In centrifuging it is important to take proper precautions against vibrations of the body and heating of the centrifuge axis, since these effects may distort the results of measurements made on the force of detachment.

In the practical use of this method for liquid media a number of special features have to be taken into consideration. The whole space in the cylinder (or cuvette) must be filled with liquid in order to prevent the latter from moving in the course of centrifuging and thus eliminate the influence of side effects. Owing to the difficulty of hermetizing the cylinder (or cuvette) the number of revolutions of the centrifuge in the methods employed is no greater than 3000 and the detaching force no greater than 10^2-10^3 g. The time of centrifuging should be about 1 min, so that hydrodynamic factors associated with the way in which the dust-laden surface is situated in the liquid medium may be fully taken into account.

The centrifugal method of measuring the value of the detaching force is the principal method used in determining forces of adhesion. The advantages of this method lie in its simplicity and accessibility, and also in the reliability of the results and the rapidity of the measurements. In addition to this, a variety of conditions may be created in the centrifuge test tubes (humidity, temperature, pressure, etc.), which widens the experimental potentialities of the method. However, in order to obtain the integral adhesion curve several measurements must be made with different numbers of revolutions.

It is possible to use the centrifugal method for determining the adhesion of a layer of particles. In this case, when calculating the detaching force, the quantity $m = V_{\rho 1}$ must be understood to mean the mass of the particles adhering to unit area of the substrate. Small particles (of under 10 μ diameter) stick so firmly to surfaces that forces corresponding to accelerations of the order of $(10^3\text{-}10^4)$ g are incapable of overcoming the adhesive forces (482). This explained the tendency to use ultracentrifuges for detaching small particles. However, an attempt at using an ultracentrifuge of the UTs-2-A type (produced by Mikrotechna of Prague) was unsuccessful. On rotating a sphere in the magnetic field of this centrifuge in vacuum, the sphere with the particles attached to it became heated. The heat melted particles consisting of fusible materials (for example, polymers) (564), and this distorted the results of the measurement."

3.4.6 Aerodynamic Method

The limitation of this method resides in the difficulty of defining aerodynamic conditions in the vicinity of adhering particles. In the absence of a well-defined velocity field results must be expressed as efficiency of particle removal versus an air velocity characteristic of the particular system used. With a well-defined velocity field it is possible to calculate, approximately, the air drag on particles at the time

of their dislodgment. The separation of particles from walls, conduits and plane surfaces has been studied by Syrkin, Rumpf, Averbukh and Shabelin, Sokolov, Bagnold, Chepi, and a good review of their work is given by Fuks (565). Bagnold (566-568) studied the separation of large sand particles lying on a sand bed, Chepie studied the erosion of soils of particle size less than 25 μ and found them uninfluenced by air streams due to their small size. Jordon (570) deposited quartz and glass dust of size 0.1-12 μ on glass slides and measured the efficiencies of removal by high velocity air jets as did Davis (569). Larson (573) studied a similar problem that of removing spheres from fibres, and recent work along these lines has been done by Löeffler (742,743,744). Orr and Dallavalle (574) studied the removal of particles from a needle tip. Gutterman and Ranz (576), and Zenz (577) studied removal from a bed and Corn, Silverman and Becker (575) studied blow-off from filter surfaces. Corn (571) and Corn and Stein (572) studied reentrainment from plane surfaces. Similar work was reported by Walker and Fish (578) who studied the adhesion of radioactive particles to glass slides. Masironi and Fish (570) and Fish (580) conducted observations on reentrainment of dust particles in a room. A field study of redispersion of dust in the submicron range was conducted by Stewart (581). His conclusions were the mechanisms by which dust is made airborne are impact processes extending from vehicle and pedestrian movement to the creep and saltation of the coarser soil particles and by the action of eddies on surfaces which protrude through the turbulent boundary layer.

From the experimental results obtained in the field it appeared that weathering processes continuously introduced changes in the surface layer so that a simple relationship between the amount of contaminant resuspended and the wind speed only applied in some situations. It was suggested that the contaminant needed to be very finely divided, micron order or less, insoluble in water and the surface to be in

equilibrium with only a minor degree of soil movement occurring for the degree of resuspension to vary with the wind speed as u^2 or u^3.

As a result of weathering processes a contaminant tends to become fixed at the site of deposition and to be dispersed in a surface layer of the order of a centimeter deep. It may be shown by simple eddy diffusion theory that only the very fine particles would be readily removed by the wind after resuspension. Some of the most pertinent work to micronized particles was reported by Corn and Stein (582) who compared air stream dispersers with centrifugal systems. The results given in Tables 7 and 8 show that 1 μ particles of atmospheric dust could be only 20% removed. As a conclusion to this method, Fuks (583) considered that for particles below 0.5 μ complete dispersion has never been achieved by air jet methods, and could not see that they would ever be of real value for this size range. Air blast studies were performed by Billings (584), and Livenbaum (585), and shock wave studies by Gerrard (586), but these had limited application.

Table 7

ACCELERATIONS REQUIRED TO DISLODGE ADHERING PARTICLES OF ATMOSPHERIC DUST, FLY ASH AND GLASS BEADS (RELATIVE HUMIDTY, 35 PER CENT, AND 20°C)

Acceleration, (g)	Size* (μ)	Efficiency of removal (per cent)			Centrifugal force (dynes)	
		Glass beads	Fly ash	Atmospheric dust	Glass beads	Fly ash
6,000	1.3	-	0.0	8.1	-	1.25×10^{-8}
24,100	1.3	-	0.0	19.1	-	5.01×10^{-8}
97,000	1.3	-	0.0	-	-	2.00×10^{-7}
6,000	3.8	-	0.0	2.8	-	3.10×10^{-7}
24,100	3.8	-	1.8	2.8	-	1.20×10^{-6}
97,000	3.8	-	2.8	-	-	5.44×10^{-6}
6,000	6.4	-	12.1	0.0	-	1.57×10^{-6}
24,100	6.4	-	9.1	3.2	-	6.31×10^{-6}
97,000	6.4	-	4.4	-	-	2.51×10^{-5}
6,000	8.9	-	13.2	16.7	-	4.33×10^{-6}
24,100	8.9	-	9.3	16.7	-	1.74×10^{-5}
97,000	8.9	-	7.9	-	-	6.93×10^{-5}
6,000	11.5	-	12.5	0.0	-	9.24×10^{-6}
24,100	11.5	-	50.0	0.0	-	3.64×10^{-5}
97,000	11.5	-	100.0	-	-	1.47×10^{-4}
1,500	5.3	50.0	-	-	3.63×10^{-6}	-
12,500	5.3	52.2	-	-	2.39×10^{-5}	-
19,500	5.3	73.4	-	-	3.67×10^{-5}	-
1,500	15.9	27.8	-	-	9.80×10^{-6}	-
12,500	15.9	85.2	-	-	6.15×10^{-5}	-
19,500	15.9	89.5	-	-	9.90×10^{-5}	-

* Projected area diameter.

Table 8

BULK AIR VELOCITY REQUIRED
TO DISLODGE ADHERING PARTICLES
OF ATMOSPHERIC DUST, FLY ASH, AND GLASS BEADS
(RELATIVE HUMIDITY, 35 PER CENT, AND 30°C)

Bulk air velocity (in/sec)	Size* (μ)	Efficiency of removal (per cent)		
		Glass beads	Fly ash	Atmospheric dust
30	1·3		0·0	0·4
90	1·3		6·0	2·5
150	1·3		21·3	4·9
30	3·8		0·0	0·0
90	3·8		20·1	4·6
150	3·8		57·4	7·9
30	6·4		4·0	5·9
90	6·4		68·0	15·7
150	6·4		100·0	31·4
30	8·9		30·8	6·7
90	8·9		76·9	20·0
150	8·9		100·0	40·0
30	11·5		0·0	0·0
90	11·5		83·3	25·0
150	11·5		100·0	50·0
30	5·3	0		
90	5·3	0		
30	15·9	0		
90	15·9	0		
117	15·9	32		

* Projected area diameter.

Separation in Liquids

There have been very few publications on the measurement of adhesion in liquids. Some already mentioned were the sloping surface method used by Buzagh (515) and the centrifugal methods reported by Krupp (478). In spite of this, many methods have been used to separate particles in liquids, particularly in industrial processes, and these are now reviewed.

3.4.7 Vibration Methods

The most common vibration methods for separating particles in liquids have involved ultrasonics. Egorov (587) pointed out that ultrasonic waves have both dispersing and coagulating effects upon suspensions. Cavitation is usually held to be the cause of the dispersing action. Several hypotheses were put forward to explain coagulation. Recent work on this subject was by Bergmann (588), Sollner (589), Kruyt (590), Tojoshina (591), Sasaki (592,593), Soboleva (594), and Deryagin (595,596, 597). The effect of ultrasonics was found to cause variations in the electrokinetic and total potential at the interface,

and thus affected the electrical double layer. The ultrasound caused a desorption of potential determining ions, and coagulation occurred. Reports on its use for dispersion were given by Agabalyants, et al. (598) who studied the dispersion of clay. It was found that the ultrasound again changed the structure of the suspension during the dispersion. The release of ion complexes from surfaces by ultrasound was reported by Lowe and Parasher (599) who studied the dispersion of soils. In contrast, Pupynin, et al. (600) coated particles with nickel during ultrasonic dispersion to produce low dispersed aluminum and cerium powders. Other pertinent studies were by Piotrowski A (601), Allegra (602,603), Rozanski (604) and Kruglitskii (605). Other studies on coagulation were by Kul'skii, et al. (606), who was concerned with the clarification of kaolin suspensions and Joung (607) who studied the clarification of mineral suspensions.

From these comments, it is clear that ultrasound has to be used with caution in dispersion studies due to the possibility of it causing coagulation. Surface modification of particles has also been shown to be possible, which makes subsequent electrokinetic studies somewhat difficult.

3.4.8 Turbulence and Shear

In industrial practice dispersion is achieved by mixing and blending powders in vehicles using various types of mixing machinery. These w ere classified by Sheppard in Parfitt's book (608) as follows:

1. Low Shear Rate Equipment - These operate at slow mixing speeds at high viscosity or high particle concentration using impellers which pass near to the walls of the mixing container to impart high shear at this point.

2. High Shear Rate Equipment - These operate by impellers which move at high peripheral speeds. The impellers generate variable high shear rates depending on the suspension rheology and the impeller design.

3. Ball Mills - These are well known to most processes and consist of free moving balls inside a sealed container. A variation of this design is the sand mill or sand grind in which the effective balls are sand grains.

4. Roll Mills - These operate by carrying the suspension between one, two or three rollers and a blade, in a closely controlled gap under pressure.

Considering first the high speed impeller mixing of particles in liquids, Patterson (609) conducted experiments with a flat paddle-type laboratory mixer and found that -

a. reducing the vehicle viscosity by solvent dilution decreased the degree of separation,
b. increasing the impeller speed increased the rate of separation,
c. cooling the mixture during mixing increased the rate of separation, and
d. increasing the number of blades on the paddle increased the degree of separation for any one mixing time.

Cozzens (610) studied the high speed mixing of various powders and liquids in a planetary-type laboratory mixer fitted with an open planar blade. He found that the rate and degree of separation were increased by increasing the vehicle viscosity, particle concentration and mixing speed, and that changes in the particle and vehicle nature drastically changed the rate and degree of separation. Other related work on high speed dispersion was reported by Guggenheim (611) and Schliesser, et al. (615). These latter authors confirmed some of the findings of the previous authors, when working with a flat paddle mixer with a four-blade impeller. They showed that better dispersions were always obtained at higher pigment concentrations, while the rate of separation only depended on the energy input and indirectly on the mixer speed. Both Wade and Taylor (612) and Ensminger (613) reported that with very high speed

impellers, a low viscosity vehicle was important. In spite of these series of experiments and reported mixing conditions, Dowling (614) reported that under optimum conditions formulation and geometry, high speed mixers were not necessary, and in fact the use of lower shear rate equipment could produce similar degrees of separation more economically. In support, a most recent paper by Armstrong (616) emphasized the usefulness of low peripheral speed impellers, in the paint industry, and using a rotary saw-tooth variety he was able to show that high particle concentration and low liquid viscosity gave higher pigment yields/batch at a lower operating temperature than high viscosity vehicles. This supported an earlier paper by Weisberg (617) who had Studied the influence of shear stress-shear rate profiles of a system on the rate and degree of dispersion of medium chrome yellow pigment. He used a smooth cylindrical impeller at slow speeds and showed that the rate of separation increased with the torque until turbulence set in. In a system of proper rheology, i.e., at a controlled Reynolds number with no turbulence, Weisberg reported that a cylindrical impeller provided a more efficient mode of power input than high speed processes. Recent studies were performed by Daniel (618) who used them for soft textured pigments.

The use of ball mills to disperse powders in liquids was reported by Daniels (619) and Shurts (620). Fisher (621) pointed out that the efficiency of ball milling was increased as the size of the ball was reduced, hence the sand mill or sand grind was introduced in which the effective ball size was one sand grain. The operation of the sand mill was discussed by Bosse (622) and by Brownlie (623) who studied TiO_2 pigments. Recent work on the efficiency of ball milling was reported by Vavra (625).

Notable comparisons of the techniques of sand milling, ball milling and impeller dispersion were reported by Ensminger (613) and Garret and Hess (624). These latter authors compared the three techniques with a fourth one - roller milling for

TiO_2 and Fe_2O_3 pigments. They found that the ball mill, sand mill, high speed impeller and triple roll mill all gave good degrees of separation, and with TiO_2 the degrees of separation were similar. The significant differences were shown in the rates of separation which varied widely. The triple roll mill was superior to all the other three methods, and it dispersed the particles in one pass. The sand and ball mills were significantly slower and the high speed impeller was the slowest of all.

With red iron oxide, differences in the degree of separation were also found. The high speed impeller never achieved the same degree of separation as the other three methods which once again were quite similar. As before the rates of separation were widely different, the triple roll mill being the fastest in achieving the best degree of separation.

From this literature search which quite surprisingly contains few references, it seems clear that several overriding factors emerge. For submicron powders high shear in a triple roll mill is desirable, and in addition high pigment concentrations in the suspension would be an advantage. In comparison with these requirements the usual laboratory separation practices of spatula shearing, milling, blending, appear to have no correlation, and one can expect inferior dispersions in the laboratory as a result. Armstrong (616) realized this when he emphasized the need to simulate industrial mixing and separating equipment in the laboratory, if quality control is to be meaningful.

3.5 Methods of Modifying Forces of Adhesion

It has been stated that the adhesive forces are largely dependent on the surface properties of the particles on surface, and hence the forces can be changed - ideally reduced - by surface modification. Lygin (627), Kiselev (628), and Babkin (629) report that surface modification by means of alkylchlorosilanes is used widely for varying the adsorption of

gases and vapors in gas chromatography. Vinogradova (630) discusses the same application to reduce the adsorption of films, Korolev (631,632,633) describes their use for reducing adhesive power of solid surfaces, Baibakov (634), Andnanov (636) and Jordon (635) for the reduction of the adhesion of ice. Zimon (475), Voronkov (638), Talaev (637) and Krotova (639) describe the use of 1% benzene solution of an alkylchlorosilane which neutralizes the hydroxyl groups on a surface replacing them by hydrophobic methyl groups. In particular they describe the use of dimethyldichlorosilane for this purpose. According to De Bruynes rule, the greater the difference in the wetting capacity of the two surfaces in contact, the smaller is the adhesion. Hence it would appear that to facilitate particle separation from a surface, one should attempt to make the surface hydrophobic and the particle surface hydrophilic. As most particles collected from the atmosphere have free water on their surfaces, agents capable of bonding to these surfaces which modify the electrical double layer to increase repulsion would be ideal. This is easier to achieve in liquid media, and much work has been done to study bonding at the hydrophilic surface in liquids.

Campbell, et al. (640) described the types of bonding that could take place between liquids and solid hydrophilic surfaces. They defined these as physical or Van der Waals, polar or principally hydrogen bonding and ion exchange. In all aqueous dispersions, there was a tendency to form hydrogen bonds between ions and the solid surface, but the main difficulties in investigating the presence of such bonds were due to a lack of knowledge of the reactivity of potentially hydrogen bonding groups. Most of the detection methods were applied to non-aqueous systems, e.g., radiation methods, solubility, etc., but Campbell, et al. was able to study the effects of various groups of solutes and correlate their hydrogen bonding tendencies in water using refractometry. Dye complexes were used specifically and they studied the role of a hydrogen attached

to an oxygen, a nitrogen and a carbon atom with regard to its hydrogen bonding character. They showed that hydrogens attached to oxygen and nitrogen were particularly prone to hydrogen bonding, even if the compounds were sulphonated. Sulphonation of a molecule with a consequent high degree of solvation in water did not impair its ability to form hydrogen bonds in aqueous solution. A hydrogen attached to a carbon formed hydrogen bonds much less readily but it could be made to do so if activated by strongly electronegative groups and such bonding, e.g., by a hydrogen in chloroform, was well known.

Similarly a carbonyl oxygen could activate a hydrogen attached to a carbon atom and it had been suggested that by these means the aldehyde group and certain ester groups could act in water as proton donors towards nitrogen atoms in a second solute. Long, et al. (641) showed that the dimensions of forces at solid interfaces, e.g., the forces of adhesion were of the same magnitude of those associated with hydrogen bonding. They studied the possibility of a monomolecular layer of water remaining on solid surfaces after vigorous heating, and showed some hydroxylation of steel surfaces still existed after heating to 800°C. They concluded that hydrogen bonding was a major component in the process of adhesion at solid surfaces. The role of a hydrogen attached to a nitrogen atoms was discussed by Schwitzer (642) who described the method by which a cationic agent attached itself to a surface. He identified the presence of secondary chemical bonds between the amine group and the surface, which became stronger when the compound was a diamine. He explained that this was the most important difference between cationic and anionic surfactants. The former act by bonding while the latter act by preferentially wetting the solid surface. The mechanism by which the amine group attached itself to the surface was most probably hydrogen bonding, and this mechanism was discussed at more length by other authors.

Although Long had proposed that hydrogen bonding was of major importance in adhesion, Trudgian and Prihoda (643) suggested that the physico-chemical affinities of materials were responsible for many other properties of materials such as miscibility, solubility, compatibility, dispersion and adhesion. To investigate this further let us first consider the case of two pure solvents. Burrell (644) developed an integrated theory on miscibility, solubility and compatibility, of two or more solvents based on two parameters, a parameter defined as the solubility parameter and a parameter defined as the hydrogen bonding value. He showed that two solvents were miscible when their solubility parameters and hydrogen bonding values were similar. For the case of a resin or a polymer dissolving in a solvent, the same rule appeared to hold. Burrell then published tables of solubility parameters and put forward hydrogen bonding values for many solvents to aid in paint formulation. These hydrogen bonding values were very crude, but were made more useful by Lieberman (645). Lieberman assigned values of hydrogen bonding numbers to solvents which Burrell had placed in the groups of poorly, moderately and strongly hydrogen bonding solvents. These numbers were 0,3, 1.0 and 1.7, respectively. If, in some cases a polymer did not dissolve in a solvent of value 1.0 or 1.7, two solvents with these values could be mixed to provide solvent with an equivalent value of 1.3, for example, when the polymer dissolved readily.

Thus, Lieberman was able to estimate the values of several other solvents by determining the solubility limits of selected polymers in mixtures of unknown solvents with those to which values had been assigned. In this way he was able to fit more precise hydrogen bonding values to solvents, polymers and resins, and produce complex tables to improve those of Burrell. By plotting the square of these values against the solubility parameter, he was able to form solubility maps which graphically showed the solubility characteristics of typical polymers. Trudgian and Prohoda (643) then published a paper in which they

discussed the application of hydrogen bonding parameters to predict not only solvent miscibility, compatibility and solubility, but resin solubility and particle dispersion. They found that solvents such as ethyl alcohol, isopropyl alcohol, ethylene glycol and n-butanol dispersed TiO_2 pigments better than any other solvents. After much searching to find the key to explain these results, they found that the hydrogen bonding values of all four solvents were identical. Extending this to other pigments, they showed generally that hydrophilic inorganic pigments dispersed well in strongly hydrogen bonding solvents, e.g., alcohols, and examples of typical pigments were yellow oxide of iron, medium chrome yellow, rutile titanium dioxide and molybdate orange. Red iron oxide dispersed in moderately hydrogen bonding solvents, e.g., ketones. Organic pigments such as phthalocyanine blue and green and lampblack, dispersed best in moderate to weak hydrogen bonding solvents, e.g., esters, while dark bon-red pigment dispersed in weakly hydrogen bonding n-nitropropane.

Hence, the hydrogen bonding value of solvents could be used effectively to separate particles from surfaces in terms of their hydrogen bonding tendencies. Strangely enough, no immediate notice was taken of this paper for several years, but in the polymer field the concept of the solubility parameter was extended quite successfully.

Gardon (646) took the work of Lieberman further by investigating the correlation between solubility parameter, hydrogen bonding value and dipole moment. Crowley, Teague and Lowe (647, 648) used these three parameters and resins, which predicted accurately the solvent type or mixture to use for any polymer. Similar work was done by Hansen (649) but in his second paper (650) he extended this to pigments. He was able to show quite clearly that pigment dispersion in pure solvents could be predicted by the 3-D mapping system. Then 13 years after his pioneering paper, Burrell summarized the progress in the subject

of solubility, and presented a review paper which is recommended for reference (651). Since this time, Rheinbeck & Lin (652) theoretically calculated solubility parameters for macromolecules by calculating the chemical group effects in the molecule, and Hoy (653) improved the solubility parameter tables, by preparing complex computer programs to calculate solubility parameters from vapor pressure data.

Lee (654) introduced a fourth parameter of interest to the dispersion field, when he studied the correlations between the three parameters above and surface tension. Finally, Eissler, Zgol and Stolp (655) studied sedimentation volumes of settled dispersions of zinc oxide and related them to the 3-D solubility parameters of che solvents used.

For more information on the hydrogen bond see Pimental & McClellan (656). It now remains to study the current literature to investigate the type of bond structure that has been experimentally found to exist between hydroxylated surfaces and adsorbed molecules.

Every, et al. (657) studied the adsorption of methyl alcohol and water on rutile from hexane and showed a high value for the heat of immersion for both water and alcohol. Wade and Hackerman (658) studied the heat of immersion (ΔH) of hexane on rutile as well as water and methyl alcohol. They showed that ΔH increased slightly with increase in the degassing temperature, but that ΔH was very much less than the ΔH for alcohol and water. They attributed the high ΔHs with alcohol and water to the formation of hydrogen bonds between the surface hydroxyls and the alcohol and water molecules. With hexane no hydrogen bonding took place as the ΔH was small. This association of high heats of immersion with hydrogen bonding was also reported by Wade & Hackerman (659). Parfitt and Wiltshire (660) studied the adsorption of alternate members of a homologous series of aliphatic straight chain primary alcohols on rutile. They studied ethanol → octadecanol from solution in p-xylene. A strong

amount of each alcohol was adsorbed at relatively low concentrations which reached a minimum at hexanol and octanol indicating the importance of water solvent interaction at the solid liquid interface. Adsorbed water on rutile caused a significant reduction in adsorption. Day and Parfitt (661) studied the thickness of the adsorbed layers of both alcohol and hydrocarbon on rutile and showed a perpendicular orientation of alcohol on the surface with a multilayer adsorption of hydrocarbon between the alcohol chains. They related this to the dual nature of the rutile surface which was heterogeneous with 58-60% of the surface positively adsorbing alcohol to the exclusion of hydrocarbon and the remainder preferentially adsorbing hydrocarbon. Day and Parfitt (662) studied the adsorption of ethanol, n-octanol and n-dodecanol on rutile from binary mixtures of p-xylene and n-heptane. Again they discussed hydrogen bonding and the interaction between the aromatic solvent and the hydroxyl groups which leads to competitive adsorption. The magnitude of this was shown to depend on the fraction of the surface covered by molecular water. The aliphatic solvent competed for the non-hydroxylated region which was again related to the water coverage.

Smith (683) studied the IR spectra of n-octadecanoic acid on rutile and found it to be conducted by two mechanisms. The reaction with surface hydroxyls to form the octadecanoate ion, or altervatively hydrogen bonding to the surface by a hydrogen bonded carboxyl group. Sherwood and Rybicka (663) studied the IR spectra of stearic acid and stearates on rutile. On simple pigments hydrogen bonding was found to predominate. The pressure of unsaturation in a molecule did not affect surface bonding, but it did change the isotherm which showed that the unsaturation was entering into the interaction resulting in an orientation of the molecule on the surface.

Livanova, et al. (664) commented on the coagulation strengths of rutile suspension structures in the presence of

impurities when treated with orthophosphate and meta-silicate. Both ions stabilized rutile but a pronounced effect was found with a dialyzed rutile when surface impurities had been removed. Masaji, et al. (665) and Krupskii, et al. (666) showed that phosphate ions can undergo specific adsorption regardless of the charge on the surface due to hydrogen bond formation. Ermolaeva, et al. (667) showed that phosphoric acid could be adsorbed on TiO_2 to a degree that increased with the amount of electrolyte added.

Dickman, et al. (668) and Kelley (669) commented that metasilicate ions adsorbed similarly to phosphate and its stabilizing action was enhanced by the adsorption of strongly hydrated silicic acid from the hydrolysis of sodium metasilicate.

Some information on the mechanism of the phosphate hydrogen bonding tendency was provided by Vissers (670) who studied the sorption of orthophosphate on the hydrated oxides of zirconium, hafnium, cerium and thorium. The sorption of the phosphate ion was throught to be related in a stoichiometric manner to the surface hydroxyls. Models of the sorption process were suggested which assumed a tetrahedral phosphate molecule. From this model they indicated that the PO_4 ion was adsorbed with a Stoichiometry of either 2 or 3 hydroxyl groups per sorbed PO_4 molecule. Low and Ramamurthy (671) investigated the adsorption of phosphoric acid on silica by IR spectroscopy, and commented on the work of Bellamy (672) in which he showed that adsorption of phosphorous compounds on oxides occured by hydrogen bonding between the >PO(OH) group and the surface hydroxyls. When this group was present the hydrogen bonding effects were very much greater than with carboxylic acids. Alternatively he showed that the P(OH) group was not hydrogen bonded and the reaction of water with surface P_4O_{10} molecules was represented by

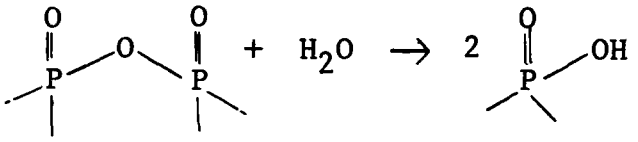

The ability of the phosphate ion to satisfy the hydrogen bonding tendency of a solid surface was demonstrated by Eissler, et al. (655). They investigated two pigments - zinc oxide and phosphate treated zinc oxide, and attempted to isolate the three effects of Hansen's three dimensional solubility maps to study the important contributors. They measured sedimentation volumes as an indicator of dispersion on flocculation and found that for the untreated zinc oxide almost all the effect on sedimentation volume took place as the hydrogen bonding tendency of the solvent was varied. With the treated pigment only, the polar parameter affected the sedimentation volume while the effect of the hydrogen bonding tendency of the solvent was nil. Here the phosphate had clearly neutralized the hydrogen bonding sites on the pigment surface.

In a similar way to TiO_2, Wade and Hackerman showed high heats of immersion for Al_2O_3, and explained them in terms of hydrogen bonding (673). Every, et al. (657) showed that methyl alcohol adsorbed very strongly on alumina, and this was confirmed by Greenler (674). Greenler showed the presence of chemisorption of CH_3OH by IR spectroscopy and found the presence of $AlOCH_3$ on the surface.

Wade and Hackerman (658) studied the adsorption of hexane on alumina and found the heat of immersion similar to that of TiO_2. They showed a slight but real increase in ΔH with outgassing temperature but that ΔHs were smaller than for water adsorption. This was explained as Van der Waals adsorption and not hydrogen bonding. Further information of the adsorption of

alcohols on alumina was provided by Ono and Keil (675) who used E.P.R. techniques.

Hasagawa and Low (676) studied the adsorption of long chain fatty acids on alumina by IR spectroscopy. In particular they studied the adsorption of stearic acid, and showed that the adsorption led to the formation of aluminum stearate and hydrogen bonded water on the surface. O'Connor, et al. (677) investigated the reactions of corundum with various ions in aqueous solution especially the effect of various mechanical and chemical treatments upon the charge density in the diffuse layer. They found that the surface layer consisted of hydroxyl groups which may be covalent or partially ionized according to the treatments. This gave rise to the structures

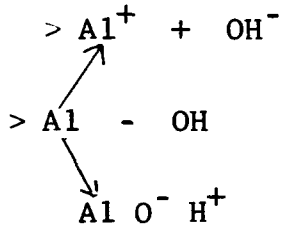

Hence, adsorption could take place by covalent bond formation or ion exchange.

Giles, et al. (678) studied the adsorption of cationic dyes on alumina and confirmed the work of O'Connor. They showed that molecules were adsorbed by either ion exchange with cations on the alumina surface, or by any hydrogen donor groups by hydrogen bonding with surface oxygen atoms. With rhodamine dyes which possessed both amine and carboxylic acid groups, they suggested that edgewise adsorption took place due to formation of a monolayer of dye formed by partial hydrogen bonding between the >NH group and the alumina surface. Somesunderan and Fuerstenau (679) studied the adsorption of sodium dodecyl sulphonate at the Al_2O_3 water interface. Adsorption was observed to proceed in three steps. At low concentration it took

place by counter ion exchange, at intermediate concentrations by two dimensional aggregates of surfactant ions and at high concentrations due to a net change of charge-zeta potential by the surfactant ions. No hydrogen bonding took place with this anionic agent.

The use of phosphates to disperse alumina was mentioned by Bakker and Bartok (680) and one can expect the same type of reaction between the phosphate ion and the surface hydroxyls as demonstrated by TiO_2. Again, like TiO_2, the use of ions to neutralize the hydrogen bonding tendency of the alumina surface was discussed by Peri (681). He studied the effect of adsorbing fluoride on surface sites on alumina, and showed that the effect of surface hydroxylation could be neutralized by fluorine treatment.

The adsorption of phosphate ions on red iron oxide was demonstrated by Tokiwa and Imamura (682) and once again the mechanism is one of hydrogen bonding. The tendency of the ferric oxide to require moderately hydrogen bonding solvents was mentioned by Trudgian and Prihoda (643). This is most probably due to the electronic configuration of the ferric oxide surface which is less electronegative than either the alumina or the titanium dioxide.

Apart from this general approach to adhesion reduction, many authors have studied the affect of specific compounds on the degree of dispersion of particles. Buckley (719) discussed the reduction in surface friction and surface adhesion of tungsten metal by the adsorption of hydrogen, oxygen, carbon dioxide, hydrogen sulphide hydrocarbons, ethylene and acetylene. The longer the hydrocarbon chain length, the less the adhesion, and also with ethane, ethylene and acetylene. It decreased with an increase in the number of carbon to carbon bonds.

Parfitt and Ramsbottom (720), Saleeb (721) and Hesselint (722) studied the effects of surfactant adsorption in liquid. Similar studies were conducted by Watanabe and

Aoki (723), McGown and Parfitt (724). Several authors patented processes for this application. Maruta, et al. (725) patented the use of anionic surfactants for urea, Linwood and Looby (726) stabilized anatase, Dicher (727) stabilized latex, Augart (728), pharmaceutical products, Yates (727), silica, Kinariwala (730), organic pigments, Augustal (731), inorganic pigments. Martynov, et al. (732), Miskarli, et al. (733), Takeshi (734), Greenwood, et al. (735), Krasnokutskaya (736), Bibik (737), Glazman and Kabysh (738), and Matijevic and Allen (739), all studied effects of surfactant adsorption on particle adhesion behavior. Theoretical work on this subject was reported by Clayfield (740) who studied the configurational behavior of adsorbed macromolecules on adhesion. Ivani and Callis (741) gave a table of useful dispersing substances for some powders in liquid and these are shown in Table 9.

The work reviewed in this section has indicated that hydrogen bonding is the most important bonding mechanism between solid particles and adsorbed ions in aqueous suspensions. These bonds are strong and permanent, and hence any agent bound to the surface in this way will not be removed without considerable effort. Alcohols appear to adsorb end-on to form a vertical chain from the surface (- at least in the monolayer), monoamines and carboxylic acids appear to do likewise. Diamines, phosphates and silicates adsorb using 2-3 surface hydroxyls per ion, and form stable surface coatings on most oxides. The oxides of silicon, titanium, aluminum, iron, hafnium, zirconium, thorium, cerium and zinc have all been shown to adsorb phosphate ions in aqueous media, and it appears to be a general rule that all hydroxylated oxides in aqueous media may be dispersed by phosphate treatments.

The use of a hydrogen bonding solvent series to predict the separation characteristics of particles appears to be most encouraging, but this has to be pursued for many types of powder before any firm conclusions can be reached.

Table 9

LIQUIDS SUITABLE FOR THE DISPERSION OF SPECIFIC POWDERS

Powder	Liquid	Dispersing Agent and Weight Concentration
Alumina	Carbon tetrachloride	
Barium carbonate	Methanol	
Bronze powder	Cyclohexanol	
Calcium carbonate	Water	0.1% Tetrasodium pyrophosphate
Calcium arsenate	1:1 Mixture of ethanol and water	
Calcium phosphate (soluble)	Isobutanol Hexane 2-Ethyl hexanol	
Calcium phosphate (insoluble)	Ethanol (absolute) Butanol	
	Water	0.1% Na_2SiO_3 and 0.02% Sterox[a]
	Water	3.1% Sodium hexametaphosphate
Cement	Glycol Paraffin oil	
	Ethanol	0.5% $CaCl_2$
Clay	Water	0.1% Sodium hexametaphosphate
Coal	Ethanol	
Copper powder	Acetone Water	
Diatomaceous Earth	Water	0.1% Sodium hexametaphosphate
Fluorspar	Water	0.02% Nitric acid
Glass particles	Butanol	
Graphite powder	Water Ethanol	0.05% Tannic acid
Gypsum	Glycol	Cobalt citrate
Iron metal	1:1 Volume mixture of acetone and soya bean oil Water	
Organic powders (cocoa, flour, starch, etc.)	Benzene Isobutanol	
Silica	Water	0.1% Tetrasodium pyrophosphate and 0.02% Sterox[a]
Sodium phosphates	Ethanol (absolute)	
Tungsten metal	Water Methanol Acetone	
Zinc metal	Butanol	

[a] For many powders more than one dispersing agent may be satisfactory.

3.6 Indexes of Dispersion

This section is concerned with the techniques that are available as indicators to inform the analyst of both the degree of separation that has been attained by a specific separation process, and the stability of the dispersion with respect to time. Measurements of differences in stability have been employed as a tool to decide which specific substance or solvent has created the best separation. For example, Trudgian and Prihoda (643) used time-dependent turbidity and Eissler, et al. (655) used changes in sedimentation volume with time to both assess their dispersions, and to comment on the usefulness of certain dispersing substances. The importance of suspension stability, in our case, is recognized, when a suspension has to be analyzed for the size distribution of the particulate phase, and the analytical time is long. One has to be sure that the degree of separation attained immediately after the separation process is maintained throughout the analytical period.

In this survey, suspension stability is not discussed in detail, as a comprehensive state of the art in the field has been prepared and reported by Parfitt (608). Our interest is only in the capability of being able to monitor small changes in the suspension stability as an indicator of the ability of an adsorbed substance to adequately or inadequately disperse a powder in aqueous media.

The three important stages of the dispersion process have been put forward by Parfitt (608) as : 1. wetting the powder; 2. breaking up agglomerates; 3. maintaining a stable dispersion. Items 1 and 3 are now discussed in detail.

The act of wetting a powder is the replacement of the solid/air interface by the solid/liquid interface. Parfitt (608) discusses this in some detail, and basically shows that wettability depends on the contact angle and surface tension of the liquid media. Hence to achieve separation, substances are used which either have small contact angles and surface tensions or

they reduce the contact angle and surface tension of the suspending medium. Examples of the former are alcohols, etc. and examples of the latter are surfactants in aqueous media. The determination of the surface tension of liquids is fairly easy and classical methods are those of the de Noüy ring, the Wilhelmy plate, the drop volume and the pendant drop. With surfactant solutions this becomes more difficult, and several useful comparisons of techniques for these solutions have been prepared by Padday & Russell (684), Drost-Hansen (685) and Boucher, et al. (686). By far the most difficult task is to determine the contact angles between a liquid and a powder. Some techniques that have been suggested for this are the contact anglometer (687), the Washburn and Bartell methods, and the one of Heertjes and Kossen. These latter three methods are discussed in references 688 and 689. Because of these difficulties, it is often impossible to theoretically predict values for the wettability of a powder, and one usually reverts to a simple empirical method. Some of these are discussed by Parfitt (608) and Mitsui and Takada (690). The effect of differences in the abilities of liquids to wet powders have been shown in previous sections of this report. Trudgian and Prihoda (643) commented that rutile TiO_2 required strongly hydrogen bonding solvents to facilitate separation. They mentioned ethyl alcohol, isopropyl alcohol, etc. as being very suitable, but found that strongly hydrogen bonding water was unsatisfactory. In this case, the inability of the water to wet the powder overrode its strong tendency for hydrogen bonding and separation. Although these factors are important, a second property of a solvent or an adsorbed substance has to be taken into account. In the maintenance of a stable suspension, these substances have to affect the electrical double layer around the particle. Ideally, not only do they wet the powder, but they adsorb and increase the zeta potential or the charge density around each particle inducing mutual repulsion of those adjacent to it. It has been shown that substances which

hydrogen bond onto titania, alumina, and ferric oxide may form stable ion structures around the particle. If these adsorbed ions cause an increase in the zeta potential, then dispersion and stability are improved. Amines, carboxylic acids, phosphates and silicates have been shown to do this, and hence are good dispersing and stabilizing agents for metal oxides. Obviously, the concentration of these substances can be critical, and the surface active agent demand or optimum surface active agent concentration has to be experimentally measured.

The most common methods of assessing the degree of separation and the suspension stability are measurements of turbidity, size distribution and sedimentation volume with respect to time. For highly concentrated suspensions, rheological properties such as the viscosity, shear strength, etc. are employed.

In this program, the first two indicators are the most important, and only if higher particle concentrations are studied will other factors be considered. In addition to these measurements, it has been shown that a change in zeta potential, pH, electrical conductivity and surface active agent concentration can induce instability in stable suspensions. Hence, measurements of these parameters have to be simultaneously recorded in any study to enable changes in a suspension to be explained and understood.

Hence, measurements that have to be made on each dispersion are ideally:

1. Suspension Turbidity and Mean Particle Size
2. Sedimentation Volume
3. Change in Mean Size and Size Distribution with Time
4. Zeta Potential
5. pH
6. Electrical Conductivity
7. Surface Active Agent Nature, Purity and Critical Concentration

The methods that are available for these determinations are now discussed in detail.

3.6.1 Suspension Turbidity and Mean Particle Size

The use of light scattering to measure the turbidity and size characteristics of suspensions has formed the subject of much literature over the last twenty-five years.

Selected literature on the use of light scattering techniques to measure physical properties of suspensions have been published and reference to the bibliographies by the Phoenix Precision Company are listed here (691,692). These bibliographies alone contain approximately 1000 references up to the year 1965. More recently, publications by Hepplestone and Lewis (693), Vavra (694), Wallace and Kratohvil (695), Maxim (696), Liversey (697), Mullaney and Dean (698), Harris (699), Perelman and Shifrin (700), and Kratohvil and Wallace (701) have added to the literature pertaining to particulate measurement using light scattering techniques.

The measurement of turbidity, dissymmetry, particle size, angular scattering and depolarization measurements can be made using a photometer of the type Brice-Phoenix Model 950. Details of the techniques necessary to make these measurements are given in the operating manual (702). Details of the methods required to measure the average particle sizes of suspensions by turbidity are given in papers by Loebel (703) and Bailey (704).

Recent usage of turbidity to follow the degree of dispersion of pigments was reported by Koglin (705) who measured the optimum concentration of pyrophosphate required to disperse zinc suspensions. Work on thoria salts was reported by Rartogil (706) and a new device was developed in Holland by an unknown author (607). Another device was developed in Russia by Novikov, et al. (708) for studying coagulation in colloidal systems.

3.6.2 Sedimentation Volume

The use of sedimentation volume to assess the state of dispersion of pigments has been widespread. Examples of the method have been given by Weisberg (709), Princen (710), Tokiwa and Imamura (682), and Eissler, et al. (655). The method merely consists of shaking a known volume of powder with either a solvent or a surface active agent solution in a tube such as the one shown in Figure 14, and then letting the suspension stand for a period of time. Frequent examination of the sediment in the tube enables the sediment volume to be measured and a plot made of sediment volume versus time. At any one time, stable suspensions will show a negligible sedimentation volume, while unstable suspensions will show a large sedimentation volume. Weisberg (709) cautioned the analyst about placing too much value on this test to measure the degree of flocculation. This was in direct conflict with the work of Dintenfass (711) who explained that the degree of flocculation could be estimated from the sedimentation volume. Weisberg's caution was based on the effect of dielectric constant on flocculation, and he advised persons using the method to check each sediment microscopically and not to place complete confidence on the sediment volume measurement. Similar work was reported by Yashiro (712). However, in most cases, Dintenfass' theory holds, and the method is considered a most convenient one for long-term studies.

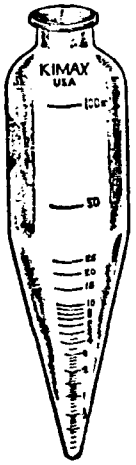

Figure 14

KIMAX TUBE
FOR SEDIMENTATION
VOLUME MEASUREMENT

3.6.3 Change in Mean Size and Size Distribution with Time

In the introduction to this report, a powder was defined as a statistical group of discrete particles, agglomerates and aggregates, and the difference between agglomerates and aggregates was defined in terms of the bonding strengths. An agglomerate was defined as a statistical group of discrete particles bound together by weak physical bonds while an aggregate was defined as a statistical group of discrete particles bound together by strong chemical bonds. Dispersion techniques then broke agglomerates down into discrete particles leaving aggregates intact.

Hence, any improvement in a dispersion would always lead to the formation of a finer size distribution and any coagulation or flocculation of the suspension would produce a coarser size distribution. Thus size analysis can be a useful tool to follow dispersion and flocculation phenomena of suspensions. The determination of only the mean size of a suspension of particles is also useful as this will change with dispersion or flocculation, but the full size distribution is better as it demonstrates the overall agglomerate sizes that are present at various times. The advantage of the former is speed of analysis, and that of the latter is more information.

Examples of the use of size analysis are given by Parfitt (608), Matthews and Rhodes (713). For submicron powders, the methods to be used are discussed in Section (5), and these will be employed in this study to provide the overall size distribution changes as a function of time.

3.6.4 Zeta Potential

The measurement of the mass transport, charge and zeta potential of particles in suspension has been used by many authors to correlate suspension stability. Many of these are recorded by Parfitt (608) and no further references are necessary. There are several types of apparatus that are available

to measure zeta-potential and these were reviewed in a paper by Sennett and Olivier (714). One of these units was later developed by these authors at the Freeport Kaolin Co., and the unit was licensed to the Micromeritics Instrument Co. for manufacture. This unit has the advantage of being used over a concentration range of 1.5%-70% by weight.

3.6.5 pH and Electrical Conductivity

There is no need to dwell on the types of measuring techniques for the determination of the pH and conductivity of suspensions. These are well known in all branches of physical chemistry. In this study, a Beckman Zeromatic pH meter can be used with a standard calomel and glass electrode system for pH, and a Fisher conductivity cell and meter will be used for the electrical conductivity. The effects of these two parameters on suspension stability have been recorded by several authors. Examples of these are Parfitt (608), McAtee (715), Petrova, et al. (716), Livanova, et al. (664), Rechman (718), and Thomas and Cremers (717).

3.6.6 Surface Active Agent Nature, Purity and Critical Concentration

The nature and purity of each surface active material can be obtained from the manufacturer, and where this is insufficiently pure for our needs, the material can be purified.

Each substance will be diluted to known active strengths in aqueous media and stored as stock solutions.

The critical concentration of each substance on the submicron powders under study can be determined by plotting the adsorption isotherms in aqueous media. For surfactants at low concentrations, this can be achieved by surface tension measurements or by the determination of conductivity. Surface tension apparatus available is the de Nouy ring and Wilhelmy plate apparatus. For phosphates and silicates, colorometric analysis can be tried, but here again, useful information may be found from conductivity measurements.

At the same time, particle size analysis can be performed by Brice-Phoenix or Disc Centrifuge and the optimum concentration of agent will be that concentration at which the mean particle size is at a minimum. This can then be correlated to the isotherm data to investigate whether this optimum occurs at a monolayer capacity or at the critical micille concentration. To do this a knowledge of the total and external surface area of the powders will be required. This data can be measured using gas adsorption and permeability, respectively.

3.7 Summary

The types of forces and bonds that are known to cause adhesion or separation of particles to surfaces, or to each other, are mechanical, Van der Waals, electrical, electrostatic, capillary, electrical double layer, covalent, ionic, metallic, and hydrogen.

In air, the force of adhesion depends on the interaction of these forces which in turn depends on the prevailing experimental conditions. In dry air, mechanical molecular, electrical and electrostatic forces are important, but in moist air with humidity >65%, the capillary forces at the liquid far outweigh any other. Such factors as surface hardness, surface roughness, particle shape, particle size and temperature affect the magnitude of the force. When suspended in liquids, many of these forces disappear or are reduced, and in fact forces of repulsion can be induced to facilitate separation. Adsorption of specific surfactants onto the particle and substrate surfaces at temperatures of 60°C cause particle separation with a minimum of energy, and the additional factors that affected the magnitude of the force in air are minimized in the liquid medium. For the most effective separation, it is important that liquids and surfactant be chosen which cause the greatest difference in wettability between surfaces and particles. Ideally, a surface should be made hydrophobic and a particle hydrophilic for good separation. In aqueous suspensions, this

can be done by selective phosphate and silicate treatments, while in non-aqueous liquids it can be done by varying the hydrogen bonding demand at the solvent. Particle adhesion forces can then be measured by several techniques, but for submicron particles, a centrifugal system appears to be the best approach. However, vibrational methods including ultrasonics, and methods of high shear in specially made roller mills should also be tried. Preliminary analysis of the degree of separations can be made using turbidity, and particle size analysis, but this is discussed in detail in Section 5.

4. MATHEMATICAL MODELS OF ADHESION AND AGGLOMERATION

The current theory for the stability of hydrophobic colloids and the adhesion of particles is now presented. The basic concepts of the former is the attraction of particles due to London-Van der Waals forces and the repulsion due to the interaction of electrical double layers. The mathematical theory for London-Van der Waals forces is discussed first followed by the double layer theory. Together these two theories give the interaction potential curve which is used to explain the stability of colloids. The next part considers how long a system is stable by considering the rate of collisions of colloidal particles. After this, the significance of the zeta potential is investigated. Finally, the adhesion forces in powders and between particle is considered.

4.1 London-Van der Waals Force of Attraction

In 1930 London (756,757,758,764) satisfactorily explained on the basis of quantum mechanics the attraction between two non-polar molecules. Since at a given moment there may be more electrons on one side of an atom than on the other, the center of the negative charge of the electrons is slightly displaced from the positively charged nucleus. This momentary asymmetry results in an instantaneous dipole moment whose field induces dipoles in neighboring molecules so that the two dipoles attract each other.

From classical physics (774) the electric field of a dipole is proportional to $1/r^3$ where r is the distance from the dipole and induces in a neighboring atom of polarizability α_o a dipole moment proportional to α_o/r^3. Since the potential energy of a dipole of strength μ in an electric field E is $-E\mu$, the potential energy of two molecules is proportional to α_o/r^6. From quantum mechanics London evaluated the constant of proportionality and found the energy of interaction

of two molecules to be:

$$V_{London} = -\frac{B}{r^6} \tag{1}$$

where:

$$B = \frac{3}{4} h\nu_o \alpha_o^2$$

h is the Planck constant and ν_o the characteristic frequency of the substance. The extra factor of α_o accounts for the fact that the two atoms mutually induce dipoles in each other.

Other methods of evaluating B are also available (761). Slater and Kirkwood (770) give:

$$B = 11.25 \times 10^{-24} Z^{1/2} \alpha_o^{3/2} \tag{2}$$

where Z is the number of electrons in the outer shell of the atom. Moelwyn-Hughes (750) modified this equation to read:

$$B = \frac{3}{4} Z^{1/2} h\nu_o \alpha_o^2 \tag{3}$$

ν_o may be calculated from optical data by means of dispersion formulas of the form (763,765):

$$n^2 = 1 + \frac{C\nu_o^2}{\nu_o^2 - \nu^2} \tag{4}$$

where n is the refractive index at frequency ν and C a constant. α_o is calculated from (763,765):

$$\alpha_o = \frac{3M}{4\pi N_o \rho} \frac{n^2-1}{n^2+2} \frac{\nu_o^2 - \nu^2}{\nu_o^2} \tag{5}$$

where ρ is the density of material of molecular weight M and N_o Avogadro's number.

Another expression may be obtained from a paper by

Neugebauer (762):

$$B = -1.62 \times 10^{-6} \alpha_o \chi \qquad (6)$$

where χ is the diamagnetic susceptibility of the atom.

As a comparison of these predictive methods, for water London's equation ($h\nu_o$ = 13 eV) gives $B = 32 \times 10^{-60}$ erg-cm^6; the Slater-Kirkwood equation (Z = 8, $\alpha_o = 1.43 \times 10^{-24}$) gives $B = 54 \times 10^{-60}$; the Neugebauer equation ($\chi = 2.2 \times 10^{-29}$) gives $B = 51 \times 10^{-60}$.

Fowkes (749) has proposed a method of estimating the Hamaker Constant $A = \pi^2 q^2 B$ where q is the number of atoms per cm^3 based on interfacial tension data. He gives:

$$A = 6\pi r_{11}^2 \nu^d \qquad (7)$$

where ν^d is surface free energy. Experimental values of ν^d for various materials are given in Table 10, and for water and elements such as oxides, metals and $-CH_2$ or -CH groups the approximation $6\pi r_{11}^2 = 1.44 \times 10^{-14}$ may be used. As a comparison with the previous for methods, Fowkes' method gives for water $A = .37 \times 10^{-12}$ erg or $B = 33 \times 10^{-60}$ erg-cm^6.

In 1954 Lifshitz (755,748) presented a completely different approach to calculating the attractive force between bodies which treats the solid as a continuum. The basis of the method is that there is a fluctuating electric field present in all materials which although it originates in the changing charge distribution in the atoms, can be investigated by means of macroscopic properties such as the complex dielectric constant. The expression for the Hamaker constant derivable from this theory is:

$$A = \frac{3h}{8\pi^2} \int_o^\infty \left(\frac{\epsilon(i\xi)-1}{\epsilon(i\xi)+1}\right)^2 d\xi \qquad (8)$$

where the dielectric constant ϵ taken along the imaginary

Table 10

ν^d AND A IN WATER FOR VARIOUS SUBSTANCES AT 20° C

Substance (No. 2)	ν^d (Exptl.), Ergs/Sq. Cm.	A Calcd. Ergs
Polyhexafluoropropylene	18	2×10^{-15}
Polytetrafluoroethylene	19.5	8×10^{-16}
Paraffin Wax	25.5	2×10^{-15}
Polymonochlorotrifluoroethylene	30.8	1×10^{-14}
Polyethylene	35	2×10^{-14}
Polystyrene	44	5×10^{-14}
Copper	60	1.4×10^{-13}
Silver	76	2.5×10^{-13}
Anatase (TiO_2)	91	3.5×10^{-13}
Iron	98	4×10^{-13}
Lead	99	4×10^{-13}
Tin	101	4×10^{-13}
Ferric Oxide	107	4.5×10^{-13}
Graphite	110	5×10^{-13}
Stannic Oxide	118	5.5×10^{-13}
Silica	123	6×10^{-13}
Rutile (TiO_2)	143	8×10^{-13}
Mercury	200	1.3×10^{-12}

frequency axis ($i\xi$) is given by the Kronig-Dramers relation (752):

$$\epsilon(i\xi) = 1 + \frac{2}{\pi}\int_{0}^{\infty} \frac{\omega\epsilon''(\omega)}{\omega^2 + \xi^2}\, d\omega \qquad (9)$$

where $2\pi h\omega$ is the photon energy. The spectra $\epsilon''(\omega)$ is determined experimentally and is presently available for only a few materials. Other papers following this approach are references 753, 754, 766 and 768.

When the interacting particles are not in a vacuum but are separated by a medium such as water, the attractive force is diminished due to the interaction between the molecules of the medium themselves and between the particles. The appropriate value of A is obtained as follows (750,751). Consider the change in energy that results when two particles initially far apart are brought close together as shown in Figure 15.

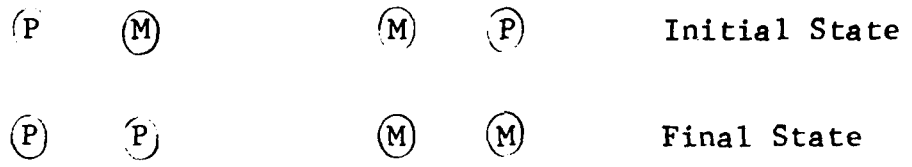

Figure 15

PARTICLES P IN MEDIUM M

The energy of the initial state is $2E_{PM}$ where the subscripts denote the mutual interactions of particle and medium atoms. The energy of the final state is $E_{PP} + E_{MM}$ where the subscripts denote interactions of particle atoms with each other and medium atoms with each other. Thus, the energy change is $E_{PP} + E_{MM} - 2E_{PM}$. Since the energy is proportional

to the Hamaker constant, the appropriate A is:

$$A = A_{PP} + A_{MM} - 2A_{PM} \tag{10}$$

If it is assumed that $A_{PM} = \sqrt{A_{PP}\, A_{MM}}$, then:

$$A = A_{PP} + A_{MM} - 2\sqrt{A_{PP}\, A_{MM}}$$

$$A = (\sqrt{A_{PP}} - \sqrt{A_{MM}})^2 \tag{11}$$

Some values of A calculated in this way are given in Table 11.

4.2 Retardation of London-Van der Waals Forces

For distances between atoms greater than the characteristic wavelength λ of the absorption spectrum of the material, London's equation must be modified. London assumed that each atom responded instantaneously to the fluctuating electric field of the other. However, due to the finite speed of light the electric field of one atom requires a certain time to reach the other so that the charge distribution in the first atom may have changed. Since the frequency with which electrons travel about the nucleus is related to the frequency of radiation emitted or absorbed by the atom, in the time it takes information concerning the charge to travel a distance λ, the charge distribution will have completely changed. Casimir and Polder (745) using quantum electrodynamics solved this problem, and their results can be presented by means of a correction function shown in Figure 16 and given analytically (751) by:

$$V_{Retarded} = V_{London}\, f(p) \tag{12}$$

where

$$p = \frac{2\pi r}{\lambda}\ ,\ \lambda = \frac{c}{\nu}$$

$$f(p) = 1.01 - .14p\ ,\ 0 < p < 3$$

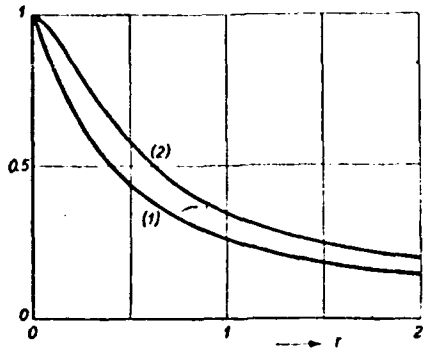

Figure 16

CORRECTION FACTOR DUE TO RETARDATION FOR THE CONTRIBUTION OF ONE EXCITED STATE TO THE USUAL LONDON ENERGY. (1) FOR THE INTERACTION BETWEEN A NEUTRAL ATOM AND A METALLIC WALL. r IS MEASURED IN UNITS 1/2 λ (2) FOR THE INTERACTION BETWEEN TWO NEUTRAL ATOMS. r IS MEASURED IN UNITS λ.

$$f(p) = \frac{2.45}{p} - \frac{2.04}{p^2} \quad , \quad 3 < p < \infty$$

and c is the speed of light.

4.3 Attraction Between Macroscopic Bodies

An important result of the quantum mechanics treatment is that to a good approximation London-Van der Waals forces between atoms are additive so that in an assembly of atoms each atom attracts all the others independent of the surrounding atoms.

Only in the case of a high density of atoms are the attractive forces slightly weakened by the dielectricum through which they are transmitted. This additive property allows one to find the London energy for macroscopic bodies by simple summation or integration over all pairs of atoms. Thus, the attractive energy between two particles contining q atoms/cm^3 without retardation is:

$$V_A = - \int_{V_1} dV_1' \int_{V_2} dV_2' \frac{q^2 B}{r^6} \qquad (13)$$

where dV_1', dV_2', V_1 and V_2 denote differential volume elements and total volumes of particles 1 and 2 respectively and r is the distance between dV_1' and dV_2'.

4.4 Two Spherical Particles (750,746)

Consider the system shown in Figure 17. The surface S_{ABC} is given by:

$$S_{ABC} = 2\pi \int_0^{\theta_o} r^2 \sin\theta d\theta \qquad (14)$$

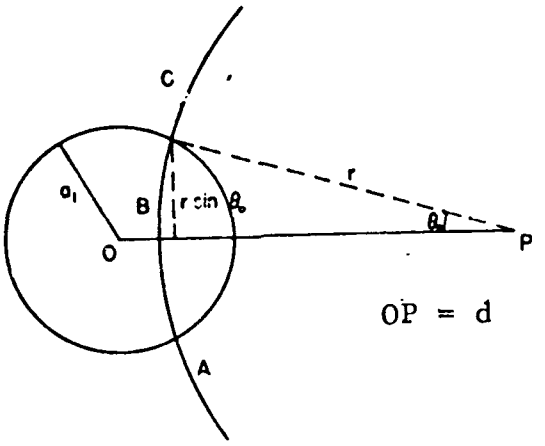

Figure 17

COORDINATE SYSTEM BETWEEN A SPHERE AND A POINT

where

$$a_1^2 = d^2 + r^2 - 2rd \cos \theta_o$$

Thus, integrating:

$$S_{ABC} = \frac{\pi r}{d}\left[a_1^2 - (d - r)^2\right] \tag{15}$$

Since $dV_1' = S_{ABC}dr$, the energy between an atom at P and a sphere at O is:

$$V_P = -\int_{d-a_1}^{d+a_1} \frac{Bq\pi}{r^6}\,\frac{r}{d}\left[a_1^2 - (d - r)^2\right] dr \tag{16}$$

Then, the energy between two spheres as shown in Figure 18 is:

$$V_A = \int_{R-a_2}^{R+a_2} V_P q\pi\,\frac{d}{R}\left[a_2^2 - (R - d)^2\right] dd \tag{17}$$

Carrying out the integration yields:

$$V_A = \frac{q^2\pi^2 B}{6}\left[\frac{2a_1a_2}{R^2 - (a_1 + a_2)^2} + \frac{2a_1a_2}{R^2 - (a_1 - a_2)^2} + \ln\frac{R^2 - (a_1 + a_2)^2}{R^2 - (a_1 - a_2)^2}\right] \tag{18}$$

For spheres of equal size $a_1 = a_2 = a$:

$$V_A = -\frac{A}{6}\left[\frac{2a^2}{R^2 - 4a^2} + \frac{2a^2}{R^2} + \ln\left(1 - \frac{4a^2}{r^2}\right)\right] \tag{19}$$

This equation is shown graphically in Figure 19.

For very small distances of separation so that $R \approx 2a$

$$V_A \approx -\frac{A}{12}\,\frac{a}{S} \tag{20}$$

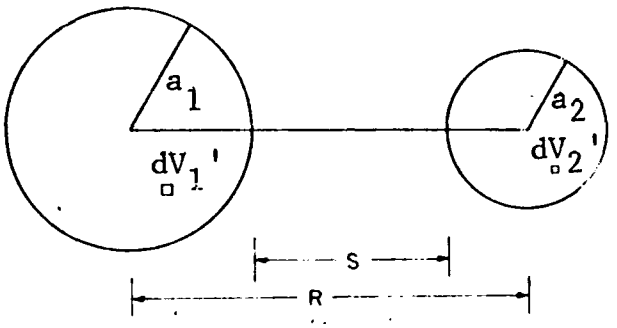

Figure 18

COORDINATE SYSTEM BETWEEN TWO SPHERES

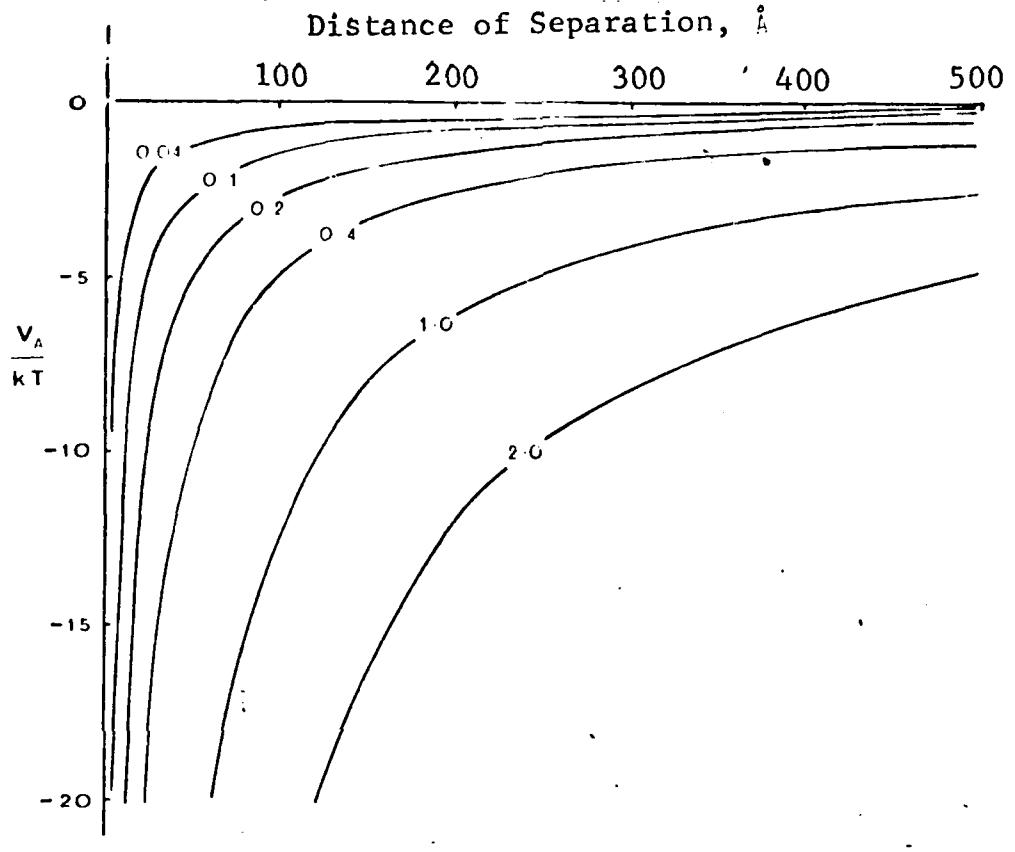

Figure 19

ATTRACTION POTENTIAL AT VARYING DISTANCES OF SEPARATION BETWEEN THE PARTICLE SURFACE, USING THE HAMAKER EQUATION FOR PARTICLES OF 0.04, 0.1, 0.2, 0.4, 1.0 AND 2.0 MICRONS DIAMETER $A_P = 1.1 \times 10^{-12}$ erg, $A_M = 5 \times 10^{-13}$ erg - Ref. 747

while for large distance R >> 2a:

$$V_A \approx - \frac{16A}{9} \frac{a^6}{S^6} \tag{21}$$

where S is the shortest distance between the spheres (see Figure 19).

These equations are valid only if retardation is neglected. In order to include retardation the corrected London equation is used, and the same integration procedure as previously given is followed. The results of Overbeek (751) are presented in graphical form in Figure 20. Schenkel and Kitchener (767,769) derived the corresponding analytical expressions for small distances S << a:

$$V_{Retarded} = \frac{Aa}{12S} \left(\frac{1}{1 + 1.77p_o}\right) , \quad 0 < p_o < 2$$

$$V_{Retarded} = \frac{Aa}{S} \left[- \frac{2.45}{60p_o} + \frac{2.17}{180p_o^2} - \frac{.59}{420p_o^3} \right] , \quad .5 < p_o < \infty \tag{22}$$

where

$$p_o = \frac{2\pi S}{\lambda}$$

while Wiese and Healy (775) extended their treatment to spheres of unequal radii giving:

$$V_{Retarded} = \frac{Aa_1a_2}{6S(a_1 + a_2)} \left(\frac{1}{1 + 1.77p_o}\right), \quad 0 < p_o < 2$$

$$V_{Retarded} = \frac{2Aa_1a_2}{S(a_1 + a_2)} \left[- \frac{2.45}{60p_o} + \frac{2.17}{180p_o^2} - \frac{.59}{420p_o^3} \right] , \quad .5 < p_o < \infty \tag{23}$$

One difficulty of these equations is that when S = 0 an infinitely large value for V_A is obtained. This is due to the face that Born-repulsion forces which prevent the interpenetration of matter were not taken into account. Thus,

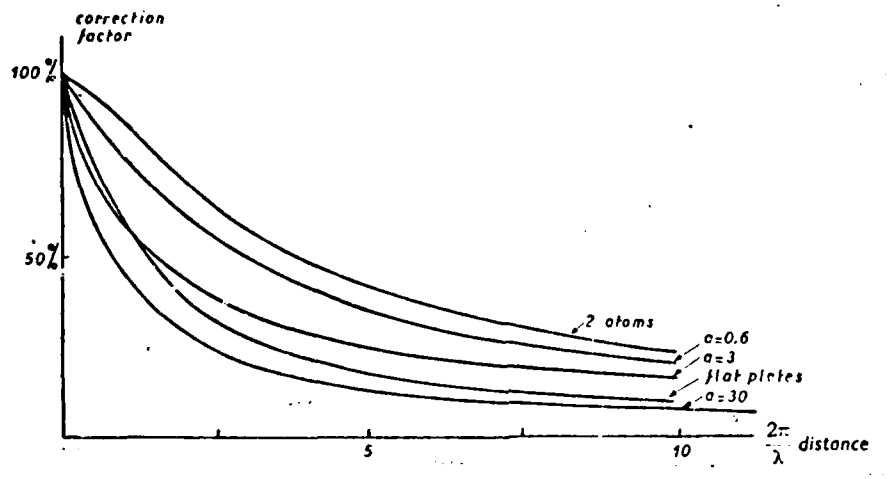

Figure 20

RETARDATION CORRECTION FACTOR TO THE LONDON ATTRACTION BETWEEN TWO EQUAL SPHERICAL PARTICLES. THE RADII OF THE PARTICLES ARE RESP. 0.6, 3 AND 30 TIMES $\frac{\lambda}{2\pi}$ WHERE λ IS THE LONDON-WAVELENGTH. THE ABSCISSA IS THE SHORTEST DISTANCE BETWEEN THE TWO SPHERES AGAIN EXPRESSED IN MULTIPLES OF $\frac{\lambda}{2\pi}$.

these equations would not be expected to be valid for distances smaller than an atomic diameter or 3Å.

4.5 Flat Surface and a Spherical Particle

Letting $X = S/2a$ and $Y = a_2/a_1$ where a is the smaller of a_1 and a_2 and taking the limit as $Y \longrightarrow \infty$, one arrives at the expression for the energy between a sphere and a flat surface:

$$V_A = -\frac{A}{12}\left(\frac{1}{X} + \frac{1}{1+X} + 2\ln\frac{X}{1+X}\right) \qquad (24)$$

When $X << 1$, one obtains the result for small distances:

$$V_A = -\frac{A}{6}\frac{a}{S} \qquad (25)$$

4.6 Other Configurations

The attractive energy for two plates of thickness δ at a distance 2d from each other is given by Verwey and Overbeek (771) as:

$$V_A = -\frac{A}{48\pi}\left[\frac{1}{d^2} + \frac{1}{(d+\delta)^2} - \frac{2}{(d+\delta/2)^2}\right] \qquad (26)$$

with the limiting cases:

$$V_A = -\frac{\delta^2 A}{32\pi d^4}, \quad d >> \delta$$

$$V_A = -\frac{A}{48\pi d^2}, \quad d << \delta \qquad (27)$$

Vold (773) has presented expressions for the attraction between anisometric particles such as rods, cylinders, and plates.

4.7 Effect of Adsorbed Layers

Vold (772) investigated the relationship between the thickness and nature of absorbed layers and the force of attraction between two spherical particles. As shown earlier, the interaction energy is the sum of the interaction energy of two solvated particles V_S and that of two phantom particles with the composition of the medium V_P minus twice that of a solvated particle and a phantom particle V_D. The individual terms are obtained as follows. Let the thickness of the adsorbed layer be δ. V_D will be obtained first. According to Hamaker's equation, the energy between a sphere of radius $R + \delta$ composed of the adsorbate (S) and a second sphere composed of the medium (M) is:

$$V_1 = -\frac{1}{12} A_{MS} H \left(\frac{S}{2(a + \delta)}, 1\right) \qquad (28).$$

where

$$H(X,Y) = \frac{Y}{X^2 + XY + X} + \frac{Y}{X^2 + XY + X + Y} + 2\ln \frac{X^2 + XY + X}{X^2 + XY + X + Y}$$

If a sphere of radius R is withdrawn from the sphere of adsorbate and replaced with a particle, the energy is decreased by:

$$V_2 = -\frac{1}{12} A_{MS} H \left(\frac{S + \delta}{2a}, \frac{a + \delta}{a}\right) \qquad (29)$$

and increased by:

$$V_3 = -\frac{1}{12} A_{PM} H \left(\frac{S + \delta}{2a}, \frac{a + \delta}{a}\right) \tag{30}$$

Thus,

$$V_D = V_1 - V_2 + V_3 = -\frac{1}{12} \left(A_{MS} H_S - A_{MS} H_{PS} + A_{PM} H_{PS}\right) \tag{31}$$

where for convenience:

$$H_S = H \left(\frac{S}{2(a + \delta)}, 1\right) \tag{32}$$

$$H_{PS} = H \left(\frac{S + \delta}{2a}, \frac{a + \delta}{a}\right) \tag{33}$$

To obtain V_S, consider a solvated particle and a sphere of adsorbate whose energy by analogy with V_D is:

$$V_3 = -\frac{1}{12} \left[A_S H_S - A_S H_{PS} + A_{PS} H_{PS}\right] \tag{34}$$

If a sphere of radius a is removed the sphere of adsorbate and replaced by a particle, the energy is decreased by:

$$V_5 = -\frac{1}{12} \left[A_S H_{PS} - A_S H_P + A_{PS} H_P\right] \tag{35}$$

and increased by:

$$V_6 = -\frac{1}{12} \left[A_{PS} H_{PS} - A_{PS} H_P + A_{PP} H_P\right] \tag{36}$$

where

$$H_P = H \left(\frac{S + 2\delta}{a}, 1\right) \tag{37}$$

Thus,

$$V_S = V_4 - V_5 + V_6 \tag{38}$$

Also,

$$V_P = A_M H_S \tag{39}$$

Combining all these equations and using the relationships $A_{PS} = \sqrt{A_P A_S}$ and $A_{MS} = \sqrt{A_M A_S}$, the total interaction energy is:

$$V_A = -\frac{1}{12}\left[(A_M^{1/2} - A_S^{1/2})^2 H_S + (A_S^{1/2} - A_P^{1/2})^2 H_P + 2(A_M^{1/2} - A_S^{1/2})(A_S^{1/2} - A_P^{1/2}) H_{PS}\right] \tag{40}$$

This equation is shown graphically in Figures 21 and 22. As can be seen, the presence of an adsorbed layer reduces the magnitude of the attractive energy, and the effect increases with increasing thickness of the adsorbed layer. For the values of the Hamaker constants used, increasing the thickness of the adsorbed layer by 50Å with particles below .2 μ has little effect while with particles about 1 μ there is little difference between adsorbed layers of 75 and 100Å. References 772, 759, and 747 present further examples.

4.8 Repulsion Forces Due to the Electrical Double Layer

When a solid particle is placed in a liquid solution, the particle may acquire an electrical charge in the following ways: (1) ionogenic groups such as -COOH present in the

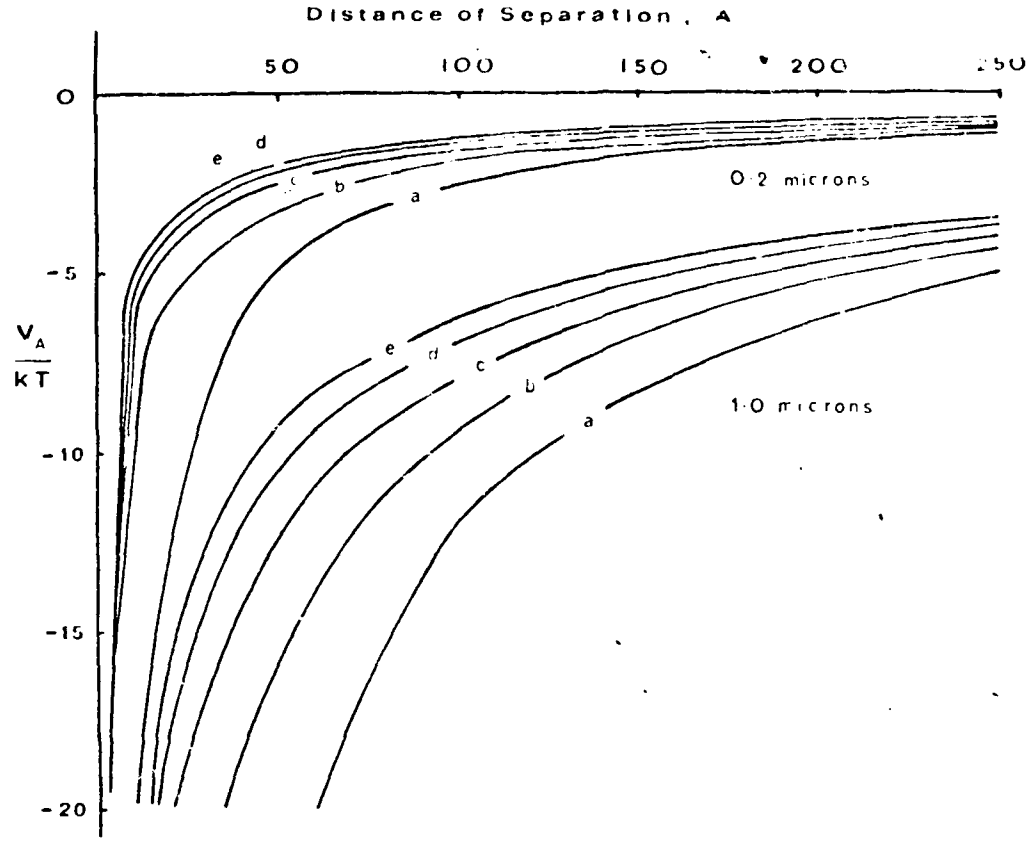

Figure 21

ATTRACTION POTENTIAL BETWEEN PARTICLES OF 0.2 AND 1.0 MICRONS DIAMETER USING THE VOLD EQUATION, WITH VARYING THICKNESSES OF ADSORBED LAYER, (a) nil (b) 25Å (c) 50Å (d) 75Å (e) 100Å, $A_P = 1.1 \times 10^{-13}$ erg, $A_S = 7 \times 10^{-13}$ erg

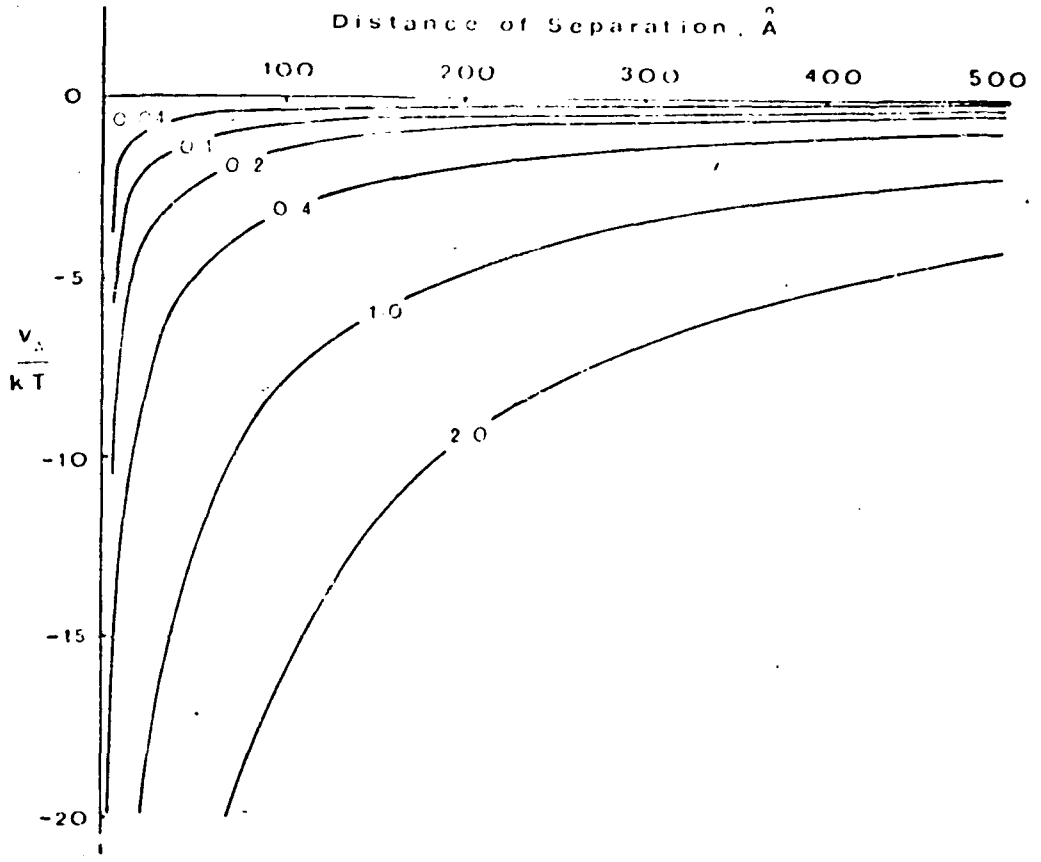

Figure 22

ATTRACTION POTENTIAL WITH ADSORBED LAYERS OF MEDIUM 50 ÅNGSTROMS THICK, AT VARYING DISTANCES OF SEPARATION BETWEEN THE OUTER SURFACES OF THE ADSORBED LAYERS, USING THE VOLD EQUATION, FOR PARTICLES OF 0.04, 0.1, 0.2, 0.4, 1.0 AND 2.0 MICRONS DIAMETER, $A_p = 1.1 \times 10^{-12}$ erg, $A_S = 7 \times 10^{-13}$ erg

particle surface dissociate; (2) the ions of which the particle is composed dissolve unequally; (3) the particle preferentially adsorbs one of the types of ions in the solution; (4) dipolar molecules are at the particle surface. In general, dispersed particles are more often negatively charged than positively because anions are usually less strongly hydrated, and thus more readily specifically adsorbed than cations. Due to this excess charge on the particle surface, ions of the opposite sign are strongly attracted to it. However, these ions are not all adsorbed on the surface because their Brownian or thermal motion resists the electrical attraction. The result is that the particle is surrounded by a layer of ions of the opposite charge.

This layer extends over a certain distance from the particle surface, and its charge diminishes gradually with increasing distance. The term "double layer" refers to the surface charge layer and this diffuse layer in the solution.

Although the total charge on the particle surface consists of discrete charges, it is mathematically convenient to treat it as homogeneous surface charge. Similarly, the liquid layer is considered as a continuous space charge instead of discrete ionic charges.

4.9 The Poisson-Boltzmann Equation (801,816,821,794,795)

The equation which relates the average electrical potential Ψ and average charge density in the electrical double layer is the well known Poisson equation from electromagnetic theory (for derivation see Appendix I, page 165):

$$\nabla^2 \Psi = - \frac{4\pi\rho}{\epsilon} \qquad (41)$$

where ∇^2 is the Laplace operator and ϵ the dielectric constant of the medium.

The average concentration n_i of ions of type i at a distance from the particle surface is given in terms of the

average electrical potential according to the Boltzmann distribution (for derivation see Appendix II, page 166):

$$n_i = n_{io} \exp - \frac{z_i e \psi}{kT} \qquad (42)$$

where n_{io} is the concentration at zero potential in the bulk of the solution, z_i valency, e charge of the electron, k Boltzmann constant and T absolute temperature. This equation accounts for the fact that negative ions concentrate at positions of positive potential while positive ones are repelled with the reverse being true for negative potentials.

The space charge density is given by the sum of the ionic charges:

$$\rho = \sum_i z_i e n_i \qquad (43)$$

Combining equations 41, 42, and 43, one obtains a differential equation which gives the potential as a function of position:

$$\nabla^2 \psi = - \frac{4\pi}{\epsilon} \Sigma z_i e n_{io} \exp \left[- \frac{z_i e \psi}{kT} \right] \qquad (44)$$

This equation is known as the Poisson-Boltzman equation.

When the solution consists only of ions of the same valency, equation 44 can be written as:

$$\nabla^2 \psi = \frac{8\pi n_o ze}{\epsilon} \text{Sinh} \left(\frac{ze\psi}{kT} \right) \qquad (45)$$

4.10 Single Flat Double Layer

For a flat double layer, equation 45 becomes:

$$\frac{d^2 \psi}{dx^2} = \frac{8\pi n_o ze}{\epsilon} \text{Sinh} \left(\frac{ze\psi}{kT} \right) \qquad (46)$$

where x is the distance from the surface and is subject to

the boundary conditions:

$$\psi = \psi_o \text{ at } x = 0 \tag{47a}$$

$$\psi = \frac{d\psi}{dx} = 0 \text{ at } x \longrightarrow \infty \tag{47b}$$

Integrating equation 46 once and using equation 47b:

$$\frac{d\psi}{dx} = -\sqrt{\frac{32\pi kTn_o}{\epsilon}} \operatorname{Sinh} \frac{ze\psi}{2kT} \tag{48}$$

From equation 48 the surface charge σ may be obtained since due to electroneutrality it must equal the total space charge. Thus,

$$\sigma = -\int_o^\infty \rho dx = \int_o^\infty \frac{\epsilon}{4\pi} \frac{d^2\psi}{dx^2} dx = -\frac{\epsilon}{4\pi} \frac{d\psi}{dx}\bigg|_{x=0}$$

$$= -\sqrt{\frac{2\epsilon kTn_o}{\pi}} \operatorname{Sinh} \left(\frac{ze\psi_o}{2kT}\right) \tag{49}$$

Integrating a second time and using equation 47a:

$$\kappa x = \ln \left[\frac{\tanh (ze\psi_o/4kT)}{\tanh (ze\psi/4kT)} \right] \tag{50}$$

where

$$\kappa^2 = \frac{8\pi n_o e^2 z^2}{\epsilon kT}$$

For small potentials equations 49 and 50 can be simplified to read:

$$\sigma = \frac{\epsilon\kappa}{4\pi} \psi_o \tag{51}$$

$$\psi = \psi_o e^{-\kappa x} \tag{52}$$

Equations 50 and 52 are illustrated in Figure 23.

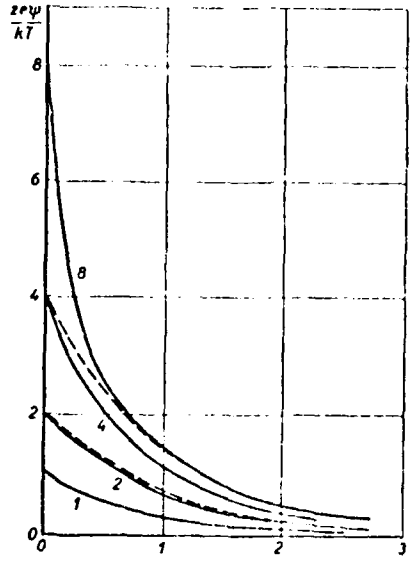

Figure 23

ELECTRIC POTENTIAL IN THE DOUBLE LAYER. THE CURVES MARKED 1, 2, 4, 8 ARE DRAWN ACCORDING TO THE EXACT EQUATION FOR $\frac{ze\psi_o}{kT}$ = 1, 2, 4 AND 8 RESP. THE DOTTED LINES FOLLOW THE APPROXIMATE EQUATION.

REF. 801

Guggenheim (792) has numerically solved the Poisson-Boltzmann equation for unsymmetrical electrolytes.

4.11 Free Energy of the Double Layer (821,801,803,804)

An important thermodynamic quantity from which the energy of repulsion between two surfaces due to the double layer is the free energy. In order to derive an expression for it, consider an imaginary charging process in which the charge of all ions is gradually increased from zero to the actual value. Let the degree of the charging process be indicated by a parameter λ which goes from zero to one. At state λ all ionic charges are increased by $z_i e d\lambda$ so that ρ and σ increase by $\rho d\lambda/\lambda$ and $\sigma d\lambda/\lambda$, respectively. Also the chemical potential of excess ions on the surface increases by $\frac{\sigma}{\lambda e} \frac{\partial \mu}{\partial \lambda} d\lambda$ for all ions per unit volume. The work done at this state is then:

$$dG = \int_{\text{Volume}} \rho \psi dV \frac{d\lambda}{\lambda} + \int_{\text{Surface}} \sigma \psi_o dS \frac{d\lambda}{\lambda} + \int_{\text{Surface}} \frac{\sigma}{\lambda e} \frac{\partial \mu}{\partial \lambda} d\lambda dS \qquad (53)$$

Integrating equation 53 with respect to λ, the free energy is:

$$G = G_0 + \int_o^1 \frac{d\lambda}{\lambda} \int_V \rho \psi dV + \int_o^1 \frac{d\lambda}{\lambda} \int_S \sigma \psi_o dS + \int_o^1 \frac{d\lambda}{\lambda} \frac{\sigma}{e} \frac{\partial \Delta\mu}{\partial \lambda} \int_S dS \qquad (54)$$

where G_0 is the free energy at $\lambda = 0$ and $\Delta\mu = \mu - \mu_o$. Since the double layer is solution in equilibrium $\Delta\mu + \lambda e \psi_o = 0$.

A convenient way to integrate equation 54 is under the condition that ψ_o is constant so that:

$$G = G_0 + \int_o^1 \frac{d\lambda}{\lambda} \int \rho\psi dV \tag{55}$$

For a flat double layer $G_0 = 0$ and:

$$G = \int_o^1 \frac{d\lambda}{\lambda} \int \rho\psi dV = -\frac{\epsilon}{4\pi} \int_o^1 \frac{d\lambda}{\lambda} \int_o^\infty \psi \frac{d^2\psi}{dx^2} dx$$

$$= \frac{\epsilon}{4\pi} \int_o^1 \frac{d\lambda}{\lambda} \int_{\psi = 0}^{\psi = \psi_o} \psi d\left(\frac{d\psi}{dx}\right) \tag{56}$$

Substituting equation 48 for $\frac{d\psi}{dx}$ into 56 with e replaced by λe:

$$G = -\sqrt{\frac{2\epsilon n_o kT}{\pi}} \int_o^1 \int_o^{\psi_o} \frac{\psi}{\lambda} \cosh\left(\frac{z\lambda e\psi}{2kT}\right) \frac{z\lambda e}{2kT} d\lambda d\psi$$

$$= -\frac{8n_o kT}{\kappa} \left[\cosh \frac{ze\psi_o}{2kT} - 1\right] \tag{57}$$

4.12 Single Spherical Double Layer (821,801)

In spherical coordinates equation 45 becomes:

$$\frac{1}{r^2} \frac{d}{dr}\left(r^2 \frac{d\psi}{dr}\right) = \frac{8\pi n_o ze}{\epsilon} \operatorname{Sinh}\left(\frac{ze\psi}{kT}\right) \tag{58}$$

subject to the boundary conditions:

$$\psi = \psi_o \text{ at } r = a$$

$$\psi = \frac{d\psi}{dr} = 0 \text{ at } r \longrightarrow \infty$$

where r is the distance from the center of the particle and a the radius of the particle. In order to obtain an analytical

solution, the hyperbolic term is linearized giving:

$$\frac{1}{r^2}\frac{d}{dr}\left(r^2\frac{d\psi}{dr}\right) = \kappa^2\psi \qquad (59)$$

The solution to equation 59 is:

$$\psi = \psi_o \frac{a}{r} e^{\kappa(a - r)} \qquad (60a)$$

$$\sigma = a\epsilon(1 + \kappa a)\ \psi_o \qquad (60b)$$

A comparison of the approximate solution given by equation 60a and the numerical solution of equation 58 by Müller (811) is given in Table 11.

Table 11

ILLUSTRATING THE DIFFERENCE BETWEEN THE APPROXIMATION AND THE THEORY OF MÜLLER FOR SPHERICAL PARTICLES

κr	$\kappa(r - a)$	$y = \frac{ze\psi}{kT}$	
		Müller	Approximate
0.2	0.0	2.83	2.78
0.5	0.3	0.82	0.82
1.0	0.8	0.25	0.25

Ref. 821

The free energy is obtain by substituting equation 59 and 60a into 55 and noting that $dV = 4\pi r^2 dr$ and $\upsilon_0 = 1/2\ \epsilon a\psi_o^2$:

$$G = -\frac{\epsilon a}{2}(1 + \kappa a)\ \psi_o^2 \qquad (61)$$

4.13 Two Flat Double Layers (821,801)

When two parallel surfaces bearing double layers approach

each other, the two diffuse layers will eventually overlap such that neither one can develop completely (see Figure 24). When the surface potentials are of the same sign, a repulsive force will act between the surfaces while if they are opposite the force will be attractive. Since the free energy, not the total energy, is a measure of the work that has to be performed against the forces resulting from the interaction of the double layers, the repulsive energy based on the free energy change is the proper potential to use in combination with the London-Van der Waals attractive potential.

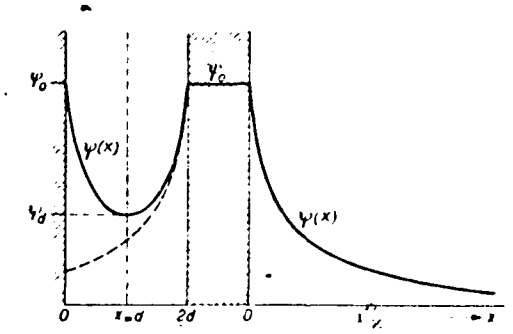

Figure 24

SCHEMATIC REPRESENTATION OF THE ELECTRIC POTENTIAL BETWEEN TWO PLATES, IN COMPARISON WITH THAT FOR A SINGLE DOUBLE LAYER

The governing equation is equation 46:

$$\frac{d^2\psi}{dx^2} = \frac{8\pi n_o ze}{\epsilon} \text{Sinh } (\frac{ze\psi}{kT}) \qquad (46)$$

subject to the boundary conditions:

$$\psi = \psi_o \text{ at } x = 0 \qquad (62a)$$

$$\psi = \psi_o \text{ at } x = 2d \qquad (62b)$$

However, the integration is more conveniently carried out by

replacing the second boundary condition with:

$$\psi = \psi_d \text{ and } \frac{d\psi}{dx} = 0 \text{ at } x = d$$

Integrating once and using the second boundary condition:

$$\frac{d\psi}{dx} = -\sqrt{\frac{8\pi kT}{\epsilon}} \sqrt{2 \cosh \left(\frac{ze\psi}{kT}\right) - 2 \cosh \left(\frac{ze\psi_d}{kT}\right)} \qquad (63)$$

Making the change of variables:

$$Y = \frac{ze\psi}{kT}, \quad Z = \frac{ze\psi_o}{kT}, \quad U = \frac{ze\psi_d}{kT}$$

and

$$\xi = \kappa x$$

simplifies equation 63 to:

$$\frac{dY}{d\xi} = -\sqrt{2 \cosh Y - 2 \cosh U}$$

which when integrated between $\xi = 0$ and $\xi = \kappa d$ gives:

$$\int_Z^U \frac{dY}{\sqrt{2 (\cosh Y - \cosh U)}} = -\kappa d \qquad (64)$$

Equation 64 can be reduced an elliptical integral to give the relation between ψ_o and ψ_d (801):

$$\kappa d = 2 \exp (-U/2) \left\{ F(e^{-U}, \pi/2) - F\left[e^{-U}, \text{Sin}^{-1} (e^{-(Z - U)/2})\right] \right\} \qquad (65)$$

where F is an elliptical integral of the first kind defined as:

$$F(k, \varphi) = \int_o^{\varphi} \frac{d\alpha}{\sqrt{1 - k^2 \text{Sin}^2 \alpha}}$$

Verwey and Overbeek (821) have tabulated equation 65, and their results are shown graphically in Figure 25.

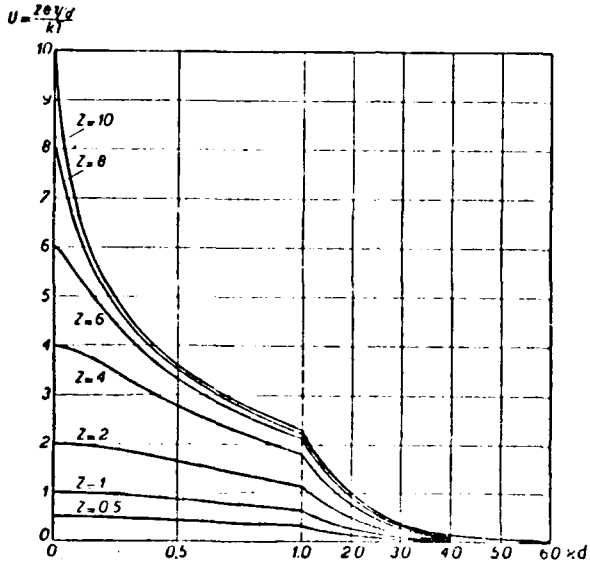

Figure 25

POTENTIAL (ψ_d) HALF-WAY BETWEEN THE PLATES AS A FUNCTION OF THE PLATE DISTANCE (2d) FOR DIFFERENT VALUES OF THE SURFACE POTENTIAL (ψ_o). IN THE FIGURE THE VALUES OF $U = \frac{ze\psi_d}{kT}$, $Z = \frac{ze\psi_o}{kT}$ AND κd ARE GIVEN

If the interaction is small so that $\kappa d \gg 1$, equation 65 can be approximated by:

$$\psi_d = \frac{8kT\nu}{ze} \exp(-\kappa d) \qquad (65a)$$

where

$$\nu = \frac{e^{Z/2} - 1}{e^{Z/2} + 1}$$

Proceeding as for the single flat double layer, it can be shown rather laborously that the free energy of each plate

is (821):

$$G = -\frac{2n_o kT}{\kappa}\left\{\frac{\kappa d}{2}(3e^{U} - 2 - e^{-U}) + 2\sqrt{2\cosh Z - 2\cosh U} - 4e^{U/2}\left[E(e^{-U}, \pi/2) - E(e^{-U}, \mathrm{Sin}^{-1}(e^{-\frac{Z-U}{2}}))\right]\right\}$$

where E is an elliptical integral defined as:

$$E(k, \varphi) = \int_o^{\varphi} \sqrt{1 - k^2 \mathrm{Sin}^2 \alpha}\, d\alpha$$

Since the change in free energy is equal to the work performed when the two surfaces are brought together from an infinite distance of separation, the potential energy of repulsion per unit area of the plates is:

$$V_R = 2(G - G_\infty) \qquad (66)$$

where

$$G_\infty = \lim_{d \to \infty} G = -\frac{2n_o kT}{\kappa}(4\cosh\frac{Z}{2} - 4)$$

When equation 66 is evaluated in conjuction with equation 65 for ψd, the repulsive potential as a function of separation can be found and is shown in Figure 26.

Alternate approaches to calculating the repulsive potential between two flat double layers have been given by Langmuir (802), Derjaquin (786), and Bergmann, Low-Beer, and Zocher (777). If two large plates with liquid between them but confined on the outside by a neutral material in contact with a liquid reservoir at pressure p_∞ and zero potential are

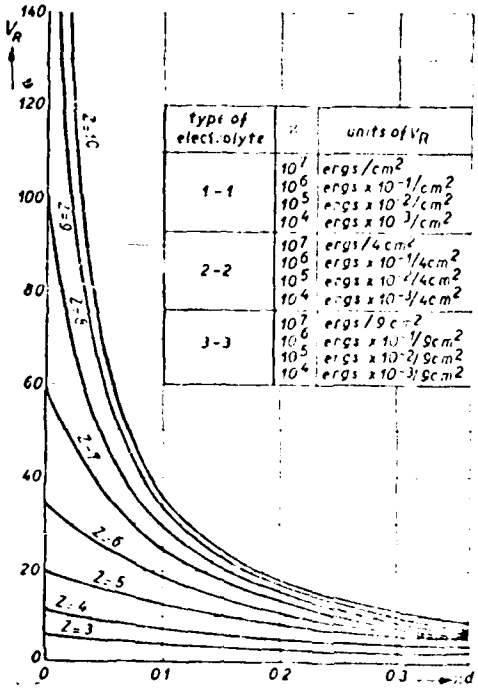

Figure 26

REPULSIVE POTENTIAL AS A FUNCTION OF κd,
FOR STRONG INTERACTION (SMALL κd)

Ref. 801

considered, a force balance on an element of liquid volume gives:

$$\frac{dP}{dx} + \rho \frac{d\psi}{dx} = 0 \qquad (67)$$

where P is the hydrostatic pressure.

Substituting for ρ:

$$\frac{dP}{dx} - \frac{\epsilon}{4\pi} \frac{d^2\psi}{dx^2} \frac{d\psi}{dx} = 0$$

$$\frac{d}{dx}\left[P - \frac{\epsilon}{8\pi} \left(\frac{d\psi}{dx}\right)^2\right] = 0$$

Integrating:

$$P - \frac{\epsilon}{8\pi} \left(\frac{d\psi}{dx}\right)^2 = \text{const}$$

Since $\frac{d\psi}{dx} = 0$ for $P = P_d$, the constant equals P_d. The difference $P_d - P_\infty$ is the force driving the plates apart so that integrating equation 67 between P_d and P_∞ or ψ_d and $\psi = 0$.

$$p = P_d - P_\infty = -\int_o^{\psi_d} \rho d\psi = \int_o^{\psi_d} 2en_o z \sinh\left(\frac{ze\psi}{kT}\right) d\psi$$

$$= 2n_o kT \left[\cosh\left(\frac{ze\psi_d}{kT}\right) - 1\right] \qquad (68)$$

The repulsive potential is then given by:

$$V_R = -2\int_\infty^d p\,d(d) \qquad (69)$$

Since the expression for ψ_d is rather complex, it is not possible to integrate equation 69 analytically. However, for small interaction, the linearized form of equation 68 may be

used:

$$p = n_o kT \left[\frac{ze\psi_d}{kT}\right]^2 \tag{70}$$

with equation 65a for ψ_d to give:

$$V_R = -2\int_{\infty}^{d} pd(d) = 64n_o kT\nu^2 \int_{\infty}^{d} e^{-2\kappa d} d(2d)$$

$$= \frac{64n_o kT}{\kappa}\nu^2 e^{-2\kappa d} \tag{71}$$

Another useful expression for V_R for small potentials can be obtained by solving the linearized Poisson-Boltzmann equation (796):

$$\frac{d^2\psi}{dx^2} = \kappa^2\psi \tag{72}$$

subject to:

$$\psi = \psi_{01} \text{ at } x = 0$$

$$\psi = \psi_{02} \text{ at } x = 2d$$

The solution is:

$$\psi = \psi_{01}\cosh \kappa X + \left[\frac{\psi_{02} - \psi_{01}\cosh 2\kappa d}{\sinh 2\kappa d}\right]\sinh \kappa x \tag{73}$$

Since the free energy can be expressed as:

$$G = -\int_o^{\psi_o} \sigma d\psi$$

The simple relation:

$$G = -\frac{1}{2}\sigma\psi_o$$

is obtained for small surface potentials since σ and ψ_o are

proportional in this case.

The surface charge density has been shown to be:

$$\sigma = - \frac{\epsilon}{4\pi} \left(\frac{d\psi}{dx}\right)\Big|_{x = 0}$$

so that:

$$\sigma_1 = - \frac{\epsilon\kappa}{4\pi} \left[\psi_{02} \text{ cosech } 2\kappa d - \psi_{01} \coth 2\kappa d\right] \qquad (74a)$$

$$\sigma_2 = \frac{\epsilon\kappa}{4\pi} \left[\psi_{02} \coth 2\kappa d - \psi_{01} \text{ cosech } 2\kappa d\right] \qquad (74b)$$

Thus, the free energy is:

$$G = - \frac{1}{2} (\sigma_1\psi_{01} + \sigma_2\psi_{02} = \frac{\epsilon\kappa}{8\pi} \left[2\psi_{01}\psi_{02} \text{ cosech } 2\kappa d - \right.$$

$$\left. - (\psi_{01}^2 + \psi_{02}^2) \coth 2\kappa d\right] \qquad (75)$$

Since

$$G_\infty = - \frac{\epsilon\kappa}{8\pi} (\psi_{01}^2 + \psi_{02}^2) \qquad (76)$$

the repulsive potential is:

$$V_R = \frac{\epsilon\kappa}{8\pi} \left[(\psi_{01}^2 + \psi_{02}^2) (1 - \coth 2\kappa d) + \right.$$

$$\left. + 2\psi_{01}\psi_{02} \text{ cosech } 2\kappa d\right] \qquad (77)$$

In Table 12 equation 77 is compared with the exact results computed numerically by Devereux and deBruyn (787). In general, there is good agreement.

4.14 Two Spherical Double Layers

Derjaquin (786) has presented a method of calculating approximately the repulsive potential between two similar spherical double layers from the potential between two flat double layers which has been extended by Hogg et al (796) to dissimilar layers. On the assumption that the thickness of the double layers is small relative to the particle size, the

Table 12

COMPARISON OF LINEAR APPROXIMATION WITH THE TABULATED FUNCTION OF DEVEREUX AND DE BRUYN

ψ_{0_1}(mV)	ψ_{0_2}(mV)	$2\kappa d$	$4\pi V_1/\epsilon\kappa$ (eqn. (15))	$4\pi V_1/\epsilon\kappa$ (Devereux and de Bruyn)
25·6	−25·6	0·01	−199·0000	−198·5000
		0·10	−19·0170	−18·9600
		1·00	1·1640	−1·1510
76·8	−76·8	0·01	−1798·0000	−1681·6500
		0·10	−171·3600	−169·3050
		1·00	−10·4850	−9·4400
		10·00	−0·0009	−0·0006
25·6	0·00	0·01	−49·5000	−49·4510
		0·10	−4·5170	−4·5070
		1·00	−0·1570	−0·1534
76·8	0·00	0·01	−445·5000	−431·2600
		0·10	−40·6530	−39·8100
		1·00	−1·4085	−1·1602
20·48	10·24	0·01	−7·5940	−7·5970
		0·10	−0·4178	−0·4140
		1·00	+0·1468	+0·1466
		5·00	+0·0044	+0·0042
153·60	76·8	0·01	−273·3840	−287·9400
		0·10	−15·0410	−9·3080
		1·00	+5·2480	+5·9800
		5·00	+0·1584	+0·1203

interaction between double layers on spherical particles can be considered to consist of the sum of interactions due to differential parallel rings on the surface of the spheres whose potential is given as that for flat double layers. Thus, the potential between two spherical double layers can be written as:

$$V_R = \int_0^\infty 2\pi h V_{R,\ plate} dh \qquad (78)$$

where $V_{R,\ plate}$ is given by equation 77 and h is the radius of the ring as shown in Figure 27.

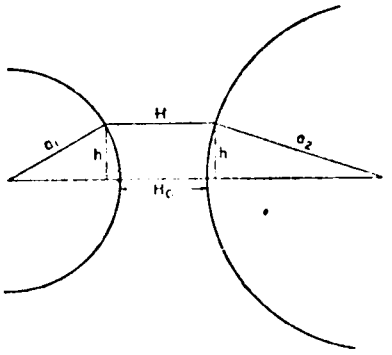

Figure 27

GEOMETRICAL CONSTRUCTION USED IN THE CALCULATION OF THE INTERACTION BETWEEN TWO DISSIMILAR SPHERICAL PARTICLES, RADII a_1 AND a_2 FROM THE INTERACTION OF TWO INFINITE FLAT PLATES

It can be seen from Figure 27 that:

$$H - H_o = a_1 + a_2 - \sqrt{a_1^2 - h^2} - \sqrt{a_2^2 - h^2}$$

so that:

$$dH = \left[\frac{1}{a_1\sqrt{(1 - h^2/a_1^2}} + \frac{1}{a_2\sqrt{1 - h^2/a_2^2}} \right] hdh$$

For $h \ll a_1$ and a_2:

$$hdh \simeq \left(\frac{a_1 a_2}{a_1 + a_2}\right) dH \qquad (79)$$

Thus, equation 78 becomes:

$$V_R = \frac{2\pi a_1 a_2}{a_1 + a_2} \int_{H_o}^{\infty} V_{R,\ plate}(H)dH$$

$$= \frac{\varepsilon a_1 a_2 (\psi_{01}^2 + \psi_{02}^2)}{4(a_1 + a_2)} \left[\frac{2\psi_{01}\psi_{02}}{\psi_{01}^2 + \psi_{02}^2} \ln \left(\frac{1 + e^{-\kappa H_o}}{1 - e^{-\kappa H_o}}\right) + \ln(1 - e^{-2\kappa H_o}) \right] \qquad (80)$$

Equation 80 is a good approximation for $\psi_o < 60$ mV and $\kappa a > 5$.

Verwey and Overbeek (821) similarly calculated the potential using the complete solution to the Poisson-Boltzmann equation by graphical integration. Their results for two equal-sized spheres along with that given by equation 80 are shown in Figure 28.

4.15 Total Potential Energy

The total interaction energy between two particle is given by the sum of the London-Van der Waals attraction potential and the double layer repulsion potential since they operate independently of each other, $V = V_A + V_R$. The general type of potential curve is shown in Figure 29. It is seen that attraction predominates at very small and very large separation distances while at intermediate distance repulsion

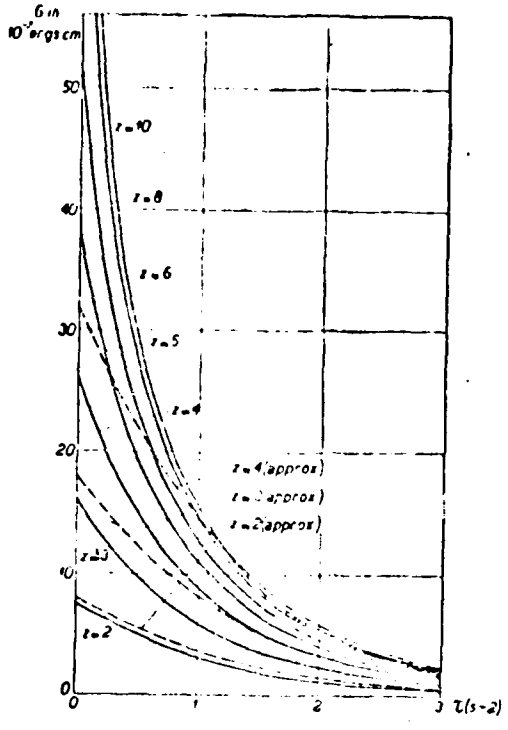

Figure 28

THE REPULSIVE POTENTIAL V_R BETWEEN TWO SPHERICAL PARTICLES, WHEN THE EXACT EXPRESSION FOR HIGH POTENTIALS IS APPLIED. DOTTED LINES = REPULSIVE POTENTIAL ACCORDING TO THE APPROXIMATED EQUATION

Ref. 821

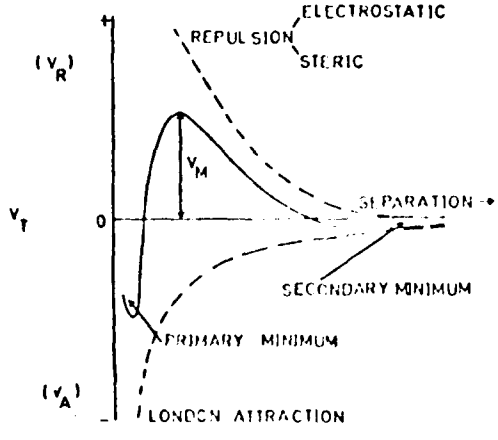

Figure 29

TOTAL POTENTIAL ENERGY (V_T) DIAGRAM FOR TWO COLLOIDAL PARTICLES

may predominate depending on the numerical values of the parameters. The important characteristics of this curve are the primary and secondary minimums and the maximum. The energy barrier due to the maximum in the curve must be overcome by particles in order for them to make lasting contact in the primary minimum. If the thermal energy kT of the particles is much smaller than the maximum, there will be few contacts. However, if the secondary minimum is much greater than kT, the particles can flocculate with a liquid film between them. Systems which have flocculated into the secondary minimum are readily dispersed while this is not true for the primary minimum. Sparnaay (818) has presented an extensive study of the secondary minimum. The effect of electrolyte concentration is shown in Figure 30 and that of surface potential in Figure 31.

4.16 Corrections to the Poisson-Boltzmann Equation

4.16.1 Stern's Correction (819,821)

In the double layer theory presented, no account was taken that the ions have finite size. As a result, unreasonably high values of the surface charge and the concentration near the surface can be calculated. In order to overcome this difficulty, Stern (819) proposed that ψ vary linearly from the surface to a certain distance δ_s and that the potential at this point be used in place of the surface potential in the solutions of Poisson-Boltzmann equation (see Figure 32). The ions in this Stern layer are considered to consist of ions held rather rigidly in place and not subject to thermal motion. If the number of ions adsorbed per unit surface is n_1, then the number of available adsorption sites is $N_1 - n_1$ where N_1 is the total number of absorption sites per unit area. The number of available positions in the solution may be taken to be approximately N/M where N is Avagadro's number and M the molecular weight of the solvent. Neglecting the effect of ions with the same charge as the

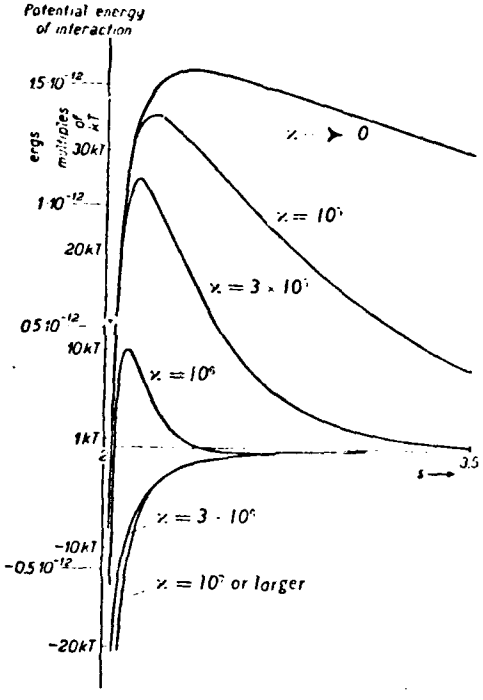

Figure 30

SHOWING THE INFLUENCE OF THE CONCENTRATION OF ELECTROLYTE (κ) ON THE TOTAL POTENTIAL ENERGY OF INTERACTION OF TWO SPHERICAL PARTICLES

$a = 10^{-5}$ cm; $A = 10^{-12}$ ergs; $\psi_o = \frac{kT}{e} = 25.6$ mV

Ref. 801

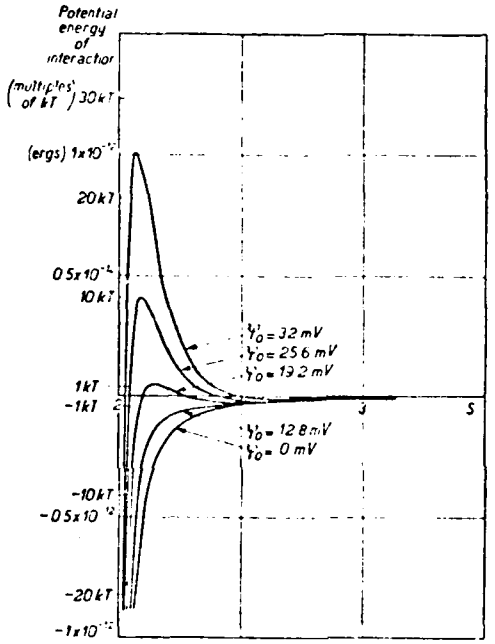

Figure 31

SHOWING THE INFLUENCE OF THE SURFACE POTENTIAL (ψ_o) ON THE TOTAL POTENTIAL ENERGY OF INTERACTION OF TWO SPHERICAL PARTICLES

$a = 10^{-5}$ cm; $A = 10^{-12}$ ergs; $\kappa = 10^{6}$ cm^{-1}

Ref. 801

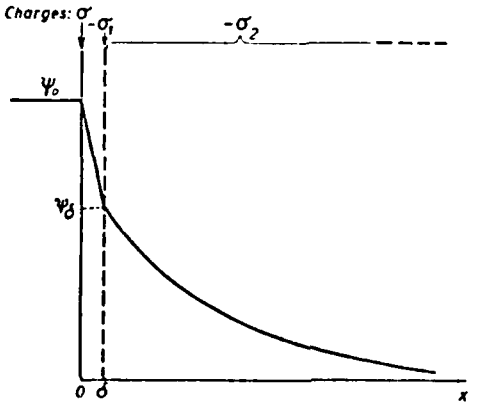

Figure 32

SCHEMATIC REPRESENTATION OF THE DOUBLE LAYER
ACCORDING TO THE THEORY OF STERN

surface, Boltzman's equation gives:

$$\frac{n_1}{n_o} = \frac{(N_1 - n_1)}{N/M} e^{ze\psi_\delta + \varphi}$$

where ψ_δ is the potential at the Stern plane and φ the specific chemical adsorption potential of the counter ion adsorbed to the surface. Davies and Rideal (824) have tabulated values of φ for various systems.

The charge at the Stern plane is thus given by:

$$\sigma_1 = n_1 ze = \frac{N_1 ze}{1 + \frac{N}{n_o M} \exp -\left[\frac{ze\psi_\delta + \varphi}{kT}\right]}$$

This equation in conjunction with the following ones:

$$\sigma = \frac{\epsilon}{4\pi\delta} (\psi_o - \psi_\delta) = c_{Stern} (\psi_o - \psi_\delta)$$

where c_{Stern} is the experimentally determined capacity of the Stern layer which is on the order of 10^7 cm,

$$\sigma_2 = \sqrt{\frac{\epsilon kTn_o}{2\pi}} \text{ Sinh } \left(\frac{ze\psi_\delta}{2kT}\right)$$

as given by the Poisson-Boltzmann equation, and:

$$\sigma = \sigma_1 + \sigma_2$$

expressing conservation of charge allows the values of σ, σ_1, σ_2 and ψ_δ to be calculated given ψ_o.

4.17 Ionic Volume Correction

As indicated before, the Poisson-Boltzmann equation can predict impossibly high concentrations due to the assumption of point charges instead of ions of finite volume. For example, for a 1N solution and a surface potential of 1 volt, a concentration of 2×10^{17} N is obtained at the surface. In

order to account the finite ionic volume, the Boltzmann distribution can be modified to reflect this space restriction. Bikerman (778) argued that the concentrations used in the Boltzmann distribution are based on the unit volume available to the ions. Thus if v_i is the volume of an individual ion of the i^{th} type, the Boltzmann distribution should be rewritten as:

$$n_i = n_{io} e^{-z_i e\psi/kT} \left[\frac{1 - \sum_j v_j n_j}{1 - \sum_j v_j n_{jo}} \right] \tag{81}$$

This equation has also been derived statistically by Schlögl (815) and by Falkenhagen and Kelbg (788) and thermodynamically by Wicke and Eigen (822), Freise (790) and Ohlenbusch (812). Since:

$$\frac{n_i}{n_j} = \frac{n_{io}}{n_{jo}} e^{-(z_i e\psi_i - z_j e\psi_j)/kT}$$

equation 81 can be written as:

$$n_i = \frac{n_{io} e^{-z_i e\psi_i/kT}}{1 + \sum_j v_j n_{jo} e^{-z_j e\psi_j/kT}} \cdot \frac{1}{1 - \sum_j v_j n_{jo}} \tag{82}$$

Therefore, the Poisson-Boltzmann equation is modified to read:

$$\nabla^2 \psi = -\frac{4\pi e}{\epsilon} \left\{ \frac{\sum_j z_j n_{jo} e^{-z_j e\psi/kT}}{1 + \frac{1}{1 - \sum_j v_j n_{jo}} \sum_j v_j n_{jo} e^{-z_j e\psi/kT}} \right\} \cdot \frac{1}{1 - \sum_j v_j n_{jo}} \tag{83}$$

For a symmetrical binary electrolyte, equation 83 becomes:

$$\nabla^2\psi = \frac{8\pi e z n_o}{\epsilon} \frac{\text{Sinh } (ze\psi/kT)}{1 + 2vn_o [\cosh (ze\psi/kT) - 1]} \quad (84)$$

A comparison of the charge as given with the corrected Boltzmann distribution and the uncorrected one is presented in Figure 33a and 33b for $2vn_o = .1$ and 1, respectively.

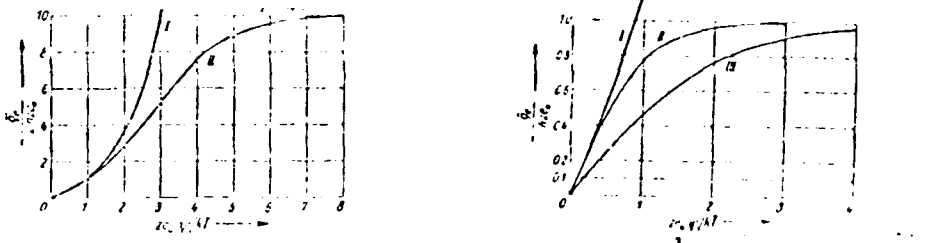

a $2n_ov = .1$ b $2n_ov = 1$

Figure 33

CHARGE VS. POTENTIAL CURVE I ACCORDING TO BOLTZMANN DISTRIBUTION; CURVE II ACCORDING TO IONIC VOLUME CORRECTION.

Ref. 822

4.18 Dielectric Saturation

In the Poisson-Boltzmann equation, the dielectric constant of the medium in the double layer is treated as a constant equal to that in the bulk of the solution. This may not be true because electric fields and high concentrations can significantly affect the dielectric constant. Malsch (808) experimentally found for field strengths in the order of 10^5 V/cm the relationship:

$$\epsilon = \epsilon_o + \alpha E^2$$

where E is the field strength, ϵ_o the dielectric constant at zero field strength, and α a constant around -3×10^{-6} for E expressed in esu units. Grahame (791) argued that a more

general empirical equation would be:

$$\varepsilon = \frac{\varepsilon_o - \varepsilon_\infty}{\left[1 + \frac{b}{m} E^2\right]^m} + \varepsilon_\infty \qquad (85)$$

where ε_∞ is the dielectric constant at infinite field strength and b and m constants. Booth (781,782) theoretically drived the equation:

$$\varepsilon = n^2 + \frac{\alpha\pi N_o (n^2 + 2)\mu_v}{E} L \left(\frac{\beta\mu_v (n^2 + 2)E}{kT}\right) \qquad (86)$$

where n is the optical refractive index, N_o the number of molecules per unit volume, μ_v the dipole moment of the water molecule, L the Langevin function and α and β are constants which have the values $\alpha = 4/3$, $\beta = 1/2$ according to Onsager (813) and $\alpha = 28/3\sqrt{73}$, $\beta = \sqrt{73}/6$ according to Kirkwood (798). Buckingham (785) has done further work to improve Booth's equation.

Calculations based on equation 86 and the experimental results of Grahame (791) indicate that the surface charge and potential are not very sensitive to the dielectric constant. Thus, it is not expected that dielectric saturation due to high field strengths is not an important correction of the Poisson-Boltzmann equation.

Hasted et al (793) examined the dependence of the dielectric constant on electrolyte concentration and found for concentrations greater than 2M the relation:

$$\varepsilon = \varepsilon_o + \delta_+ c_+ + \delta_- c_- \qquad (87)$$

where $c_{+(-)}$ is the ion concentration in mole/liter, and δ_+ and δ_- constants whose values for Na^+ and Cl^- are -8 ± 1 and -3 ± 1, respectively. Thus, the accumulation of ions in the double layer can have a significant effect on the dielectric constant.

4.19 Ion Polarization

When an ion moves in an aqueous solution, it exchanges places with water dipoles so that in an inhomogeneous electric field work must be done to displace the dipoles. This polarization contributes an extra energy term E_p to the Boltzmann equation which is rewritten as:

$$n_+ = n_{+o} \exp \left[- \frac{1}{kT} (e\psi + E_{p+}) \right] \tag{88}$$

Following Böttcher (783), Bolt (780) by considering an ion as a spherical cavity of radius a and dielectric constant ϵ_c derived:

$$E_{p+} = - \frac{a_+^3}{6} \frac{3\epsilon_o(\epsilon_c - \epsilon_o)E^2}{(2\epsilon_c + \epsilon_o)} \tag{89}$$

Levine (805) has pointed out that the denominator of equation 89 should be $(2\epsilon_o + \epsilon_c)$. Sparnaay (817) used the expression as found by Prigogine (814):

$$E_{p+} = - \frac{E^2}{8\pi} \left(\frac{\partial \epsilon}{\partial n_+}\right)_{t,v,n,E} \tag{90}$$

to obtain:

$$E_{p+} = - \frac{E^2}{8\pi} \delta_+$$

by using equation 87.

4.20 The Self-Atmosphere Effect of the Ions

Due to the interaction between neighboring ions, work must be done against an ion's own atmosphere in bringing it from infinity to its final position. Loeb (807) and Williams (823) have both considered this correction to the Poisson-Boltzmann equation. Following the approach of the latter, Bolt (780) gives as the energy E_s resulting from coulombic

interaction between ions:

$$E_s = - \frac{z^2 e \tilde{K}}{2\epsilon} \frac{(1 - e^{-2\tilde{K}x})}{2\tilde{K}x} \qquad (91)$$

where

$$\tilde{K} = \sqrt{\frac{8\pi z^2 e^2 n/2}{\epsilon kT}}$$

and x is the distance of an ion to the particle surface.

The first term of the right-hand side of equation 91 is the energy of interaction proper while the second term is due to image effects caused by a discontinuity in the dielectric represented by the colloidal surface. Except for very small distances on the order of Angstroms, the image term can be neglected so that equation 91 becomes:

$$E_s = - \frac{z^2 e \tilde{K}}{2\epsilon} \qquad (92)$$

This energy term is used in the Boltzmann distribution as in the previous section.

The self-atmosphere effect reduces the potential and the correction amounts to not more than 10%.

4.21 The Combined Effect of the Corrections

Brodowsky and Strehlow (784) considered the combined corrections for ionic volume and dielectric saturation. They found that the ionic volume and dielectric saturation corrections work in the same direction to give higher surface potentials for given charge densities. The increase in the potential due to the correction can be greater than 30% for surface charges of 16 μ coulomb/cm^2.

Sparnaay (817) considered the ionic volume, dielectric saturation, and polarization corrections. He found the net correction of the potential to be on the order of a few per

cent, 2-3%.

Bolt (780) considered all four of the corrections except that he omitted the effect of the electrolyte on the dielectric constant. He found that the dielectric saturation and polarization corrections almost exactly offset each other and that the self-atmosphere and ionic volume effects tend to cancel each other.

Haydon (794) has conveniently summarized the results of these investigations.

Below 10^{-2} M electrolyte and $\psi_o \sim 100$ mV, the net correction to the value of ψ_o is likely to be $\sim$ 0 to + 2-3%, and will be sensitive to the ionic volume of the counter ion. For $< 10^{-2}$ M electrolyte and $\psi_o > 100$ mV, we may expect that deviations will still be very small ($\sim$ 2%) since the corrections for the self-atmosphere and ionic volume effects tend to increase, but balance each other.

For $> 10^{-2}$ M and $\psi_o \sim 100$ mV, the self-atmosphere effect becomes less, and the ionic volume more important. Dielectric saturation and polarization will remain relatively small, and the correction to ψ_o will be positive and sensitive to the ionic volume; probably > + 3%. For $> 10^{-2}$ M and $\psi_o > 100$ mV, there seems little doubt that the ionic volume correction will ultimately become much larger than all the others, although dielectric saturation may also become rapidly larger. Both these corrections work in the same direction and correction to ψ_o will be positive and perhaps very large (up to 30-40%).

4.22 The Statistical Mechanics Approach to the Electrical Double Layer

The treatment of the electrical double layer using the Poisson-Boltzmann equation has been criticized on grounds that it is a short cut to avoid applying the principles of statistical mechanics. Although the statistical mechanics approach has not been developed as far as the Poisson-Boltzmann equation

method, it does present a rigorous formulation of the problem which introduces in a natural way all the corrections previously discussed.

The starting point is the canonical distribution (779):

$$D_N = Q_N^{-1} \exp\left[-\varphi_N/\theta\right] \tag{93}$$

where D_N is the probability distribution for the positions of all N molecules, $\theta = kT$, φ_N the potential energy of the system and Q_N the partition function:

$$Q_N = \int_V \cdots\cdots \int_V \exp\left[-\varphi_N/\theta\right] d\underset{\sim}{q}_1 d\underset{\sim}{q}_2 \cdots d\underset{\sim}{q}_N$$

where $q_i(q_i^{\,1}, q_i^{\,2}, q_i^{\,3})$ denotes the position of the i^{th} molecule.

If equation 93 is logarithmically differentiated:

$$\frac{\partial D_N}{\partial q_1^{\,\alpha}} + \frac{1}{\theta} \frac{\partial \varphi_N}{\partial q_1^{\,\alpha}} D_N = 0, \quad \alpha = 1, 2, 3$$

When this equation is multiplied by V^s and integrated over $q_{s+1}, \ldots q_N$, it can be shown that in the limit $N \to \infty$ one obtains the Bogolyubov equation which gives the concentration, $G_a(z_a)$, of particles of type a at a distance z_a from the surface of a solution (779,809).

$$\frac{\partial G_a(z_a)}{\partial z_a} + \frac{G_a(z_a)}{\theta} \frac{\partial U_a(z_a)}{\partial z_a} +$$

$$+ \frac{1}{\theta} \int_{z_1 \geq 0} \sum_b \nu_b G_{ab}(\vec{r}_a, \vec{r}_b) \frac{\partial \Phi_{ab}(\vec{r}_a, \vec{r}_b)}{\partial z_a} d\vec{r}_b = 0 \tag{94}$$

where ν_a is the number of particle of type a per unit volume

of solution, $U_a(z_a)$ is the energy of a type a particle in the external field, $\Phi_{ab}(\vec{r}_a, \vec{r}_b)$ is the energy of interaction of particles of types a and b, $\vec{r}_a$ is the radius vector of the a particle, and $G_{ab}(\vec{r}_a, \vec{r}_b)$ is a binary function satisfying the boundary conditions:

$$G_{ab} \to G_a(Z_a)G_b(Z_b) \text{ when } r_{ab} = \left|\vec{r}_a - \vec{r}_b\right| \to \infty,$$

$$G_{ab} \to f(\vec{r}_a, \vec{r}_b)\exp[-\Phi_{ab}^{(s)}(r_{ab})/\theta] \to 0,$$

$$f \geq 0 \text{ when } r_{ab} \to 0 \qquad (95)$$

$\Phi_{ab}^{(s)}$ being the energy of the Born repulsion forces which assure particle rigidity.

It is convenient to write the expression for G_{ab} as:

$$G_{ab} = g_a g_b \exp\left[-\Phi_{ab}^{(s)}/\theta\right](1 + g_{ab})$$

where

$$G_a = g_a, \quad \lim_{r_{ab} \to \infty} g_{ab}(\vec{r}_a, \vec{r}_b) = 0$$

Substitution of this expression into 94 leads to:

$$\frac{\partial \ln g_a}{\partial z_a} + \frac{\partial U_a}{\theta \partial z_a} + \frac{1}{\theta} \int_{z_b \geq o} \sum_b \left[\nu_b g_b (1 + g_{ab}) \cdot \right.$$

$$\left. \cdot\, e^{-\Phi_{ab}^{(s)}/\theta} \frac{\partial \Phi_{ab}}{\partial z_a} \vec{dr}_b = 0\right] \qquad (96)$$

The summation of 96 extends over all types of particles present in the solution.

It is necessary to know the forms of U_a and Φ_{ab} in order to specify the system. The general expression for the energy

of an ion in the neighborhood of the interface between two media is:

$$U_a = \Phi_a^{(coul)} + \Phi_a^{(im)} + \Phi_a^{(ad)} \qquad (97)$$

Here $\Phi_a^{(coul)} = e_a[\psi_o - (2\pi\eta/\epsilon)z_a]$ is the electrostatic energy of a charge e_a located at a distance z_a from a surface carrying a charge η, ϵ is the dielectric constant of the solvent located in the semi-space $z \geq 0$,

$$\Phi_a^{(im)} = \frac{e_a^2}{2\epsilon} \frac{\epsilon - \epsilon'}{\epsilon + \epsilon'} \cdot \frac{1}{2z_a}$$

is the energy of interaction of an ion with its own image, as determined by the difference in polarizabilities of the solvent and the external medium (the dielectric constant of the latter is ϵ'), and $\Phi_a^{(ad)}$ is the ion-external medium interaction energy, resulting from the presence of nonelectrical forces. The ion-pair interaction energy is, on the other hand, expressed by:

$$\Phi_{ab} = \Phi_{ab}^{(coul)} + \Phi_{ab}^{(im)} + \Phi_{ab}^{(s)}, \qquad (98)$$

$\Phi_{ab}^{(coul)} = (e_a e_b/\epsilon)(1/r_{ab})$ being the energy of coulombic interaction of two point-charges, and

$$\Phi_{ab}^{(im)} = \frac{e_a e_b}{\epsilon} \frac{\epsilon - \epsilon'}{\epsilon + \epsilon'} \frac{1}{r_{ab}}$$

the energy of interaction of ion a with the image of ion b.

Martynov (809,810) has shown that under certain conditions the Poisson-Boltzmann equation can be shown to be limiting cases of the general theory. Fowler (789) using different manipulations of the canonical distribution also verified the Poisson-Boltzmann equation for dilute solutions and obtained a first order correction due to fluctuations in the potential. Similar work has been done by Kirkwood (799),

Kirkwood and Poirier (800), Stillinger and Kirkwood (820), and Levine and Bell (776,806). The statistical mechancis approach has not led to any really new, useful or practical expressions and has been restircted to treating only the single flat double layer. However, one important result is that it tends to support the Stern layer concept.

4.23 APPENDIX I - Derivation of Poisson's Equation (797)

In electromagnetic theory, the displacement vector Field $\vec{D}$ is defined as follows: the magnitude of the displacement field D at a given point is measured by and is equal to the surface charge density induced on a test plate inserted at this point and oriented to acquire the greatest induced charge. It is an experimental fact that a charge placed inside a conducting enclosure induces an equally large charge of opposite sign on the inner surface of the enclosure. This induced charge is given by the displacement integrated over the surface of the enclosure:

$$q_{induced} = \oint_{surface} D\,ds$$

The enclosed charge can be expressed in terms of a volume density charge ρ integrated over the enclosed volume:

$$q_{enclosed} = \int_{volume} \rho\,dV$$

Since

$$q_{enclosed} = -q_{induced}$$

$$\oint_{s} \vec{D} \cdot d\vec{S} = \int_{v} \rho\,dV$$

$$\int_V \nabla \cdot \vec{D} dV = \int_V \rho dV$$

or

$$\nabla \cdot \vec{D} = \rho \tag{99}$$

The displacement is related to the electric field $\vec{E}$ whose magnitude at a point is equal the force exerted on a positive unit charge at that point by:

$$\vec{D} = \frac{\epsilon}{4\pi} \vec{E} \tag{100}$$

where ϵ is the dielectric constant of the medium. The electric field is further related to the electrical potential ψ which represents the potential energy of a unit positive charge in the electric field by:

$$\vec{E} = - \nabla \psi \tag{101}$$

Substituting equation 100 and 101 into 99 yields:

$$\nabla \cdot (\epsilon \nabla \psi) = - 4\pi\rho \tag{102}$$

For ϵ constant, equation 102 becomes the Poisson equation:

$$\nabla^2 \psi = - \frac{4\pi}{\epsilon} \rho \tag{103}$$

4.24 APPENDIX II - Derivation of the Boltzmann Distribution (816)

Consider a system of N particles which consist of N_1 particles each with energy ϵ_1; N_2, each with energy ϵ_2; etc. such that:

$$N = \sum_i N_i \tag{104}$$

and the total energy E of the system is:

$$E = \sum_i N_i \epsilon_i \tag{105}$$

The number of way in which the N particles can be arranged in groups of N_i is:

$$G = \frac{N!}{N_1!\, N_2!\, N_3! \cdots N_i! \cdots} \tag{106}$$

The problem is to determine the most likely values of each N_i for given N and E. This corresponds to maximizing G subject to equations 104 and 105.

Taking the log of equation 106:

$$\ln G = \ln N! - \sum_i \ln N_i! \tag{107}$$

which using the Stirling approximation $\ln\xi = \xi\ln\xi - \xi$ for large ξ becomes:

$$\ln G = N\ln N - N - \sum_i (N_i \ln N_i - N_i) \tag{108}$$

Lagrange's method may now be applied to equation 108 subject to the constraints given by equation 104 and 105:

$$\delta(\ln G) - \alpha\delta N - \beta\delta E = 0$$

$$\sum_i (\ln N_i + \alpha + \beta\epsilon_i)\ \delta N_i = 0$$

where δ is the variation operator and α and β undetermined multipliers. Since the undetermined δN_i are arbitrary:

$$\ln N_i + \alpha + \beta\epsilon_i = 0$$

$$N_i = e^{-\alpha} e^{-\beta\epsilon_i} \tag{109a}$$

Substituting equation 109a into 104:

$$e^{-\alpha} \sum_i e^{-\beta\epsilon_i} = N \tag{109b}$$

and then eliminating α from equation 109b:

$$\frac{N_i}{N} = \frac{e^{-\beta\epsilon_i}}{\sum_j e^{-\beta\epsilon_i}} \qquad (110)$$

By evaluating the average energy per particle and equating it to that for a perfect gas which is known to be $\frac{3}{2}$ kT, it can be shown that:

$$\beta = \frac{1}{kT}$$

where k is Boltzmann's constant and T temperature. Denoting N_o as the number of particles for which the energy is zero equation 110 can be written as:

$$N_i = N_o e^{-\frac{\epsilon_i}{kT}} \qquad (111)$$

4.25 Constant Surface Potential vs. Constant Surface Charge

In most colloid systems, the electrical double layer around a particle is due to an equilibrium distribution of "potential determining" ions between the particle surface and the medium. For example, in the AgI/H_2O system the double layer potential is determined by the concentration of the Ag+ or I- ions in solution (866). In an aqueous solution of 10^{-6} eg. Ag^+ ions/liter and AgI particles are uncharged so that the surface potential ψ_o is zero. Upon increasing the Ag^+ concentration ten fold, there is a slight excess of Ag^+ ions on the particle surface when equilibrium is established. The result is that the particles are now positively charged.

Since the excess of Ag^+ ions is extremely small and that these excess ions are indistinguishable from the original Ag^+ ions of the surface and bound there in the same way, the chemical potential μ may be considered a constant independent of the double layer potential.

Since the change in chemical potential $\Delta\mu = kT\ln C/C_o$ where C_o is the concentration at zero charge equals the electrical work $e\psi_o$, ψ_o can be given by:

$$\psi_o = \frac{kT}{\varepsilon} \ln \frac{C}{C_o} \qquad (112)$$

The surface potential for 10^{-5} eq. Ag^+ ions/liter is then 57 millivolts.

The important point of these remarks is that the equilibrium of the potential determining ions determines the surface potential independently of all other variables such as other electrolytes.

The theory presented for the interaction of double layers considered the surface potential to be constant with the surface charge changing during the interaction. This means that equilibrium is rapidly established and continuously maintained. However, it is conceivable that the implied transition of charge carriers from one phase to another is much slower than the time of a collision of two Brownian particles (867). In this case, the surface charge, not the surface potential, should be considered as constant.

A similar argument can be made when the dissociation of certain groups fixed at the surface determine the surface charge due to their slow desorption.

The experiments of Frens, Engel, and Overbeek (868) have indicated that equilibirum for the AgI/H_2O system is established very flowly. On the basis of this result, Frens (869) replaced the condition of constant surface potential with that of constant surface charge and investigated how this would modify the double layer interaction. Jones and Levine (870) carried out a similar analysis. The conclusions drawn from these studies is that differences in the interaction due to these two conditions become significant only at small surface potentials. It was also found that for the condition of

constant surface charge the surface potential tends to infinity as the separation between the particles approaches zero. This suggests that neither the constant surface potential nor charge condition is completely correct, but that the true situation lies somewhere between these two limiting conditions.

4.26 The Relationship Between the Surface Potential and the Zeta Potential

The zeta potential ζ is a quantity which is indirectly determined from electrokinetic experiments in which the relative movement between the liquid and solid allows according to theoretical considerations the calculation of the potential at the shear plane which located is somewhere within the double layer. For example, a common technique is to measure the velocity at which colloidal particles migrate in a known external electric field. It has been long realized the zeta and surface potentials are not identical, but it is believed that the zeta potential should resemble the potential at the Stern Plane. However, due to both experimental and theoretical difficulties, this cannot be proved so that it has been generally accepted that the zeta and Stern potentials are approximately equivalent.

An expression relating the zeta potential to the observed mobility of a colloid particle can be obtained as follows. Consider a portion of the surface of a particle moving in a liquid as shown in Figure 34. The forces acting on an element of liquid in the vicinity of the particle's surface are the viscous frictional force and the force exerted by the electric field on the charge ρ in the double layer. Since the net force on a liquid dement must equal zero:

$$\rho E \Lambda \Delta x + \tau A\Big|_{x + \Delta x} = \tau A\Big|_{x}$$

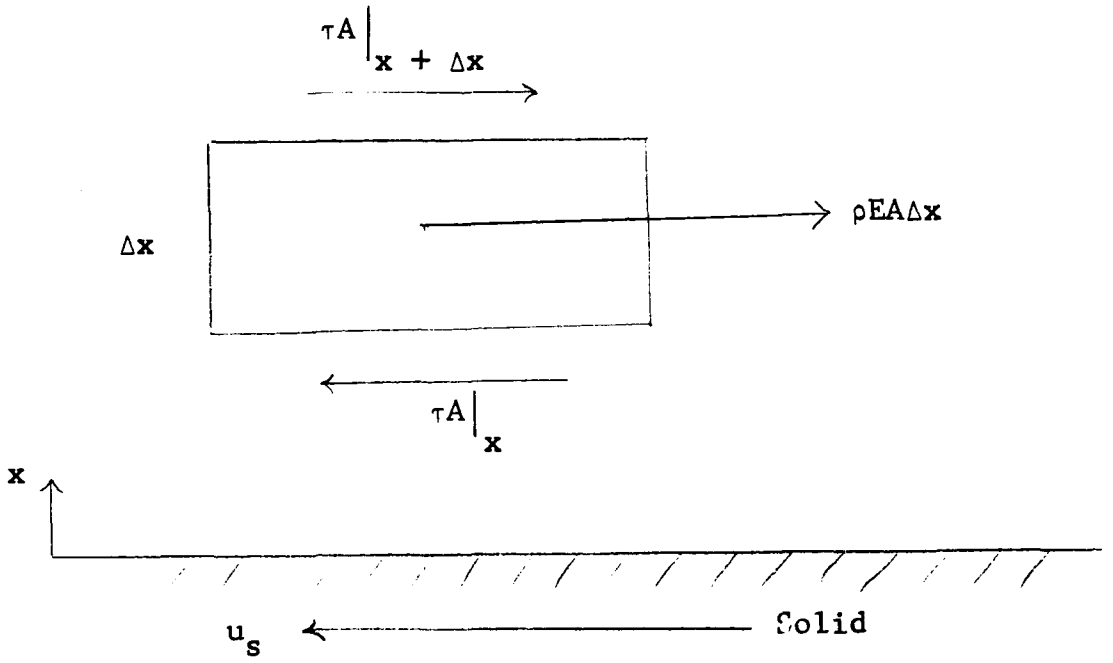

τ, shear force
A, area
u_s, velocity of solid

Figure 34

FORCES ACTING ON AN ELEMENT OF LIQUID
IN AN ELECTRICAL FIELD

For a Newtonian fluid:

$$\tau = - \mu \frac{du}{dx}$$

where μ is the viscosity of the liquid and u its velocity so that:

$$- \rho EA = \left[- \mu \frac{du}{dx} A \Big|_{x + \Delta x} + \mu \frac{du}{dx} A \Big|_{x} \right] / \Delta x$$

Taking the limit as $\Delta x \longrightarrow 0$:

$$\rho E = \frac{d}{dx} \left(\mu \frac{du}{dx} \right) \tag{113}$$

Using Poisson's equation to eliminate ρ:

$$\rho = - \frac{1}{4\pi} \frac{d}{dx} \left(\epsilon \frac{d\psi}{dx} \right)$$

equation 113 becomes:

$$\frac{d}{dx} \left(\epsilon \frac{d\psi}{dx} \right) = - \frac{4\pi}{E} \frac{d}{dx} \left(\mu \frac{du}{dx} \right) \tag{114}$$

Integrating equation 114 once:

$$\epsilon \frac{d\psi}{dx} = - \frac{4\pi}{E} \mu \frac{du}{dx} + C_1 \tag{115}$$

where the integration constant C_1 is zero because at far away from the particle $\frac{d\psi}{dx} = \frac{du}{dx} = 0$. Integrating again with ϵ and μ considered constant:

$$\psi = - \frac{4\pi\mu}{E\epsilon} u + C_2 \tag{116}$$

At the shear plane, the liquid moves at the velocity of the particle so that $u = u_s$ and $\psi = \zeta$ there. Thus,

$$C_2 = \zeta - \frac{4\pi\mu}{E\epsilon} u_s \tag{117}$$

and equation 116 becomes:

$$\psi - \zeta = - \frac{4\pi\mu}{E\epsilon} (u + u_s) \tag{118}$$

Further, since far away from the particle, $u = \psi = 0$, equation 118 gives the Smoluchowski equation:

$$\zeta = \frac{4\pi\mu u_s}{E\epsilon} \tag{119}$$

Equation 119 although derived from a plane double layer is applicable to all other particle shapes provided the thickness of the double layer is small in comparison to the radius of curvature of the particle.

For spherical particles, a similar expression can be obtained. The viscous resistance is given by Stokes law:

$$F = 6\pi\mu a u_s$$

and the electrical force by:

$$F = QE$$

where

$$Q = a\epsilon(1 + \kappa a)\zeta$$

as obtained previously for a spherical double layer.

Equating these forces, the zeta potential for spherical particles is obtained:

$$\zeta = -\frac{6\pi\mu u_s}{\epsilon E(1 + \kappa a)} \tag{120}$$

Equation 119 and 120 do not take in account two effects; (1) the retardation caused by the movement of counter ions in the opposite direction to that of the particle under the influence of the applied field, and (2) the retardation resulting from the deformation of the otherwise symmetrical double layer around a charged particle when it is moving in the applied field. The former is known as the electrophoretic effect and the latter as the relaxation effect. These effects become important when the counter ions in solution have low mobilities, the zeta potential is high, and κa is in the range $0.2 < \kappa a > 50$.

Henry (872) took into account the electrophoretic effect and obtained for spherical particles:

$$u_s = \frac{E\varepsilon\zeta}{6\pi\mu}\,[1 + \lambda f(\kappa a)] \qquad (121)$$

where

$$\lambda = \frac{\sigma_e - \sigma_s}{2\sigma_e - \sigma_s}$$

and

$$f(\kappa a) = \frac{(\kappa a)^2}{8} - \frac{5(\kappa a)^3}{24} - \frac{(\kappa a)^4}{48} + \frac{(\kappa a)^5}{48} - \left[\frac{(\kappa a)^4}{4} - \frac{(\kappa a)^6}{48}\right] e^{\kappa a} \int_{\infty}^{\kappa a} \frac{e^{-t}}{t}\, dt$$

and σ_e and σ_s are the electrical conductivities of the electrolyte solution and particles, respectively. He showed that equation 119 and 120 are limiting forms of equation 121 at low and high values of κa, respectively.

The correction factor for a non-conducting spherical particle $1 + 1/2\ f(\kappa a)$ is given in Table 13.

Table 13

VALUES FOR $[1 + 1/2\ f(\kappa a)]$ IN THE HENRY EQUATION FOR A RANGE OF κa VALUES

κa	0·01	0·1	0·3	1	3	5	10	20	50	100	1000
$[1+\frac{1}{2}f(\kappa a)]$	1·000	1·001	1·004	1·027	1·100	1·160	1·239	1·340	1·424	1·458	1·495

Overbeek (875) considered both the electrophoretic and relaxation effects, and obtained a series solution for terms up to ζ^3 with the restriction $eT/kT < 1$:

$$u_s = \frac{E\epsilon\zeta}{6\pi\mu}\left[f_1(\kappa a) - z^2\left(\frac{e\zeta}{kT}\right)^2 f_3(\kappa a) - \right.$$

$$\left. - \frac{\beta_+ + \beta_-}{2e}\ \frac{\epsilon kT}{6\pi\mu e}\left(\frac{e\zeta}{kT}\right)^2 f_4(\kappa a)\right] \qquad (122)$$

For symmetrical electrolytes and:

$$u_s = \frac{E\epsilon\zeta}{6\pi\mu}\left[f_1(\kappa a) - (z_- - z_+)\frac{e\zeta}{kT} f_2(\kappa a) - \right.$$

$$\left. - \frac{z_+\beta_+ + z_-\beta_-}{(z_+ + z_-)e}\ \frac{\epsilon kT}{6\pi\mu e}\left(\frac{e\zeta}{kT}\right)^2 f_4(\kappa a)\right] \qquad (123)$$

for unsymmetrical electrolytes.

The functions $f_1(\kappa a)$, $f_2(\kappa a)$, $f_3(\kappa a)$ and $f_4(\kappa a)$ are tabulated in Table 14, and equations 122 and 123 are illustrated in Figures 35 and 36 respectively. Booth (871) has obtained similar results.

Table 14

VALUES OF CORRECTION TERMS IN EQUATIONS 122 AND 123

κa	$f_1(\kappa a)$	$f_2(\kappa a)$	$f_3(\kappa a)$	$f_4(\kappa a)$
0.01	1.000036	0.0006	0.00009	0.0006
0.1	1.000515	0.0125	0.00090	0.0107
0.3	1.00398	0.0279	0.0044	0.0218
1	1.0267	0.0411	0.0116	0.0387
3	1.1069	0.053	0.020	0.051$_5$
5	1.160	0.057	0.022	0.054$_6$
10	1.239	0.05$_6$	0.021	0.05$_3$
20	1.34	0.04	0.014$_5$	0.01
50	1.424	0.0188	0.00706	0.0177
100	1.458	0.0102	0.00111	0.00992
1000	1.465	0.0011	0.0005	0.0011

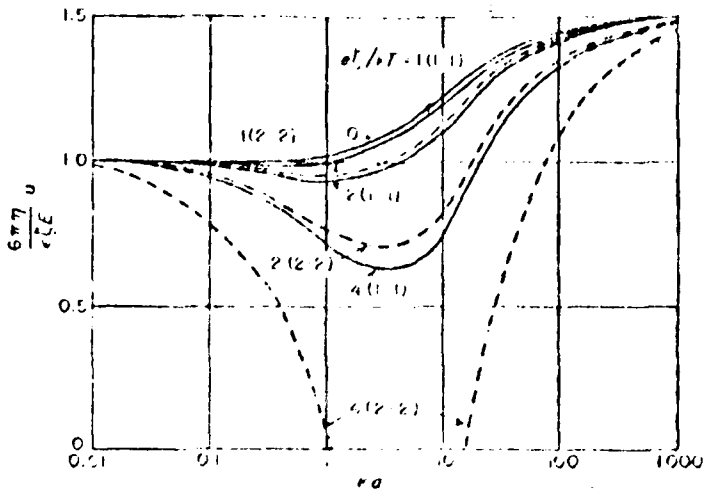

Figure 35

ELECTROPHORETIC MOBILITY IN SYMMETRICAL ELECTROLYTES (Eq. 122). VALUES OF $e\zeta/kT$ AND 1, 2, AND 4 OR ζ ABOUT 25, 50, AND 100 mv., RESPECTIVELY. THE LINE MARKED 0 FORMS THE LIMIT FOR VERY SMALL VALUES OF THE ZETA POTENTIAL. FULL LINES FOR MONOVALENT AND BROKEN LINES FOR BIVALENT ELECTROLYTES.

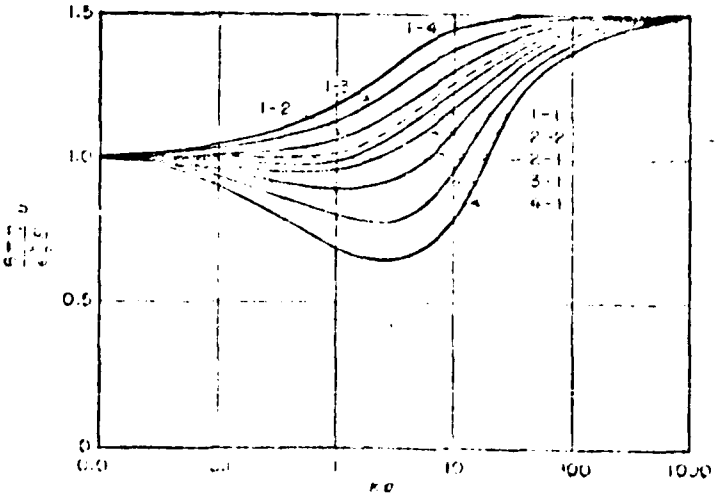

Figure 36

ELECTROPHORETIC MOBILITY IN UNSYMMETRICAL ELECTROLYTES (Eq. 123). FOR ALL THE CURVES $e\zeta/kT$ VALUES EQUAL 2 OR ζ ABOUT 50 mv.

The equations of Overbeek have been superceded in range of validity and convenience of use by the latter work of Wiersema, Loeb, and Overbeek (876) who used a digital computer to avoid making approximations. Table 15 shows a selection of their results.

Table 15

PARTICLE MOBILITIES IN μ/SEC PER VOLT/CM AS A FUNCTION OF THE ZETA POTENTIAL AT VARIOUS VALUES OF κa FOR PARTICLES SUSPENDED IN AQUEOUS SOLUTION AT 25°C CONTAINING ONLY 1:1 ELECTROLYTE WITH IONIC MOBILITIES CORRESPONDING TO $\lambda = 70$ ohm^{-1} cm^{-2} eq^{-1}

$\frac{\kappa a}{\zeta(mV)}$	0	0·05	0·1	0·5	1·0	2·0	5·0	10	20	50	100	200	500	∞
25·7	1·33	1·33	1·33	1·32	1·35	1·39	1·51	1·63	1·77	1·89	1·93	1·96	1·99	2·00
51·4	2·67	2·65	2·63	2·56	2·55	2·57	2·78	3·03	3·35	3·68	3·83	3·91	3·96	4·00
77·1	4·00	3·95	3·87	3·62	3·50	3·47	3·66	4·08	4·57	5·23	5·60	5·79	5·94	6·00
102·8	5·34	5·20	5·04	4·48	4·17	3·99	4·10	4·58	5·29	6·39	7·18	7·58	7·87	8·00
128·5	6·67	6·40	6·12	5·07	4·58	4·27	4·23	4·63	5·47	7·00	8·30	9·18	9·78	10·00
154·1	8·00	7·55	7·18	5·48	4·84	4·36	4·11	4·46	5·25	7·03	8·86	10·54	11·65	12·00

In all of the treatments discussed, it has been assumed that ϵ and μ are constant. However, this may not be true where the electric field strength is sufficiently high to increase μ and decrease ϵ significantly. Both these effects would reduce the particle's mobility for a given zeta potential. Lyklema and Overbeek (874) investigated this problem and concluded that the effect of field strength on ϵ could be neglected but perhaps not on μ. The difficulty is that the equation relating μ to field strength:

$$\mu = \mu_o \left[1 + f_o \left(\frac{d\psi}{dx}\right)^2\right]$$

where μ_o is the viscosity at zero field strength, contains the viscoelectric constant f_o which is not known with any certainty.

However, Hunter (873) has recently concluded that the two effects are of the same magnitude and are both of not great significance.

4.27 The Rate of Agglomeration

The curves of the total potential energy of interaction given previously can only provide a qualitative criterion for the stability of colloids by saying that stability is expected if the maximum of the potential curve is greater than kT which is the termal energy of the particles. This criterion can be greatly improved by considering the rate at which the particles collide so that one can determine how long a system is stable. The controlling factors are the Brownian motion of the particles and their interaction when they approach one another.

4.28 The Collision Rate (830)

The cause of Brownian motion of a particle is its collisions with molecules of the surrounding medium. In a liquid, a particle will undergo about 10^{21} collisions per second. Since each collision produces a kink in the particle's path one cannot follow its path on a fine scale.

The theory of Brownian motion starts with Langevin's equation:

$$m \frac{du}{dt} = - \beta u + A(t) + K(\vec{r}, t) \qquad (124)$$

where u is the particle's velocity, t time, and $\vec{r}$ position. This equation is simply a statement of Newton's 2nd law of motion. The left-hand side is the product of the particle's mass m and its acceleration; the first term on the right-hand side is the frictional force exerted on the particle by the

medium; the second term is the fluctuating force due to molecular collisions; and the third term is the force on the particle due to a force field. According to Stokes' law for a sphere:

$$\beta = 6\pi a\mu \tag{125}$$

where a is the radius of the particle and μ the viscosity of the medium. It is assumed that A(t) is independent of u and varies very much faster than u. The latter assumption is to assure that for time intervals of interest Δt, u(t), and $u(t + \Delta t)$ only differ slightly and that there no longer exist any correlation between A(t) and $A(t + \Delta t)$.

From these concepts, Chandrasekhar (830) showed that the probability P that a Brownian particle released at the point $\vec{r}_o$ in a force field is at $\vec{r}$ some time later is governed by the following equation for time intervals much greater than β^{-1}:

$$\frac{\partial P(\vec{r},\ t/\vec{r}_o)}{\partial t} = \nabla\cdot\left[\mathcal{D}\nabla P(\vec{r},\ t/\vec{r}_o) - \frac{K}{\beta} P(\vec{r},\ t/\vec{r}_o)\right] \tag{126}$$

where the Brownian diffusivity $\mathcal{D} = \frac{kT}{\beta} = \frac{kT}{6\pi a\mu}$ and K is the acceleration per unit mass due to the force field.

For a system of particles, the probability P_i of finding any particle of the i^{th} type is obtained by integrating equation 126 over all particles of the i^{th} type or equivalently over $\vec{r}_{io}$:

$$\frac{\partial \mathcal{P}_i}{\partial t} = \nabla\cdot(\mathcal{D}_i\nabla\mathcal{P}_i - \frac{K_i}{\beta_i}\mathcal{P}_i) \tag{127}$$

Since

$$\mathcal{P}_i = \frac{N_i}{N_t}$$

where N_i is the particle number density of the i^{th} type and

N_t the total density, equation 127 becomes:

$$\frac{\partial N_i}{\partial t} = \nabla.(\mathcal{D}_i \nabla N_i - \frac{K_i}{\beta_i} N_i) \tag{128}$$

According to equation 128, the stationary or time independent diffusional flux J_i of particles of the i^{th} type to a point is given by:

$$J_i = -\mathcal{D}_i \nabla N_i + \frac{K_i}{\beta_i} N_i \tag{129}$$

Since K_i can be expressed in terms of the interaction potential V_i so that:

$$K_i = -\nabla V_i \tag{130}$$

then equation 129 can be written as:

$$J_i = -\mathcal{D}_i \nabla N_i - \beta_i^{-1} N_i \nabla V_i \tag{131}$$

Suppose that the origin of the coordinate system is attached to a particle of type j also in Brownian motion. Then $\mathcal{D}_i$ must be replaced by $\mathcal{D}_{ij} = \mathcal{D}_i + \mathcal{D}_j$. This follows from the fact that the average relative displacement of particles i and j is:

$$\overline{(\Delta X_i - \Delta X_j)^2} = \overline{\Delta X_i^2} + \overline{\Delta X_j^2} - 2\,\overline{\Delta X_i X_j} \tag{132}$$

Since the Brownian motion of a particle is independent of the other particle, the correlation term $\overline{\Delta X_i \Delta X_j} = 0$. Using Einstein's expression for the diffusivity $\mathcal{D} = \Delta X/2\Delta t$, equation 132 becomes:

$$\overline{(\Delta X_i - \Delta X_j)^2} = 2(\mathcal{D}_i + \mathcal{D}_j)\,\Delta t = 2\mathcal{D}_{ij}\Delta t \tag{133}$$

Also, since $\beta_i^{-1} \nabla V_i$ is the velocity of i^{th} particle due to the force field, it must be replaced by the relative velocity

of particles i and j, $\beta_{ij}^{-1}\nabla V_{ij}$, where V_{ij} is the interaction potential between particle i and j and $\beta_{ij}^{-1} = \beta_i^{-1} + \beta_j^{-1}$. Thus, equation 131 is rewritten as:

$$J_i = -\mathcal{D}_{ij}\nabla N_i - \beta_{ij}^{-1} N_i \nabla V_{ij} \tag{134}$$

Since the rate at which particles of the i^{th} type reach the surface of a particle of the j^{th} type gives the desired collision rate, equation 134 is to be solved in spherical coordinates (832):

$$J_i = 4\pi r^2 \left[\mathcal{D}_{ij} \frac{dN_i}{dr} + \beta_{ij}^{-1} \frac{dV_{ij}}{dr} N_i\right] \tag{135a}$$

where r is the radial distance measured from the center of the j^{th} particle suject to the boundary conditions:

$$N_i = 0 \text{ at } r = a_i + a_j = a_{ij} \tag{135b}$$

$$N_i - N_{io} \text{ at } r = \infty \tag{135c}$$

where N_{io} is the bulk density of particles of the i^{th} type. The first boundary condition states that due to the absorption of particles of the i^{th} type by a particle of the j^{th} type, there can be no i particles in the close vicinity of a j particle. The second condition accounts for the fact that far away from the j particle, the density of i particles equals their bulk density.

The general solution of a first order differential equation of the form:

$$\frac{dN_i}{dr} + \alpha(r)N_i = \gamma(r) \tag{136}$$

with the condition that at $r = r_o$, $N_i = \tilde{N}_i$ is well-known to be:

$$N_i = \tilde{N}_i \exp\left[-\int_{r_o}^{r} \alpha(r')dr'\right] +$$

$$+ \exp\left[-\int_{r_o}^{r} \alpha(r')dr'\right]\int_{r_o}^{r} \gamma(\lambda) \exp\left[\int_{r_o}^{\lambda} \alpha(r')dr'\right] d\lambda \qquad (137)$$

Comparing equations 135 and 136, it is seen that:

$$\alpha(r) = \frac{1}{\beta_{ij}\mathscr{D}_{ij}} \frac{dV_i}{dr} = \frac{1}{kT}\frac{dV_{ij}}{dr}$$

$$\gamma(r) = (4\pi r^2 \mathscr{D}_{ij})^{-1} J_i$$

Letting $r_o = \infty$ and $\tilde{N}_i = N_{io}$ and evaluating equation 137 at $r = a_j$ where $N_i = 0$ yields:

$$N_{io} + \int_{\infty}^{a_{ij}} \frac{J_i}{4\pi\lambda^2\mathscr{D}_{ij}} \exp\left[\int_{\infty}^{\lambda} \frac{1}{\beta_{ij}\mathscr{D}_{ij}} \frac{dV_{ij}}{dr} dr\right] = 0$$

$$N_{io} - \frac{J_i}{4\pi\mathscr{D}_{ij}} \int_{a_{ij}}^{\infty} \frac{e^{V_{ij}/\beta_{ij}\mathscr{D}_{ij}}}{r^2} dr = 0$$

$$J_i = \frac{4\pi\mathscr{D}_{ij} N_{io}}{\int_{a_{ij}}^{\infty} \frac{e^{V_{ij}/\beta_{ij}\mathscr{D}_{ij}}}{r^2} dr} \qquad (138)$$

Since J_i is the rate at which particles of the i^{th} type arrive at the surface of one particle of the j^{th} type, the

total number of collisions between i and j particles assuming binary collisions only is:

$$J_{ij} = \frac{4\pi \mathscr{D}_{ij} N_{io} N_{jo}}{\int_{a_{ij}}^{\infty} \frac{e^{V_{ij}/\beta_{ij}\mathscr{D}_{ij}}}{r^2} dr} \tag{139}$$

For collisions of particles of the same type, equation 139 should be multiplied by 1/2. Thus,

$$J_{ij} = \frac{4\pi \delta_{ij} \mathscr{D}_{ij} N_{io} N_{jo}}{\int_{a_{ij}}^{\infty} \frac{e^{V_{ij}/\beta_{ij}\mathscr{D}_{ij}}}{r^2} dr} \tag{140}$$

where

$$\delta_{ij} = \begin{cases} 1 \text{ for } i \neq j \\ 1/2 \text{ for } i = j \end{cases}$$

The case for which there is no interaction between the particles known as rapid coagulation is obtained by setting $V_{ij} = 0$ in equation 140. The result as found first by Smoluchowski (858) is:

$$J_{ij} = 4\pi \delta_{ij} \mathscr{D}_{ij} a_{ij} N_{io} N_{jo} \tag{141}$$

The stability ratio (862,852) W_{ij} which is defined as the multiplicative factor by which the number of collisions as given for rapid coagulation is modified due to the presence of an interaction potential:

$$W_{ij} = a_{ij} \int_{a_{ij}}^{\infty} \frac{e^{V_{ij}/\beta_{ij}\mathscr{D}_{ij}}}{r^2} dr \tag{142}$$

allows equation 140 to be written as:

$$J_{ij} = 4\pi\delta_{ij}\beta_{ij}a_{ij}W_{ij}^{-1}N_{io}N_{jo} \tag{143}$$

Another simplification can be made by introducing the coagulation constant K_o:

$$K_o(a_i, a_j) = 4\pi\delta_{ij}\beta_{ij}a_{ij}W_{ij}^{-1} \tag{144}$$

so that:

$$J_{ij} = K_o(a_i, a_j)N_{io}N_{jo} \tag{145}$$

4.29 The Kinetic Equation (849,857,848)

The rate at which particles of mass m are formed is:

$$B = \frac{1}{2}\int_o^m K_o(m', m - m')N_o(m', t) \cdot N_o(m - m', t)dm' \tag{146}$$

The factor 1/2 is to avoid counting collisions twice. It should be noted that mass has been used instead of the radius of a particle because with agglomeration the mass is additive but not the radius.

The rate at which particles of mass m disappear is:

$$D = N_o(m, t)\int_o^\infty K_o(m, m')N_o(m', t) \cdot dm' \tag{147}$$

A material balance for particles of mass m states that the rate of accumulation equals the net generation of these particles so that:

$$\frac{\partial N_o(m, t)}{\partial t} = B - D$$

$$\frac{\partial N_o(m,\ t)}{\partial t} = \frac{1}{2} \int_o^m K_o(m',\ m - m')N_o(m',\ t)\ .$$

$$.\ N_o(m - m',\ t)dm' -$$

$$- N_o(m,\ t) \int_o^\infty K_o(m,\ m')N_o(m',\ t)dm' \qquad (148)$$

Equation 148 is an integro-differential equation and is subject to the initial distribution $N_o(m,\ o)$. It can only be solved analytically for the not very plausible case where K_o is a constant. Its solution was first given by Smoluchowski (858).

Define the n^{th} moment of the distribution N_o as:

$$\mu_n(t) = \int_o^\infty m^n N_o(m,\ t)dm \qquad (149)$$

Applying this definition to equation 148 gives:

$$\frac{d\mu_n}{dt} = \int_o^\infty m^n(B - D)dm \qquad (150)$$

The right hand side of equation 150 is evaluated as follows. If a mean value for K_o is used so that it can be taken outside the integral sign:

$$\int_o^\infty m^n Ddm = \overline{K}_o\mu_o(t) \int_o^\infty m^n N_o(m,\ t)\ dm =$$

$$= \overline{K}_o\mu_o\mu_n \qquad (151)$$

$$\int_o^\infty m^n B dm = \frac{1}{2} \bar{K}_o \int_o^\infty m^n dm \cdot \int_o^\infty N_o(m - m', t) N_o(m', t) dm' =$$

$$= \frac{1}{2} \bar{K}_o \int_o^\infty dm \int_o^\infty m^n N_o(m - m', t) N_o(m') dm' \quad (152)$$

Equation 152 can be integrated by letting (849):

$$y = m - m', \quad dy = dm$$

$$m^n = (y + m')^n = \sum_{\nu=o}^{n} \binom{n}{\nu} y^{n-\nu} m'^{\nu}$$

Thus,

$$\int_o^\infty m^n B dm = \frac{1}{2} \bar{K}_o \int dy \int_o^\infty \sum_{\nu=o}^{n} \binom{n}{\nu} y^{n-\nu} m'^{\nu} \cdot$$

$$\cdot N_o(y, t) N_o(m', t) dm'$$

$$= \frac{1}{2} \bar{K}_o \sum_{\nu=o}^{n} \binom{n}{\nu} \left[\int y^{n-\nu} N_o(y) dy \right] \cdot$$

$$\cdot \left[\int_o^\infty m'^{\nu} N_o(m') dm' \right]$$

$$= \frac{1}{2} \bar{K}_o \sum_{\nu=o}^{n} \binom{n}{\nu} \mu_{n-\nu} \mu_\nu \quad (153)$$

Therefore, equation 150 can be written as:

$$\frac{d\mu_n}{dt} = \bar{K}_o \left[\frac{1}{2} \sum_{\nu=o}^{n} \binom{n}{\nu} \mu_\nu \mu_{n-\nu} - \mu_o \mu_n \right] \quad (154)$$

or

$$\frac{d\mu_o}{dt} = -\frac{1}{2}\overline{K}_o\mu_o^2$$

$$\frac{d\mu_1}{dt} = 0$$

$$\frac{d\mu_2}{dt} = \overline{K}_o\mu_1^2$$

The solution to equation (154) subject to the initial condition:

$$\mu_n(0) = \lambda_n$$

is

$$\mu_o = \frac{2\lambda_o}{2 + \lambda_o\overline{K}_o t} \qquad (155)$$

$$\mu_1 = \lambda_1$$

$$\mu_2 = \lambda_2 + \lambda_1^2\overline{K}_o t$$

Thus, it is seen that μ_o which gives the total number of particles is inversely proportional to time for long times; the total mass μ_1 remains constant; the sum of the squares of the particle masses increases proportionately with time.

4.30 Methods of Solving the General Kinetic Equation

The most obvious way of solving the general kinetic equation for agglomeration as given by equation 148 is to replace the integrals with summations by using quadrature formulas (842,844,845). Equation 148 can then be written as:

$$\frac{dN_o(m_k, t)}{dt} = \frac{1}{2} \sum_{\ell=1}^{k} K_o(m_\ell, m_k - m_\ell) \cdot$$

$$\cdot N_o(m_\ell, t) N_o(m_k - m_\ell, t) -$$

$$- N_o(m_k, t) \sum_{\ell=1}^{\infty} K_o(m_k, m_\ell) \cdot N_o(m_\ell, t) \quad (156)$$

$$\text{for } k = 1,2, \ldots, \infty$$

subject to the initial distribution $N_o(m_k, o)$ where the values of the m_k are determined by the quadrature formula chosen and need not be evenly spaced. Equation 156 defines a set of simultaneous first order nonlinear ordinary differential equations which can be solved numerically by a digital computer. However, in order to do this, an upper limit k_{max} must be set on the value of k so that the system is finite. Thus, equation 156 becomes:

$$\frac{dN_o(m_k, t)}{dt} = \frac{1}{2} \sum_{\ell=1}^{k} K_o(m_\ell, m_k - m_\ell) \cdot$$

$$\cdot N_o(m_\ell, t) N_o(m_k - m_\ell, t) -$$

$$- N_o(m_k, t) \sum_{\ell=1}^{k_{max}} K_o(m_k, m_\ell) N_o(m_\ell, t) \quad (157)$$

$$k = 1,2 \ldots, k_{max}$$

subject to the initial distribution $N_o(m_k, o)$.

The value of k_{max} is selected such that the value of $m_{k_{max}}$ is so large that $N_o(m_{k_{max}}, t)$ is always negligibly small for the times of interest.

The drawback of this approach is the excessive amount of computation time required. This is due to the fact that in order to obtain accurate numerical solutions the number of equations or k_{max} must be very large while the integration

step size Δt must be very small because $N_o(m_k, t)$ varies strongly with time. Beeckmans (827) used 80 equations, Fair and Gemmell (837) 100, and Hidy (843) 400 and 600.

In attempting to explain the similarity in shape of the particle distribution of stratospheric aerosols, Swift and Friedlander (861,838,839) presented a similarity argument. It is assumed that $N_o(m, t)$ can be expressed as:

$$N_o(m, t) = g(t)\psi(\eta) \tag{158}$$

where

$$\eta = \frac{m}{m^+(t)}$$

and $m^+(t)$ is a scaling factor.

The functions $g(t)$ and $M^+(t)$ can be found by evaluating the zero and first moments of $N_o(m, t)$ in terms of equation 158:

$$\mu_o(t) = \int_o^\infty N_o(m, t)\, dm = g(t)m^+(t) \int_o^\infty \psi(\eta)d\eta =$$

$$= c_1 g(t)m^+(t)$$

or

$$g(t) = \frac{\mu_o(t)}{c_1 m^+(t)} \tag{159}$$

$$\mu_1(t) = \int_0^\infty mN_o(m,\ t)\ dm = \left[m^+(t)\right]^2 g(t) \int_0^\infty \eta\psi(\eta)d\eta$$

$$= c_2 \left[m^+(t)\right]^2 g(t) = \frac{c_2}{c_1}\,\mu_o(t)m^+(t)$$

or

$$m^+(t) = \frac{c_1}{c_2}\,\frac{\mu_1(t)}{\mu_o(t)} \tag{160}$$

Substituting equations 159 and 160 into 158:

$$N_o(m,\ t) = c_2\,\frac{\mu_o^{\,2}(t)}{\mu_1(t)}\,\psi\left[\frac{c_2}{c_1}\,\frac{\mu_o(t)}{\mu_1(t)}\,m\right] \tag{161}$$

In order to determine $\psi(m)$, equation 161 is substituted into equation 148 which upon simplification results in an integro-differential equation to be solved for $\psi(m)$. Swift and Friedlander (861) did this for the case of no interaction potential and obtained:

$$\left[1 + \int_o^\infty \tilde{\eta}^{1/3}\psi_1(\eta)d\eta \int_o^\infty \tilde{\eta}^{1/3}\psi_1(\tilde{\eta})d\tilde{\eta}\right]\left[2\psi_1(\eta) + \eta\frac{d\psi_1}{d\eta}\right] +$$

$$+ 1/2 \int_o^\eta \psi_1(\tilde{\eta})\psi_1(\eta - \tilde{\eta})\ [\tilde{\eta}^{1/3} +$$

$$+ (\eta - \tilde{\eta})^{1/3}]\left[\frac{1}{\tilde{\eta}^{1/3}} + \frac{1}{(\eta - \tilde{\eta})^{1/3}}\right]\ d\tilde{\eta} -$$

$$- \psi_1(\eta) \int_o^\infty \psi_1(\tilde{\eta})\ [\eta^{1/3} +$$

$$+ \tilde{\eta}^{1/3}]\left[\frac{1}{\eta^{1/3}} + \frac{1}{\tilde{\eta}^{1/3}}\right] d\tilde{\eta} = 0 \tag{162}$$

Unfortunately, this equation for $\psi(m)$ is no more easily solved than the original equation for $N_o(m, t)$, and in fact because it is much more non-linear, it may be more difficult to solve.

A similar approach was taken by Martynov and Bakanov (854) who used a series decomposition method to obtain a general but not very practical solution for the initial stages of agglomeration.

Another approach that has been used is the so-called "approximation technique" (826). It consists of choosing a specific distribution function for $N_o(m, t)$ whose parameters are taken as functions of time. Cohen and Vaughan (833) used a log-normal distribution and justified this on the grounds that the experimental results of Lindauer and Castleman (853) indicate such a distribution for short times.

$$N_o(m, t) = \frac{\mu_o(t)}{\sqrt{2\pi V(t)}} \exp \left\{ - \left[\frac{\ln \frac{m}{\bar{m}(t)}}{\sqrt{2V(t)}} \right]^2 \right\} \frac{1}{m} \quad (163)$$

where $V(t)$ is the logarithmic variance and $\bar{m}(t)$ the geometric mean mass of a particle. The parameters $\mu_o(t)$, $\sigma(t)$ and $\bar{m}(t)$ are unknown functions to be determined.

This is accomplished by rewritting equation 148 in terms of the moments of $N_o(m, t)$ as defined by equation 149:

$$\frac{d\mu_n}{dt} = \frac{1}{2} \int_o^\infty \int_o^\infty m^n K_o(m', m - m') N_o(m', t) \cdot$$

$$\cdot N_o(m - m', t) dm'dm -$$

$$- \int_o^\infty \int_o^\infty m^n K_o(m, m') N_o(m', t) N_o(m, t) dm'dm \quad (164)$$

$$n = 1, 2 \ldots\ldots$$

The moments μ_n can be expressed in terms of the parameters for a log-normal distribution as:

$$\mu_n(t) = \mu_o(t)\ [\bar{m}(t)]^n \exp\left\{\frac{n^2}{2} V(t)\right\} \qquad (165)$$

so that:

$$\bar{m}(t) = \frac{\mu_1^2}{\sqrt{\mu_o^3 \mu_2}} \qquad (166a)$$

$$V(t) = \ln\left(\frac{\mu_o \mu_2}{\mu_1^2}\right) \qquad (166b)$$

By substituting equations 165 and 166 into equation 164, a set of three first order nonlinear ordinary differential equation for $\mu_o(t)$, $\bar{m}(t)$ and $V(t)$ results whose solution can be obtained by numerical integration with a computer. The advantage of this method is a considerable reduction in computation time. Unfortunately, the disadvantage of this method is that the accuracy of the solution depends very heavily on choosing the proper form of the distribution function for $N_o(m, t)$ and that there is no way of checking the validity of the solution other than comparing it with that given by directly solving the integro-differential equation 148.

Hulburt and Katz (849) have shown that a distribution function f(r) can be expanded in series in terms of its moments, the chi-square distribution, and Laguerre polynomials.

$$f(r) = \frac{\lambda}{a} p^{(\lambda)}\left(\frac{\lambda r}{a}\right) \sum_{k=o}^{\infty} k_n L_n^{(\lambda)}\left(\frac{\lambda r}{a}\right) \qquad (167)$$

where

$$p^{(\lambda)}(z) = z^{\lambda-1}e^{-z}/(\lambda - 1)!$$

$$L_n^{(\lambda)}(z) = \sum_{j=o}^{n} (-1)j \frac{n!(n + \lambda - 1)!}{j!(n - j)!(n + \lambda - 1 - j)!} z^{n-j}$$

The parameters are λ, a, and the k_n. The k_n may be expressed in terms of the moments of f(r) as:

$$k_n = \sum_{j=o}^{n} (-1)^j \frac{(\lambda - 1)!}{j!(n + \lambda - 1 \cdot j)!} \frac{(\lambda/a)^{n-j}}{(n - j)!} \mu_{n-j}$$

This gives for the first three terms:

$$k_o = \mu_o$$

$$k_1 = (\mu_1/a) - \mu_o .$$

$$k_2 = \frac{1}{2a^2} \left(\frac{\lambda}{\lambda + 1}\right) \mu_2 - \frac{\mu_1}{a} + \frac{1}{2} \mu_o$$

Thus, the two parameters, λ and a can be chosen arbitrarily.

A trial form for $N_o(m, t)$ is chosen by truncating the series at the ℓ^{th} term and substituting this expression into equation 148, which gives a set of ℓ first order nonlinear ordinary differential equations for the μ_ℓ.

In order to check the accuracy of the solution and thus determine if ℓ terms were sufficient, the system is solved again for $\ell + 1$ terms. If the two results do not differ, then no higher terms are needed, and convergence is obtained. Since λ and a are arbitrary, they can be selected such that the number of terms ℓ is a minimum and convergence is as rapid as possible.

Of all the methods of solution, this technique is the most desirable. However, it has not been extensively used, and for those cases where it has, the problems were of a

fairly simple nature (848).

4.31 Mean Free Path Effect

For very small particles such that the Knudsen number Kn defined as the ratio of the mean free path of the medium λ and the diameter of the particle is greater than .1, the increased mobility of the particles is accounted for by empirically correcting the Brownian diffusion coefficient by means of the Stokes-Cummingham factor (834,851,855).

$$\mathcal{D}_i = \frac{kT}{6\pi\mu a_i} (1 + A_i Kn_i) \tag{168}$$

where

$$A_i = 1.125 + .400 \exp [-1.10\ Kn_i^{-1}]$$

$$Kn_i = \frac{\lambda}{a_i}$$

This equation is valid up to Kn $\approx$1.

When Kn $\geq$ 10, the continuum approach must be completely abandoned in favor of the kinetic theory of gases. The rate of collisions between particles of types i and j is then given by the usual expression (846).

$$J_{ij} = \int_0^\infty \int_0^\infty \int_0^{2\pi} \int_0^{a_{ij}} f_i(v_i, t) f_j(v_j, t) \delta_{ij} \cdot g_{ij} b\,db\,d\epsilon\,dv_i\,dv_j \tag{169}$$

where f_i and v_i are the distribution function and velocity of the i^{th} type particle g_{ij} the absolute value of the relative velocity of the particles $|v_i - v_j|$, b impact parameter, and ϵ an angle. The distribution f has the known form (846).

$$f_i(v_i,\ t) = N_o(m_i,\ t)\left[\frac{m_i}{2\pi kT}\right]^{3/2} \cdot$$

$$\cdot\ \exp\left\{-\frac{1}{kT}\left[\frac{1}{2}\,m_i v_i^{\,2} + \varphi\right]\right\} \qquad (170)$$

where φ is an interaction potential.

If equation 170 with $\varphi = 0$ is substituted into equation 169 and the integration carried out, the result is (846):

$$J_{ij} = 2N_o(m_i,\ t)N_o(m_j,\ t)a_{ij}^{\,2} \cdot$$

$$\cdot\ \sqrt{2\pi kT\left(\frac{1}{m_i} + \frac{1}{m_j}\right)} \qquad (171)$$

This expression is to be used in place of the rate expression based on continuum theory.

Block and Hidy (829) have gone through this procedure for a Sutherland potential with Debye-Huckel shielding.

For the transition region $1 \leq Kn \leq 10$, only an approximate estimate of the collision rate can be made following the approaches of Arendt and Kallaman (825), Fuchs (840), and Zebel (864,865). The kinetic gas theory is applied up to a distance of one mean free path of a particle ℓ from the particle's surface while diffusion theory is used from that point on. The two theories are coupled together by requiring that the concentrations and fluxes as given by them are equal at a distance ℓ.

$$J_i\Big|_{\text{diffusion}} = 4\pi(a_{ij} + \ell_{ij})\mathcal{R}_{ij}\delta_{ij}W_{ij}^{-1} \cdot$$

$$\cdot\ [N_{io} - N_{i\ell}] \qquad (172)$$

where $N_{i\ell}$ is the concentration at a distance $\ell_{ij} = \ell_i + \ell_j$,

$$J_i \Big|_{\substack{\text{kinetic} \\ \text{theory}}} = 2N_{i\ell}a_{ij}^2 \sqrt{2\pi kT\left(\frac{m_i + m_j}{m_i m_j}\right)} \qquad (173)$$

Equating equations 172 and 173, solving for $N_{i\ell}$, and substituting this expression into equation 172 yields:

$$J_{ij} = 4\pi\delta_{ij}\mathfrak{D}_{ij}(a_{ij} + \ell_{ij})W_{ij}^{-1}N_{io}N_{jo}\left(\frac{1}{1 + G_{ij}}\right) \qquad (174)$$

where

$$G_{ij} = \frac{4\mathfrak{D}_{ij}\delta_{ij}W_{ij}^{-1}}{a_{ij}(1 + \ell_{ij}/a_{ij})^{-1}} \sqrt{\frac{m_i m_j}{m_i + m_j}\frac{\pi}{8kT}}$$

Thus, the effect of taking the particle's mean free path into account is to modify the coagulation constant to read:

$$K_o(a_i, a_j) = 4\pi\delta_{ij}\mathfrak{D}_{ij}a_{ij}W_{ij}^{-1}F_{ij} \qquad (175)$$

where

$$F_{ij} = \frac{1 + \ell_{ij}/a_{ij}}{1 + G_{ij}}$$

This is the result obtained by Zebel (864,865) in a more general form. Unfortunately, equation 175 does not agree with the limiting cases given by the continuum and kinetic gas theories so that its validity is doubtful. However, in a similar manner Fuks (840) found for equal sized particles and no interaction potential:

$$F_{ii} = \frac{1}{2}\left[\frac{a_i}{a_i + \delta/2} + \frac{\pi\ell_i}{2\sqrt{2}a_i}\right]^{-1} \qquad (176)$$

where δ is the thickness of the region where kinetic theory applies.

In order to agree with the limiting cases, he required

that in the limits Kn → 0 and Kn >> 1, $\delta = \ell_i$ and that:

$$\ell_i = \frac{8}{\pi} \mathcal{D}_i \left(\frac{8kT}{m_i \pi}\right)^{-1/2}$$

An alternate but much more complex approach has been presented by Brock and Hidy (829) in which the kinetic gas theory has been extended rather than the continuum theory.

4.32 Effect of Hydrodynamic Interaction

Derjaguin (835,836) observed that at small interparticle distances colloidal particles do follow Stokes law:

$$F = 6\pi\mu a u$$

where F is the force exerted on the particle and u its velocity. Stimson and Jeffery (860) showed that the proper equations are:

$$\begin{aligned} F_i &= -\kappa_i u_i + \lambda_i u_j \\ F_j &= -\kappa_j u_j + \lambda_j u_i \end{aligned} \qquad (177)$$

where the κ_i, κ_j, λ_i, λ_j are positive coefficients proportional to the viscosity and related to the dimensions and separation of the particles by complicated functions. Following this theory, Spielman (859) showed that the resistance coefficient β_{ij} is given by:

$$\beta_{ij} = \frac{\kappa_i \kappa_j - \lambda_i \lambda_j}{\kappa_i + \kappa_j - \lambda_i - \lambda_j} \qquad (178)$$

This means that in order to incorporate the hydrodynamic interaction effect into the theory presented so far one merely uses a different but more complex function for β_{ij} in place of the simple expression:

$$\beta_{ij} = 6\pi\mu \frac{a_i a_j}{a_i + a_j} \qquad (179)$$

An asymptotic equation for very small separations is given by (831):

$$\beta_{ij} = \frac{6\pi\mu a_i}{\frac{s}{a_i}(1 + a_i/a_j)^2}, \quad \frac{s}{a_i} << 1 \qquad (180)$$

A similar approach was taken for the case of spheres with equal radii by Honig et al (847) who used an expression for β given by Brenner (828). The results of both these studies indicated that hydrodynamic interaction can significantly reduce the rate of coagulation as computed without it being accounted for.

4.33 Other Mechanisms of Agglomeration

Two other mechanisms which can contribute to the collision of colloidal particles are gravity and turbulence. Due to gravity, particles will fall at velocities dependent on their size according to Stokes' law so that large particles will tend to sweep past small ones, thus, causing collisions. Turbulence can cause collisions due to motion caused by entrainment of the particles by eddies. In order to account for these mechanisms, the expression for the rate of collisions is modified to read (841,863):

$$J_{ij} = \left\{ K_o(a_i, a_j) + K_c(a_i^2 - a_j^2)(a_i + a_j)^2 + \right.$$
$$\left. + K_T(a_i + a_j)^3 \right\} N_{io}N_{jo} \qquad (181)$$

where

$$K_c = \frac{32\pi\rho g}{9\mu}$$

$$K_T = \frac{32}{3}\left(\frac{d\bar{u}}{dz}\right)$$

and $\frac{d\bar{u}}{dz}$ is the mean rate of shear due to turbulence.

4.34 Agglomeration of Charged Particles in a Non-Aqueous Medium

For particles in a non-aqueous medium, the potential due to the electrical double layer reduces to the coulomb potential which describes the force between two charges because there are no ions in the medium:

$$V_{ij}^{(coul)} = \frac{q_i q_j}{r} \tag{182}$$

where q_i is the charge of the i^{th} particle and r the distance between the centers of the particles. This potential is used in place of the double layer potential V_R so that the total potential is:

$$V_T = V_A + V^{(coul)} \tag{183}$$

Therefore, the theory given so far remains unaltered except a minor modification of the kinetic equation due to the fact that in this case a particle is characterized by not only its size or mass but also its charge.

Thus, the kinetic equation is modified to read (864,865):

$$\frac{\partial N_o(m, q, t)}{\partial t} = \frac{1}{2} \int_{-\infty}^{\infty} \int_{o}^{m} K_o(m', m-m', q', q-q') N_o(m', q', t) \cdot$$

$$\cdot N_o(m-m', q-q', t) dm'dq' -$$

$$- N_o(m, q, t) \int_{-\infty}^{\infty} \int_{o}^{\infty} K_o(m, m'; q, q') \cdot$$

$$\cdot N_o(m', q', t) dm'dq' -$$

$$- 4\pi\beta^{-1} q N_o(m,q,t) \int_{-\infty}^{\infty} \int_{o}^{\infty} q' N_o(m,q',t) \cdot dmdq' \tag{184}$$

where $N_o(m, q, t)$ is number density of particles with mass m and charge q. The first term of the right hand side of this equation says that a particle with mass m and charge q is formed if two particles with masses m' and m-m' and charges q' and q-q' collide. The second term states that a particle of mass m and charge q disappears if it collides with any other particles. The last term is due to the electric field which is caused by an excess charge if the positive and negative charges do not balance. The derivation of this equation is similar to that given earlier and is presented by Zebel (864,865).

4.35 Agglomeration of Non-Spherical Particles

In order to determine the collision rate of non-spherical particles, one proceeds as for the spherical case and considers this rate to be governed by the diffusion of the surrounding particles i to the absorbing surface of the collecting particle j. As shown before the diffusion equation:

$$\frac{\partial N_i}{\partial t} = \nabla \cdot (\beta_{ij} \nabla N_i + \beta_{ij}^{-1} N_i \nabla V_{ij}) \qquad (185)$$

is to be solved subject to the boundary conditions:

$N_i = 0$ on the absorbing surface S

$N_i = N_{io}$ at a very large distance from the absorbing surface

and the initial condition:

$N_i = N_{io}$ at $t = 0$

From this solution the collision rate is obtained by evaluating the flux of particles at the absorbing surface:

$$J_i = - \int_S \beta_{ij} \nabla N_i \Big|_S dS' \qquad (186)$$

Since the stationary solution is required, $\frac{\partial N_i}{\partial t} = 0$ so that the system to be solved becomes:

$$\nabla \cdot (\mathcal{D}_{ij} \nabla N_i + \beta_{ij}^{-1} N_i \nabla V_{ij}) = 0 \qquad (187a)$$

subject to:

$$N_i = 0 \qquad \text{on S} \qquad (187b)$$

$$N_i = N_{io} \qquad \text{at infinity} \qquad (187c)$$

The only further treatment of this problem was given by Müller (856,840) in 1928 for the case of ellipsoidal particles with no interaction potential. For this case equation 187a simplifies to:

$$\nabla^2 N_i = 0 \qquad (188)$$

subject to:

$$N_i = 0 \qquad \text{on S}$$

$$N_i = N_{io} \qquad \text{at infinity}$$

If the change of variables:

$$\psi = N_i - N_{io}$$

is made, equation 188 becomes:

$$\nabla^2 \psi = 0 \qquad (189)$$

subject to:

$$\psi = -N_{io} \qquad \text{on S}$$

$$\psi = 0 \qquad \text{at infinity}$$

Equation 189 is of the same type of system used in electrostatic theory.

The concentration and its gradient are analogous to the electrostatic potential and the field strength. It is well

known from electrostatics that the field strength is large at points of sharp curvature. Thus, since the flux is proportional to the concentration gradient it is expected that collisions between particles would occur mainly at their most sharp points.

Taking advantage of this analogy, equation 186 may be written as:

$$J_i = 4\pi \beta_{ij} C_{ij} N_{io} \tag{190}$$

This follows from the fact that:

$$\nabla N_i \Big|_S = \nabla \psi \Big|_S = -4\pi\sigma \tag{191}$$

where σ is the surface charge density so that substituting equation 191 into 186:

$$J_i = 4\pi \beta_{ij} \int_S \sigma dS' = 4\pi \beta_{ij} q \tag{192}$$

where q is the total surface charge. Introducing the capacitance of the surface:

$$C_{ij} = \frac{q}{\psi} = \frac{q}{N_{io}} \tag{193}$$

into equation 192, equation 190 is obtained. The value of introducing the capacitance is that equations are available for it for various shapes from electrostatic theory. For example, the capacitance for the case of spheres diffusing to an ellipsoidal particle is (850):

$$C_{ij} = \sqrt{D^2 - E^2} \; / \; \ln \frac{D + \sqrt{D^2 - E^2}}{E} \tag{194}$$

where

$$D = d + a$$

$$E = e + a$$

and d, e are the semi-axes of the ellipsoid and a the radius of the spheres.

Another problem of non-spherical particles that has not been treated is the rotation of the particles due to their Brownian motion.

4.36 The Strength of Agglomerates

The main bonding mechanisms of fine particles are, (1) solid bridges, (2) capillary pressure at freely moving liquid surfaces, (3) adhesion and cohesion forces in agglutinate bridges not in free motion, (4) from-closed bonding, and (5) attraction forces between solid particles.

Solid bridges between particles can be formed by sintering, chemical reactions, melting, hardening agglutinates, and crystallization, and tend to occur at points of contact, especially where there are sharp peaks or edges.

Moist particles adhere to each other due to capillary pressure at freely moving liquid surfaces. As shown in Figure 37, there are four ways in which the liquid may be distributed between the particles. In type A, there is such a small amount of liquid that the liquid forms bridges around contact points. In type C, the void space is completely filled with liquid while type B is an intermediate case between types A and C. In type D the liquid completely envelops the particles so that a droplet filled with particles is formed.

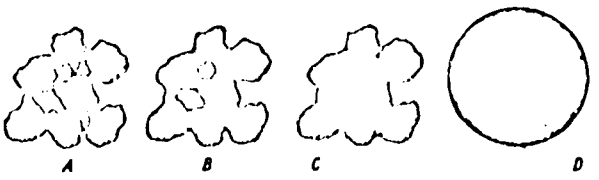

Figure 37

POSSIBLE LIQUID DISTRIBUTIONS IN PARTICLE PILES

Non-freely moving bridges are formed by thin layers of viscous binders adhearing to the particles and also by thin adsorption layers.

Form-closed bonds result from particles interlocking with each other.

Attraction between particles can also be caused by molecular or Van der Waals forces and electrostatic charges.

Rumpf (877) derived a basic equation for the tensile strength of agglomerates held together by adhesion forces at their contact point. He assumed the particles were monosized spheres, and obtained for the tensile strength σ_z:

$$\sigma_z = \frac{9}{8} \frac{1 - \epsilon}{\pi d^2} kH \qquad (195)$$

where ϵ is porosity, d particle diameter, k mean coordinate number, and H the adhesion force at a contact point. Cheng (881) has obtained a similar but not as useful result.

Rumpf (877,878) and also Pietsch (879,880) have evaluated equation 195 for several of the bonding mechanisms by using suitable theoretical and empirical expressions for H. For solid bridges:

$$\sigma_z = \psi_B \epsilon \sigma_B \qquad (196)$$

where ψ_B is the degree of filling of the agglutinant and σ_B its tensile strength.

For liquid bridges of type A:

$$\sigma_z = \frac{9}{8} 2.5 \nu \frac{1 - \epsilon}{\epsilon} \frac{1}{d} \qquad (197)$$

where ν is surface tension while for type C:

$$\sigma_z = \alpha \frac{1 - \epsilon}{\epsilon} \alpha \frac{1}{d} \qquad (198)$$

where α is a constant between 6 and 8.

For molecular attraction:

$$\sigma_z = \frac{9}{8} \frac{1 - \epsilon}{\epsilon} \frac{A}{24S^2} \frac{1}{d} \tag{199}$$

where A is the Hamaker constant and S distance between particles.

For electrostatic attraction:

$$\sigma_z = \frac{9}{8} \frac{1 - \epsilon}{\epsilon} \frac{3\varphi^2}{(1 + \frac{S}{d})^2} \tag{200}$$

where φ is the surface charge density.

These equations are summarized in Figure 38 where the tensile strength of the agglomerate is plotted against particle size.

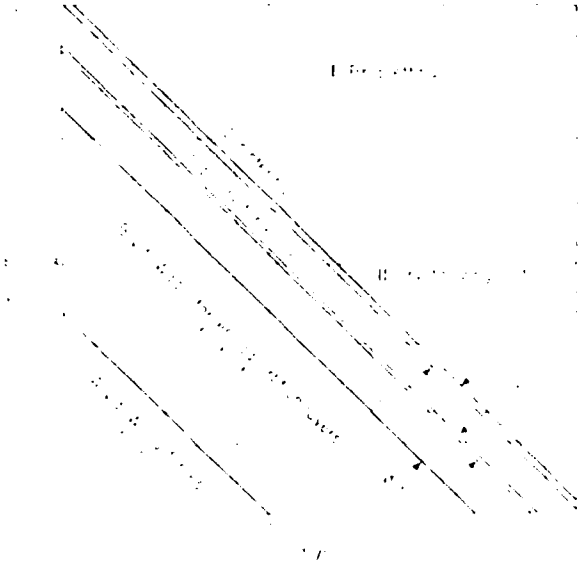

Figure 38

THEORETICAL TENSILE STRENGTH OF AGGLOMERATES: CURVE 1, FLUID BRIDGES; CURVE 2, COMPLETELY FILLED VOID VOLUME. 2a UNIFORMLY SIZE; 2b RRS DISTRIBUTION, n = 0.8; 2c RRS DISTRIBUTION, n = 1.4 (878).

4.37 Adhesion of Small Particles to a Flat Plate

A consistent theory of adhesion of small particles to a flat plate has been presented by Krupp and his associates (888,889,890). The assumptions on which the model is based are: (1) the system is a sphere adhering to a smooth flat plate, (2) no external force is applied to press them together, (3) the force of adhesion is that force normal to the plate required to tear the particle away, (4) the range of temperature is around ambient, (5) the attractive force is of the Van der Waals and electrostatic type, and (6) the environment is a vacuum or inert gas.

Consider the system shown in Figure 39.

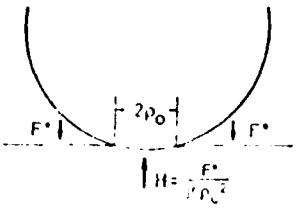

Figure 39

MODEL OF PARTICLE ADHESION

Equilibrium of the forces acting the particle yields:

$$F^o = \pi \rho_o^2 H \tag{201}$$

where F^o is the attractive force acting outside the contact area, ρ^o the radius of the circular area of contact, and H the Meyer hardness of the softer of the two adherents. Empirically, it has been found from stress-strain diagrams that H is a function of the duration t of stress application of the form:

$$\frac{1}{H} = \frac{1}{H_o} + \frac{1}{H_\tau}\left(1 - e^{-t/\tau}\right) + \frac{t}{\eta} \tag{202}$$

where H_o and H_τ are the values of H at Z = 0 and t = τ respectively and τ and η constants.

Across the surface of contact there is an attractive force per unit area denoted as P. Thus, the force F required to remove the particle is:

$$F = F^o + \pi\rho_o{}^2 P \tag{203}$$

or using equation 201:

$$F = F^o(1 + P/H) \tag{204}$$

The forces P and F^o can be evaluated as follows. The Van der Waals component P_{vdw} of P is given by the expression for two flat plates:

$$P_{vdw} = \frac{A}{6\pi S^3} \tag{205}$$

where S is the distance between adherents at the contact area and A the Hamaker constant. S may be taken to be about 4Å. Similarly, the Van der Waals component $F^o{}_{vdw}$ of F^o is given by the expression for a sphere and a flat plate:

$$F^o{}_{vdw} = \frac{Aa}{6S^2} \tag{206}$$

Thus, in the absence of additional electrostatic forces, equations 202, 205, and 206 may be substituted into equation 204 to give:

$$F = \frac{Aa}{6S^2}\left\{1 + \frac{A}{6\pi S^3}\left[\frac{1}{H_o} + \frac{1}{H_\tau}(1 - e^{-t/\tau}) + \frac{t}{\eta}\right]\right\} \tag{207}$$

Attractive forces can also originate from the electronic energy levels of the adherents. From the equations for the electrostatic force between two plates and a sphere and a flat plates, the electrical components P_{el} and $F^o{}_{el}$ are

given by:

$$P_{el} = \epsilon_o U^2/2S^2 \tag{208}$$

and

$$F^o_{el} = \pi\epsilon_o(\frac{U^2}{S})a \tag{209}$$

where U is a potential difference and ϵ_o a constant equal to 8.86×10^{-4} Å sec/V cm.

4.38 Adhesion Due to Capillary Condensation

Condensation of water vapor can take place in the gap between bodies on contact due to air humidity as shown in Figure 40. The meniscus formed draws the bodies together due to surface tension and reduces the pressure of the liquid. The two effects cause attractive forces (885):

$$F_1 = 2\pi a_1 \nu \tag{210}$$

and

$$F_2 = \nu\pi a_1^2(\frac{1}{a_2} - \frac{1}{a_1}) \tag{211}$$

respectively, where ν is surface tension and a_1 and a_2 the radii of curvature of the free liquid surface. The total attractive force is then:

$$F = F_1 + F_2 = \frac{\pi a_1 \nu(a_1 + a_2)}{a_2} \tag{212}$$

The radii of curvature can be expressed in terms the radius a of the bodies in contact from simple geometry as (885):

$$a_1 = a(1 + \tan\alpha - \sec\alpha) \tag{215}$$

$$a_2 = a(\sec\alpha - 1) \tag{214}$$

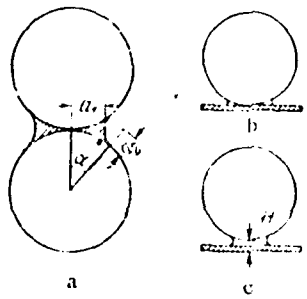

Figure 40

CAPILLARY CONDENSATION ASSOCIATED WITH THE CONTACT OF TWO PARTICLES (a) AND OF A PARTICLE WITH A SURFACE (b, c). a, b) WITHOUT ANY INTERMEDIATE LAYER; c) WITH AN INTERMEDIATE LAYER IN THE CONTACT ZONE.

Substituting equations 215 and 214 into equation 212 gives:

$$F = \frac{2\pi\nu a}{(1 + \tan \frac{\alpha}{2})} \qquad (215)$$

For unwetted surface euqation 215 should be multiplied by cos θ where θ is the wetting angle. Similar but more exact and complicated models have been proposed by Gillespie and Settineri (882), Melrose (883), Radushkevich (884), Picknett (887) and Princen (886).

4.39 Summary

The theory of the stability of colloidal systems has been presented from a mathematical point of view. It was shown that the force acting between colloidal particles consists of an attractive part due to London-Van der Waals forces and a repulsive part due to the interaction of the electrical double layers of the particles. Equations were derived for the purpose of determining these forces. This allowed the stability of a colloidal system to be described by means of a calculated potential energy of interaction curve. The result

is that the stability of a system can be qualitatively assessed by the magnitude of the curve's maximum value. The larger this value is, the more stable is the system. The theory is able to explain most of the experimentally observed phenomena of colloidal systems. However, the one important thing that it cannot do is to predict how long a system will be stable. In order to accomplish this, the collision rate of particles had to be investigated. The analysis yielded an integro-differential equation to be solved. This equation can only be solved analytically for situations that are not likely to occur in practice while in all other cases a computer must be used. Current numerical techniques demand the simultaneous solution of hundreds of differential equations which require excessive computer time. Also, in the cases investigated in this way, only simple systems were considered where there were no interaction forces between the particles. However, in these cases the theory was in agreement with data. It should be also noted that mainly spherical particles have been treated and to a very slight extent particles of other shapes.

Equations were also presented for the tensile strength of powders, the force between a particle in contact with plate, and bodies bonded together by capillary forces. These equations are in general agreement with data but it should be kept in mind that their purpose is more to give an order of magnitude rather than exact values.

5. METHODS OF SAMPLING, COLLECTING AND ANALYZING SUBMICRON PARTICLES

The three previous sections have described ways of removing particles from surfaces, stabilizing them and dispersing them into fluids. In this section, the methods available for their sampling, collection and analysis are reviewed. It is realized that for the requirements of this program, every particle dispersed has to be collected for analysis and so sampling may appear to be an unnecessary step. However, as particles have to be drawn into the device in which they are to be collected, many of the problems associated with sample line loss, for example, are involved in the collecting device itself and need to be defined. Although the method of collection in a suitable form for analysis is by far the most important step, an analytical method has to be employed, which is sensitive enough to indicate how efficient the methods of separation and collection have been. High efficiency can be defined as a good state of separation of the particles on the collecting substrate, with no loss of particles during the separating, dispersing, sampling and collecting stages. Literature is now presented relating to all of these pertinent areas, and it has been assembled so as to investigate sampling collection and analysis of both particles in air and liquid.

5.1 Particles in Air

5.1.1 Sampling

The transport of airborne particles to and deposition on surfaces is of considerable importance in industry, meteorology and in life sciences. The case of general significance is the deposition of particles in systems designed to transport gases containing particles to points of release to the atmosphere, to storage zones, to a sample collector or analyzer. The deposition and retention of particles in ducts, sampling lines and collecting instruments may materially influence the assessment, or the safety of the gaseous release.

In most cases, the analytical device is invariably separated from the sample probe by some distance. In transporting the aerosol to the collecting or analytical device, changes can occur in the nature of the aerosol. Agglomeration can occur due to Brownian motion, eddy fluctuations, thermal turbulence, and electrostatic effects. Losses to the walls of the transportation system can occur by diffusive and gravitational precipitation in laminar flow, or by turbulent diffusion in turbulent flow. There could be deposition losses due to acoustic resonance if sonic vibrations occur which are near to the resonant frequency of the transported particles. Another, often neglected, means of deposition of particulate matter is due to particle space charge and induced electrostatic effects. The various mechanisms of particle deposition in sampling lines were recently discussed in detail by Davies (893).

An accurate determination of the significance of particle deposition in a given circumstance requires knowledge of the many parameters which control the behavior of particles in an air stream. The important variables are the velocity of the carrying gas and its dynamic fluid properties, the friction of the surfaces or walls in the case of closed conduit, the charge on the particles, and finally the inertial properties of the particles themselves. The effect of particle diameter on deposition velocity is shown in Figure 41. From this figure, it is seen that there is a size range at which minimum deposition occurs. This is between 0.2 and 0.8 micron dependent on the Reynolds number. To the right of this minimum, deposition increases due to inertial and gravitational mechanisms, but to the left of the minimum, i.e., in the size range of interest in this report, deposition increases due to the diffusional and electrostatic mechanisms. Hence, for this study, electrostatic charge will be of major importance and will have to be eliminated for dispersions of aerosol in air.

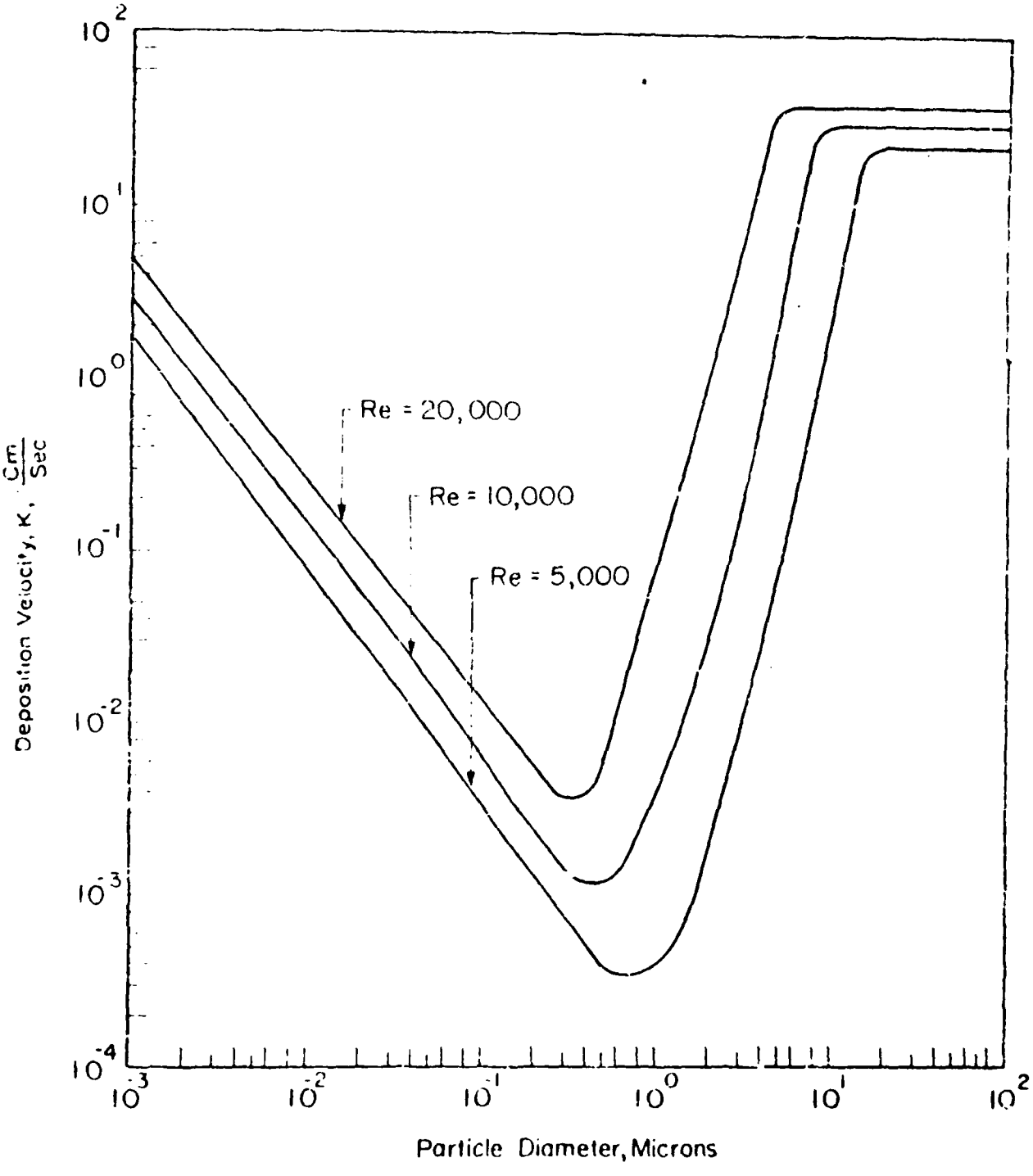

Figure 41

EFFECT OF PARTICLE DIAMETER ON DEPOSITION VELOCITY

Various theories and empirical correlations have been proposed to predict the turbulent deposition of particles in vertical and horizontal tubes. Both phenomenonlogical and stochastic approaches to this problem have been presented to predict a particulate velocity of deposition, K_L, in tubes.

$$K_L = \frac{\text{Number of particles deposited/cm}^2 \text{ sec.}}{\text{Number of Particles/cm}^3}$$

Recent reviews on this subject are readily available (891-899, 901-905). Most of these correlations or theoretical predictions were valid for smooth tubes and held for particle sizes $\geq$1 micron when deposition due to Stokes'-Einstein diffusivity was negligible. A unified approach was developed by Beal (891), Sood, Lieberman, Wasan (900), Davies (893), and Sehmel (905), which covered a particle size range from molecular size to the order of tens of microns. The method of analysis employed by Sood, et al. (900) was very similar to the method used by Beal (891), except that a different and more realistic correlation for eddy diffusivity, as proposed by Wasan was used. In this study, experimental values of deposition were compared with theoretically predicted values for different values of Reynolds number of flow through the tube for neutral particles. A good agreement between theory and experimental data was obtained for the small particle sizes.

When the theoretical results were compared with experimental data when the natural charge on aerosol particles was not eliminated, much higher experimental values of deposition for small particles were obtained; the theory, which did not account for electrostatic charge on particles, did not adequately describe the transport loss phenomena of charged aerosol consisting of small particles (<1 micron). This was because electrostatic forces between charged aerosol particles and the image charge on the conduit wall overshadowed the forces due to gravity, eddy motion and inertia. Moreover, the

presence of bipolar charged particles led to enhanced coagulation resulting in larger particles which then deposited at a higher rate.

Larger particles, > 3 μ, however, deposited to a smaller extent than expected from theory both for charged and uncharged aerosols. This was because in the theoretical analysis the pipe wall was assumed to be a perfect sink and no account was taken of particle reentrainment. Reentrainment of 6 μ particles began at Reynolds number of approximately 5000; that of 3 μ particles at Re = 8000, and that of 1.5 μ particles at Re = 16,000, both for charged and neutral particles. This agreed with the observations of previous investigators (893,895,902). Larger particles were more easily reentrained from the wall since they projected further into the gas stream. To eliminate sample line loss, it was considered conceivable that solid particle deposition could be prevented by using a porous sampling tube constructed out of a fine pore, sintered metal. The tube could then be surrounded by an annular space containing clear air at a higher pressure. The air would "transpire" through the tube wall into the main stream, thus providing a sheath of air next to the wall and reducing the rate at which the particles reached the tube wall.

This was implemented in a second study at IIT Research Institute (906) in which a simplified theoretical analysis based on the concept of the transverse flow through the porous walls of the tube was presented. Equations were employed to estimate the gas transpiration rate to minimize the solid particle deposition losses while designing or evaluating aerosol instrumentation and pollution control devices.

The sampling collection and analysis of dusts and fumes in mines, factories, and industrial plants was the subject of other work in this field. A review of the practices in coal mines was reported by the Aerosol Technology Committee of the American Industrial Hygiene Association (907). This report

was concerned with respirable mass sampling, and a listing of all current instruments capable of performing this task was included for reference. Background to this report was provided by Lippman (908) who discussed the factors that affect the parameters that describe particle deposition and retention in the human respiratory tract. A comprehensive review of the effect of air pollutants on the human lung was presented in a series of papers given at the Conference of Inhalation Carcinogenesis sponsored by the U.S. Atomic Energy Commission. Individual papers are not referenced here, but readers are directed to the proceedings of this conference (909). In assessing the concentration and size distribution of particles found in many aerosol systems, the representative sampling of the system is of the utmost importance. Yanada and Charlson (910) gave an account of a study performed to investigate the effect of differently sized sample inlet lines in the continuous monitoring of air pollution sources. Sehmel and Schwendiman (911) recorded the amount of particle deposition that took place in a curved sampling probe, and Kneen and Strauss (912) proposed a mathematical expression for the deposition rate of particles from turbulent gas streams. On the same subject, Wehner, at al. (913) studied the effect of unipolar charge on aerosol particles, and related it to their deposition in tubes and pipes.

From these references, it was found that particles are lost from aerosol systems by many different mechanisms. For submicron particles of particular importance are electrostatic charge and diffusion. Charge can be reduced and eventually removed by a source of bipolar ions, e.g., from a Whitby ionizer (900). Total line loss can be eliminated by the use of transverse flow of air around the aerosol stream. These experimental findings should be implemented into a collecting device if submicron particles are to be collected with high efficiency from transported aerosols.

5.1.2 Collection

There are several types of collection systems for particles in air. These include:

Gravity Sedimentation
Centrifugal Sedimentation
Impaction
Centrifugal Impaction
Impingement
Thermal Precipitation
Electrostatic Precipitation
Filtration

For submicron particles, the most useful collecting devices operate under centrifugal, thermal and electrostatic fields. Other devices are of no value for this size range of aerosol (914). The merits of each of these systems are now reviewed with reference to recent literature.

5.1.3 Centrifugal Systems

These can be subdivided into three categories: (a) cyclones, (b) classifiers, and (c) spectrometers.

Basically, cyclones separate all particles from the air and collect them together; classifiers separate any two size fractions and collect them separately; and spectrometers collect the whole size distribution over a known area in bands of particles with the same aerodynamic diameter.

5.1.4 Cyclones

In 1960, Hyatt, et al. (915) determined the particle size collection efficiencies of several size-selective samplers including cyclones. Similar work was reported by Lippman and Harris (916), Wesley, Mayfield and McCaskill (917), Knuth (918), Sutton (919), and Tomb and Raymond (920). The latter authors used monodispersed aerosols to calibrate their instruments for use in respiratory studies.

Experiments by these and various other authors indicated that two-stage or size-selective cyclone samplers could be designed to provide a more accurate estimate of the inhalation hazard than was provided by the measurement of gross air concentrations. The lower size limit explored by many of these authors was 0.5 μ. Unfortunately, there was much disagreement as to the proper flow rate for small cyclones which were ideally suited for personal air sampling. This was partially due to the use of different definitions of particles size in initial calibrations. It is accepted now that particle aerodynamic diameter is the size parameter defining lung deposition, and any sampler calibration has to be in terms of this size parameter. Several authors discussed this fact, amongst them were Muschelkhautz and Krambroch (921), Ettinger and Royer (922), and Steltzer, Lynch and Bernaski (923). The aerodynamic characteristic of airborne particles is dependent to some degree on the particle shape. Leroy, Balzer and Tebbins (924) conducted experiments with a cyclone and a hexlet elutriator to investigate their potential as collectors for fibrous aerosols, but for this particular shape neither unit proved satisfactory. The work of Lippman and Kydonius (925) involved the design of a multistage cyclone collector incorporating six cyclones that operated in parallel. Stelzer (923) evaluated the Dorr-Oliver cyclone using radioactive aerosols and Errington and Powell (926) designed a new cyclone for sampling particles in the field.

Watson (927), Mercer (928), Beeckmans (929), and Mukhapad and Chowdhury (930) calculated the theoretical ratios of the fraction passing cyclones to the fraction deposited in the lung. Theoretical work along these lines was performed by Lynch (931) and Thompson & Strauss (932). The latter authors applied vortex theory to the design of cyclone systems. Shoub (933) investigated the use of an MRC (Isleworth) sampler and a Dorr-Oliver 10 mm nylon cyclone, and Knight and Lichti (934) expanded this work on the latter by operating at four different flow rates with overy thirty dusts.

The effect of other parameters such as geometrical shape, gas-dust loading, etc., were investigated by Gloger and Jugel (935) who studied their effect upon the degree of separation and pressure loss in cyclone separators. Most of this previous work involved particles >1 μ. The only work specifically involving the removal of submicron particles was reported by Freudenthal (936) and Dennis, Coleman and First (937). They reported that industrial cyclones presently in operation were considered inefficient for particles less than 1 μ. Examples would be those manufactured by Dyna-Therm Corporation (938), Bauer Brothers Corp. (939), Fisher-Klosterman, Inc. (940), R. P. Adams (941), Dorr-Oliver, Inc. (942), Equipment Engineering, Inc. (943), and Buell Engineering, Inc. (944). Freudenthal (936) investigated the efficiency of the Aerotec-3 cyclone for submicron particles and found that particles having an aerodynamic diameter of 0.6 μ were removed by the cyclone operating at 60 cu ft per minute with an efficiency of only fifty percent. Hence, on these results, it appeared that no current cyclone could remove particles of 0.01-1 μ with one hundred percent efficiency as required in this program. On this evidence cyclones have to be excluded from the list of possible collection devices.

5.1.5 Classifiers

When a dust laden stream is fed into a centrifugal classifier, the dust is subdivided into two parts which are collected separately. Current instruments that can be commercially obtained have long standing and have numerous publications on their use. Examples are Alpine (945), Bauer (946), Dietert (947), Donaldson (948), Geoscience (949), Micromeritics (950), Neu (951), Vortec (952), and Walther (953). Of these, only the Donaldson claims to be able to separate submicron particles. Recent work that appeared on this subject was by Plitt (954), Leschonski (955), Black and Williams (956), Jones (957), and Zverev and Ushakov (958). In most circumstances, the application of

classifiers to the problem of collecting submicron particles from air was again of little value, and these devices must also be disregarded as potential submicron collecting devices.

5.1.6 Aerosol Spectrometers

Aerosol spectrometers were developed for the study of aerocolloidal components of the atmosphere, in particular to determine the size and mass distribution of the particulates closely representative of those in the airborne state.

In 1957, Goetz (959) developed an instrument to quantitatively separate and size classify airborne particles down to 0.2 μ in size. This instrument was applied to various studies (960,961). An improved version of this device was reported in 1959 (962,963,964). Applications of this later device were concentrated on studying the stability of submicron atmospheric aerosols and, in general, their whole physical behavior (965, 969). In 1962, the modified spectrometer was the basis of a paper presented to the Air Pollution Control Association in Chicago (970), where it was shown that it could sample and collect particles of size 0.03-3 μ. In this device, particles were separated from a steady laminar air flow inside a pair of symmetrical channels represented by helical grooves on the outer surface of a rapidly turning rotor. The outer wall of these channels was formed by the inner surface of a tightly fitting detachable cup lined with a removable foil upon which the particles were deposited during high centrifugal acceleration (30,000 g). Good size separation of the particles was obtained on this foil, which could be easily removed for particle examination. This unit is now commercially available from Zimney Corporation (971), Figure 42, and has been investigated along with other commercial units in a recent study (914).

In 1967, Stöber (972) designed and developed a similar device in Vienna, for the collection and separation of airborne submicron radioactive particles. Extremely good resolution of the particles was found, and this was confirmed by Berner and

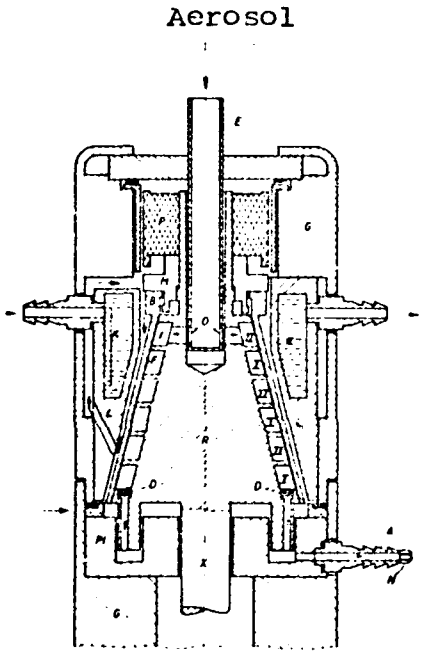

NOTE—G—Rotor housing, P—air-bearing assembly, E—stationary inlet tube with outlet ports O, R—rotor with outer helical channels I, II, leading to jets D, B—conical cup seating I, II, lined inside with foil F and attached to R by ring nut M, L—stationary insert, surrounding R contains coolant cavity K in L, X—drive shaft of rotor R, P1—stationary insert with circular groove leading channel outflow (arrows) to outlet A with calibrated restriction H. Heat exchange between L and R by air flow indicated by arrows.

Figure 42

GOETZ SPECTROMETER

Reichert (973). In the design of the latter authors, a rotating ring slit was used in a cylindrical instrument. This allowed the complete inlet system to rotate with the spectrometer avoiding the need for rotating seals. Upon rotation, a pressure gradient was developed between the inlet and outlet nozzles, and air flowed through the device. The rate of flow was controlled by both the nozzle size and the speed of rotation. Hochrainer and Brown (974) built two devices, one similar to the one described above, and the other a conical design somewhat similar to the Goetz. Their two spectrometers deposited aerosol particles on removable foils in centrifugal fields up to 5000 g. Good size resolution was obtained for aerosols of size 0.1-5 μ. These devices are shown in Figures 43 and 44.

In 1969, Stöber and Flachbart (975) at the University of Rochester designed and built a modified conifuge collector, Figure 46, which had an inlet in the form of a ring slit. The conifuge was originally the design of Sawyer and Walton (976), Figure 45. This ring slit was conceived to facilitate high aerosol sampling rates with reasonable size resolutions in terms of aerodynamic diameters. Particles of size 0.1-4 μ could be collected and resolved at a sampling rate of 1 liter/min. For the size range 0.1-0.06 μ the flow rate had to be reduced to 0.1 liter/min to obtain good resolution. Once again the aerosol was collected on a removable foil for the purposes of analysis. Further work by these authors was given in a later paper (977) in which they described the separation of aerosol particles in a spinning spiral duct. Along similar lines, Flesch (978) reported his studies on the calibration of a centrifugal aerosol size classifier for submicron particles. Hochrainer and Zebel in two papers (979,980) gave an account of a new type of separator for the size classification of aerosols. Stöber, Boose and Flachbart (981) in 1971, compared aerosol collecting devices against the spiral centrifuge that

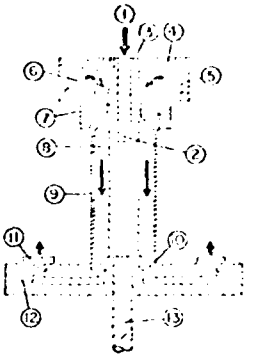

1. Aerosol Inlet
2. Flow Limiting Nozzle
3. Inlet Holes
4. Flow Duct
5. Centrifuge Body
6. Inlet Chamber
7. Inlet Head
8. Centrifuge Chamber
9. Cylindrical Wall
10. Conical Body
11. Six-Outlet Nozzle
12. Bottom Plate
13. Motor Shaft

Figure 43

HOCHRAINER AND BROWN CYLINDRICAL CENTRIFUGE

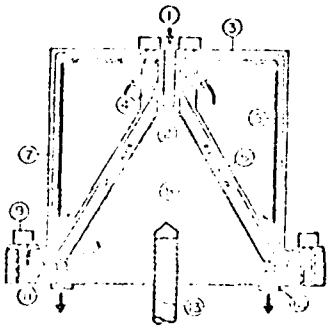

1. Aerosol Inlet
2. Flow Restriction Nozzle
3. Flow Channel
4. Clean Air Ring Slit
5. Cylinder
6. Deposition Cone
7. Inner Cylinder Surface
8. Conical Body
9. Mounting Screws
10. Outlet Ring Slit
11. O-Ring Seal
12. Flow Limiting Nozzles
13. Motor Shaft

Figure 44

HOCHRAINER AND BROWN CONICAL CENTRIFUGE

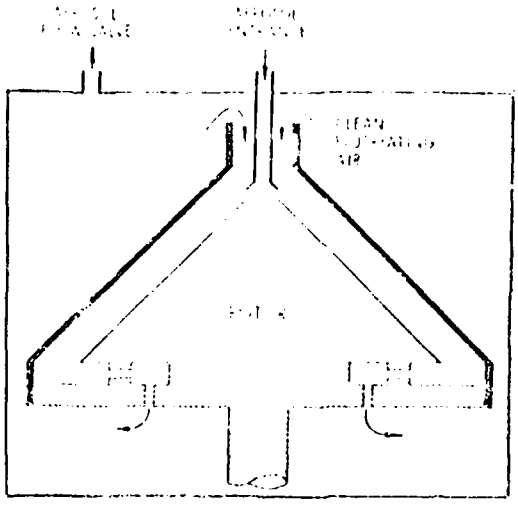

Figure 45

CONIFUGE

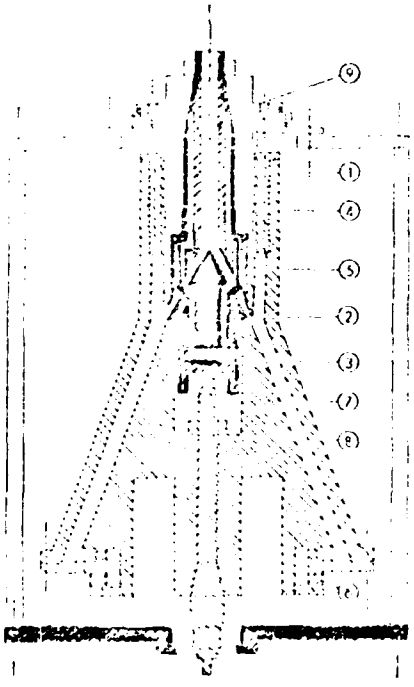

1. Non-Rotating Cylindrical Duct
2. Adjustable Annular Slit
3. Conical Section
4. Vertical Capillaries
5. Annular Duct
6. Six-Outlet Jets
7. Cone
8. Funnel-Shaped Lid
9. Cooling Duct

Figure 46

STÖBER AND FLACHBART RING SLIT CONIFUGE

they had developed. Resolution in this instrument was found to be better than many of the other types of systems.

One problem with sampling very small aerosol particles was the possibility of contamination of the deposit if the carrier gas was not particle free and clean. This problem was studied by Litvinov (982) who studied ways of effectively purifying gas used as a carrier for any centrifugal device. Very recently, Hochrainer (983,984) developed another centrifugal collector. In design, this collector was perhaps the most simple of the ones discussed so far. It required no special cooling systems, rotating seals or auxiliary devices such as pumps or filters, and was able to resolve the distribution of particles in the range 0.2-1.1 μ. This is shown in Figure 47.

From the literature found on the subject of aerosol spectrometers, there is no doubt that these instruments offer the best solution so far to the problem of collecting dispersed submicron particles from an air stream in such a manner that they can be readily analyzed. Most of the authors cited in this section commented on the high resolution and separation of the particles sampled. Monodispersed aerosols appeared as single bands on the metal foil collectors and multi-sized aerosols were collected in a spectrum dependent on their aerodynamic diameter. Proper selection of instrument sampling speed, particle dilution, etc., was shown to result in a well separated and resolved deposit of aerosols of size 0.03-1 μ, the range required in this program.

5.1.7 Thermal Precipitation

The deposition of particles in a thermal precipitator is accomplished by the radiometric force which an airborne particle experiences in a temperature gradient. The particle moves from the vicinity of a hot source and is collected on a cold surface. In the Casella and Willson thermal precipitator (985, 986) the dust laden air is drawn through a channel in a sampling head in which there is stretched a hot nichrome wire. Particles

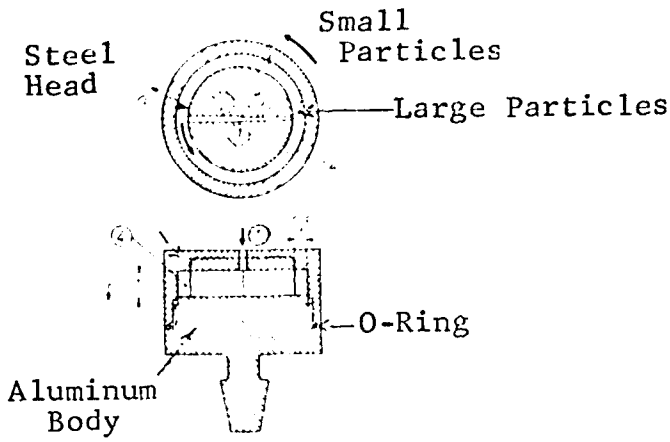

1. Aerosol Inlet
2. Radial Channel 1
3. Radial Channel 2
4. Thin Annulus
5. Outlet Duct

Figure 47

HOCHRAINER CENTRIFUGE

are deflected from this source onto two microscope cover glasses on each side of the channel. Measurements of the collection efficiency shows that virtually all particles from 5 to 0.01 μ and smaller are collected, but significant penetration of the sensing zone takes place with particles 10 μ and above (987, 988,989,990). This means that the upper limit of size that should be collected is between 5 and 10 μ. The original design of a thermal precipitator was by Watson (991). This was later modified by Donohue (992), Walkenhorst (993) and Burdekin and Dawes (994). New designs were developed by Beadle and Kitto (995) in which particles were deposited as 12 dust strips on a standard microscope slide. An elutriator was employed to remove coarse particles, e.g., 5 μ and above before entering the thermal zone. These instruments had the disadvantage that for good resolution, sample had to be taken over a very short period of time, or the deposit became too concentrated and particle overlapping occurred. For long period sampling and to obtain a uniform deposit, several devices were specially designed.

Cember, et al. (996) developed one in which the sample slide rotated continuously. Walton (997) devised one in which the slide oscillated. Orr and Martin (998) replaced the microscope slide by a transparent tape moving past the hot wire. In the long period sampler developed by Hamilton (999,1000) the dust laden air first entered through an inlet elutriator where coarse particles were removed, it then passed through a gravity spectrometer in which 3-1 μ particles settled out, and finally the fumes and particles were deposited by a hot wire onto a microscope slide. Large volume samplers such as the one devised by Wright (1001, 1002) deposited amounts of dust large enough to weight. At the present time, many of these instruments can be commercially obtained. The "Thermopositor" (1003) is made by Aminco and uses a small thermal gradient between two metal discs. The Casella/Willson instrument (985,986) incorporates a hot wire between two cover glasses. A similar design

to this is the unit made by Corner House Laboratories in South Africa (1004). The Orr-Martin precipitator (999) is marketed by Numinco (1005) and uses a hot wire to precipitate particles onto a continuous tape.

Joseph Ficklen, Inc. (1006) manufactures several types of precipitator including the Konisampler (1007), the continuous (1008), oscillating (1009), gravitational (1010) and micro (1011) units. The former incorporates a hot wire and is a portable unit; the continuous model uses a hot wire and deposits particles on a slide which moves at 1 mm/hr; the oscillating unit produces a similar deposit but the slide moves back and forth across a wide area every 3 minutes; and in the "gravimetric" unit the slide does not move but the dust is deposited over an area 5 cm square by a heated plate.

The one major problem with thermal precipitators is that very often the deposits are not uniform. Work by Hasenclever (1012), Ashford (1013), Dawes and Maguire (1014) showed particle overlapping takes place. In some areas dense deposits were found, in which particles were not separated at all. As a general rule, oscillating and continuous samplers operating at low dust concentration give the most uniform and separated deposits. A good review of the various instruments and the problems encountered in thermal precipitation was given by Hodkinson (1015) and several papers by the same author are fundamental in this field (1016,1017 and 1018).

From the literature cited, the thermal precipitation method is satisfactory for the collection of particles in this program. The only problem in the use of this device is the non-uniformity of the deposit and the possibility of overlapping. If this can be eliminated, thermal precipitation would be highly successful in the collection of the submicron particles from air.

5.1.8 Electrostatic Precipitation

The electrostatic precipitator relies on producing an electric charge on the particle to be collected and then directing the charged particle by electrostatic force to the collecting electrodes. The electrostatic precipitator operation involves several basic steps:

1. Electrostatic charge is applied to each dust particle.
2. The ionized particle with its negative charge is attracted to the grounded electrode. This precipitation force is the product of the field strength between the electrodes and the acquired charge on the particle.
3. The acquired charge is discharged to the collecting electrode.

Most precipitators are presently designed to operate at efficiencies approaching 100 percent. High efficiency is the result of a careful balance between gas velocity and active length of the unit. A large precipitator with low gas velocity permits maximum efficiencies. Uniform gas velocity distribution is extremely important so that arrangement of inlet and outlet ducts requires careful study.

The electrostatic precipitator collection efficiency is related to the time of particle exposure to the electrostatic field and the resistivity of the dust particle. The exposure time can be increased either by increasing the cross section area of the precipitator or its length in the direction of gas flow.

Particulate matter, having moderate electric resistivity, is easier to collect in an electrostatic precipitator than that having higher or lower values (1019). Several recent studies have been published on the properties of aerosols in electrostatic fields.

Theoretical work on the electrical properties of aerosols was done extensively at the University of Minnesota. Diffusion and field charging studies of submicron aerosols were made. A new diffusion charging theory was developed by Liu, et al. (1020), and several collection and particle size analytical instruments were devised (1020). A two-stage aerosol sampler was developed in which size classification of the deposited aerosol was presented by a new pulsed precipitating field. Sampling efficiencies and uniformity of deposit was determined for fluorescent aerosols over a size range 0.028-3.2 μ. The sample was very satisfactory for light and electron microscopical analysis (1021). A continuous sampling-sizing system composed of a nuclei counter, an electrical counter and an optical counter was developed (1022). The electrical counter was the forerunner of the Whitby Aerosol Analyzer now marketed by Thermo-Systems (1023). The effect of corona charging of particles in an electrostatic precipitator was the subject of much research at the Carnegie Institute of Technology. Work on orientation, adhesion (1024), particle trajectory (1025,1026), and other parameters during electrostatic precipitation was reported (1027-1030).

In order to record the behavior of particles during electrostatic precipitation, photographs were taken using periodically interrupted light. This, both direction and velocity could be determined at any point along the path of a particle. A very intense light had to be used because the particle was in one position for only a few microseconds. There had to be almost no reflection of light from a stationary surface toward the camera lens because the camera shutter had to be open for a relatively long time.

In the usual theory of electrostatic precipitation, it is assumed that particles are driven to the collecting surface by electrostatic forces and that the particles are collected when they touch the collecting surface. Photographic records of the paths of 100 μ particles bounced off from the surface

without losing their electric charge. Thus the actual path more nearly resembled a golf ball striking a paved road. When a striking layer of previously deposited fine particles, the larger particle not only bounced but knocked off some of the previously deposited fine particles. When there was a deposit of high resistivity dust on the collecting electrode, the paths of particles were often very irregular, indicating local regions having a high density of positive ions. According to the usual theory, there should be only negative ions present.

The effect described above resulted in both a non-uniform deposit on the collector surface, and a reduction in the particle collection efficiency.

Other operating parameters such as eddy turbulence effects on particle motion in a precipitator were studied by Williams and Jackson (1031), Cooperman (1032) and Robinson (1033,1034) and a state of the art summary of the effects of this parameter was published by Robinson (1035). These authors devised a modified diffusion theory to account for wallward particle migration under the action of electrostatic forces. The nature of the turbulence generated in precipitators was from both aerodynamic and corona discharge sources, the latter being referred to as the electric wind. The magnitude of the two sources was studied experimentally using helium tracer gas. The results showed that under the normal operating conditions of the corona discharge unit, the electric wind eddies were predominant and that previous attempts to describe precipitator performance without allowances for this factor were seriously in error. For a summary of the effects of most parameters on electrostatic precipitators reference should be made to recent publications (1036-1039), the latter being a manual on electrostatic precipitation generated for the National Air Pollution Control Administration. From these summary reports, it was found that near 100% collection efficiency can be expected for submicron particles, but this is a function of gas velocity,

dimensions of the instrument, design of the inlet and outlet ducts, the time of particle exposure to the electrostatic field, the resistivity of the particle, the particle size distribution and the strength of the corona discharge.

Submicron particles suffer little effects of particle bounce or reentrainment, and if they are non-metals they have a very high collection efficiency in currently available commercial precipitators. The major factor influencing the state of the deposit is the design of the instrument and the collecting surface.

Several designs of precipitators have been developed for submicron particles or ions. The Wait ion counter, consisting of two concentric cylindrical electrodes is widely used for meteorological measurements (1040,1041). Daniel (1042) described a unit with parallel plates with the collector electrode enclosed in a guard ring to reduce stray leakage to the ground. Better resolution was found by using two sets of electrodes in series to produce a two-stage system. A device was designed by Langer, Radnik and Templeton (1043) to collect a submicron platinum aerosol of size range 0.06-0.1 μ. The aerosol was introduced as a stable filament into a parallel plate collector system surrounded by an air sheath. The latter used clean dry air to prevent any leakage problems with the supporting insulators. The results showed the collection of particles of minimum size 0.01-0.02 μ with a very high degree of resolution. Other very recent designs of precipitator for the monitoring of fission products were reported in Denmark and Sweden by Teodosic (1044) and Strindehag (1045). Several commercial units are available with widely different design features. Bendix (1046) markets a unit with a cylindrical collector plate on which can be placed rolled paper, metal foil, metal sheet for easy removal and examination of the deposit. Flow rates of 3-8 cu ft/min can be obtained and collection efficiencies of 98% were reported for submicron lead and iron

dust. Similar designs at precipitators are available from Del Electric Corporation (1047) which operates at 96% efficiency at 27 cf/m and MSA (1048) which operates at about the same efficiency but at lower flow rates. Environmental Research Corporation (1049) markets a precipitator termed a leap sampler. In this device, air is drawn into the instrument through a calibrated nozzle and flows through the center of a high voltage plate. The air then flows radially out between this plate and a rotating grounded collection disc. A ring of needles located on the high voltage plate and concentric with the air inlet emit a continuous negative corona. The charged are then collected on the collector plate, which is continuously washed by a thin film of liquid under centrifuge force. This flows across the plate carrying the collected particles into a collector dish. For particles of size 0.1-1 μ less than 90% efficiency is claimed at 500 liters/min flow rate. An almost identical unit is available from Litton Systems, Inc. (1050). Collection efficiencies of 98% at 1000 1/min are claimed, but this falls to 88% for particles of size 0.1 μ. A portable type of precipitator is sold by Thermo-Systems (1051) and flow rates of 4-10 1/min are possible but no collection efficiency is given.

Two original types of precipitators are also available from the same company (1052,1053) in which particles are precipitated onto a piezzo-electric crystal collector that records the mass collected. Near 100% collection efficiencies are claimed for particles of size 0.01-10 μ at a flow rate of 1 1/min. A continuous particle size distribution measurement on an aerosol of size 0.02-1 μ can be made by another unit marketed by Thermo-Systems termed the Whitley Aerosol Analyzer (1023). Although this operates by electrostatic precipitation no collection of the total sample is available for examination.

From the survey of available instrumentation, it has been found that for particles of size 0.01-1 μ collection, efficiencies of between 88% and 98% can be expected. In some samplers,

the final deposit is in a suitable form for examination, but uniformity of the deposit will be variable depending on the operating parameter. These devices, therefore, appear inferior to centrifuges for the purpose of collecting submicron particles, when 100% recovery is demanded.

5.1.9 Analysis

In the preceding two sections the problems of sampling and collecting aerosols has been discussed. Let us suppose that the aerosol has been generated from the original matrix of submicron particles, and after their separation, every particle has been collected on a suitable collecting surface for examination and analysis. For the purposes of this program, this collection of the separated particles would be the final stage, but for the purposes of research into the efficiency of separation, analysis has to be performed to determine this efficiency value. In this present section, the analysis of a deposit by optical microscope, electron microscope and scanning electron microscope is not being discussed, as this applies equally well to collected particles from liquids. The discussion of microscopic analysis will be provided in that particular section rather than here. For the present, we are concerned with the dynamic analysis of submicron particles in the aerosol form for rapidly investigating the efficiency of the separating technique. For this purpose, differences in the particle size distributions are considered the best way of measuring this in air, and, consequently, techniques that measure this parameter have to be studied. Submicron particles can be instantly sized in the aerosol form by several techniques.

The best known is by the technique of light scattering using optical counters. Examples of these units are the Climet (1054), Dynac (1055), Royco (1056), Research Appliance (1057), Coulter (1058) and Bausch and Lomb (1086) counters. The ranges of operation are from 0.3 to 0.5 to above one micron. From this information, the counters do not count a size range low enough

for the range required in this program, but they could be useful for the preliminary studies.

An alternative method would be to use the Whitby Aerosol Analyzer (1023) which covers the range 0.01-1 μ. Undoubtedly, this would be the superior technique but the instrument is costly and unavailable to the program team. As an alternative, instead of measuring the actual size involved, one could count the number of particles generated using a condensation nuclei counter. Examples are Environmental One Corporation (1060), General Electric (1061), Research Appliance Co. (1062) and Singo, Inc. (1063). The principle of operation is that if an aerosol of 0.002-0.1 μm particles with water vapor is suddenly expanded, the water vapor condenses on most particles causing them to grow. Such particles are called condensation nuclei. Depending on the thermodynamic properties of the system, particles larger than about 20 Å grow, most particles are in the 0.1 to 1.0 μm size range and are quite uniform in size, composition, and optical properties. A photometer then senses the concentration of the resulting aerosol. The measurement can be calibrated in terms of particle number concentration. The measurement is overwhelmingly dominated by submicron particles which do not contain much mass (1064).

Recent work was published in this area by Fawcett and Gardner (1065), Skala (1066), Pollak (1067), McGreevy (1068), Peterson and Paulus (1069), and Pedder (1070). The range of operation of these instruments if from 0.001-1 μ at concentration ranging from 300-10^7 nuclei/ml at flow rates of about 20 cc/sec.

Finally, two other techniques appeared in the literature which seemed to be very promising. One of them reported by Pircher, et al. (1071) scanned aerosol particles in the submicron range in the nuclear medical field, and the other by Binek and Dohnalova (1082) counted particles of size less than

0.5 μ by a scintillation-type counter. This is presently being manufactured by Sartorius-Werke in Prague.

From this literature, the separation efficiency of particles in air would best be measured dynamically by the Whitby Aerosol Analyzer. This would be very rapid, e.g., a complete distribution in 4 minutes for a 0.01-1 μ size range, but it is very costly and unavailable to the program team. Empirical studies could be performed using a condensation nuclei counter in which no sizing would be made, and separation efficiency would be based on total particle frequency only.

5.2 Particles in Liquid

5.2.1 Sampling

The problems outlined under the heading "Sampling of Particles in Air" were numerous, and in consequence had to be studied carefully in order to first define them and later either predict or eliminate their behavior. Submicron particles in liquid media present little problem in sampling, if, the suspension is stable. Consequently, no importance is placed on this particular operation in this section. However, to be certain, the use of a liquid sheath to surround a suspension entering a collector would be a useful engineering modification.

5.2.2 Collection

There are several methods of removing particles from liquids, but unlike "particles in air" submicron particles can only be removed in a dispersed state from a suspension by centrifugation. However, liquid centrifugal systems can be subdivided into three categories, hydrocyclones, centrifugal classifiers and centrifuges. The use of hydrocyclones and classifiers for the collection of submicron particles in a suitable state for analysis has been very limited. In fact, only two references to the use of classifiers in liquid systems have been found. These w ere Kristek (1075) who developed a new classifier in Czechoslovakia, and by Colon, et al. (1076)

in the Netherlands who doubt even the validity of using centrifugal classification methods in liquids. Also only two on hydrocyclones have appeared. These were by Trawinski (1073) who reviewed the use of centrifuges, hydrocyclones and sludge thickeners, and Neesse (1074) who used a hydrocyclone as a turbulence separator.

5.2.3 Centrifuges

The only useful technique for collecting and analyzing submicron particles in liquids appears to be by centrifugation. The literature on liquid centrifuges can be subdivided into two basic categories, those that operate on homogeneous suspensions and those that employ line-start systems. In homogeneous systems, a random homogeneous suspension is placed in a centrifuge which is then started and rotated to remove particles. In a line-start system, a layer of suspension is fed into an already spinning centrifuge filled with clean liquid. This injected suspension then forms a layer on the liquid surface from which particles can move out into the clean liquid and be separated. The theory involved in these operations has been well reviewed by Allen who has included centrifugal theory in over twenty fundamental papers (1077-1097). Very recent work in this area was also done by Abarbane & Viner (1098) and Bennert (1099).

Various designs of centrifuge have appeared, and use this theory in the separation of submicron particles. Norton and Speil (1079) constructed a centrifuge large enough so that standard glass jars could be used. Kamack (1095) described a system of withdrawal pipettes which could be operated while the centrifuge was in motion. Marshall (1100), and later Whitby (1101) designed a centrifuge which collected particles according to size in a capillary at the base of a centrifuge tube. This system was later made commercially available by MSA (1102) and several papers have appeared on its use (1103-1108). For this program this type of centrifuge is of little use as the particles

are collected as a packed bed and are not collected in a separated manner suitable for analysis.

Of more use are the series of instruments known as disc centrifuges. In 1955, Donahue and Bostock (1093) developed a disc centrifuge for the collection and particle size analysis of very fine particles.

The principle of this disc centrifuge is shown in Figure 48. On the rim of each step were placed two roughened thin metallic strips which covered between them one-half of the perimeter of the step. The pieces were placed so as to be at a maximum distance from the withdrawal tube E. When the lid was in place, the stepped tank formed by the two portions of the rotor was filled with suspension and the system spun at the desired speed. Particles settled out onto each step and each step represented a different sediment height. After a given centrifuge time, the supernatant suspension was withdrawn through the tubes E and E_1, through the central pillar C while the centrifuge was still spinning. After the fluid had been withdrawn, the centrifuge was run at a higher speed to consolidate the powder settled on each strip. The strips were then removed from the centrifuge, dried, and the accumulated powder determined gravimetrically. The use of the stepped bowl enabled several points on the particle size distribution curve to be determined concurrently.

In 1958, Kaye (1109) developed a disc centrifuge purely for particle size analysis, but this will be discussed in a later section. In 1962, Atherton and Cooper (1110) patented a disc centrifuge which was later built and sold commercially by Joyce Loebi (1111). In this unit, samples were removed from the liquid by a probe which inserted into the suspension at preselected times. Particles collected in this way consisted of fractions with known stokes diameters, but were collected in the form of near monosized suspensions. Two further devices were built for particle size analysis by Hildreth and Patterson (1083) in 1964 and Slater and Cohen (1096) in 1962, but these were of

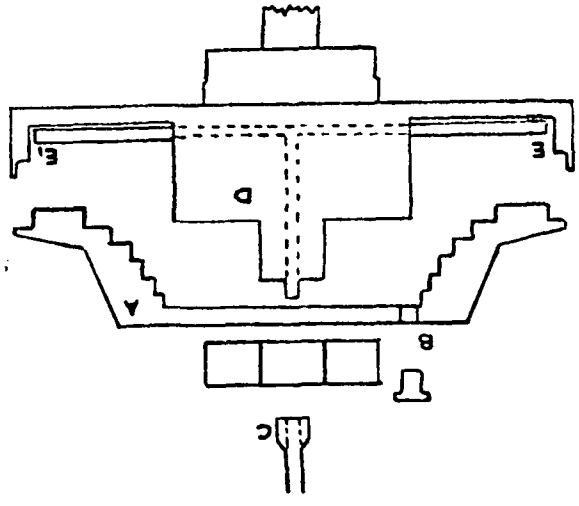

Figure 48

DONOHUE AND BOSTOCK CENTRIFUGE

little use for the collection of submicron particles. Of particular value for this application is the centrifuge devised by Hausner (1112-1114) and marketed by Sharples (1125) termed the supercentrifuge.

The supercentrifuge devised by Hausner and Lynn (1114) is shown in Figure 49. It rotated at several thousand revolutions per minute, and could be used to purely collect submicron particles or to determine their particle size distribution. For the latter, the usual experimental procedure involved successive fractionation of the suspension and weighing of the fractions collected on a removable liner in the bowl.

The suspension was fed into the bottom of the bowl and the particles moved in a spiral path until they reached the wall. The liquid was then discharged in an annular layer over the overflow dam.

If Q is the rate of flow of suspension that causes a particle of size D to be deposited at a height h above the feed inlet, it was shown that:

$$Q = khD^2$$

If the removable liner is divided into idential strips, dried and weighed, the weight deposited on each strip may be used to find the size distribution. The constant k was evaluated from curves given by Hauser and Lynn or a nomograph developed by Saunders could be used (1116).

This method of determining size distributions could not be recommended for routine analysis and a method developed by Bradley was preferred (1118). For the collection of submicron particles, the centrifuge was run at a speed sufficient to collect the smallest particle present, and then the whole size distribution was collected as a size spectrum on the removable liner. Analysis could be performed by the direct examination of this deposit. A more common version was the instrument manufacted by Sharples (1115). This is shown in Figure 50.

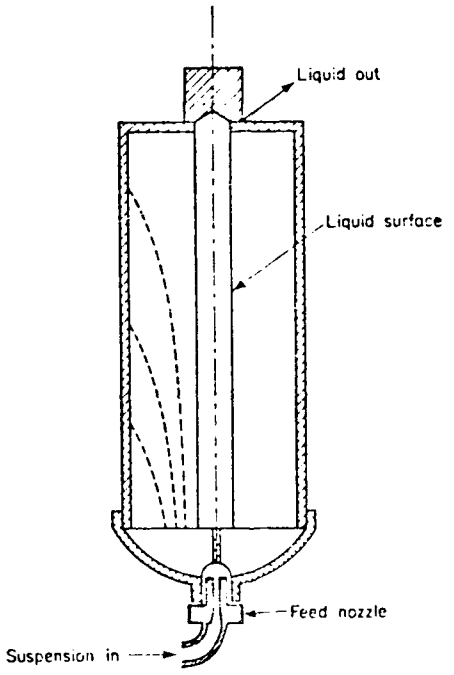

Figure 49

DIAGRAMMATIC SECTION OF THE HAUSER LYNN CENTRIFUGE

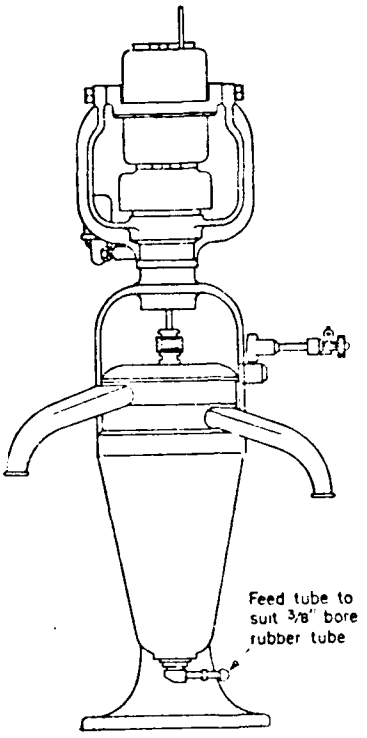

Figure 50

SHARPLES SUPERCENTRIFUGE

The main advantage of this unit is the very high speeds of rotation that are possible, e.g., 8,000-50,000 revs/min. Its disadvantages are the uncertain end effects in the bowl, but for our purposes this is not serious.

In 1920-1935, Svedberg (1119) and coworkers in Uppsala, Sweden, developed a high speed analytical centrifuge which they termed the ultra centrifuge. This ran at speeds approaching 80,000 rpm, and was driven by oil turbines. The centrifuge cell was made of steel and revolved in an atmosphere of cooled hydrogen. Ultra centrifuges of different design were developed later, an example being the one developed by Pickels (1120) which was electrically driven. Examples of the use of these instruments on colloids and emulsions were given by McCormick (1117), Brodriyan (1119), Svedberg and Nichols (1121), and McInnes, et al. (1122). Svedberg and Nichols (1121) reported that particles of 0.001 μ could be separated and collected, according to their stokes diameters.

In addition to these centrifuges that separated particles according to their settling velocities, another class of centrifugal separators, termed zonal centrifuges, employed a density gradient to separate particles according to their density. This method was used very widely in the biological and medical fields and a review of the method, containing 196 references, was published by Schumaker (1123). The method is based on the capability of preparing several layers with an increasing density gradient throughout the centrifuge. The density layers can be delivered to the centrifuge while at rest (statically) or while rotating (dynamically). The operation of the zonal rotors is shown in Figure 51. Following the static loading of the density gradient through (A), the vertical gradient is reoriented by acceleration (B), and is transformed into a radial gradient (C). Several isodense layers in the gradient are depicted by parallel lines within each compartment. A radial gradient may be produced directly by dynamic

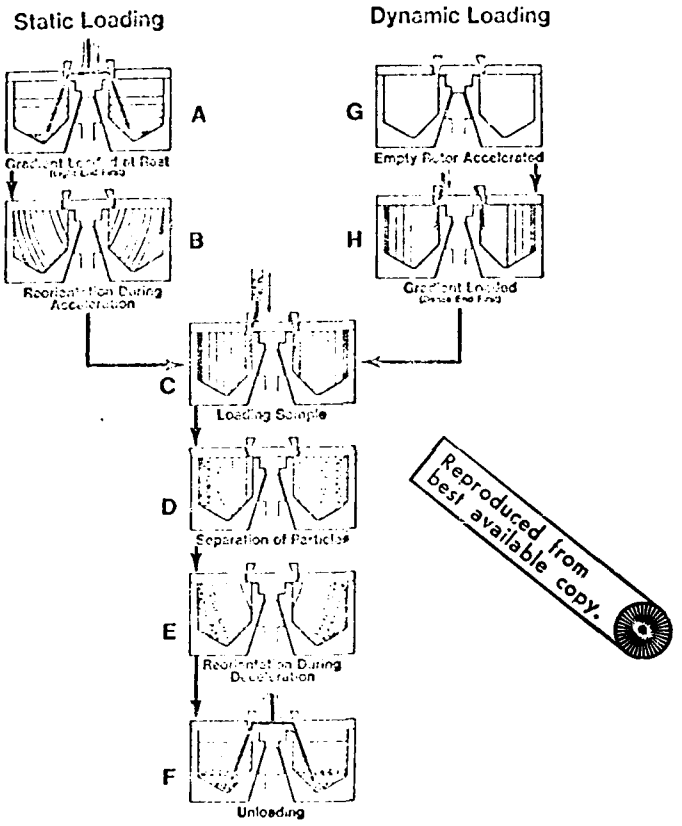

Figure 51

OPERATION OF THE REORIENTING GRADIENT ZONAL ROTORS

loading of the empty rotor through the core lines (G and H). The sample is introduced onto the reoriented gradient through the core lines (C) and following acceleration of the rotor to operating speed, the particles in the sample sediment radially to form a series of concentric zones (D). These zones, together with the gradient, are reoriented during deceleration (E) and are withdrawn in sequence from the rotor at rest through the lines (F).

These operations, as shown in Figure 51, was found in a very recent paper by Scheeler, et al. (1124). He described the use of ultracentrifugation and compared the results of comparative testing of several devices. In this way, he was able to concentrate particles of known density within each gradient and separate them from other compounds. This was particularly useful for the separation of submicron organic particles from submicron inorganic ones. In addition to this mode of operation, particles could be separated by using their rates of sedimentation through the density gradients. Work on this application was reported by Halsall (1125) who calculated sedimentation rates in a zonal ultracentrifuge and Hsu, et al. (1126) who investigated a method of obtaining the true bandwidth of a density layer during the actual centrifugation operation. Finally, applications of this method were reported by Kornguth, et al. (1127) and Wilcox, et al. (1128) for biological systems.

From this literature it was found that centrifugal collections such as the supercentrifuge and the ultracentrifuge were most suitable for the collection of submicron particles from liquids. The design of Hausner and Lynn appeared to be the best for our current needs, as this deposited particles in a removable liner in the form of a size spectrum most suitable for analytical purposes. The use of zonal centrifugation was useful for the separation of organic from inorganic matter but, of course, this would have to be followed by supercentrifugation to produce size spectra of organic matter on one liner and

inorganic matter on a second liner.

5.2.4 Analysis

As in the section on "Particles in Air", the use of analytical systems in this program is solely to indicate the efficiency and degree of separation achieved by the submicron separation process. This can be done in two ways. Firstly, by measuring the particle size distribution by a microscopic or static examination of a collected size spectrum, or by an on-stream or dynamic analytical method. For preliminary testing, the latter is more rapid and less tedious to use. For the final results, the former is essential as only in this way can the real state of subdivision be measured. This section on analysis is begun by first investigating dynamic methods and it is ended by a summary of those using static systems.

5.2.5 Dynamic Methods

The first method of use to determine the particle size distribution of submicron particles in liquids is centrifugation. Several instruments were mentioned under centrifugal collectors which could be used as collectors and analyzers. These included the Donahue and Boxtock (1097), Kamack (1095), Kaye (1109), Slater and Cohen (1096), Atherton/Joyce Loebl (1110), Hildreth and Patterson (1083), and Whitby (1100,1101). Others include the Moser and Schmidt (1129), Martin Sweets (1130), ICI/Jiskoot (1131) and Norsk Hydro (1132). Most of these devices are classified as disc-centrifuges and all of them employ the line-start sedimentation method. In this method, a suspension is injected into the centrifuge so as to form a thin layer on the surface of the clean sedimentation fluid. Particles move out of this layer according to their stokes velocities and are detected after a known length of travel by various methods including light extinction, packing rate in a capillary, extraction and weighing and extraction and chemical analysis. All of these methods suffer from a common error which is described as

"instability" in the injected layer. Many papers have appeared on this subject (1133-1143) and to date, reliable and accurate size distributions have been difficult to obtain because of it. Very recently, there have appeared several papers directly concerned with analysis of submicron particles using these devices, amongst them were papers by Toyoshima (1144,1145) and an unknown author (1148) who used the Joyce Loebl, Haug and Zorll (1146) and Cast (1147). Burkholz (1149) measured size down to 0.1 μ by the use of a new centrifugal sedimentation balance, which recorded the direct weight settled at various times as a method of computing the size distribution. The theory involved in all the methods mentioned above was developed by many authors already referenced, and their work appears in references 1077 through 1108.

As an alternative to centrifugation, two new instruments appeared in the literature which used x-ray absorption as a means of detecting particle concentration charges within a suspension and hence particle size distribution. These were the subjects of papers by Allen and Svarovsky (1155,1156) and Smithwick, Orr and Hendrix (1157,1158). The instrument used by the latter was used for submicron pigments in the size range 0.1-1 μ with some success. Reasonably high concentrations of particles are required, but direct recording of the distribution in a rapid time is one major advantage. Other miscellaneous methods were reported by Schmidt (1150), Elaaser (1151), Davidson, et al. (1152), DeBlois and Bean (1153) and Muta and Watanabe (1154). These include small x-ray scattering from suspensions, flow ultra-microscopy and resistance pulse measurement.

Of these dynamic methods, the use of the x-ray sedimentometer is considered the most valuable for the rapid size analysis of submicron particles in liquid, but centrifugal analyzers such as the Kaye Disc Centrifuge and the Joyce Loebl are not to be ignored.

5.2.6 Static Method

The most common method of analyzing submicron particles in a static manner, i.e., when the particles have been collected on a surface, is by microscopy. Literature on methods of microscopy is abundant and cannot be comprehensively referenced here. Satisfactory treatises on particle size analysis by this method are given in Allen (6), Dallavalle (5), Herdan (4) and Orr and Dallavalle (3).

Basically, particles are magnified and their projected diameters or areas, determined by vernier or reticule devices using optical, transmission electron, or scanning microscopes.

The accuracy of a particle size distribution depends to a great extent on the statistics of the determination, or more precisely, on the number of particles counted. For a wide distribution, i.e., in which a tenfold size range is involved, e.g., 1-1.0 μ, particles in the order of 10-20,000 should be counted. This is impossible by manual methods. For the purposes of this program, if a static method was employed, it would be advantageous to count and size particles by the use of an automatic microscope. Examples of current instruments are given in references 1159-1152. Ideally, an automatic microscope such as the Quantimet 720 interfaced with a transmission electron microscope would be the ultimate goal. With such a system, all particles on the collector surface could be counted and sized and their interparticle distances and degree of agglomeration rapidly measured. Such a measuring device would be most desirable for the studies on the forces of adhesion discussed in Section 3. Here the sample surface coated with particles would be examined after each increase in rotational speed and hence the percent removal of particles and their sizes could be rapidly assessed. For this part of the study, a method similar to this has to be used, which in the absence of automatic microscopy, would involve taking electron

micrographs of the whole sample surface, followed by a tedious manual counting procedure. The lack of a rapid analytical tool was the cause of slow progress in this field in the past, and it also was one reason why only larger particles, >10 μ, were used in adhesion studies. Alternative static sizing methods for submicron particles include x-ray diffraction, line broadening and scattering, but it is considered that they have little direct application in this program as routine measuring methods.

5.3 Summary

For particles in air, the survey has shown that extreme care has to be taken in sampling submicron particles in air, as diffusion and electrostatic charge can cause serious losses to the walls of sampling tubes and collecting instrument inlets. Submicron particles from 0.01-1 μ can be collected very easily using current high speed centrifugal spectrometers, in which the size spectrum is deposited in a manner suitable for analysis. In liquid media, sampling is not critical for submicron particles provided that the suspension is stable, and they can be readily collected using a supercentrifuge of the type developed by Hausner and Lynn.

To test the degree of separation that has been attained in the separation method, the collected particles from air or liquid are best analyzed statically by interfacing an electron-microscope with a Quantimet 720 automatic microscope, so that particle size distributions interparticle distance and degree of agglomeration can be quickly measured on the collector surface.

For preliminary testing of the dispersing system, a dynamic analytical method is recommended. For this purpose the Whitby Aerosol Analyzer is best for measurement in air, and the Micromeretics X-Ray Analyzer or Kaye Centrifuge in liquid.

6. CONCLUSIONS

The literature survey has shown that in the four main areas of search, i.e., the nature of atmospheric aerosols, the studies in adhesion, the mathematical models used to represent forces of adhesion, and the sampling, collection and analysis of submicron particles, there has been an abundance of literature published.

Unfortunately in adhesion studies, very little work has been reported on submicron particles. The reasons for this are fairly simple. Most of the studies performed in adhesion have been academic in nature, and have been performed in air. In this medium, the handling and analysis of particles is difficult for sizes below 5 microns. This is because particle-surface characterization becomes very difficult for particles below this size, and the surfaces used for particle-surface adhesion studies have roughness values of the same order of magnitude as the particle diameters themselves. Also as the particle mass for sizes below 5 μ is very small, many of the simple techniques used for measuring the forces of adhesion between macro-particles cannot be used and more sophisticated ones developed.

In order to make progress in submicron separation studies, the survey shows that the best approach is to perform the separation in liquid media, where the forces of adhesion can be minimized. Much work has been reported on the basic separation of bulk submicron powders in liquids, particularly by paint pigment, chemical, rubber, plastics and pharmaceutical industries. Their experience can be used in a study of this kind. Suitable models of collected atmospheric aerosols can be devised as a result of the survey, and at the beginning these could include mixtures of ammonium sulphate, sodium chloride, carbon black and ferric oxide powders. At a later time, atmospheric aerosol particles should be used, perhaps from a high volume air sampler which has collected submicron particulates

from Chicago city air over a several month period. The forces of adhesion can then be measured on first the model system and later the atmospheric aerosol by the use of a high speed centrifuge in liquid media. The force of adhesion and the degree of separation should be measured in the presence of various surfactants and organic solvents, and optimum conditions of type, concentration and energy input for the different types of particles and surfaces determined. This will define the amount of force that has to be applied under those conditions to separate specific particles from each surface. In order to compare this experimental data with theory, the mathematical expressions found in the literature survey to describe the various forces first have to be modified and computor programs written, so that experimental values can be inserted into the modified expressions and the force of adhesion calculated. This will permit the design of a separating apparatus to be made so that separation can be performed on any type of submicron particle that has been studied.

Collection systems should then be implemented after the separator to collect the separated submicron particles in a manner suitable for single particle analysis. This could be achieved using a modified Hausner and Lynn centrifuge. Separation efficiencies could be determined by particle size analysis of the collected product. For this, an electron microscope interfaced with a Quantimet 720 automatic analyzer would be the ideal approach. From such a system, the size analysis, interparticle distance and degree of agglomeration could be rapidly assessed. From a measure of separation efficiencies, the need for any modification to the prototype separation unit could be instantly observed.

REFERENCES

INTRODUCTION

1. Zimon, A. D., Adhesion of Dust and Powder, Plenum Press 1969.

2. Orr, C., Fine Particle Technology, McMillan Press 1966.

3. Orr, C., and Dallavalle, J. M., Fine Particle Measurement, McMillan 1956.

4. Herdan, H., Small Particle Statistics, Butterworth 1960.

5. Dallavalle, J. M., Micromeritics, Pitman Publishing Corp. 1948.

6. Allen, T., Particle Size Measurement, Chapman and Hall 1968.

7. Wentworth, C. K., A Method of Measuring and Plotting Shape of Pebbles, US Geol Survey Bull 730B 91 1922.

8. Cox, E. P., Method of Assigning Numerical and Percentage Values to the Degree of Roundness of Sand Grains, J Paleontology 1 (3) 179 1927.

9. Tester, A. C., Measurement of the Shapes of Rock Particles, J. Sed. Petrol., 1 3 1931.

10. Wadell, H., Volume and Shape of Rock Particles, J Geol 40 443 1932.

11. Wadell, H., Volume, Shape and Roundness of Quartz Particles, J Geol 43 250 1935.

12. Krumbein, W. C., Measurement of the Geological Significance of Shape and Roundness of Sedimentary Particles, J Sed Petrol 11 (2) 64 1941.

13. Flemming, N. C., Form and Function of Sedimentary Particles, J Sed Petrol 35 (2) 381 1965.

14. Cohan, L. H., and Watson, J.H.L., Shape Factor and Other Fundamental Properties of Carbon Black, Rubber Age 68 (6) 687 1951.

15. Medalia, A. L., Morphology of Aggregates, J Coll & Int Sci 24 393 1967.

16. Medalia, A. L., Pattern Recognition Problems in the Study of Carbon Black, Pattern Recognition (in press).

17. Medalia, A. L., and Heckman, F. A., Morphology of Aggregates Carbon 7 567 1969.

18. Hausner, H., Characterization of Powder Particle Shape, Part Size Conference, Loughborough, England 1966.

19. Kaye, B. H., Some Aspects of the Efficiency of Statistical Methods of Part Size Analysis, ASTM/IITRI Conf, Part Size Anal 1968.

20. Church, T., Problems Associated with the Use of Martins to Ferets Diameter as a Profile Shape Factor, ASTM/IITRI Conf 1968.

21. Mandelbrot, B., How Long is the Coast of Britain, Science 156 636 1967.

22. Steinhaus, H., Colloquium Math 3 1 1954.

23. Dwyer, J. L.. et al, Small Particle Measurement on the ΠMC Measurement Computer System, Part Size Anal Conf, Bradford, England 1970.

24. Stöber, W., and Flachbart, H., Environ Sci & Tech 3 1280 1969.

25. Stein, F., and Corn, M., Atmos Environ 3 443 1969.

26. Burke, K., and Freeth, S. J., Det of Shape, Sphericity and Size of Gravel Fragments, J Sed Petrol 39 797 1969.

27. Robins, W.J.M., Measurement of the Thickness of Fine Particles, Nature 170 583 1952.

28. McCullough, D. S., and Briggs, L., Hydraulic Shape of Sand Particles, J. Sed. Petrol., 32 (4) 645, 1962.

29. Zingg, T. H., Beitrag zur Schotteranlyse Min V Pet Mitt 15 39 1935.

30. Wadell, H., Sphericity and Roundness of Rock Particles, J Geol 41 1933.

31. Callieux, A., Bull Soc Geol France 5 (13) 125 1945.

32. Cloos, E., Oolite Deformation in Maryland, Geol Soc Am Bull 58 843 1947.

33. Oftedahl, C., Deformation of Quartz Conglomerates in Norway, J Geol 56 476 1948.

34. Nadai, Plasticity, McGraw Hill 295 1931.

35. Corey, A. T., Influence of Shape on the Fall Velocity of Sand Grains, M Sc Dissert, Colorado A & M Coll 1949.

36. Luttig, G., Eine neue, einfache Gerollmorphometrische, Eiszeitalter Gegenwort 13 1956.

37. Flinn, D., Deformation of the Funzie Conglomerate Shetland J Geol 64 480 1956.

38. Flinn, D., Folding during 3-D Progressive Deformation, J Geol 64 480 1956.

39. Sneed, E. D., and Folk, R. L., Pebbles in the Lower Colorado River, J Geol 66 114 1958.

40. Rosenfelder, R., Contribution a l'analyse texturale des Sediments, Thesis Univ Algiers p. 356 1960.

41. Aschenbrenner, B. C., A New Method of Expressing Particle Sphericity, J Sed Petrol 26 (1) 15 1956.

42. Kuenan, P. H., Experimental Abrasion of Pebbles, J Geol 64 336 1956.

43. Poser, H., Hövermann, Study on the Morphology of Pebbles, Abhandl Braunschwerg, Wiss, Ges 4 12 1952.

44. Valeton, I., Petermanns Geographischer Mitteilung 99 13 1955.

45. Waltz, H., and Hermite, R., Methodes Generales d'Essaix et de Controle 1 Eyrolles Paris 1959.

46. Blenk, M., Sonderdruck aus Zeitschr fur Geomorphologic 4 (3) 202 1960.

47. Carr, Gleason, R., and King, A., Significance of Pebble Size and Shape in the Sorting by Waves, Sedimentary Geology 4 89 1970.

48. Medalia, A. I., Dynamic Shape Factors of Particles, Powder Technology 4 (3) March 1971.

49. Gregg, S. J., Surface Chemistry of Solids, Chapman and Hall 1965.

50. Seitz, F., Modern Theory of Solids, McGraw Hill, 1940.

51. Mott, N. F., and Jones, H., Theory of Metals and Alloys, Oxford Univ Press 1940.

52. Stone, F. E., Chemistry of the Solid State, Butterworth 1955.

53. Gray, T. J., The Defect Solid State, Interscience 1957.

54. Wright, D. A., Semiconductors, Methuen, 1958.

55. Cottrell, A. H., Dislocations and Plastic Flow in Crystals, Oxford Univ Press 1953.

56. Reid, T. A., Dislocations in Crystals, McGraw Hill 1953.

57. Bunn, C. W., Chemical Crystallography, Oxford Univ Press 1946.

58. Harkins, W. D., Physical Chemistry of Surface Films, Reinhold 1952.

59. Adam, N. K., Physics and Chemistry of Surfaces, Oxford Univ Press 1942.

60. Ross, S., and Olivier, J. P., On Physical Adsorption, Interscience 1964.

61. Gregg, S. J., and Sing, K.S.W., Adsorption, Surface Area and Porosity, Academic Press 1967.

62. Young, D. M., and Crowell, A. D., Physical Adsorption of Gases, Butterworth 1962.

63. DeBoer, J. H., Dynamical Character of Adsorption, Oxford Univ Press 1953.

64. Parfitt, G. D., Dispersion of Powders in Liquids, Elsevier 1969.

65. Kruyt, Colloid Science Vols 1 and 2, Elsevier, 1949.

66. Verwey, E.J.W. and Overbeek, T., G., Theory of the Stability of Lyophobic Colloids, Elsevier 1948.

67. Fischer, E. K., Collidal Dispersions, Wiley & Son 1950.

68. Davies, J. T., and Rideal, E. K., Interfacial Phenomena, Academic Press 1963.

69. Overbeek, T. G., Prins, W., and Zettlemoyer, A. C., Advances in Colloid and Interface Science, Elsevier 1967.

70. Arthur, W. A., Electrical Aspects of Surface Chemistry, 1960.

71. Bikerman, J. J., Surface Chemistry, Academic Press 1958.

72. Azaroff, L. V., Introduction to Solids, McGraw Hill 1960.

73. Bowden, V. P., and Tabor, D., Friction and Lubrication in Solids, Clarendon Press 1964.

74. Bonis, L. J., Fundamental Phenomena in the Material Sciences Vol 1, II & III, Plenum Press 1964.

ATMOSPHERIC AEROSOLS

75. Sheesley, D., C., Pate, J. B., Frank, E. R., and Lodge, J. P., Jr., April 1970, Symposium Proceedings on Environment in Amazonia - Part I, Measurement of Particles in the Non-Urban Atmosphere, Instituto Nacional de Pesquisas da Amazonia (INPA), Manaus, Amazanas, Brazil.

76. Houghton, H. G., 1951 Compendium of Meterology; editor T. Malone, p 178 Boston Amer. Meterol. Soc.

77. Smith, J. G., Kassner, J. L., Jr., and Biermann, A. H. Evaporation of Small Droplets in a Wilson Cloud Chamber, Properties of Residual Nuclei, J Rech Atmospheriques, 3(1-2), 41-44, 1968.

78. Goetz, A., and Pueschel, R., 1967, Atmos. Environ. 1, 287-306.

79. Junge, C. E., 1963, Air Chemistry and Radioactivity, Academic Press, New York, N.Y. p 117.

80. Green, H., and Lane, W., Particulate Clouds: Dusts, Smokes and Mists, London: E & F.N. Spon Ltd., 2nd edition 1964.

81. Anonymous, Chemical and Engineering News, pp 40-41, Aug. 16, 1971.

82. Diamant, R.M.E., The Prevention of Pollution, Heating Ventilating Engr. J Air Conditioning (London), 44 (523): 385-394, Feb. 1971.

83. Critchlow, A., and Maguire, B. A., Airborne Dust in Man's Environment, Environ. Eng., No. 85:12-20, Nov. 1968.

84. Israel, Hans, Trace Gases and Aerosols in the Atmosphere, Naturw. Rundschau, 20(8):329-336, Aug. 1967.

85. Chovin, Paul, Chemical Pollution of the Atmosphere, Sci. Progr. Decour., No. 3417; 35-40, Jan. 1970.

86. Georgii, H. W., Natural Aerosol in Clean and in Polluted Air, Schriftenreihe Ver. Wasser Boden Lufthyg. Berlin No. 30:13-18, 1970.

87. Corn, M., Nonviable Particles in Air, In: Air Pollution, v.I. Air Pollution and Its Effects, Ed. by A. C. Stern, New York, Academic Press 1968.

88. Johnston, H., Reactions in the Atmosphere, In: Project Clean Air, California Univ. Berkeley, Task Force 7, Vol. 4, Section 3, 25p., Sept. 1, 1970.

89. Knop, Wilhelm, Industrial Dusts and Waste Gases, Wasser Luft Betrieb, 14(1):20-23, Jan. 1970.

90. Anonymous, Reference Book Summary of Nationwide Emissions, Preprint 36p, 1969, APTIC 12496.

91. Hidy, G. M. and Brock, J. R., An Assessment of the Global Sources of Troposheric Aerosols, 2nd Clean Air Congress, Inter. Union of Air Pollution Prevention Associations, Wash., D.C., Dec. 1970.

92. Ivliev, L. S., 1967: Role of Distribution Mechanisms and Sources of Atmospheric Aerosol. Prob. Fiz. Atm. 5, 240-244.

93. Vandegrift, A. E., Shannon, L. J., Sallee, E. E., Gorman, P. G., and Park, W. R., Particulate Air Pollution in the United States, J. Air Pollution Control Assoc., 21, 321 (1971).

94. Dreisbach, R. H., Handbook of the San Francisco Region Palo Alto, Calif., Environment Studies, 1969, p. 284-309.

95. Crouse, W. R., and Flynn, N. E., Source Inventory IBM System for Particulate and Gaseous Pollutants, J Air Poll. Control Assoc., 17,508 (1967).

96. Selezneva, E. S., Investigations of Condensation Nuclei and the Chemical Composition of Atmospheric Precipitation of Atmospheric Precipitation, Tr. Gl. Geofiz. Observ. (Leningrad), no. 218-266-276, 1967. Israel Program for Scientific Translations, Jerusalem 11p., 1970. CFSTI:TT-68-50493.

97. Burt, R., and Thomas, A., Aerosol Pollution from Internal Combustion Engines, Royal Society of London, Philosophical Transactions Series Mathematical and Physical Sciences, 307(1489): 183-194, Oct. 29, 1968.

98. McKee, H. C., and McMahon, W. A., Automobile Exhaust Particulates - Source and Variation, J Air Poll Control Assoc, 10,456 (1960).

99. Marchesani, V. J., Towers, T., and Wohlers, C., Minor Sources of Air Pollutant Emissions, J Air Pollution Control Assoc., 20(1): 19-22, Jan. 1970.

100. Windom, H., Griffin, J., and Goldberg, E. D., Talc in Atmospheric Dusts,Env. Sci. & Tech. 1(11),923-6 (Nov 1967).

101. Parkin, D. W., Phillips, D. R., Sullivan, R.A.L., and Johnson, L., Airborne Dust Collections over the North Atlantic. J Geophys Res 75(9):1782-1793, March 1970.

102. Vohra,K. G., Vasudevan, K. N., and Nair, P.V.N., Mechanisms of Nucleus-Forming Reactions in the Atmosphere. J Geophys Res, 75(15):2951-2960, May 1970.

103. Vohra, K. G., and Nair, P.V.N., Recent Thinking on the Chemical Formation of Aerosols in the Air by Gas Phase Reactions, Aerosol Sci, Vol 1:127-133, 1970.

104. Mohnen, V. A., and Lodge, J. P. Jr., 1969: On Gas to Particle Conversion, Puzzling Features, In Proc. 7th Int. Conf. Condensation and Ice Nuclei, J. Podzimek, Ed., Czechoslovak Acad. Sci., Prague, 69-91.

105. Mosher, J. C., MacBeth, W. G., Leonard, M. J., Mullins, T. P., and Brunelle, M. P., The Distribution of Contaminants in the Los Angeles Basin Resulting from Atmospheric Reactions and Transport, J. Air Pollution Control Assoc., 20(1):35-42, Jan. 1970.

106. Goldsmith, J. B., Los Angeles Smog, Science J., 5(3):44-49, March 1969.

107. Altshuller, A. P., Analytical Chemistry, 41, 1R, 1969.

108. Mueller, P. K., Analytical Chemistry, 43, 1R, April 1971.

109. Germogenova, O. A., Friend, J. P., and Sacco, A. M., 1970: Atmospheric Haze: A Review, Bolt, Beranek, and Newman, Inc., Cambridge, Mass. 184 pp. Final Rept., prepared for Coordinating Research Council, Inc., New York (March).

110. Terry, E. R., Greene, B. R., Gadecki, E. V., Newman, E., Record, P. A., Boer, G. J., Wong, E.V.J., and Nicolopoulos, H., Bibliography on Atmospheric Transport, Dispersion and Depletion Processes, Vol. II, GCA Corp., Bedford, Mass., Technology Div., Contract DAAD 09-27-C-0128, RDT and E Proj. DA 1V025001A128, TR-67-26-G (II), 287 p.,Feb. 1969.

111. Lomaya, O. V., Dependence Between the Concentration of Aerosols and the Intensity of Turbulent Interchange in Lower Atmosphere, Soobshch. Adak. Nauk Gruz. SSR, 53(1):77-80, 1969.

112. Spirtas, R., and Levin, H., Patterns and Trends in Levels of Suspended Particulate Matter, J. Air Pollution Control Assoc., 21,329 (1971).

113. Spirtas, R., and Levin, H. J., Characteristics of Particulate Patterns 1957-1966, Public Health Service, Raleigh, N.C., National Air Pollution Control Administration, 101 p. March 1970, CESTI:PB 192223 NAPCA AP-61.

114. Gunn, R., The Secular Increase of the Worldwide Fine Particle Pollution, J. Atmospheric Sci., 21(2): 168-181, March 1964.

115. Porch, W. M., Charlson, R. J., and Radke, L. F., Atmospheric Aerosol: Does a Background Level Exist, Science 170(3955):315-317, Oct, 1970.

116. Dufour, L, 1967: L'aerosol Atmospherique, Ciel et Terre (Brussels) 83(9/10), 269-317.

117. Dufour, L., 1969: The Atmospheric Aerosol, Transl. by G. B. Hoidale, White Sands Missile Range, Atm. Sci. Lab. 47 pp., D.A. Task 1T 06112 B53A-18 (March).

118. McCaldin, R. O., Johnson, L. W., and Stephens, N. T., 1969: Atmospheric Aerosols, Sci. 166, 381-382.

119. McCrone, W. C., Morphological Analysis of Particulate Pollutants, In: Air Pollution. v. II. Analysis, Monitoring, and Surveying, Ed. by A. C. Stern, New York, Academic Press, 1968, p. 281-301.

120. Whitby, K. T., Aerosol Measurements in Los Angeles Smog, Vol. I, Air Pollution Control Office Publication No. APTD-0630, Nov. 1970.

121. Harris, F. S., 1970: Aerosols and Air Pollution in Los Angeles, Paper 70-146, Air Pollution Control Assn. Meeting, St. Louis, Mo., (June).

122. MacPhee, R. D., and Bokian, A. H., 1967: Suspended Particulates in the Los Angeles Atmosphere, J. Air Poll. Control Assn. 17,580.

123. Murthy,Bh. V. R., Roy, A. K., and Kapoor, R. K., 1965: Aerosols at Delhi, In Proc. Int. Conf. Cloud Physics, Tokyo and Sapporo (May-June), 67-72.

124. Vigliani, E. C., Chemical Composition and Particles Size Measurement of Air-Borne Dust in the Atmosphere of Milan, World Health Organization, Copenhagen (Denmark), Regional Office for Europe, Proc. Conf. Public Health Aspects Air Pollution Europe, Milan, Italy, 1957, p. 299-302 (Nov. 6-14).

125. Laamanen, A., Total Particle Fall and the Composition of Particulates in the Air of Some Finnish Urban Areas, Work-Environ-Health, 6(1):23-30, 1969.

126. Kneip, T. J., Eisenbud, M., Strehlow, C. D., and Freudenthal, C., Airborne Particulates in New York City, J. Air Pollution Control Assoc., 20(3): 144-149, March 1970.

127. Yagi, K., Konokawa, H., Inoue, T., Aizaki, M., and Masuda, S., Atmospheric Pollution from Foundries, Taiki Osen Kenkyu (J. Japan Soc. Air Pollution), 4(1):145, 1969. (Proceedings of the 10th Annual Meeting of the Japan Society of Air Pollution, 1969.)

128. Junge, C. E., Studies in the Chemistry of Unpolluted Atmospheres. Stanford Research Institute, Menlo Park, Calif., Final Rept., Contract Cwb-11151, 98 pp.

129. Valko, P., 1964: The properties of Atmospheric Aerosols in the Southern Foothills of the Alps, Arch. Meteor. Geophys. Biokl., Ser. B., 12, 458-474.

130. Junge, C. E. Robinson, E., and Ludwig, F. L., 1969: Study of Aerosols in Pacific Air Masses, J. Appl. Meteorol. 8, 340-347.

131. Cadle, R. D., Fischer, W. H., Frank, E. R., et al., 1968: Particles in Antarctic Atmosphere, J. Atmos. Sci. 25, 100-103.

132. Sheesley, D. C., Pitombo, L.R.M., Pate, J. B., Wartburg, A. F., Frank, E. R., and Lodge, Jr., J. P. (1971a), Atmospheric Sampling (Chemical) in Amazonas VI. Particles, in Symposium Proceedings on Environment in Amazonia, Part III, 14-17 June 1971, Instit, Nacion. Pesq. Amazon., Manaus, Brazil, to be published.

133. Schaefer, V. J., Condensation Nuclei: Production of Very Large Numbers in Country Air, Science, 170 (3960):851-852, Nov. 20, 1970.

134. Sekhon, R. S., and Murtphy, Bh. V. R., 1966: Some Characteristic Features of Hygroscopic and Non-hygroscopic Aerosols at Delhi. J. Atmos. Sci. 23,771.

135. Winkler, P., 1969: Growth of Atmospheric Aerosols with Relative Humidity. In Proc. 7th Int. Conf. Condensation and Ice Nuclei, Prague-Vienna, Czechoslovak Acad. Sci. (Sept.), 55.

136. Pueschel, R. G., Charlson, R. J., and Ahlquist, N. C., 1969: On the Anomalous Deliquescence of Sea-spray Aerosols. J. Appl. Meteorol. 8, 995-998.

137. Winkler, P., 1969: Untersuchungen über das Grössenwachstrum Naturlicher Aerosoltelichen mit der Relativen Feuchte Nach Einer Wägemethod. Ann. Meteorol. 4, 134-137.

138. Morachevsky, V. G., 1969: Structure of the Adsorption Layers of Atmospheric Aerosols. In Proc. 7th Int. Conf. Condensation and Ice Nuclei, J. Podzimek, Ed., Czechoslovak Acad. Sci., Prague, 33.

139. Hoidale, G. E., and Blanco, A. J., 1969: Infrared Absorption Spectra of Atmospheric Dust over an Interior Dust Basin. Pure Appl. Geophys. 74, 151-164.

140. Rozenberg, G. V., 1967: Properties of an Atmospheric Aerosol from Optical Data. Izv. Atm. Oceanic Phys. 3(9), 545-552.

141. Gushchin, G. P., 1968: Spectrophotometric Investigations of Characteristics of Atmospheric Aerosols in Various Geographic Regions of the USSR. Leningrad, Glav. Geofiz. Obs., Trudy 223, 65-80.

142. Hänel, G., 1968: The Real Part of the Mean Complex Index of Refraction and the Mean Density of Atmospheric Aerosol Particles. Tellus 20, 371-379.

143. Sears, P. B., Tell-tale Dust. American Scientist, New Haven, 52(1): 1-15, March 1964.

144. Flanigan, D. F., and DeLong, H. P., Spectral Absorption Characteristics of the Major Components of Dust Clouds. (Def. Dev. Eng. Lab., Edgewood Arsenal, Md.). Appl. Opt. 1971, 10(1), 51-7 (Eng).

145. Hoidale, G. B., Blanco, A. J., Johnson, N. L., and Doorey, R. V., Variations in the Absorption Spectra of Atmospheric Dust. Army Electronics Command, Fort Monmouth, N.J., DA Task 1T061102B53A-20, ECOM-5274, 31p., Oct. 1969.

146. Smith, R. M., and Twiss, P. C., Extensive Gaging of Dust Deposition Rates. Trans. Kansas Acad. Sci., 68(2): 311-321, Aug. 1965.

147. Game, P.M., Observations on a Dustfall in the Eastern Atlantic, Feb. 1962. J. of Sedimentary Petrology, Tulsa, Okla., 34(2):355-359, June 1964.

148. Prospero, J. M., and Bonatti, E., 1969: Continental Dust in the Atmosphere of the Eastern Equatorial Pacific. J. Geophys. Res. 74, 3362-3371.

149. Ferguson, W. S., Griffin, J. J., and Goldberg, E. D., Atmospheric Dusts from the North Pacific - A Short Note on a Long-Range Eolian Transport. J. Geophys. Res., 75(6):1137-1139, Feb. 20, 1970.

150. Kashina, V. I., Dust Content of the Atmospheric Layer near the Ground in Deserts and Semi-deserts in Central Asia and Kazakhstan. Adademiia Nauk Kazakhskoi SSR, Alma-Ata. Astrofizicheskii Institut, Trudy, 3:115-121, 1962.

151. Andreyev, B. G., and Lavrinenko, R. F., Some Data on the Chemical Composition of Atmospheric Aerosols in Central Asia. Meteorol. 1 Gidrol., No. 4:63-69, 1968.

152. Pitty, A. F., 1968: Particle Size of the Saharan Dust which Fell in Britian, July 1968. Nature 220, 364,

153. Prospero, J. M., Bonatti, E., Schubert, C., and Carlson, T. N., Dust in the Caribbean Atmosphere Traced to an African Dust Storm, Earth Planet Sci. Lett., 9(3):287-293, Oct. 1970.

154. Chester, R., and Johnson, L. R., Atmospheric Dusts Collected off the West African Coast. Nature (London) 229(5280):105-107, Jan., 8, 1971.

155. Junge, C. E., Airborne Dust at Barbados and its Relation to Global Tropospheric Aerosols. Geochim Cosmochim. Acta, Vol. 32:1219-1222, 1968.

156. Kawai, S., Takada, Y., Takenobu, Y., and Tada, T., Measurement of Particulate Matter by High Volume Air Samples. Taiki Osen Kenkyu (J. Japan Soc. Air Pollution), 4(1):30, 1969. (Proceedings of the 10th Annual Meeting of the Japan Society of Air Pollution, 1969.)

157. Sakabe, H. Matsushita, H., Hayashi, H., and others. Mineral Components and 3, 4-Benzpyrene in Air Pollutants of Tokyo. Indus. Health, v. 3: 126-139, 1965.

158. Hoidale, G. B., Smith, S. M., Blanco, A. J., and Barber, T. L., A Study of Atmospheric Dust, White Sands Missile Range, N. Mex., Atmospheric Sciences Lab., Task 1P620901-A199-05, ECOM-5067. (Mar. 1967). AD654990.

159. Friend, J. P., Atmospheric Aspects of the Global Sulfur Cycle, Meteorology and Oceanography, School of Engineering and Science, University Heights, Bronx, N.Y. 10453. 162nd Natl. Mtg. ACS, Sept. 12-17, 1971, Wash., D.C.

160. Robinson, E., and Robbins, R. C., Gaseous Sulfur Pollutants from Urban and Natural Sources. J. Air Pollution Control Assoc., 20(4):233-235, April 1970.

161. Cadle, R. D. and Allen, E. R., Atmospheric Photochemistry. Science, Vol. 167:243-249, Jan. 16, 1970.

162. Sulfur Oxides and other Sulfur Compounds - A Bibliography with Abstracts. PHS Publication #1093, Bibliographic Series #56, Wash., D. C., U.S. Government Printing Office.

163. Urone, P., and Schroeder, W. H., SO2 in the Atmosphere: A Wealth of Monitoring Data, but Few Reaction Rate Studies. Environ. Sci. Technol., 3(5):436-445, May 1969.

164. Proceedings of the Symposium on the Physico-Chemical Transformation of Sulphur Compounds in the Atmosphere and the Formation of Acid Smogs. Physico-Chem. Transformation Sulfur Compounds Atmosphere Formation Acid Smogs Proc. Symp., Mainz, West Germany, 1967. (June 8-9).

165. Heard, M. J., and Wiffen, R. D., 1969: Electron Microscopy of Natural Aerosols and the Identification of Particulate Ammonium Sulfate. Atmos. Environ. 3, 337-340.

166. Lodge, J., and Frank, E., Chemical Identification of Some Atmospheric Components in the Aitken Nucleus Size Range. Journal De Recherches Atmospheriques, p 140 (1966).

167. Good, A. and Thynne, J.C.J., Reaction of Free Radicals with Sulphur Dioxide. Part I. Methyl Radicals. Trans. Faraday Soc., 63(11):2708-2714, 1967.

168. Quon, J. E., Siegel, R. P., and Hulburt, H. M., Particle Formation from Photolysis of Sulfur Dioxide in Air, Preprint, Int'l Union of Air Pollution Prevention Assoc., 30 p., 1970. (Presented at the Int'l. Clean Air Congress, 2nd, Washington, D.C., Dec. 6-11, 1970, Paper CP-1D).

169. McKay, H.A.C., The Atmospheric Oxidation of Sulphur Dioxide in Water Droplets in Presence of Ammonia, Atmos. Environ. 5(1):7-14, Jan. 1971.

170. Cox, R. A. and Penkett, S. A., Oxidation of Atmospheric SO2 By-products of the Ozone-Olefin Reaction, Nature (London), 230(5292):321-322, April 2, 1971.

171. Okita, T., Measurements of the Concentration of Sulphur Compounds in the Atmosphere and Laboratory Experiments on the Oxidation of Sulphur Dioxide at the Surface of Particles. Proc. Symp. Physico-Chemical Transformation Sulphur Compds. Atmosphere, Formation Acid Smogs, Mainz (West Germany), 1967, p. 75-86 (June 8-9, Paper 9.)

172. Hill, A. E., and Fitzgerald, T. E., The Compounds of Sulfur Dioxide with Various Amines. J. Am. Chem. Soc., Vol. 57:250-254, Feb. 1935.

173. Kimura, K., Kunotsuki, K., Tada, O., and Nakaaki, K., On the Atmospheric Oxidation of Sulfur Dioxide. Translated from Japanese. Rodo Kagaka, 41 (10): 501-511, 1965.

174. Goetz, A., and Pueschel, R., Atmos. Environ; 1,287 (1967).

175. Smith, B. M., Wagman, J., and Fish, B. R., Interaction of Airborne Particles with Gases, Environ. Sci. Technol. 3,558 (1969).

176. Urone, P., Lutsep, H., Noyes, C., Parcher, J., Enrion. Sci. Technol., 2,611 (1968).

177. Bowen, H.J.M., Elementary Cycles and Pollution. Missouri Univ., Columbia, Proc. Missouri Univ. Second Annu. Conf. Trace Substances Environ. Health, Columbia, Mo., 1968, p. 171-179. (July 16-18.)

178. Lodge, J., and Pate, J., Atmospheric Gases and Particulates in Panama, Science, 153, 408 (1966).

179. Fishcer, W., Lodge, J., Pate, J., and Cadle, R., Antarctic Atmospheric Chemistry: Preliminary Exploration. Science, 164;66 (1969).

180. Fischer, W., Lodge, J., Warburg, A., and Pate, J., Estimation of Some Atmospheric Trace Gases in Antarctica. Environ. Sci. Technology, 2,464 (1968).

181. Cadle, R., Fisher, W., Frank, E., and Lodge, J., Paricles in the Antarctic Atmosphere, J. Atmospheric Sci. 25,100 (1968).

182. Bufalini, M., Oxidation of Sulfur Dioxide in Polluted Atmospheres - A Review, Environ. Sci. Technol., 5, 685 (1971).

183. Wagman, J., Lee, R. E. Jr., and Axt, C. J., Influence of Some Atmospheric Variables on the Concentration and Particle Size Distribution of Sulfate in Urban Air. Atmos. Environ., v. 1:479-489, July 1967.

184. Garland, J. A., Condensation on Ammonium Sulphate Particles and its Effect on Visibility. Atmos. Environ., 3(3):347-354, May 1969.

185. Cadle, R. D., Warburg, A. F., Frank, E. R., et al., 1967: Particles in Volcanic Fume. Nature 213, 581.

186. Junge, C., and Scheich, G., Determinations of the Acid Content of Aerosol Particles, Atmos. Environ. 5, 165 (1971).

187. deBarry, E., and Junge, C., Distribution of Sulfur and Chlorine over Europe, Tellus, XV, 370 (1963).

188. Eggleton, A.E.J., The Chemical Composition of Atmospheric Aerosols on Tees-side and its Relation to Visibility. Atmos. Environ., 3(3):355-372, May 1969.

189. Kapoor, R. K., and Murthy, Bh. V., 1966: Sulfate Aercsol at Delhi in Relation to Associated Chloride Component. J. Appl. Meteorol. 5, 493-499.

190. Okita, T., Tezuka, T., and Umino, H., Concentration of Sulfate in Aerosol and Fog Water. Collection of Aerosol by Using a High-Volume Cascade Impacter; and Analysis of the Sulfate and other Inorganic Components. Taiki Osen Kenkyu (J. Japan Soc. Air Pollution), 2 (1):96-98, 1967. APTIC 23450

191. Georgii, H. W., Jost, D., and Schaefer, R. J., The Spatial and Temporal Distribution of Sulfur Dioxide and Sulfate Aerosols in the Lower Troposhere. Frankfurt Univ. (West Germany). Institut fur Meteorologie und Geophysik, Contract T483-J-203, 88 p., Feb. 1968. APTIC 12218.

192. Ludwig, J. H., Morgan, G. B., and McMullen, T. B., Trends in Urban Air Quality. Trans. Am. Geophys. Union, 51(5):468-475. May 1970.

193. Maienthal, E. J., Analysis of Air Pollutants. National Bureau of Standards, Wash., D. C., Micro-chemical Analysis Section, TN-505, p. 34-36, Oct. 1969.

194. Schroeder, H. A., Airborne Metals. Sci. Citizen, 10(3):83-88, April 1968.

195. Covert, D. S., Charlson, R. J., and Ahlquist, N. C., 1970: A Study of the Relationship of Chemical Composition and Humidity with Light Scattering by Aerosols. Bull. Am. Meteorol. Soc. 51, 1010.

196. Chow, T. J., and Earl, J. L., 1970: Lead aerosols in the atmosphere: Increasing Concentration. Sci. 169, 577γ580.

197. Atkins, P. R., Lead in a Suburban Environment, J. Air Pollution Control Assoc., 19(8):591-594, Aug. 1969.

198. Chow, T. J., Earl, J. L., and Bennett, C. F., Lead Aerosols in Marine Atmosphere. Environ. Sci. Technol., 3(8):737-740, Aug. 1969.

199. Murozumi, M., Chow, T. J., and Patterson, C., Lead, Dust, and Salt in Firn and Ice From Camp Century and Byrd Station. Antarctic J. U. S., 4(5):218, Sept.-Oct. 1969.

200. Daines, R. H., Motto, H., and Chilko, D. M., Atmospheric Lead: Its Relationship to Traffic Volume and Proximity to Highways. Environ. Sci. Technol. 4(4):318-322, April 1970.

201. Kobayashi, Y., Hori, M., and Tsuchiya, K., Horizontal and Vertical Distribution of Lead Particulates in Air around a Busy Road in Yokohama City. Nippon Koshu Eisei Zasshi (Japan J. Public Health), 17 (6):307-312, June 15, 1970.

202. Yunghans, R. S., and McMullen, B., Ambient Air Fluoride Concentrations in the United States. Preprint, Public Health Service, Cincinnatti, Ohio, National Air Pollution Control Administration, Aug. 1969.

203. Thompson, R., McMullen, T., and Morgan, G., Fluoride Concentrations in the Ambient Air, J. Air Poll. Control Assoc., 21,484 (1971).

204. Lovelock, J. E., Origin and Movement of Fluorine Compounds, Nature, 230, 379 (1971).

205. Jepsen, A. F., Measurement of Mercury Vapor in the Atmosphere. Environmental Measurements, Inc., 215 Leidesdorff St., San Francisco, Calif., 94111. 162nd Nat'l. Mtg. ACS, Sept. 12-17, 1971, Wash., D.C.

206. Kothny, E. L., The Three Phase Equilibrium of Mercury in Nature, Air & Industrial Hygiene Laboratory, California State Dept. of Public Health, 2151 Berkeley Way, Berkeley, California 94705. 162nd Nat'l. Mtg., ACS, Sept. 12-17, 1971, Wash., D. C.

207. Lakin, H. W., The Geochemical Cycle of Selenium in our Environment. U. S. Geological Survey, Denver Federal Center, Building 25, Lakewood, Colorado 80225. 162nd Nat'l. Mtg. ACS, Sept. 12-17, 1971, Wash., D. C.

208. Hashimoto, Y. and Winchester, J., Selenium in the Atmosphere, Environ. Sci. Technol. 1(4), 340-2 (April 1967).

209. Sullivan, R. J., Preliminary Air Pollution Survey of Nickel and its Compounds: A Literature Review. Litton Systems, Inc., Silver Spring, Md., Environmental Systems Div., Contract PH22-69-25, NAPCA Pub. APTD 69-41, 69 p., Oct. 1969.

210. Zoller, W. H., Gordon, G. E., Gladney, E. S., and Jones, A. G., The Sources and Distribution of Vanadium in the Atmosphere. Department of Chemistry, University of Maryland, College Park, Md., 20742. 162nd Nat'l. Mtg. ACS, Sept. 12-17, 1971, Wash., D. C.

211. Robinson, E., and Robbins, R., Gaseous Nitrogen Compound Pollutants from Urban and Natural Sources, J. Air Pollution Control Assoc., 20,303 (1970).

212. Haentzsch, S., and Lahmann, E., Ammonia Determination in the Urban Atmosphere, Schriftenreihe Ver. Wasser Boden Lufthyg. (Berlin), no. 33:35-39, 1970.

213. Petriconi, G. L., and Papee, H. M., On the Decomposition of Ammonium Nitrate in the Atmosphere. J. Atmospheric Sci., 27(1):164-166, Jan. 1970.

214. Voronkov, P. P., Hydrochemical Study of Atmospheric Precipitation. Sb. Rab. Gidrol., No. 8:67-81, 1968.

215. Petrenchuk, O. P., Chemical Composition of Cloud Water in Regions of Western Siberia. In: American Institute of Crop Ecology Survey of USSR Air Pollution Literature. Vol. IV. Meteorological and Chemical Aspects of Air Pollution; Propagation and Dispersal of Air Pollutants in a Number of Areas in the Soviet Union. M. Y. Nuttonson (ed.), Silver Spring, Md., American Institute of Crop Ecology, 1970, p. 87-93. (Also: Tr. Gl. Geofiz. Observ. (Leningrad), no. 234: 130-136, 1968.)

216. Osokin, I. M. Chemical Composition of Snow Cover in the USSR, Akademiia, Nauk SSSR, Izvestiia, Ser. Geogr., No. 3:26-34, May/June 1963.

217. Rancitelli, L. A., Perkins, R. W., Tanner, T. M. and Thomas, C. W., Stable Elements of the Atmosphere as Tracers of Precipitation Scavenging, Battelle Memorial Inst. Richland, Wash., Pacific Northwest Lab. and Atomic Energy Commission, Wash., D. C., Fallout Studies Branch Precipitation Scavenging Proc. Symp., Richland, Wash. 1970, p. 99-108. (June 2-4).

218. Lazrus, A., Lorange, E., and Lodge, J. P., Lead and Other Metal Ions in United States Precipitation, Environmental Sci. Tech., 4,55 (1970).

219. McMullen, T. B., Faoro, R. B., and Morgan, G. B., Profile of Pollutant Fractions in Nonurban Suspended Particulate Matter. J. Air Pollution Control Assoc., 20(6):369-372, June 1970.

220. Pate, J. B., Pitombo, L.R.M., Wartburg, A. F., Sheesley, D. C., Lahue, M. D., and Lodge, Jr., J. P. (1971a). Atmospheric Sampling (Chemical) in Amazonas V. Gases, in Symposium Proceedings on Environment in Amazonia, Part III, 14-17 June 1971, Instit. Nacion. Pesq. Amazon., Manaus, Brazil, to be published.

221. Strackee, L., Electron Spin Resonance of Ferromagnetic Particles in Airborne Dust, Nature, 218, 498 (1968).

222. Goetz, A., 1965: Constitution of Aerocolloidal Particles above the Ocean Surface. In Proc. Int. Conf. Cloud Physics, Tokyo and Sapporo (May-June).

223. Winchester, J. W., and Duce, R. A., The Global Distribution of Iodine, Bromine, and Chlorine in Marine Aerosols. Naturwissenschaften (Berlin), 54(5):110-113, March 1967.

224. Dudey, N. D., Ross, L. E., and Noshkin, V. F., Application of Activiation Analysis and GE(LI) Detection Techniques for the Determination of Stable Elements in Marine Aerosols. In: Modern Trends in Activation Analysis. James P. DeVoe (ed.), Vol. 1, Washington, D. C., Dept. Commerce, NBS SP312, June 1969.

225. Lazrus, A. L., Baynton, H. W., and Lodge, Jr., J. P., Trace Constituents in Oceanic Cloud Water and their Origin, Tellus (Uppsala), 22(1):106-114, 1970.

226. Hoffman, G. L., Duce, R. A., and Zoller, W. H., Vanadium, Copper, and Aluminum in the Lower Atmosphere between California and Hawaii, Environ. Sci. Technol., 3,1207 (1969).

227. Wilkniss, E., and Bressan, D. J., Geochemical Aspects of Inorganic Aerosols near the Ocean-Atmosphere Interface, Naval Res. Lab., Code 8330, Wash., D. C., 20390, 162nd Nat'l. Mtg. ACS, Sept. 1 -17, 1971, Wash., D. C.

228. Matveey, A. A., and Bashmakova, O. I., Removal of Soluble Substances from the Atmosphere at the Surface of Small Bodies of Water. Gidrokhim. Materialy, vol. 44:5-15, 1968.

229. Egorv, V. V., Zhigalovskaya, T. N., and Malakhov, S. G., Microelement Content of Surface Air above the Continent and the Ocean. J. Geophys. Res., 75(18): 3650-3656, June 20, 1970.

230. Selezneva, Ye. S., Petrenchuk, O. P., and Svistov, P. F., Distribution and Chemical Composition of Natural Aerosols over Various Regions of the European Sector of the USSR. Tr. Gl. Geofiz. Observ. (Leningrad), no. 234:125-129, 1968.

231. Dyer, A. J., and Hicks, B. B., 1968: Global Spread of Volcanic Dust from the Bali Eruption of 1963. Quart. J. R. Met. Soc. 94, 545-554.

232. Friend, P. P., 1970: Volcanic Sources of Atmospheric Aerosol. Bull. Am. Meteorol. Soc. 51, 1009.

233. Bigg, E. K., Kviz, Z., and Thompson, W. I., Electron Microscope Photographs of Extraterrestrial Particles, Tellus, 23, 247, (1971).

234. Rosinski, J., Extraterrestrial Magnetic Spherules: Their Association with Meteor Showers and Rainfall Frequency, J. Atmospheric Terr. Phys., 32, 805 (1970).

235. Lininger, R. L., et al., 1966: Chlorine, Bromine, Iodine and Lead in Aerosols from Cambridge, Massachusetts. J. Geophys Res. 71, 2457-2463.

236. Thompson, R. J., 1970: Trace Metal Analysis in Atmospheric Particulates. In 11th Conf. Methods in Air Pollution, Industrial Hygiene Studies, Berkeley, Calif. (March-April).

237. Guerin, M. R., and Shultz, W. D., Air Quality Survey. In: Analytical Chemistry Division Annual Report for Period Ending September 30, 1968. Oak Ridge National Lab., Tenn., Analytical Chemistry Div., Rept. ORNL-4343, UC-4-Chemistry, p. 19-20, Dec. 1968.

238. Rahn, K., Wesolowski, J., John, W., and Ralston, H., Diurnal Variation of Aerosol Trace Element Concentrations in Livermore, California., J. Air Poll. Control Assoc., 21,406 (1971).

239. Harrison, P., Rahn, K., Dams, R., Robbins, J., Winchester, J., Brar, S., and Nelson, D., Areawide Trace Metal Concentrations Measured by Multielement Neutron Activation Analysis, J. Air Poll. Control Assoc., 21(9); 563-570 (1971).

240. Dams, R., Robbins, J., Rahn, K., and Winchester, W., Pair and Cluster Correlations among Trace Elements in Air Particulates over the Industrialized Area of Northwest Indiana. Dept. of Oceanography, Florida State University, Tallahassee, Florida 32306. 161st Nat'l. Mtg. ACS, March 28, 1971, Los Angeles, Calif.

241. Baugh, J. O., and Russell, I. J., Source Identification of Atmospheric Aerosols by Neutron Activation Analysis, Chemistry Dept., Boston College, Chestnut Hill, Massachusetts, 02167. 161st Nat'l. Mtg. ACS, March 28, 1971, Los Angeles, Calif.

242. Brar, S. S., Nelson, D. M., Kline, J. R., Gustafson, P. F., Kanabrocki, E. L., Moore, C. E., and Hattori, D. M., Instrumental Analysis for the Trace Elements Present in Chicago Area Surface Air. J. Geophys. Res., 75(15):2939-2945, May 20, 1970.

243. Loucks, R. H., Winchester, J. J., Matson, W. R., and Tiffany, A., The Halogen Composition of Aerosol Particles over Lake Michigan. In: Modern Trends in Activation Analysis. James R. DeVoe (ed.), vol. 1, Washington, D. C., National Bureau of Standards SP312, Dept. of Commerce, 1969, p. 36-42.

244. Dams, R., Robbins, J. A., Rahn, K. A., and Winchester, J. W., Nondestructive Neutron Activation Analysis of Air Pollution Particulates. Anal. Chem., 42(8): 861-867, July 1970.

245. Lindsey, A. J., Some Observations on the Relative Quantities of Air Pollutants in Various Locations. Nat. Cancer Inst. Monograph, No. 9:235-250, 1962.

246. Hettche, H. O., Benzopyrenes and Trace Elements in the Atmosphere of a Large City, Intern. J. Air Water Pollution (London), vol. 8:185-191, 1964.

247. Aleksandrov, N. N., Panichev, N. A., Rzhaksinskaya, M. A., and Turkin, M. I., Spectral Method of Determining a Number of Elements in Atmospheric Aerosols. Text in Russian. Tr. Gl. Geofiz. Observ. (Leningrad), No. 234:196-204, 1968.

248. Masek, V., The Composition of Dusts on Work Sites and in the Close Vicinity of Iron Works, Staub, Reinhaltung Luft, 31(2):66-68, Feb., 1971.

249. Hasegawa, T., and Sugimae, A., Trace Metals in Suspended Par iculates in Osaka Prefecture. Part I. Taiki Osen Kehkyu (J. Japan Soc. Air Pollution), 4(1):143, 1969. (Proceedings of the 10th Annual Meeting of the Japan Society of Air Pollution, 1969).

250. Hasegawa, T., Sugimae, A., Fujii, J., Matsuo, Y., and Okuyama, Y., Trace Metals in Suspended Particulates. Part II. Taiki Osen Kenkyu (J. Japan Soc. Air Pollution), 5(1):310, 1970. (Proceedings of the Japan Society of Air Pollution, Annual Meeting, 11th, 1970.)

251. Kiyoura, R., Iguchi, S., Kuramoto, T., Munidasa, M., Naito, N., and Uenishi, Y., Characteristics of Air Borne Particulates in the Atmosphere in Industrial Complexes and Urban Areas. Taiki Osen Kenkyu (J. Japan Soc. Air Pollution), 5(1):232, 1970. (Proceedings of the Japan Society of Air Pollution, Annual Meeting, 11th, 1970.)

252. Kiyoura, R., Kuramoto, T., Munidasa, M., Kawasaki, G., Naito, N., and Uenishi, Y., Characteristics of Heavy Metals in Air-Borne Particulates in Industrial Complexes and Urban Areas. Taiki Osen Kenkyu (J. Japan Soc. Air Pollution), 5(1):233, 1970. (Proceedings of the Japan Society of Air Pollution, Annual Meeting, 11th, 1970.)

253. Himi, Y., Mori, O., Tanaka, H., and Muramatsu, T., Air Pollution Due to Dust and Smoke in Keihin Industrial Area. (Report 18). Taiki Osen Kenkyu (J. Japan Soc. Air Pollution), 5(1):209, 1970. (Proceedings of the Japan Society of Air Pollution, Annual Meeting, 11th, 1970.)

254. Iki, S., and Yoshinaga, S., Heavy Metals in the Atmospheric Deposit in Kita-Kyushu City. Taiki Osen Kenkyu (J. Japan. Soc. Air Pollution), 4(1): 108, 1969. (Proceedings of the 10th Annual Meeting of the Japan Society of Air Pollution, 1969.)

255. Iki, S., Yoshinaga, S., Nishimura, T., and Matsumoto, M., The Contents of Heavy Metals in the Atmospheric Deposits in Kitakyushu City. Kyushu Sangyo Daigaku Kogakubu Kenkyu Hokoku (Kyushu Ind. Coll. Res. Rept), vol. 7:1-26, June 1970.

256. Oya, T., Kudo, T., Miyazaki, H., Himi, K., Hasegawa, H., Iki, S., Saruta, N., Suzuki, T., Kobayaski, Y., Ito, K., Koyama, O., Terabe, M., Saruta, K., Takeuchi, H., Nakano, M., and Jujii, T., Investigation of Air Pollutants. Taiki Osen Kenkyu (J. Japan Soc. Air Pollution), 1(2):87-96, 1967.

257. Sato, A., Takahashi, M., and Kudo, T., Studies on Atmospheric Pollution in Iwate Prefecture. No. 9. Heavy Metal Content in Settling Dusts. Part II. Iwate-Ken Eisei Kenkyusho Nenpo (Ann. Rept. Iwate Inst. Public Health), no. 12:71-99, 1968. Part I. Ibid, no. 12:44-70, 1968.

258. Went, F. W., Dispersion and Disposal of Organic Materials in the Atmosphere. Desert Research Inst. Reprint Series No. 31. Apr. 1966.

259. Spengler, C., and Haupt, G., Formation of Scot and Polycyclic Aromatic Hydrocarbons in Simple Hydrocarbon Flames and its Inhibition by Fuel Additives. Erdoel Kohle (Hamburg), 22(11):679-684, Nov. 1969.

260. Lindsey, A. J., and Stanbury, J. R., A Study of Air Pollution by Analysis of Particulate Material Collected from Air Filtration Plants. Part II. Determination of Polycyclic Aromatic Hydrocarbons in Total Air Solids. Intern. J. Air Water Pollution (London), vol. 6:387-390, 1962.

261. Sawicki, E., Stanley, T. W., and Elbert, W. C., Analysis of the Urban Atmosphere and Air Pollution Source Effluents for Phenalen-1-One and 7 H-Benz(De) Anthracen-7-One. Mikrochimica Acta (Wien), v. 5-6: 1100-1123, 1965.

262. Sawicki, E., Airborne Carcinogens and Allied Compounds. Arch. Environ. Health, v. 14: 46-53, 1967.

263. Sawicki, E., Corey, R. C., Dooley, A. E., Gisclard, J. B., Monkman, J. L., Neligan, R. E. and Ripperton, L. A., Tentative Method of Analysis for Polynuclear Aromatic Hydrocarbon Content of Atmospheric Particulate Matter. Health Lab. Sci. Suppl., 7(1):31-59, Jan. 1970.

264. Saringer, M. K., Morik, J., Benzpyrene Content of Dust Samples Collected on Urban and Rural Settlements and in Industrial Plants 3,4. Egeszegtudomany, 14(2): 105-115, Feb. 1970.

265. Clemo, G. R., Some Constituents of City Smoke. Tetrahedron, vol. 23:2389-2393, April-June 1967.

266. Fujie, K., Gas Chromatographic Analysis of Polycyclic Aromatic Hydrocarbons Associated with Particulates in Osaka Air. Taiki Osen Kenkyu (J. Japan. Soc. Air Pollution), 3(2): 126-133, 1969.

267. Barrett, W. J., Identification of Organic Compounds in the Atmosphere. (Summary Report). Southern Research Inst., Birmingham, Ala., Grant AP 00454, Proj. 1791, Rept. 1, Dec. 27, 1968.

268. Gilbert, J.A.S., and Lindsey, A. J., The Determination of the Amount and Distribution of Atmospheric Smoke Pollution by Analysis of Snow. Chem. Ind. (London), vol. 45:1439-1440, Nov. 5, 1955.

269. Bosco, G., and Grella, A., Determination of Aromatic Polycyclic Hydrocarbons in the Hazy Atmosphere of Siena, Italy. Nuovi Ann. Igiene Microbiol. (Rom) 17 (4):297-300 (1966.)

270. Semenov, A. D., Nemtseva, L. I., Kishkinova, T. S. and Pashanova, A. P., Organic Substances in Atmospheric Precipitates. Doklady Akad. Nauk SSSR, 173(5): 1185-1187, 1967.

271. Fujie, K., Determination of Sugars and other Alpha-Clycolic Derivatives in Airborne Particulates. Taiki Osen Kenkya (J. Japan. Soc. Air Pollution), 3(3):153-158, Dec. 1, 1969.

272. Tabor, E. C., Contamination of Urban Air through the Use of Insecticides. Trans. New York Acad. Sci., v. 28:569-578, 1966.

273. Stanley, C. W., Barney, J. E., Heltos, M. R., and Yobs, A. R., Measurement of Atmospheric Levels of Pesticides, Environ. Sci. Technol., 5,430 (1971).

274. Sharkey, A., Shultz, J., Appell, H., and Friedel, R., Research Development, August, (1971).

275. Tabor, E. C., and Fair, D. H., Relation of Benzene Soluble Organic Matter to Suspended Particulate Matter in the Atmosphere. Preprint, Air Pollution Control Association, New York City, 1960. (Presented at the Air Pollution Control Association Annual Meeting, 534d, Cincinnatti, Ohio, May 22-26, 1960.)

276. Keng, E.Y.H., Gaseous Impurities and Nuclear Condensation on Airborne Sodium Chloride Particles, Environmental Sci. Tech., 4,417 (1970).

277. Nix, N., Condensation and Evaporation at Single Particles of Small Aerosols. Staug, Reinhaltung Lufte, 29(5):15-19, May 1969.

278. Levy, II, H., Normal Atmosphere: Large Radical and Formaldehyde Concentrations Predicted, Science, 173, 141 (1971).

279. Lewis, J., Peroxyacyl Nitrates. In: Project Clean Air California Univ., Berkeley, Task Force 7, Vol. 4, p. 4-1 to 4-9, Sept. 1, 1970.

280. Stephens, E. R., The Formation, Reactions, and Properties of Peroxyacyl Nitrates (PANS) in Photochemical Air Pollution. In: Advances in Environmental Sciences and Technology, J. N. Pitts, Jr., and R. L. Metcalf (eds.), Vol. 1, New York, Wiley-Intersciences, 1969, p. 119-146.

281. Glasson, W., and Tuesday, C. S., Hydrocarbon Reactivities in the Atmospheric Photooxidation of Nitric Oxide. Environ. Sci. Technol. 4(11):916-924, Nov. 1970. 29 refs. (Presented at the American Chemical Society, 150th Meeting, Div. of Water, Air, and Waste Chemistry, Atlantic City, N.J., Sept. 1965.)

282. Stephens, E. R., and Price, M. A., Smog Aerosol Infrared Spectra. Science, 168, 1584-6, 1970.

283. Fatiadi, A. J., and Cohen, A., Photochemistry of Aromatic Air Pollutants. National Bureau of Standards, Washington, D. C., TN-427, p. 17-31, Oct. 1967.

284. Went, F. W., 1967: Formation of Aerosol Particulates Derived from Naturally Occurring Hydrocarbons Produced by Plants. J. Air Poll. Control Assn. 17, 579-580.

285. Went, F. W., The Nature of Aitken Condensation Nuclei in the Atmosphere. Proc. Natl. Acad. Sci. U. S., 51(6):1259-1267, June 1964.

286. Fish, B., Electrical Generation of Natural Aerosols from Vegetation. 45th Natl. Coll. Sym., June 1971, Oak Ridge Natl. Lab.

287. Smidt, A. X., and Marlies, C. A., Principles of High-Polymer Theory and Practice, McGraw-Hill Book Company, Inc. 1948.

288. Cukor, P., Ciaccio, L. L., Lanning, E., and Rubino, R. L., Characterization of the Organic Fraction in Air Particulate Matter, GTE Laboratories, 208-20 Willets Point Blvd., Bayside, NY 11360, 152nd Nat'l. Mtg. ACS, Sept. 12-17, 1971, Wash., D. C.

289. Hunt, Madison and Marvel, C. S., The Reaction between Sulfur Dioxide and Olefins. II. Propylene. J. Am. Chem. Soc., vol. 57:1691-1696, Sept. 1935.

290. Staudinger, H., and Ritzenthaler, B, A Study of High Polymer Compounds: 104th Report: The Addition of Sulfur Dioxide to Ethylene Derivatives. Chem. Ber., vol. 68:455-471, 1935.

291. Jellinek, H.H.G., Chain Scission of Polymers by Small Concentrations (1 to 5 rpm) of Sulfur Dioxide and Nitrogen Dioxide, Respectively, in Presence of Air and near Ultraviolet Radiation. J. Air Poll. Control Assoc. 20 (10):672-4 (Oct. 1970).

292. Shearer, E. C., Formaldehyde, Methane, and Krypton. Arkansas Univ., Fayetteville, Thesis (Ph.D.), 1969, 135 p. CFSTI:TID-25286.

293. Cavanagh, L. A., Schadt, C. F., and Robinson, E., Atmospheric Hydrocarbon and Carbon Monoxide Measurements at Point Barrow, Alaska. Environ. Sci. Technol., 3(3):251-257, March 1969.

294. Sheesley, D. C., Pitombo, L.R.M., Neuscheler, R., Lahue, M. L., Pate, J. B., Wartburg, A. F., and Lodge, Jr., J. P. (1971b), Atmospheric Sampling (Chemical) in Amazonas VII. Organic Compounds. in Symposium Proceedings on Environment in Amazonia, Part III, 14-17 Sept. 1971, Instit. Nacion. Pesq. Amazon., Manaus, Brazil, to be published.

295. Garrett, W. D., Stabilization of Air Bubbles at the Air-Sea Interface by Surface-Active Material, Deep Sea Research, 14,661 (1967).

296. Barger, W. R., and Garrett, W. D., Surface Active Organic Material in the Marine Atmosphere, J. Geophys. Res. 75(24):4561-4566, Aug. 20, 1970. (Presented at the American Chemical Society National Meeting, 159th, Houston, Tex., Feb. 1970.)

297. Blanchard, D. C., 1968: Surface Active Organic Material on Airborne Salt Particles. Proc. Int. Conf. Cloud Physics, Toronto (August), 25-29.

298. Junge, C. E., Large Scale Distribution of Micro-organism in Atmosphere, Proc. Atmos. Biol. Conf., p. 117, 1965.

299. Ackermann, H., Research on Air Fungi Isolated by Culture since 1940. Rev. Can. Biol. 27(1):61-68, March, 1968.

300. Reifferscheid, H., The Biological Component of Aerosol and its Measurement. Germany (Federal Republic), Deutscher Wetterdienst, Berichte, 12(91):92-95, 1963.

301. Reddi, C., A Comparative Survey of Atmospheric Pollen and Fungus Spores at Two Places Twenty Miles Apart. Acta Allergol. 25 (2-3):189-215, 1970.

302. Varonier, H., Study of the Aero-Allergen Potential (due to pollen and fungi) in Geneva. Acta Allergol., 24(6):410-420, Dec. 1969.

303. Grigorashchenko, O., and Kharmats, L. M., Data on the Study of Bacterial Contamination of Atmospheric Air of tge City of Odessa. Mikrobiol. Zh. (Kiev), 25(1):35-41, 1963.

304. Seisaburo, Sekido, Kiyoko, K., and Tatsuko, N., Free Dust Particles and Airborne Microfloba. Osaka Shiritsu Daigaku Kaseigakubu Kiyo (Repts. of the Sci. of Living, Osaka City Univ.), 4(3):31-37, March 31, 1959.

305. Schlichting, H. E., Jr., The Importance of Airborne Algae and Protozoa. J. Air Pollution Control Assoc., 19(12):946-951, Dec. 1969.

306. Wright, T. J., Greene, V. W., Paulus, H. J., and Ciagne, R. P., Viable Microorganisms in an Urban Atmosphere, Univ. of Minnesota, 61st Annual Mtg. APCA, St. Paul, Minn., June 23-27, 1968.

307. Gregory, P. H., Atmospheric Microbial Cloud Systems. Science Progress (London), v. 55:613-628, 1967.

308. Laseter, J. L., and Valle, R., Organics Associated with the Outer Surface of Airborne Urediospores, Environ. Sci. Technol., 5,631 (1971).

309. Junge, C. E., 1963: Air Chemistry and Radioactivity. Academic Press.

310. Stewart, K., Principal Characteristics of Radioactive Contaminants which May Appear in the Atmosphere. Progr. Nucl. Energy, Ser. 12, pp. 321-60, 1969.

311. McEachern, P., Myers, W. G., and White, F. A., Uranium Concentrations in Surface Air at Rural and Urban Localities within New York State, Environ. Sci. Technol. 5,700 (1971).

312. Breslin, A. J., Glauberman, H., Investigation of Radioactive Dust Dispersed from Uranium Tailing Piles, Proc. Symp. Environ. Surveillance Vicinity Nucl. Facil. 1968 (Pub. 1970), 249-53 (Eng.), Edited by Reinig, William C. Thomas: Springfield, Ill.

313. Jones, I. S., and Pond, S. F., Some Experiements to Determine the Resuspension Factor of Plutorium from Various Surfaces, Proc. Symp. on Surface Contamination, Gatlinburg, Tenn., p. 83-92, 1964.

314. Madelaine, G. J., Formation and Evolution of Aerosols in Filtered Air and in Natural Air. Effect of Radioactivity. Commissariat a l'Energie Atomique, Fontenay-aux-Roses (France), Service Technique D'Etudes de Protection, Rept. CEA-R-3614, Dec. 1968.

315. Kozlova, M. V., Korenkov, I. P., Novikov, Yu V. and Granovskava, D. D., The Study of the Concentrations of Long-Duration Radioactive Aerosols of Atmospheric Air in its Relation to the Amount of Dust. Moscow Municipal Epidemic Hospital (USSR) and Erisman Research Inst. of Hygiene, Moscow (USSR). Translated from Russian. Army Foreign Science and Technology Center, Wash., D. C., 5p., Sept. 18, 1969. AD 695177

316. Volchok, H. L. and Kleinman, M. T., Radionuclides and Lead in Surface Air. In: Health and Safety Laboratory Fallout Program Quarterly Summer Report. Appendix. Atomic Energy Commission New York, Health and Safety Lab., p. 1-6, 78-81, July 1, 1970.

317. Chen, T. S., and Kuroda, P. K., Worldwide Movement of Fallout Particles from Nuclear Explosion. Health Physics, 20,139 (1971).

318. Machta, L., List, R. J., Smith, Jr., M. E., and Oeschger, H., Use of Natural Radioactivities to Estimate Large-Scale Precipitation Scavenging. Battelle Memorial Inst., Richland, Wash., Pacific Northwest Lab. and Atomic Energy Commission, Wash., D. C., Fallout Studies Branch, Precipitation Scavenging Proc. Symp, Richland, Wash., 1970, p. 465-74. (June 2-4).

319. Karol, I. L., and Malakhov, S. G., International Symposium on Atmospheric Trace Constituents and Atmospheric Circulation (8-13 September 1969, Heidelberg, Germany). Bull. Acad. Sci. USSR, Phys. Atmos. Oceans (English translation from Russian of: Izv. Akad. Nauk SSSR. Fiz Atmosfery i Okeana), 6(3):180-182, March 1970.

320. International Symposium on Atmospheric Trace Constituents and Atmospheric Circulation, Heidelberg, Germany, Sept., 1969, Reprinted from J. of Geophys. Res. 75, Nos. 9, 12, 15 and 18. Ed. by E. A. Martell and K. K. Turekian.

321. Cadle, R. D., Particles in the Atmosphere and Space, Reinhold Book Division (1966).

322. Cole, A. E., 1965: Precipitation, Clouds and Aerosols. In Handbook of Geophys. and Space Environ., S. L. Valley, Ed., Ch. 5, McGraw-Hill Book Co.

323. Bibliography on Nuclei in the Atmosphere, Met. Abs., 6(8,9):1163-1197; 1037-1343, Aug., Sept. 1955.

324. Bibliography on Weather Modification and Microphysics of Clouds (Nuclei), Met. Abs., 14(1): 144-244, Jan. 1963.

325. Recent Literature on Nuclei and Nucleation Processes, Met. Abs., 15(6):1306-1337, June 1964.

326. Rosinski, J., Solid Water - Insoluble Particles in Hailstones and their Geophysical Significance. J. Applied Meteorology, 5,481 (1966).

327. Rosinski, J., Langer, G., Nagamoto, C., Kerrigan, T., and Prodi, F., Natural Ice Forming Nuclei in Severe Convective Storms, J. Atmos. Sci., 28,391 (1971).

328. Hidy, G. M., Bleck, R., Blifford, Jr., I. H., Brown, P. M., and Langer, G., Observations of Aerosols over Northeastern Colorado. National Center for Atmospheric Research, Boulder, Colo., NCAR-TN-49, 64 p., June 1970.

329. Went, F. W., 1966: The Nature of Aitken Condensation Nuclei. Tellus 18, 549-556.

330. Bricard, J., Billard, F., and Madelaine, G., 1968: Formation and Evolution of Nuclei of Condensation that Appear in Air Initially Free of Aerosols. J. Geophys. Res. 73, 4487.

331. Radke, L. F., and Hobbs, P. V., Measurement of Cloud Condensation Nuclei, Light Scattering Coefficient: Sodium-Containing Particles, and Aitken Nuclei in the Olympic Mountains of Washington. J. Atmos. Sci., 26(2):281-288, March 1969.

332. Cadle, R. D., Bleck, R., Shedlovsky, J. P., Blifford, I. H., Rosinski, J., and Lazrus, A. L., 1969: Trace Constituents in the Vicinity of Jet Streams. J. Appl. Meteorol. 8, 348-356.

333. Ludwig, F. L., and Robinson, E., 1970: Observations of Aerosols and Droplets in California Stratus. Tellus 22, 94-105.

334. Jiusto, J. E., 1967: Aerosol and Cloud Microphysics Measurements in Hawaii. Tellus 19, 359-368.

335. Cowan, G. A., Gregory, Jr., T. G., Guthals, I. R., Sedlacek, W. A., and Smith, E. L., Characterization and Tracking of Aerosol Sources with the Use of Aircraft Sampling. Univ. of California, Los Alamos Scientific Lab., P.O. Box 1663, Los Alamos, New Mexico 87544. 161st Nat'l. Mtg. ACS, March 28, 1971, Los Angeles, Calif.

336. Kishko, Yu. G., Quantitative Content of Microorganisms in High Atmospheric Layers. Mikorbiol. Zh. (Kiev), 22(6):77-81, 1960. 15 refs. Translated from Russian, Foreign Technology Div. Wright-Patterson AFB, Ohio, Translation Div. 8 p., Feb. 26, 1970, CFSTI,DDC: AD 703889.

337. Pilipowsky, S. Weinman, J. A., Clemesha, B. R., Kent, G. S., and Wright, R. W., 1968: Investigation of the Stratospheric Aerosol by Infrared and Lidar Techniques. J. Geophys. Res. 73, 7553.

338. Elterman, L., Wexler, R., and Chang, D. T., 1969: Features of Tropospheric and Stratospheric Dust. Appl. Optics 8, 893-903.

339. Shahi, G. M., Study of Aerosols in the Atmosphere by Twilight Scattering. Tellus (Uppsala), 22(1): 82-93, 1970.

340. Elterman, L., 1966: Aerosol Measurements in the Troposphere and Stratosphere. Appl. Optics 5, 1769-1776.

341. Blifford, I. H., and Ringer, L. D., 1968: Elemental Composition of Aerosols in the Troposphere. Bull. Am. Meteorol. Soc. 49, 1031.

342. Pötzl, I., 1970: Inorganic Chemical Analyses of Nonpolluted Aerosols Sampled at 1800 Meters Altitutde. J. Geophys. Res. 75, 2347-2352.

343. Rosen, J. E., 1968: Simultaneous Dust and Ozone Soundings over North and Central America. J. Geophys. Res. 73, 479.

344. Kelley, J. J., Jr., 1969: Investigations of Atmospheric Trace Gases and Suspended Particulate Matter on Mount Olympus, Washington. J. Geophys. Res. 74, 435-443.

345. Blifford, I. H., Jr., 1970: Tropospheric Aerosols. J. Geophys. Res. 75(15):3099-3103.

346. Gillette, D., and Blifford, I., Composition of Tropospheric Aerosols as a Function of Altitutde. National Center for Atmospheric Research, to be published.

347. Rosen, J. E., 1969: Possible Identification of Volcanic Dust in the Stratosphere. University of Minnesota, School of Physics and Astronomy, ONR Contract N00014-67-A0113-0004, Rept. No. AP-28.

348. Mossop, S. C., 1964: Volcanic Dust Collected at an Altitude of 20 km. Nature 203, 824.

349. Martell, E. A., 1966: The Size Distribution and Interaction of Radioactive and Natural Aerosols in the Stratosphere. Tellus 18, 486.

350. Rosen, J. E., 1969: Stratospheric Dust and its Relationship to the Meteoric Influx. Space Sci. Rev. (Netherlands) 9, 58-59.

351. Volz, F. E., 1969: Twilights and Stratospheric Dust before and after the Agung Explosion. Appl. Optics 8, 2505.

352. Cadle, R. D., Lazrus, A. L., Pollock, W. H., and Shedlovsky, J. P., 1970: Chemical Composition of Aerosol Particles in the Tropical Stratosphere. Bull. Am. Meteorol. Soc. 51, 298.

353. Cadle, R. D., 1968: Particles in the Stratosphere and Mesosphere. Bull. Am. Meteorol. Soc. 49, 842.

354. Chagnon, C. W., and Junge, C. E., 1961: The Vertical Distribution of Sub-Micron Particles in the Stratosphere. J. Meteorol. 18, 746.

355. Friend, J. P., 1966: Properties of the Stratospheric Aerosol. Tellus 18, 465-473.

356. Grams, G., and Fiocco, G., 1967: Stratospheric Aerosol Layer during 1964 and 1965. J. Geophys. Res. 72, 3523.

357. Junge, C. E., Chagnon, C. W., and Manson, J. E., 1961: Stratospheric Aerosols. J. Meteorol. 18, 81-108.

358. Junge, C. E., and Manson, J. E., 1961: Stratospheric Aerosol Studies. J. Geophys. Res. 66, 2163-2182.

359. Mossop, S. C., 1965: Stratospheric Particles at 20 km Altitude. Geochim. Cosmochim. Acta 29, 201-207.

360. Newkirk, G. A., and Kroenig, J. L., 1965: Aerosols in the Stratosphere: A Comparison of Techniques of Estimating their Concentration. J. Atmos. Sci. 22, 567-570.

361. Pittock, A. B., 1966: A Thin Stable Layer of Anomalous Ozone and Dust Content. J. Atmos. Sci. 23, 538-542.

362. Rosen, J. E., 1964: The Vertical Distribution of Dust to 30 km. J. Geophys. Res. 69, 4673.

363. Volz, F. E., 1970: On Dust in the Tropical and Mid-latitude Stratosphere from Recent Twilight Measurements. J. Geophys. Res. 75, 1641-1646.

364. Bigg, E., Ono, A., and Thompson, W., Aerosols at Altitudes between 20 and 37 km, Tellus. XXII, 550 (1970).

365. Bigg, E. K., Stratospheric Pollution and Volcanic Eruptions. Weather (London) 26(1):13-18, Jan. 1971.

366. Junge, C. E., Recent Investigations in Air Chemistry. Tellus (Uppsala), vol. 8:127-139, May 1956.

367. Jaenicke, R., and Junge, C., Studies of the Upper Size Limit of the Natural Aerosol, Beiträge zur Physik der Atmosphare, 40(1/2):129-143, 1967.

368. Benarie, M. M., About the Validity of the Log-Normal Distribution of Pollutant Concentrations. Preprint, Int'l. Union of Air Pollution Prevention Assoc., 9p., 1970. (Presented at the Int'l. Clean Air Congress, 2nd, Wash., D. C., Dec. 6-11, 1970, Paper SU-18D.)

369. Twomey, S., and Severynse, G. T., 1964: Size Distributions of Natural Aerosols below 0.1 Micron. J. Atmos. Sci. 21, 558.

370. Misaki, Masao, Submicron Aerosol. Shizen (Nature), 25(12):72-74, Dec. 1970.

371. Clark, W. E., and Whitby, K. T., 1967: Concentration and Size Distribution Measurements of Atmospheric Aerosols and a Test of the Theory of Self-preserving Size Distribution. J. Atmos. Sci. 24, 677-687.

372. Friedlander, S. K., and Hidy, G. M., 1969: New Concepts of Aerosol Size Spectrum Theory. In Proc. 7th Int. Conf. Condensation and Ice Nuclei, Prague and Vienna (September), 21-25.

373. Friedlander, S. K., and Wang, C. S., 1966: The Self-preserving Particle Size Distribution for Coagulation by Brownian Motion. J. Coll. Interface Sci. 22, 126-132.

374. Friedlander, S. K., 1965: Theory of Self-preserving Size Distribution in a Coagulating Dispersion. In U.S. Atomic Energy Commission Symp. Ser., Vol. 5, 253-259.

375. Friedlander, S. K., 1962: The Similarity Theory of the Particle Size Distribution of the Atmospheric Aerosol. In Aerosols, Physical Chemistry and Applications, Proc. 1st Int. Conf. Aerosols, Prague (Octgber), 115.

376. Junge, C. E., Clark, W. E., and Whitby, K. T., 1969: Concentration and Size Distribution Measurements of Atmospheric Aerosols and a Test of the Theory of Self-preserving Size Distribution. J. Atmos. Sci. 26, 603-608.

377. Noll, K. E., 1967: A Procedure for Measuring the Size Distribution of Atmospheric Aerosols. The Trend in Engineering 19(2):21. (Quart. J. University of Washington, College of Engineering, Seattle.)

378. Pich, J., Friedlander, S. K., and Lai, F. S., 1970: The Self-preserving Particle Size Distribution for Coagulation by Brownian Motion. III. Smoluchowski Coagulation and Simultaneous Maxwellian Condensation. J. Aerosol. Sci. 1(2), 115-126.

379. Quon, J. E., and Mockros, L. F., 1965: Equilibrium Size Distribution of an Aerosol Continually Reinforced with Particles. Air Water Poll. 9(5); 279-290.

380. Blifford, I. H., and Ringer, L. D., 1969: Size and Number Distribution of Aerosols in the Continental Troposphere. J. Atmos. Sci. 26(4):716-726 (MGA 21.1-566).

381. Clark, W. E., 1966: The Concentration and Size Distribution of Atmospheric Aerosol. M. S. Thesis, University of Minnesota.

382. Friedlander, S. K., and Pasceri, R. E., 1965: Measurements of Particle Size Distribution of the Atmospheric Aerosol. I. Introduction and Experimental Methods. J. Atmos. Sci. 22, 571-576.

383. Gass, M., Saran, and Steierstadt, K., 1965: Das Grössenspektrum des Natürlichen Atmosphärischen Aerosoles. Zeits. Physik 185, 269-277.

384. Meszaros, A. (Nagy), 1965: Size Distribution of Atmospheric Aerosol Particles Captured in a Membrane Filter. Idojaras 69, 71-76.

385. Meszaros, E., 1968: On the Size Distribution of Water Soluble Particles in the Atmosphere. Tellus 20, 443-448.

386. O'Donnell, H., Montgomery, T. L., and Corn, M., 1970: Routine Assessment of the Particle Size-weight Distribution of Urban Aerosols. Atmos. Environ. 4(1):1-7.

387. Pasceri, R. E., and Friedlander, S. K., 1965: Measurement of the Particle Size Distribution of Atmospheric Aerosol. II. Experimental Results and Discussion. J. Atmos. Sci. 22, 577-584.

388. Peterson, C. M., Paulus, H. J., and Foley, G. H., 1969: Number-Size Distribution of Atmospheric Particulates during Temperature Inversion. J. Air Poll. Control Assc. 19, 795-801.

389. Rich, T. A., and Mohnen, V. A., 1969: A Proposed Size Distribution Function for Natural Aerosols. In Proc. 7th Int. Conf. Condensation and Ice Nuclei, Prague-Vienna, (September), J. Podzimek, Ed., Czechoslavak Acad. Sci., Prague, 40.

390. Sarkisov, S. L., Stepanov, G. V., and Khorgani, V. G., 1969: The Size Distribution of Natural Aerosol Particles. Nal'check USSR, Vysokogornyi Geofiz. Inst., Trudy 13, 88-96 (MGA 21.11-373).

391. Twomey, S., and Severynse, G. T., 1963: Measurements of Size Distributions of Natural Aerosols. J. Atmos. Sci. 20, 392.

392. Whitby, K. T., and Liu, B.Y.H., 1969: Atmospheric Aerosol Size Distribution. In Proc. 7th Int. Conf. Condensation and Ice Nuclei, J. Podzimek, Ed., Prague and Vienna (September), Czechoslovak Acad. Sci., 54-55.

393. Noll, K. E. Atmospheric Aerosol Size Distribution, 45th National Colloid Symposium, June 19, 1971.

394. Sholtes, R. S., and Emery, L. H., 1968: Elevated Particulate Distribution in Polluted Atmosphere. Paper 68-108, Air Pollution Control Assn. 61st Annual Mtg. (June), St. Paul, Minn.

395. Noll, K. E. and Pilat, M. J., Size Distribution of Atmospheric Giant Particles, Atmospheric Environment 5,527 (1971).

396. Sekihawa, T., and Kojima, H., 1969: Charged Friction and Charged Equilibrium on the Submicron Aerosol Particles in the Atmosphere. Meteorol. Soc. Japan (Tokyo) J. 47(5):329-334.

397. Lee, R. E., and Goranson, S., The NASN Cascade Impactor Network: First Year Operation. 162nd Nat'l. Mtg. ACS, Sept. 12-17, 1971, Wash., D. C. (84).

398. Whitby, K. T., and Liu, Y. H., Atmospheric Aerosol Size Distributions. Summary of Research. Preprint, Conf. on Methods in Air Pollution and Industrial Hygiene Studies, 11th, Berkeley, Calif., 1970.

399. Waller, P. E., Brooks, A.G.F., and Cartwright, J., An Electron Microscope Study of Particles in Town Air. Intern. J. Air Water Pollution (London), vol. 7:779-786, 1963, 1963.

400. Shalmon, E., 1969: Sizing of Atmospheric Aerosols by Light and Electron Microscopy. In Assessment of Airborne Radioactivity, Proc. Symp. on Instruments and Techniques for the Assessment of Airborne Radioactivity in Nuclear Operations, Vienna (July), Int'l. Atomic Energy Agency, 335-348.

401. Byers, R. L., Davis, J. W., White, E. W., and McMillan, R. E., A Computerized Method for Size Characterization of Atmospheric Aerosols by the Scanning Electron Microscope. Environ. Sci. Technol., 5,517 (1971).

402. Noll, K. E., A Procedure for Measuring the Size Distribution of Atmospheric Aerosols. The Trend in Engr. 19(2):21-7 (Apr. 1967).

403. Horvath, H., 1967: A Comparison of Natural and Urban Aerosol Distributions Measured with the Aerosol Spectrometer. Environ. Sci. Technol. 1(8):651-655.

404. Abel, N., Winkler, P., and Junge, C., 1969: Studies of Size Distribution and Growth with Humidity of Natural Aerosol Particles. I. A sensitive large ion counter for studying size distributions in the atmospheric aerosol particles with radii smaller than 0.1μ. II. Investigation of the composition of atmospheric aerosol particles by measurement of particle growth due to absorption of water vapor and organic vapor. Max. Planck Institut für Chemie, Mainz. AFCRL 69-0205, Final Rept. Contract AF 61(052)-965.

405. Pilat, M. J., and Charlson, R. J., 1966: Theoretical and Optical Studies of Humidity Effects on the Size Distribution of a Hygroscopic Aerosol. J. Rech. Atmos. 4, 165-170.

406. Ahlquist, N. C., and Charlson, R. J., 1968: Measurement of the Vertical and Horizontal Profile of Aerosol Concentrations in Urban Air with the Integrating Nephelometer. Environ. Sci. Technol. 2(5):363-366.

407. Rozenberg, G. V., 1968: Optical Investigations of Atmospheric Aerosols. Soviet Physics Uspekhi 11, 353-380.

408. Penndorf, R., 1954: The Vertical Distribution of Mie Particles in the Troposphere. Geophys. Res. Papers, No. 25, U. S. Air Force.

409. Quenzel, H., 1970: Determination of Size Distribution of Atmospheric Aerosol Pargicles from Spectral Solar Radiation Measurements. J. Geophys. Res. 75, 2915-2921.

410. Volz, F. E., Atmospheric Turbidity after the Agung Eruption of 1963 and Size Distribution of the Volcanic Aerosol. J. Geophys. Res. 75(27):5185-5193, Sept. 20, 1970.

411. Gladney, E. W., Zoller, W. H., and Gordon, G. E., Size Fractionation of Trace Elements on Urban Aerosols. 161st Nat'l. Mtg. ACS, March 28, 1971, Los Angeles, Calif.

412. Lundgren, D. A., Atmospheric Aerosol Composition and Concentration as a Function of Particle Size and of Time. J. Air Pollution Assoc., 20(9):603-608, Sept. 1970.

413. Lee, Jr., R. E., Patterson, R. K., and Wagman, J., Particle-size Distribution of Metal Components in Urban Air. Environ. Sci. and Technol., v. 2:288-290, Apr. 1968.

414. Nifong, G. D., Winchester, J. W., and Boettner, E. A., 1970: Particle Size Distribution of Trace Metals in Aerosols from Northwest Indiana. Bull. Am. Meteorol. Soc. 51, 1010.

415. Nifong, G. D., Particle Size Distributions of Trace Elements in Pollution Aerosols. Michigan Univ., Ann Arbor, Dept. of Meteorology and Oceanography, AEC Contract AT(11-1)-1705, ORA Proj. 08903, 263 p., Aug. 1970.

416. Nifong, G. D., Boettner, E. A., and Winchester, J. W., Particle Size Distribution of Trace Elements in Pollution Aerosols. Amer. Ind. Hyg. 32,51 (1971).

417. Rahn, K. Wesolowski, J., John, W., and Ralston, H., Diurnal Variation of Aerosol Trace Element Concentrations in Livermore, California. J. Air Pollution Control Assoc., 21,406 (1971).

418. Rahn, K. A., Dams, R., Robbins, J. A., and Winchester, J. W., Diurnal Variations of Aerosol Trace Element Concentrations as Determined by Nondestructive Neutron Activation Analysis. In: I. Occurrence of Halogens in Atmospheric Aerosols and Precipitation. II. Air Pollution Inputs of Trace Metals to Lake Michigan Water. Michigan Univ., Ann Arbor, Dept. of Meteorology and Oceanography, and Michigan Univ. Ann Arbor Great Lakes Research Div., AEC Contract AT(11-1)-1705, ORA Proj. 08903, PR-3, May 1970.

419. Friedlander, S. K., Characterization of Aerosols Distributed with Respect to Size and Chemical Composition. J. Aerosol Sci. 1(4), 295-307, 1970.

420. Lee, R. E., Patterson, R. K., Crider, W. L., and Wagman, J., Concentration and Particle-Size Distribution of Particulate Emissions in Automobile Exhaust. Atmos. Environment 5,225(1971).

421. Stockham, J. D., and Betz, H., Study of Visible Exhaust Smoke from Aircraft Jet Engines. National Air Transportation Meeting, Atlanta, Ga., May 10-13, (1971).

422. Robinson, E., and Ludwig, F. L., Particle Size Distribution of Urban Lead Aerosols. J. Air Poll. Control Assoc., 17,664 (1967).

423. Meszaros, E., 1970: Seasonal and Diurnal Variations of the Size Distributions of Atmospheric Sulfate Particles. Tellus 22, 235-238.

424. Ludwig, F. L., and Robinson, E., 1968: Variations in the Size Distributions of Sulfur-containing Aerosols. Atmos. Environ. 2, 13-24.

425. Meszaros, E., 1969: Size Distribution of Nitrate and Soluble Calcium Particles. Ann. Meteorol. 4, 132-133.

426. Lee, R. E., Jr., and Patterson, R. K., 1969: Size Determination of Atmospheric Phosphate, Nitrate, Chloride and Ammonium Particulate in Several Urban Areas. Atmos. Environ. 3,257-280.

427. Hoidale, G. B., and Blanco, A. J., 1968: Infrared Spectroscopic View of the Nature of Giant and Large Particle Atmospheric Dust. J. Rech. Atmos. 4, 293-299.

428. Efendi-zade, M. M., and Shteyngart, B. M., Precipitating Aerosols in the Air of the City of Baku and their Sanitary-Hygienic Significance. Azerb. Med. Zb., no. 1:67-71, 1955.

429. Laudien, K., Size Distribution and Concentration of Aerosols in the Atmosphere and in Closed Volumes. Z. Phys. Chem. (Leipzig) 247(1-2), 60-4, 1971.

430. Asakuno, Kunihiko, Inokushi, Y., Yamamoto, T., Shinozaki, Y., and Odaira, T., Studies on Size Spectra of Particulate Pollutants. Taiki Osen Kenkyu (J. Japan Soc. Air Pollution), 5(1):212, 1970. (Proceedings of the Japan Society of Air Pollution, Annual Meeting, 11th, 1970).

431. Asakuno, K., Yamazaki, H., Inokoshi, Y., and Yamamoto, T., Analysis of Sub-micron Particles in Air Pollution at Tokyo Tower. Tokyo-to Kogai Kenkyusho-ho (Ann. Rept. Tokyo Metropol. Res. Inst. Environ. Protection), Sect. 1:132-135, Jan. 1970.

432. Bignardi, L., and Mastrolelli, M., 1970: About the Smoke Emission of Heating Plants. Termotecnica (Milan) 24(2):99-104.

433. Zavodsky, D., 1957: Study of the Atmospheric Aerosol Concentration on the Ground Layer in Bratislava-Koliba. Meteorologicke Zpravy 20(5):128-130.

434. Antal, S., 1969: Distribution of Large and Giant Atmospheric Aerosol Particles over Hungary. Időjaras 73(2):92-98.

435. Keresz-Saringer, M., Meszaros, E., and Varkonyi, T., Size Distribution of Benzo(a)pyrene Containing Particles in Urban Air. Atmos. Environ. 5(6):429-31, 1971.

436. Hoidale, G. B., and Smith, S. M., 1968: Analysis of Giant Particle Component of the Atmosphere over an Interior Desert Basin. Tellus 20, 251-268.

437. Blifford, I. H., and Ringer, L. D., 1968: Size and Number Distribution of Tropospheric Aerosols over the Oceans. Trans. Am. Geophys. Union 49, 690.

438. Duce, R. A., Woodcock, A. H., and Moyers, J. L., 1967: Variations of Ion Ratios with Size Among Particles in Tropical Oceanic Air. Tellus 19, 369-379.

439. Carder, K. L., Beardsley, G. F., and Pak, H., Particle-size Distributions in Eastern Equatorial Pacific. J. Geophysical Res. 76,5070 (1971).

440. Hamilton, W. L., 1968: Change in the Size Distribution of Dust Falling in Polar Regions over the Past Fourteen Centuries. Polarforschung 36(1/2), 107-112.

441. Hamilton, W. L., Microparticle Deposition on Polar Ice Sheets. Ohio State Univ., Columbus, Inst. of Polar Studies, NSF Grant GA 530, Rept. 29, RF 2262, 77 p., May 1969.

442. Rosen, J. E., 1969: The Vertical Distribution of Particulate Material near the Surface of the Earth. J. Air Poll. Control Assn. 19, 106-108.

443. Carnuth, W., 1970: Aerosol Size Distribution at 700-, 1800- and 3000-meter Altitudes. J. Geophys. Res. 75, 2999-3005.

4444. Ivlev, L. S., Bursakova, N. S., and Surikov, O. M., Measuring the Ground-layer Distribution of Atmospheric Aerosol. Probl. Fiz. Atmo. No. 6:77-78, 1968.

445. Junge, C., and McLarien, E., Relationship of Cloud Nuclei Spectra to Aerosol Size Distribution and Composition. J. Atmospheric Sci., 28, 382 (1971).

446. Andreev, B. G., 1967: Regularities of Vertical Distribution of Very Small Atmospheric Particles in the Atmospheric Boundary Layer. Izv. Atm. Oceanic Phys. 3(9):571-576.

447. deBary, E., and Rössler, F., 1966: Size Distributions of Atmospheric Aerosols Derived from Scattered Radiation Measurements Aloft. J. Geophys. Res. 71, 1011.

448. Biswas, K. R., Paul, S. K., and Murthy, Bh. V., 1968: Giant Size Aerosols in Lower Troposphere. Proc. Int. Conf. Cloud Physics, Toronto (August), 50-56.

449. Borovikov, A. M., Mazin, I. P., and Nevzarov, A. N., 1965: Some Properties of the Distribution of Large Particles in Various Clouds. Izv. Atm. Oceanic Phys. (1(15):291-301.

450. Bunakova, A. M., and Ivlev, L. S., 1967: Vertical Distribution of Aerosol, and Aerosol Layers in the Atmosphere. Probl. Fiz. Atm. (Leningrad) 5, 206-214.

451. Carnuth, W., and Reiter, R., 1966: Simultaneous Measurements of the Aerosol Particle Size Spectra at 700, 1800 and 3000 m. above Sea Level. J. Rech. Atmos. 2, 261.

452. Fenn, R. W. Gerber, H. R., and Weickmann, H. K., 1965: Distribution of Aerosol Particles in the Troposphere. In Proc. Int. Conf. Cloud Physics, Tokyo and Sapporo (May-June), Tokyo, 62-66.

453. Kondrat'yev, K. Ya., Badinov, I. Ya., Ivlev, L. S., and Nikol'shy, G. A., 1969: Aerosol Structure of the Troposphere and Stratosphere. Izv. Atm. Oceanic Phys. 5, 270-276.

454. Melton, C. E., 1967: Aerosol Samples Obtained from 9- to 12-km Altitude. Smithsonian Contrib. Astrophys. 11, NASA Spec. Publ. 135, 293-299.

455. Meszaros, E., 1969: Vertical Profile of Large and Giant Particles in the Lower Troposphere. 7th Int. Conf. Condensation and Ice Nuclei, Prague and Vienna (September), Abstracts, 32.

456. Mikirov, A. E., 1967: Average Size of Particles at the 70-450 km Height. Geomag. Aeronomiia 7, 748-750; English transl. in Geomag. and Aeron. (MGA 19.2-140).

457. Mikirov, A. E., 1967: Mean Particle Sizes at 70-450 km heights. In Space Research, Vol. 7, Proc. 7th Int. Space Science Symposium, Vienna (May 1966) (MGA 18.11-226).

458. Rieter, R., Carnuth, W., and Sladkovic, R., 1968: Effects of Atmospheric Fine Structure Characteristics on the Vertical Distribution of Aerosols. Arch. Meteorol. Geophys. Biokl., Serv. A., 17(4), 336-365.

459. Rieter, R., 1968: Atmospheric Aersols between 700 and 3000 m above Sea Level: (2) A Study of the Effects of Atmospheric Fine Structure Characteristics on the Vertical Distribution of Aerosols. Fraunhofer-Gesellschaft zur Förderung der Angewandten Forschung EV, Physikalisch-Bioklimatische Forchungsstelle, Garmisch-Partenkirchen, Final Tech. Rept., Contract DA-JA-37-67C-0254, 43 pp.

460. Rieter, R., and Jaffe, A., 1967: Atmospheric Aerosols between 700 and 3000 m above Sea Level: A Study of the Effects of Atmospheric Fine Structure Characteristics on the Vertical Distribution of Aerosols. Fraunhofer-Gellelschaft zur Förderung der Angewandten Forschung EV, Physikalisch-Bioklimatische Forschungsstelle, Garmisch-Partenkirchen, Final Tech. Rept., Contract DA-91-EUC-3936.

461. Rössler, F., 1967: The Aerosol Layer in the Stratosphere. In Proc. 10th Committee on Space Research (COSPAR), A. Mitra et al., Eds, London, 633-636.

462. Unz, F., 1969: Konzentration des Aerosols in Troposphäre und Stratosphäre aus Messungen der Polarisation der Himmelstrahlung im Zenit. Beitr. Phys. Atmos. 42, 1-35.

463. Volz, F. E., 1969: Stratospheric Dust Striations. Bull. Am. Meteorol. Soc. 50, 16.

464. Makhon'ko, K. P., Character of the Spectrum of Natural Radioactive Dust Particles. Akademiia Nauk SSSR, Izvestiia, Ser. Geofiz., No. 1:183-187, Jan. 1963.

465. Ernst, F., Preining, O., and Sedlacek, M., Sizing of the Fall-out at Vienna. Nature, London, 195(4845): 986-987, Sept. 8, 1962.

466. Junge, C. E., and Chagnon, C. W., The Size Distribution of Radioactive Aerosols in the Upper Troposphere, J. Applied Meteorology, 4,329 (1965).

467. Vitton, O., Size Distribution of Airborne Magnetic "Black Spherubs" in the 1-5μ Range. J. Geophys. Res., 75, 371 (1970).

468. Nagamoto, C., and Rosinski, J., Size Distribution of Magnetic Spheroids, to be published in J Atmospheric Terrestrial Physics, late 1971.

469. Corn, M., Stein, F., and Esmen, N., The Shape of Atmospheric Particles. (Progress Report). Pittsburgh Univ., Pa., Dept. of Occupational Health, Research Grant AP 00431-04, Rept. 6, March 1, 1969.

470. Corn, M., Stein, F., and Esmen, N., The Shape of Atmospheric Particles. Univ. of Pittsburgh, Pa., Dept. of Occupational Health, Progress Report Apr. 1, 1966-Aug. 30, 1967, Nov. 1, 1967.

471. Corn, M., Montgomery, T. L., and Esmen, N. A., Suspended Particulate Matter: Seasonal Variation in Specific Surface Areas and Densities. Environ. Sci. Technol. 5, 155 (1971).

472. Stein, F., Esmen, N. A., and Corn, M., 1969: The Shape of Atmospheric Particles in the Pittsburgh Air. Atmos. Environ. 3, 443-453.

ADHESION OF ATMOSPHERIC PARTICLES

473. Krupp, H., Particle Adhesion Theory and Experiment Advances in Colloid and Interface Science, Edition 1, pp. 111, J. Wiley & Son 1967.

474. Salomon, V. J., and Houwink, A. D., Adhesion and Adhesives Vol. 1 & 2, 1967.

475. Zimon, A. D., Adhesion of Dust and Powder, Plenum Press 1969.

476. Voyutskii, R., Reference 27, 28 Quoted by Salomon and Houwink (474).

477. Orr, C., Particulate Technology, MacMillan Press 1966.

478. Krupp, H., Adhesion of Small Gold Particles to Solid Substrates Immersed in Water and in Aqueous Solution of Surfactants and of Alkaline Salts. J. Colloid and Int. Sci. 24 (1):170 1968.

479. Newett, D. M., and Conway Jones, J. M., Contribution to the Theory of Granulation, Trans. Inst. Chem. Eng. 36 422 1958.

480. Billings, C. E., and Wilder, J., Handbook of Filter Technology Vol. 1, Fabric Filter System Study. Contract CPA-22-69-38 Prepared for NAPCA 1970.

481. Oweberg, T. G., et. al, Investigation of the Force of Adhesion between Powder Particles, Aerojet Corp. Contract DA-18-108-405-CML-829 March 1963.

482. Deryaguin, B. V., Zimon, A. D., and Kollord, Z., 23 454 1961.

483. Penney, G. W., and Klinger, E. H., AIEE Paper CP6/184 1961.

484. Donald, D. L., Electrostatic Contribution to Powder Particle Adhesion, J. Appl. Phys. 40 3013 1969.

485. Kunkel, W. B., J. Appl. Phys. 21 820 1950.

486. Kunkel, W. B., J. Appl. Phys. 21 833 1950.

487. Orr, C., Burson, J., and Linoya, K., Nature 200, 360 1963.

488. Morgan, B. B., Brit. Coal Util. Res. Assoc. Monthly Bull. 25, 125, 1961.

489. Priesing, C. P., Ind. Eng. Chem. 54, 38, 1962.

490. Rumpf, F. H., "Agglomeration" in "Strength of Granules and Agglomerates in W. A. Knepper, J. Wiley & Son 1962.

491. Zimon, A. D., and Koll, Z., 25, 317, 1963.

492. Kordecki, M. C., and Orr, C., Am. Med. Assoc. Archives Ind. Health 1 (1) 1960.

493. Corn, M., Adhesion of Particles, Aerosol Science, Acad. Press, 1966.

494. Meldau, R., Handbuch der Staubtechnik 1 Dusseldorf, 1956.

495. Renmuth, H., Staub 22 (8) 301, 1962.

496. Nishivaki, V., Atomic Sci. (4), 279, 1955.

497. Zimon, A. D., Volkova, T. S., and Kollord, Z., 27 (3) 365, 1965.

498. Bohme, G., et al., Z Angew. Phys. 16 (6) 486, 1964.

499. Corn, M., J. Air Poll. Control Assoc. 11, 523, 1961.

500. Corn, M., J. Air Poll. Control Assoc. 11, 566, 1961.

501. Akhmatov, A. S., Res. on Surface Forces Izd. Acad. Nauk, 1961.

502. Akhmatov, A. S., Molecular Physics of Boundary Friction, 1963.

503. Fuks, G. I., Study and Classification of the Effectiveness of Gas Flame Treatment, N.I.I.Ch.A.SPROM, 1963.

504. Deryaguin, B. V., Zimon, A. D., Koll, Z. 23, 544 1961.

505. Stone, W., Phil. Mag. 9 (58) 610, 1930.

506. McFarlane, J., and Tabor, D., Proc. Roy. Soc. A220 (1069) 224, 1950.

507. Bradley, R. S., Phil. Mag. 13 (86) 853, 1932.

508. Bradley, R. S., Trans. Farad. Soc. 32 (8) 1088, 1936.

509. Howe, P. L., et al., Can. J. Chem. 33 (9) 1375 (1955).

510. Malkina, A. D., and Koll, A., 12(6) 431, 1950.

511. Zimon, A. D. and Petunin, Y. P., Lakokrasochye Materialy i ikh Primenenie No. 2, 63, 1963.

512. Zimon, A. D., Deryaguin, B. V., and Kollard, Z., 25 (2) 159, 1963.

513. Fuks, G. I., et al., Doklady Akad. Nauk SSSR 65(3) 307, 1959.

514. Fuks, G. I., Scientific Report Dl Mendeleev Chem. Soc. No. 3, 33, 1949.

515. Buzagh, A., Ann. Univ. Sci. Budapest., Sect. Chim., 1:32 (1959).

516.- Buzagh, Koll.-Z., 47:370 (1929); 51:105, 230 (1950);
520. 52:46 (1939); 53:294 (1939); 79:1956 (1937).

521. Buzagh, A., and Szabo, Z., Koll.-Z., 83:139 (1938).

522. Buzagh, A., and Dux., K., Koll.-Z., 84-279 (1938).

523. Buzagh, A. Koll.-Z., 85:329 (1938).

524. Buzagh, A., and Zimmerman, J., Koll.-Z., 84:15 (1938).

525. Buzagh, A., Acta Chim. Hung., 1:181 (1950).

526. Buzagh, A., Koll.-Z., 125:14 (1951).

527. Fuks, G. I., and Klychnikov, V. M., Transactions of the All-Union Scientific-Research Institute of Fertilizers, Agricultural Technology, and Soil Science (VIUAA), No. 28 (1948), p. 215: (1949), pp. 186, 215.

528. Zimon, A. D., and Kishin, N. G., Kolloidn. Zh., 27(5):685 (1965).

529. Fuks, G. I., and Tsyganova, E. V., Collections of Papers on Oil Technology, No. 1.

530. Taylor, A., and Wood, F., Trans. Faraday Soc. 53(4) 523, 1956.

531. Fuks, G. I., and Kaverina, N. I., Kolloidn. Zh., 21(6):718 (1959).

532. Kirk, P. L. (1951), Quantitative Ultramiscroscopy, Ch. 4. John Wiley, New York.

533. Cahn, L., and Schultz, H. R. (1962), Vacuum Microbalance Techniques, Vol. 2, pp. 7-18. Plenum Press, New York.

534. Hamaker, H. C. (1937), Physica, 4, 1058.

535. Bradley, R. S. (1936), Trans. Faraday Soc. 32, 1088.

536. Stone, W. (1930), Phil. Mag. 9, 610.

537. Tomlinson, G. A. (1928), Phil. Mag. 6, 695.

538. Tomlinson, G. A. (1930), Phil. Mag. 10, 541.

539. Overbeek, J. Th. G., and Sparnaay, M. (1954), Discuss. Faraday Soc. 18, 12.

540. Deryagin, B. V., Abriksova, I. I., and Lifshitz, E. M. (1956), Quart. Rev. Chem. Soc. 10, 295.

541. Tekenev, Zh., Interaction of Dust Particles from an Air Flow with the Surface of an Obstacle, Master's Thesis, Tashkent (1962).

542. Tekenov Zh. and Mazitov, B., in collection: Some Questions of Applied Physics, Izd. Akad. Nauk UzSSR, Tashkent (1961), p. 11.

543. Corn, M., J. Air Pollution Control Assoc., 11 (11:523 (1961); 11(12):566, 584 (1961).

544. McFarlane, J., and Tabor, D., Proc. Roy. Soc., A220(1069):224 (1950).

545. Beischer, D., Kolloid-Z., 89(2):214(1939).

546. Schubert, H., and Wibowo, W., Chemie Ingeneu-Technik, 42 (8) 541, 1970.

547. Cremer, E., Conrad, F., and Kraus, Th. Angew Chem., 64(1):10 (1952).

548. Batel, W., Chim.-Ingr.-Tech., 31(5):343 (1959).

549. Patat, F., and Schmid, W., Chem. Ind. Techn., 32(1): 8 (1960).

550. Zimon, A. D., Kolloidn. Zh., 24(4):459 (1962).

551. Pecht, H., Chem.-Ingr.-Tech., 33(10):691 (1961).

552. Moses, S., Ind. Eng. Chem., 41:2339 (1949).

553. Larsen, R. I., Am. Ind. Hyg. Assoc. J., 19(4):265 (1958).

554. Zimon, A. D., Dovnar, N. I., Belkina, G. A., and Nozdrina, G. V., in collection: Research on Surface Forces, Izd. "Nauka" (1964), p. 330.

555. Deryagin, B. V., Toporov, Yu. P., Tomfel'd, I. N., Aleinikova, I. N., and Parfanovich, B. N., Lakokrasochnye Materialy i ikh Primenenie, No. 4:62 (1964).

556. Kordecki, M. C., Gladden, J. K., and Orr, C., Jr., Adhesion between Solid Particles and Solid Surfaces, Final Report Proj. No. B-148, Engineering Experiment Station, Georgia Institute of Technology, Atlanta, Ga., 1959.

557. Böhme, G., Krupp, H., Rabenhorst, H., and Sandstede, G., Trans. Inst. Chem. Eng., London, 40, 252, 1962.

558. Böhme, G., Kling, W., Krupp, H., Lange, Sandstede, G., and Walter, G., Preprint, Intern. Congr. Surface Activity, 4th Brussels, 1964, paper B/III.16.

559. Bohme, G., et. al., Z. Angew, Phys., 16, 486, 1968, through Chem. Abstr., 63, 2423C, 1965.

560. Böhme, G., et. al., Angew. Phys., 19, 265, 1965;
and through Phys. Abstr., 69, 48, 1966.
561.

562. Krupp, H., and Angew, Z., Phys., 19, 259, 1965;
and through Phys. Abstr., 69, 4832, 1966.
563.

564. Deryagin, B. V., Toporov, Yu. P., and Aleinikov, I. N., ibid., 26, 335, 1964.

565. Fuks, N. A., Mechanics of Aerosols, CWL Spec. Pub. 4-12, 1955.

566. Bagnold, R. A., Physics of Blown Sand and Desert Dunes, Methuen, London, 1941.

567. Bagnold, R. A., The Flow of Chohesionless Grains and Fluids. Phil. Trans. A249, 235, 1956.

568. Bagnold, R. A., The Re-entrainment of Settled Dusts. Int. J. Air Poll. 2, 357, 1960.

569. Davies, C. N., Aylward, M., and Leacey, D., Impingement of Dust from Air Jets. AMA Arch. Ind. Hyg. and Occ. Med. 4, 354, 1951.

570. Jordan, D. W., The Adhesion of Dust Particles. Brit. J. Appl. Phys. 3, S194, 1954.

571. Corn, M., The Adhesion of Solid Particles to Solid Surfaces, I and II. J. Air Pollut. Control Assoc. 11, 523, 566, 1961.

572. Corn, M., and Stein, F., Re-entrainment of Particles from a Plane Surface. Amer. Ind. Hyg. Assoc. J. 26, 325, 1965.

573. Larsen, R. I., The Adhesion and Removal of Particles Attached to Air Filter Surfaces. Amer. Ind. Hyg. Assoc. J. 19, 265, 1958.

574. Orr, C., Jr., and Dallavalle, J. M. (1956). Studies and Investigations of Agglomeration and Deagglomeration of Solid Particles. Semifinal Report, Project A-233, Georgia Institute of Technology, Engineering Experiment Station, Atlanta.

575. Corn, M., and Silverman, L. (1961), Amer. Ind. Hyg. Assoc. J. 25, 337.

576. Gutterman, B., and Ranz, W. E. (1959), Proc. A.S.C.E., J. San. Eng. Div. SA4, 25.

577. Zenz, F. A. (1964), I.E.C. Fundamentals, 3, 65.

578. Walker, R. L., and Fish, B. R., Proc. Sym. of Surface Contaminants, 61, 1964.

579. Masironi, L. A., and Fish, B. R., Proc. Sym. of Surface Contaminants, 61, 1964.

580. Fish, B. R., et al., Proc. Sym. of Surface Contaminants, 61, 1964.

581. Stewart, K., Proc. Sym. of Surface Contaminants, 61, 1964.

582. Corn, M., and Stein, F., Nature 211, 60, 1966.

583. Fuks, N. A., and Sutugin, A. G., Generation and Use of Monodisperse Aerosols Given in"Aerosol Science," C. N. Davies, Acad. Press, 1966.

584. Billings, C. E., Silverman, L. Dennis, R., and Levenbaum, I. H., Shock Wave Cleaning of Air Filters, J. Air Pollut. Control Assoc. 10, 318, 1960.

585. Jacobs, M. B., Monoharan, A., and Goldwater, L. J., Int. J. Air and Water Pollution 6, 205 1962.

586. Girrard, J. H., An Experimental Investigation of the Initial Stages of the Dispersion of Dust by Shock Waves, Brit. J. Appl. Phys. 14, 186, 1963.

587. Egorov, P. A., Kolloid Zhumal 30 (3) 363, 1968.

588. Bergmann, L, Ultrasonics (Russian translation), Izd-vo Inostr. Lit. (1956).

589. Sollner, K., In: Colloid Chemistry (ed. by J. A. Alexander), Vol. 5 (1944), p. 337.

590. Kruyt, H. R., Colloid Science (Russian translation), Izd-vo Inostr. Lit. (1955).

591. Tojoshima, Y., Kogyo Esui, 39 (1961).

592. Sasaki, N., Om Denki Zasshi, 47, 75 (1960).

593. Sasaki, Tanken, 10, 161 (1959).

594. Soboleva, N. I., Bol'shakov, A. G., and Kortnev, A. V., Kolloidn. Zh., 20, 742 (1958).

595. Deryagin, B. V., Proceedings of the Third All-Union Conference on Colloid Chemistry (in Russian), Izd-vo AN SSSR (1956), p. 235.

596. Deryagin, B. V., Kolloidn. Zh., 23, 361 (1961).

597. Voyutskii, S. S., Kolloidn. Zh., 23, 353 (1961).

598. Agabal'yants, E. G., et al, Dopov. Akad. Nauk Ukr. RSP. Ser. B. 32 (9) 813, 1970.

599. Lowe, L. E., and Parasher, C. D., Can. J. Soil Sci. 51(1) 136, 1971.

600. Pupynin, V. P., et al., Zhunal Met. Abst. 11G403, 1969.

601. Piotrows, A., Propagation of Ultrasonic Waves in Suspensions and Emulsions. I. Investigation of Emulstions and Pigment Suspensions by an Acoustic Method. Ultrasonics, 9, 14, 71, 13R, N1, I1188.

602. Allegra, J. R., Attenuation of Sound in Suspensions of Solid Particles, 8 Am. Phys. S. 16, 186, 71, M iR N2, 13979.

603. Allegra, J. R., Hawley, S. A., and Holton, G., Propagation of Ultrasound in Suspensions and Emulsions. 8 Am. Phys. S 15, 98, 70, M, 3R, N1 F1692.

604. Rozanski, W., Frydrych, J., Kusinski, and Klosowska, B., Use of Ultrasound for Dispersing Powder Suspensions, Pol. Akad., Nauk-Oddzial Krakowie, Pr. Kom. Met. - Odlew., Met., pp. 85-98, 1969.

605. Kruglitskii, V., et al., Ukr. Khim. Zh 32(9), 971, 1966.

606. Kul'skii, L. A., et al., Fiz. Khim. Mekh. Liohe'nost. Dispersinikk Sist. 291, 1968.

607. Joung, U. S., Chosun. Kwahakwan Tongbo, 5, 24, 1966.

608. Parfitt, G. D., Dispersion of Powders in Liquids, Elsevier, 1969.

609. Patterson, J. K., Ph.D. Thesis, Purdue Univ., 1953.

610. Cozzens, S. L., NPIRI Project Report 44, Lehigh Univ., 1960.

611. Guggenheim, S., Official Digest, 30 (402), 729, 1958.

612. Wade, W. G., and Taylor, B. A., Paint Manuf. 30, 355, 1960.

613. Ensminger, R. I., Official Digest 71, Jan. 1963.

614. Dowling, D. G., J. Oil & Col. Chem. Assoc., 44, 188, 1961.

615. Schlieser, R. H., et al., Official Digest 265, March 1962.

616. Armstrong, W. G., J. Paint Tech., 41 (530) 179, 1969.

617. Weisberg, H. E., Official Digest, 1261, Nov. 1964.

618. Daniel, F. R., J. Oil Col. Chem. Assoc. 54 84, 1971.

619. Daniels, F. K., Natl. Paint Varnish Laquer Assoc. Sci. Sect. Circ. 744 (1950).

620. Shurts, R. B., Natl. Paint Varnish Laquer Assoc. Sci. Sect. Cir. 745 (1950).

621. Fischer, E. K. Colloidal Dispersions, J. Wiley & Son, N. Y., 1950.

622. Bosse, D. G., Official Digest, 30 (398), 251, 1958.

623. Brownlie, G., J. Oil & Col. Chem. Assoc. 43, 1960.

624. Garrett, M. D., and Hess, W. M., J. Paint Tech. 40 (524), 367, 1968.

625. Vavra, J., (FR) Efficiency of Dispersion in a Ball-Mill. Chim. Ind. GC 103 358 70 NO R N3 F5668.

626. Smith, A. L., Proc. Sym. on Adhesion, Karlsruhe, 1969.

627. Lygin, V. I., Kovaleva, N. V., Kavtaradze, N. N. and Kiselev, A. V., Kolloidn. Zh., 22(3):334(1960).

628. Kiselev, A. V., Korolev, A. Ya., Petrova, R. S., and Shcherbakova, K. D., Kolloidn. Zh., 22(6):671 (1960).

629. Babkin, I. Yu. Kiselev, A. V., and Korolev, A. Ya., Dokl. Akad. Nauk SSSR, 136(2):373 (1961).

630. Vinogradova, L. M., and Korolev, A. Ya., Fifth All-Union Conference on Colloid Chemistry, Summaries of Contributions, Izd. Akad. Nauk SSSR (1962), p. 82.

631. Korolev, A. Ya., in collection: Glues and Glue Technology, Oborongiz (1962), p. 35.

632. Korolev, A. Ya., Davydov, P. V., and Vinogradova, A. M., in collection: Adhesion of Polymers, Izd. Akad. Nauk SSSR (1963), p. 3.

633. Vinogradova, L. M., Korolev, A. Ya., Davydov, P. V., and Kuchenkova, R. V., Ibid., p. 137.

634. Baibakov, A. Z., Bulletin of Scientific and Technical Information on Agricultural Physics, No. 3, 4, Agrofizicheskii NII (1957).

635. Jordan, D. W., Brit. J. Appl. Phys., Suppl. No. 3:194 (1954).

636. Andrianov, K. A., Deryagin, B. V., Zakhavaeva, N. N., Sobolevskii, M. V., and Talaev, M. V., Zh. Prikl. Khim., 32(12):2682 (1959).

637. Voronkov, M. G., and Dolgov, B. N., Priroda, No. 5:22 (1954).

638. and 639. Krotova, N. A., and Morozova, L. P., in collection: Research on Surface Forces, Izd. Akad. Nauk SSSR (1961), p. 83; Kolloidn. Zh., 24(4):473 (1962).

640. Campbell, D.S.E., Cathcart, D., and Giles, C. H., J. Soc. Dyers & Colorists, 73, 546, 1957.

641. Long, J. S. et al., Official Digest, 11, Jan. 1963.

642. Schwitzer, M. K., Official Digest 33, 1111, 1961.

643. Trudgian, L., Prihoda, H., Official Digest, 1211, Nov. 1963.

644. Burrell, H., Official Digest, 726, Oct. 1955.

645. Lieberman, E. P., Official Digest, 30 Jan. 1962.

646. Gardon, J., J. Paint Tech., 38 (492) 43, 1966.

647. Crowley, J. D., Teague, G. S., and Lowe, J. W., J. Paint Tech., 38 (496) 269, 1966.

648. Crowley, J. D., Teague, G. S., and Lowe, J. W., J. Paint Tech., 39 (504) 19, 1967.

649. Hansen, C. M., J. Paint Tech., 39 (505) 104, 1967.

650. Hansen, C. M., J. Paint Tech., 39 (511) 505, 1967.

651. Burrell, H. J. Paint Tech., 40 (520) 197, 1968.

652. Rheinbeck, A. E., and Lin, K. F., J. Paint Tech., 40 (527) 611, 1968.

653. Hoy, K. L., J. Paint Tech., 42 (541) 76, 1970.

654. Lee, L. H., J. Paint Tech. 42 (545), 365, 1970.

655. Eissler, R. L., Zgol, R., and Stolp, J. A., J. Paint Tech. 42 (548), 483, 1970.

656. Pimental, McClellan, "The Hydrogen Bond," Reinhold, N.Y., 1960.

657. Every, R. L., Wade, W. H., and Hackerman, N., J. Phys. Chem., 65 937, 1971.

658. Wade, W. H., and Hackerman, N., J. Phys. Chem., 66, 1823, 1962.

659. Wade, W. H., and Hackerman, N., J. Phys. Chem., 65, 1681, 1961.

660. Parfitt, G. D., and Wilshire, I. J., J. Pnys. Chem., 12, 3545, 1964.

661. Day, R. E., and Parfitt, G. D., J. Phys. Chem. 71, 3073, 1967.

662. Day, R. E., and Parfitt, G. D., J. Phys. Chem., 71, 815, 1967.

663. Sherwood, A. F., and Rybicka, S. M., J. Oil & Col. Chem. Assn., 49, 648, 1966.

664. Livanova, N. M., et al, Kolloid Zhurnal, 31 (6) 875, 1969.

665. Masaji, M., et al, J. Sci. Hiroshima Univ. Ser A-II, 30, 57, 1966.

666. Krupskii, N. I., et al., Ionites and Ion Exchange, Nauka 139, 1966.

667. Ermolaeva, T. A., et al., Lakokrasochnye Materialy i Ikh, Primenerie, (3), 14, 1964.

668. Dickman, S. R., et al., Soil Science, 52, 263, 1941.

669. Kelley, J. B., et al, Soil Science, 55, 167, 1943.

670. Vissers, D. R., J. Phys. Chem., 72(9) 3236, 1968.

671. Low, M.J.D., and Ramamurthy, P., J. Phys. Chem., 72 (9), 3161, 1968.

672. Bellamy, G., Infra Red Spectra of Complex Molecules, p. 319, J. Wiley & Son, N. Y., 1960.

673. Wade, W. H. and Hackerman, N., J. Phys. Chem., 64, 1196, 1960.

674. Greenler, S., J. Chem. Phys., 37, 2094, 1962.

675. Ono, Y., and Keii, T., J. Phys. Chem., 72 (8), 2851, 1968.

676. Hasagawa, M., and Low, M.J.D., J. Coll. & Int. Sci., 30 (3), 378, 1969.

677. O'Connor, et al., Trans. Farad Soc., 178, 1113, 1956.

678. Giles, C. H., et al, J. Appl. Chem., 9, 457, 1959.

679. Somasunderan, P., and Fuerstenau, D. W., J. Phys. Chem. 70, 90, 1966.

680. Bakker, W. T., and Bartok, D., Am. Ceram. Soc. Bull., 45 (6) 582, 1966.

681. Peri, J. B., J. Phys. Chem., 72 (8), 2917, 1968.

682. Tokiwa, F., and Imamura, T., J. Am. Oil Chem. Assn., 46, 572, 1969.

683. Smith, I. T., Nature 201 (4914) 67, 1964.

684. Padday, J. F., and Russell, D. R., J. Coll. Sci., 15, 503, 1960.

685. Drost-Hansen, W., Chem. & Phys. of Interfaces, Am. Chem. Soc., 1965.

686. Boucher, E. A. et al., J. Coll. & Int. Sci., 23, 600, 1967.

687. Contact Anglometer, Micromeritics Inst. Co., Norcross, Ga.

688. Kossen, N.W.F., and Heertjes, P. M., Chem. Eng. Sci., 20 593, 1965.

689. Heertjes, P. M., Kossen, N.W.F., Pow. Tech., 1, 33, 1967.

690. Mitsui, T., and Takada, S., J. Soc. Cosmetic Chem., 20, 335, 1969.

691. Selected Bibliography on Light Scattering, Phoenix Precision Inst. Co., Philadelphia, Pa.

692. Supplement No. 1 to Selected Bibliography on Light Scattering, Phoenix Preciaion Inst. Co., Phila., Pa.

693. Hepplestone, G. W., and Lewis, P. C. Brit. J. Appl. Phys., 1, (22), 199, 1968.

694. Vavra, B., J. Metals, 21 A, 20, 1969.

695. Wallace, T. P., and Kratohvil, J. B., Abs. Pap. Acs, PO54, 1969.

696. Maxim, L. D. et al, J. Polym. Sci., 195, 1969.

697. Liversey, P. J., and Billmeyer, F. W., J. Coll & Int. Sci., 30, 447, 1969.

698. Mullaney, P. F., and Dean, P. N., Appl. Optics, 8, 2361, 1969.

699. Harris, G. W., Pow. Tech., 3, 107, 1969.

700. Perelman, A. Y., and Shifrin, K. S., Opt. Spect. 26, 548, 1969.

701. Kratohvil, J. P., and Wallace, T. P., J. Phys. D., 3, 221, 1970.

702. Light Scattering Photometer Operation Manual OM-2000 Phoenix Precision Inst. Co., Phil., Pa.

703. Loebel, A. B., Ind. & Eng. Chem. 51 (2), 117, 1959.

704. Bailey, E. D., Ind. & Eng. Chem., 18 (6), 365, 1946.

705. Koglin, B., Chem. Ing. Tech. 41, 1926, 1969.

706. Rastogi, M. C., et al., Kolloid Z Polyn. 232, 804, 1969.

707. Anon. Optical Sedimentometer Nederland Patent 6715882, 1969.

708. Novikov, A. N., Koll Zhurnal 31 (4) 559, 1969.

709. Weisberg, H. E., Official Digest, 1155, Nov. 1962.

710. Princen, L. H., Official Digest, 766, July 1965.

711. Dintenfass, L., J. Oil & Col. Chem. Assoc., 41, 125, 1958.

712. Yashero, Y., Nagoya Kogyo 9, 261, 1957.

713. Matthews, E. A., and Rhodes, C. T., J. Coll. & Int. Sci., 32 (2), 332, 1970.

714. Sennett, P., and Olivier, J. P., I & E C 57, 32, 1965.

715. McAtee, J., et al., Amer. Minerologist, 54, 869, 1969.

716. Petrova, T. T., et al., Koll. Zhur., 31 (5) 741, 1969.

717. Thomas, H. C., and Cremers, A., J. Phys. Chem. 74 (5) 1072, 1970.

718. Rechman, H., Fatipec-Kongressbuch 3-18, 1964.

719. Buckley, D. M., J. App. Physics, 39 (9) 4224, 1968.

720. Parfitt, G. D., and Ramsboth, J., Study of Surface Properties of Coated Titanium-Dioxide Pigments by Electrophoresis. J. Oil Col. C 54 356 71 16R N4 J1094.

721. Saleeb, F. Z., Adsorption of Surface Active Agents at Solid-Liquid Interface. 1. Adsorption of Aerosol-OT. Z Phys. Ch L 244 85 70 21R 1-2 H4541.

722. Hesselin, F. T., Theory of Stabilization of Dispe. ons by Adsorbed Macromolecules. 1. Statistics of Cha· ,e of Some Configurational Properties of Adsorbed Macromolecules on Approach of an Impenetrable Interface. J. Phys. Chem. 75 65 71 50R N1 I1686.

723. Watanabe, A., and Aoki, I., Yukagatu 17 (3) 193, 1968.

724. McGown, D.N.L., and Parfitt, G. D., Kolloid Z Polym. 220 (1) 56, 1967.

725. Maruta, I., et. al., U.S. Patent 3554947, 1971.

726. Linwood, E., and Looby, T., German Patent 2044510, 1971.

727. Dreher, E., French Patent 1597521, 1970.

728. Augart, H., German Patent 1935939, 1971.

729. Yates, P. C., German Patent 2022347, 1970.

730. Kinanivala, N. P., German Patent 1901733, 1969.

731. Augustat, S., German Patent (East) 75,515, 1970.

732. Martynov, G. A., Issled. Obl. Poverkh. Sil. Sb. Dokl. Konf. 3rd, 256, 1966.

733. Miskarli, A. K., Dokl. Akad. Nauk. Azerb. 26 (7) 27, 1970.

734. Takeshi, Y., Kogyo Kagaku Zasshi 73 (10) 2081, 1970.

735. Greenwood, F. G., et al., Amer. Chem. Soc. Div. Water, Air Waste Chemicals Preprints 7 (2) 114, 1967.

736. Krasnokutskaya, M. E., et al., Issled. Obl. Poverkh. Sil. Sb. Dokl. Konf. 3rd, 319, 1966.

737. Bibik, E. E., et al., Ibid., 232, 1966.

738. Glazman, Y., and Kabysh, G. M., Koli Zhurnal 31 (1) 27, 1969.

739. Matijevic, E., and Allen, L. H., Environ. Sci. & Tech., 264, 1970.

740. Clayfield, E. J., Proc. Symp. on Adhesion, Karlsruhe, 1969.

741. Irani, R. R., and Callis, C. F., Particle Size Measurement Interpretation and Application, J. Wiley & Son, N. Y.

742. Löffler, F., On the Adhesion of Solid Particle to Fibre and Particle Surfaces, Proc. Conf. Physics of Adhesion, Karlsruhe, 1969.

743. Die Berechrung von Flich Kraft Abscheidem Staub - Reinh d Luft 30 (12) 497, 1970.

744. Abscheidegrad and Duckverlust von Filter-Stoffen verschiedener Struktur bei Unter Schiedlichen Bedingungen Staub. Reinh d Luft 30 (12) 518, 1970.

745. Casimir, H.B.G., and Polder, P., Phys. Rev. 73, 360 360 (1948).

746. Chu, B., Molecular Forces, Interscience Publ. 1967.

747. Crowl, V. T., J. Oil and Color Chemists Assoc., 50, 1023 (1967).

748. Derjaguin, B. V., Abrikosova, I. I., and Lifshitz, E. M., Quart. Rev. (London) 10, 295 (1956).

749. Fowkes, F. M., Ind. Eng. Chem. 56 40 (1964).

750. Hamaker, H. C., Physica, 4, 1058 (1937).

751. Kruyt, H. R., Colloid Science, Vol. 1, 1952, Elsevier, Amsterdam.

752. Landau, L. D., and Lifshitz, E. M., Electrodynamics of Continuous Media, Pergamon, Oxford, 1960.

753. Langbein, D., Physics of Adhesion, Karlsruhe, 1969.

754. Langbein, D., Phys. Rev. B 2, 3371 (1970).

755. Lifshitz, E. M., Soviet Physics, J.E.T.P., 2, 73 (1956).

756. London, F., Z. Physik, 63, 245 (1930).

757. London, F., Trans. Faraday Soc. 33. 8 (1937).

758. Margenau, H., Rev. Mod. Phys. 11, 1 (1939).

759. Mathai, K. G., and Ottewill, R. H., Trans. Faraday Soc., 62, 759 (1966).

760. Moelwyn-Hughes, E. A., Physical Chemistry, 2nd Ed. Pergamon, London, 1961.

761. Napper, D. H., Sci. Progr. 55, 91(1967).

762. Neugebauer, T. H., Z. Physik. 107, 785 (1937).

763. Ottewill, R. H., and Wilkins, D. J., Trans. Faraday Soc. 58, 608 (1962).

764. Overbeek, J.Th.G. and Sparnaay, M. J., Disc. Faraday Soc., 18, 12 (1954).

765. Parfitt, G. D., Dispersion of Powders in Liquids, Elsevier, Amsterdam, 1969.

766. Renne, M. J., Physics of Adhesion, Karlsruhe, 1969.

767. Schenkel, J. H., and Kitchener, J. A., Trans. Faraday Soc. 56, 161 (1960).

768. Schram, K., Physics of Adhesion, Karlsruhe, 1969.

769. Sherman, P., Emulsion Science, Chapter 2, Academic Press, New York, 1968.

770. Slater, J. C., and Kirkwood, J. G., Phys. Rev. 37, 682 (1931).

771. Verwey, E.J.W. and Overbeek, J.Th.G., Theory of the Stability of Lyophobic Colloids, Elsevier, Amsterdam, 1948.

772. Vold, M. J., J. Coll. Sci. 16, 1 (1961).

773. Vold, M. J., J. Coll. Sci., 9, 451 (1954).

774. Winterton, R.H.S., Contemp. Phys., 11, 559 (1970).

775. Wiese, G. R. and Healy, T. W., Trans. Faraday Soc. 66, 490 (1970).

776. Bell, G. M., and Levine, S., Trans. Faraday Soc., 53, 143 (1957).

777. Bergmann, P., et al., Z. Physik. Chem. A181 (1938) 301.

778. Bikerman, J. J., Phil. Mag. 33, 38A (1942).

779. Bogoliukov, N. N., Problems of a Dynamical Theory in Statistical Physics. In: Studies in Statistical Mechanics, Vol. I. 1962.

780. Bolt, G. H., J. Coll. Sci. 10, 206 (1951).

781. Booth, F., J. Chem. Phys., 19, 391, (1951).

782. Booth, F., J. Chem. Phys. 23, 453 (1955).

783. Bottcher, C.J.F., Theory of Electric Polarization, 1952, Elsevier, Amsterdam.

784. Brodowsky, H., and Strehlow, H., Z. Elektro Chem. 63, 262 (1959).

785. Buckingham, A. P., J. Chem. Phys. 25, 428 (1956).

786. Derjaguin, B., Trans. Faraday Soc. 36, 203 (1940).

787. Devereux and deBruyn, Interaction of Parallel Plane Double Layers, (M.I.T. Press, Cambridge, Mass. 1963).

788. Falkenhagen, H., and Kelbg, G., Ann. Physik, 11, 60 (1953).

789. Fowler, R. H., Trans. Faraday Soc. 23, 434 (1927).

790. Freise, V., Z. Elektrochem. 60 607 (1952).

791. Grahame, D. C., J. Chem. Phys. 18, 903 (1950).

792. Guggenheim, E. A., Trans. Faraday Soc. 55, 1714 (1959).

793. Hasted, J. B., et al., J. Chem. Phys. 16, 1 (1948).

794. Haydon, D. A., in Recent Progress in Surface Science, 1964, p. 94.

795. Haydon, P. A. and Taylor, F. H., Roy. Soc., Phil. Trans. A253, 255 (1960).

796. Hogg, R. et al., Trans. Faraday Soc. 62, 1638 (1966).

797. Jefimenko, O. P., Introduction to the Theory of Electric Fields Appleton-Century-Crofts, New York, 1966.

798. Kirkwood, J. G., J. Chem. Phys. 7, 911 (1939).

799. Kirkwood, J. G., J. Chem. Phys. 2, 767 (1934).

800. Kirkwood, J. G., and Poirier, J. C., J. Phys. Chem. 58, 591 (1954).

801. Kruyt, H. R., Colloid Science, Vol. I, 1952, Elsevier, Amsterdam.

802. Langmuir, I., J. Chem. Phys. 6, 893 (1938).

803. Levine, S., Proc. Phys. Soc. A66, 357 (1953).

804. Levine, S., Proc. Phys. Soc. A66, 365 (1953).

805. Levine, S., J. Phys. Chem. 64, 1195 (1960).

806. Levine, S., and Bell, G. M., J. Phys. Chem. 64, 1188 (1960).

807. Loeb, A. L., J. Coll. Sci. 6, 75 (1951).

808. Malsch, J., Physik, 29, 770 (1928).

809. Martynov, G. A., in Research in Surface Forces, Vol. 2, (1966), p. 75, 84, 94.

810. Martynov, G. A., and Muler, A. L., in Research in Surface Forces, Vol. 3 (1971) p. 210.

811. Müller, H. Kolloidchem. Beihefte, 26, 257 (1928).

812. Ohlenbush, H. P., Z. Elektrochem. 60, 607 (1956).

813. Onsager, L., J. Am. Chem. Soc. 58, 1486 (1936).

814. Prigagine, I., et al, J. Chim. Phys. 50, 146 (1953).

815. Schlögl, R., Z. Phys. Chem. 202, 379 (1954).

816. Sheehan, W. F., Physical Chemistry, Allyn and Bacon, Boston, 1970.

817. Sparnaay, M. J. Rec. Trav. Chim. 77, 872 (1958).

818. Sparnaay, M. J., in Rheology of Emulsions, 1962, p. 2[illegible].

819. Stern, O., Z. Elektrochem. 30, (1924) 508.

820. Stillinger, F. H., and Kirkwood, J. G., J. Chem. Phys. 33, 1282 (1960).

821. Verwey, E.J.W. and Overbeek, J.Th.G., Theory of the Stability of Lyophobic Colloids, Elsevier, Amsterdam 1948.

822. Wicke, E., and Eigen, M., Z. Elektrochem. 56, 551, (1952).

823. Williams, W. E., Proc. Phys. Soc. A66, 372 (1953).

824. Davies, J. T., and Rideal, E. K., Interfacial Phenomena, Academic Press, New York, 1963.

825. Arendt, P., and Kallmann, H., Z. Phys. 35, 421 (1926).

826. Baroody, E. M., J. Appl. Physics, 38, 4893 (1967).

827. Beeckmans, J. M., Can. J. Chem. 43, 2312 (1965).

828. Brenner, H., Chem. Eng. Sci. 16, 242 (1961).

829. Brock, J. R., and Hidy, G. M., J. Appl. Phys. 36, 1857 (1965).

830. Chandrasekhar, S., Rev. Mod. Phys. 15, 1 (1943).

831. Charles, G. E., and Mason, S. G., J. Coll. Sci. 15, 236 (1960).

832. Chu. B., Molecular Forces, Interscience, 1967.

833. Cohen, E. R., Vaughan, E. U., J. Coll. Sci. 35, 612 (1971).

834. Davies, C. H., Proc. Phys. Soc. 57, 259 (1945).

835. Derjaguin, B. V., Disc. Faraday Soc. 42, 317 (1966).

836. Derjaguin, B. V., and Muller, V. M., Dokl. Akad. Nauk. SSSR, 176, 738 (1967).

837. Fair, G. M., and Gemmell, R. S., J. Coll. Sci. 19, 360 (1964).

838. Friedlander, S. K., J. Meteorol, 17, 479 (1960).

839. Friedlander, S. K., J. Meteorol, 18, 753 (1961).

840. Fuchs, N. A., The Mechanics of Aerosols, MacMillan, 1964.

841. Green, H. L., and Lane, W. R., Particulate Clouds: Dusts, Smokes, and Mists, Var Nostrand, 1957.

842. Greenfield, M. P., et al., J. Coll. Sci. 35, 102 (1971).

843. Hidy, G. M., J. Coll. Sci. 20, 123 (1965).

844. Hidy, G. M., and Brock, J. R., J. Coll. Sci. 20, 477 (1965).

845. Hidy, G. M., and Lilly, P. K., J. Coll. Sci. 20, 867 (1965).

846. Hirschfelder, J. O. et al, Molecular Theory of Gases and Liquids, Wiley, New York (1954).

847. Honig, E. P., et al., J. Coll. Sci. 36, 97 (1971).

848. Hulburt, H. M., and Akiyama, T., I. & E.C. Fund, 8, 319 (1969).

849. Hulburt, H. M., and Katz, S., Chem. Eng. Sci. 19, 555 (1964).

850. Jeans, J. H., The Mathematical Theory of Electricity and Magnetism, Cambridge (1920).

851. Knudsen, M., and Weber, S, Ann. Phys. 36, 482 (1911).

852. Kruyt, H. R., Colloid Science, Vol. 1, 1952, Elsevier.

853. Lindauer, G. C., and Castleman, A. W., Trans. Amer. Nucl. Soc. 12, 897 (1969).

854. Martynov, G. A., and Bakanov, S. P., Research in Surface Forces, Vol. I, p. 182 (1967).

855. Millikan, R. H., Phys. Rev. 22, 1, (1923).

856. Müller, H., Kolloid Chem Beihefte, 27, 223 (1928).

857. Müller, H. Kolloid Chem Beihefte, 26, 257 (1928).

858. Smoluchowski, M., Von Physik, 17, 557 (1916); Z. Physik Chem. 92, 129 (1917).

859. Spielman, L. A., J. Coll. Sci. 33, 562 (1970).

860. Stimson, M., and Jeffery, G. B., Proc. Roy. Soc. London Ser. 111, 110 (1926).

861. Swift, D. L., and Friedlander, S. K., J. Coll. Sci. 19, 621 (1964).

862. Verwey, E.J.W. and Overbeek, J.Th.G., Theory of the Stability of Lyophobic Colloids, Elsevier, 1948.

863. Whytlaw-Gray, R., and Patterson, H. S., Smoke, Arnold, 1932.

864. Zebel, G., Kolloid-Zeitschrift, 156, 102 (1958); 157, 37 (1958).

865. Zebel, G., in Aerosol Science, C. N. Davies (Ed.) Chapt. II, Academic Press, 1966.

866. Verwey, E.J.W., and Overbeek, J.Th.G., Theory of the Stability of Lyophobic Colloids, Elsevier, Amsterdam, 1948.

867. Kruyt, H. R., Colloid Science, Elsevier, Amsterdam, 1948.

868. Frens, G., et al., Trans. Faraday Soc. 63, 418 (1967).

869. Frens, G., Thesis, Utrecht, Netherlands, 1968.

870. Jones, J. E., and Levine, S., J. Coll. Sci. 30, 241, (1969).

871. Booth, F., Proc. Roy. Soc. A203, 514 (1950).

872. Henry, P. C., Proc. Roy. Soc. A133, 106 (1931).

873. Hunter, R. J., J. Coll. Sci. 22, 231 (1966).

874. Lyblema, J., and Overbeek, J.Th.G., J. Coll. Sci. 16, 501 (1961).

875. Overbeek, J.Th.G., Adv. in Coll. Sci. Vol. 3, p. 97.

876. Wiersema, P. H., et al., J. Coll. Sci. 22, 78 (1966).

877. Rumpf. H., in Agglomeration, Wm. A. Knepper (ed.) Interscience Publ. 1962, p. 379.

878. Rumpf, H., Chem.-Ing.-Tech. 30, 144 (1958).

879. Pietsch, W.. Staub, 27, 24 (1967).

880. Pietsch, W., et al., IAEC Prod. Res. Develop., 8, 58 (1969).

881. Cheng, D. C., Chem. Eng. Sci. 23, 1405 (1968).

882. Gillespie, T., and Settineri, W. J., J. Coll. & Interf. Sci. 24, 199 (1967).

883. Melrose, J. C., AICHE J. 12, 986 (1966).

884. Radushkevich, L. V., Izv. Akad. Nauk. 69, 1008 (1952).

885. Zimon, A. D., Adhesion of Dust and Powder, Plenum Press, New York, 1969.

886. Princen, H. M., J. Coll. Sci. 26, 249 (1968).

887. Picknett, R. G., J. Coll. Sci. 29, 173 (1969).

888. Krupp, H., and Sperling, G., J. Appl. Phys. 37, 4176 (1966).

889. Kottler, W., et al., Z. für anglwandte Physik, 24, 219 (1968).

890. Krupp, H., and Sperling, G., Int. Cong. on Chemistry, Physics and Application of Surface Active Substances, p. 447, (1964).

METHODS OF SAMPLING, COLLECTING AND ANALYZING SUBMICRON PARTICLES

891. Beal, S. K., Nuclear Sci. & Eng. 40, 1 (1970).

892. Chamberlain, A. C., Proc. Roy. Soc. (London) 296A, pp. 45-70, 1967.

893. Davies, C. N., Aerosol Science, Academic Press, 1966.

894. Flygger, H., and Rosenbaum, H. C., Nature, Vol. 205, p. 62, January 1965.

895. Friedlander, S. K., and Johnstone, H. F., Ind. and Eng. Chemistry, pp. 1151-1156, July 1957.

896. Fuchs, N. A., The Mechanics of Aerosols, CWL Special Publications, 1955.

897. Gowariker, V. R., V. K. Atomic Energy Commission AERE-1085, 1962.

898. Kneen, T., and Strauss, W., Atmosh-Environ., Vol. 3, pp. 55-67, 1969.

899. Rouhiainen, P. O., and Stachiewicz, J. W., J. Heat Transfer, pp. 169-177, February 1970.

900. Sood, S. K., Lieberman, A., and Wasan, D. T., Aerosol Transport, Tech. Documents M. & P., IIT Research Institute, August 1968, Chicago, Ill.

901. Hutchinson, P., Hewitt, G. F., and Dukler, A. E., Chem. Eng. Sci., 26, 419 (1971).

902. Sehmel, G. A., Aerosol Sci., 2, 63 (1971).

903. Sehmel, G. A., Am. Ind. Hyg. Assoc. Jor., 758, Nov.-Dec. (1970).

904. Sehmel, G. A., J. Geophys. Res., 75, 1766 (1970).

905. Sehmel, G. A., Particle Diffusivities and Deposition Velocities over a Horizontal Smooth Surface, paper presented at the 45th National Colloid Symposium, Atlanta, June 21-23, 1971.

906. Wasan, D., et al., Aerosol Transport - Sampling Line Loss and its Prevention. Int. Symp. Coll. & Int. Sci., Atlanta, Ga., 1971.

907. Anonymous, Guide to Respirable Mass Sampling, Amer. Ind. Hyg. Assn. J., 132 (Apr. 1970).

908. Lippmann, M., Respirable Dust Sampling, Amer. Ind. Hyg. Assn. J., 31, p. 138 (April 1970).

909. Proceedings of Conference on Inhalation Carcinogeneis, U. S. At. Energy Comm., Oak Ridge, Tenn., October 1969.

910. Yanada, V. M., and Charlson, R. J., Proper Sizing of the Sampling Inlet Line for a Continuous Air Monitoring System, Environ. Sci. Technol., 3 (5), 483 (1969).

911. Sehmel, G. A., and Schwendiman, L. C., Particle Deposition within a Curved Sampling Probe, Pacific N.W. 1967 Annu. Rep. 88, 1968.

912. Kneen, T., and Strauss, W., Deposition of Dust from Turbulent Gas Streams, Atmos. Environ., 3 (1), 55 (1969).

913. Wehner, A. P., et al., Unipolar Charged Aerosols, Effect on Deposition in Tubes and on Droplet Size, Arch. Environ. Health, 20, 28 (1970).

914. Particle Size Analysis, IITRI Project C8109. Final Report Dec. 1969.

915. Hyatt, E. C., et al., A Study of Two-Stage Air Samplers Designed to Simulate the Upper and Lower Respiratory Tract, 13th Int'l. Cong. on Occupational Health, 1960.

916. Lippmann, M., and Harris, N. B., Size Selective Samplers for Estimating Respirable Dust Concentration Health Physics 8, 155, 1962.

917. Wesley, R. A., Mayfield, W. D., and McCaskill, O. L. An Evaluation of Cyclone Collector, Agr. Eng. 51 590 70.

918. Knuth, R. H., Recalibration of Size-Selective Samplers, Amer. Ind. Hyg. Assoc. J. 30, 379 (1969).

919. Sutton, G. W., Calibration of Aerodynamic Size versus Efficiency for a Miniature Cyclone. Presented at the American Industrial Hygiene Conference, Pittsburgh, Pa., (1966).

920. Tomb, T. F., and Raymond, D. L., Evaluation of the Collection Characteristics of Horizontal Elutriator and of 10 mm Nylon Cyclone Gravimetric Dust Samplers. Presented at the American Industrial Hygiene Association Conference, Denver, Colo. 1969.

921. Muschelknautz, E., and Krambroch, W., Aerodynamic Parameters of a Cyclone Separator on Basis of New and Improved Measurements. Chem-Ing-T 42 247, 1970.

922. Ettinger, H. J., and Royer, G. W., Calibration of a Cyclone 2 Stage Air Sampler, Am. Ind. Hyg. 31 15 1970.

923. Stelzer, D. F., Lynch, J. R., and Bernaski, W. J., Evaluation of Size-Selective Presamplers. Efficiency of 10 mm Nylon Cyclone. Am. Ind. Hyg. 31 15, 1970.

924. Leroy Balzer, J., and Tebbins, B. D., Size Selective Sampling of Fibrous Materials. Am. Ind. Hyg. Assoc. 31 14 1970.

925. Lippmann, M., and Kydonieus, A., Multistage Aerosol Sampler for Extended Sampling Intervals. Am. Ind. Hyg. Assn. J. 31, 14 1970.

926. Errington, F. P., and Powell, E. O., A Cyclone Separator for Aerosol Sampling in Field. J. Hyg. Camb. 67 387, 1969.

927. Watson, H. H., Dust Sampling to Simulate the Human Lung. Brit. J. Ind. Med. 10: 93 (1953).

928. Mercer, T. T., Air Sampling Problems Associated with the Proposed Lung Model. Proceedings of the 12th Annual Meeting of the Bioassay and Analytical Chemistry Socieity, Gatlinburg (1953).

929. Bleckmans, J. M., Correction Factor for Size-Selective Sampling Results. Based on a New Computed Alveolar Deposition Curve. Ann. Occup. Hyg. 8: 221 (1965).

930. Mukhopad, S. N., and Chowdhury, K. C., Collecting Efficiency of a Cyclone Separator, Br. Chem. Eng. 15 529, 1970.

931. Lynch, J. R., Evaluation of Size-Selective Presamplers. 1. Theoretical Cyclone and Elutriator Relationships. Am. Ind. Hyg. 31 548, 1970.

932. Thompson, B. W., and Strauss, W., Application of Vortex Theory to Design of Cyclone Collectors, Chem. Eng. SC 26 125, 1971.

933. Shour, E. P., Dust Measurement in Connection with Coal Workers Pneumoconiosis. Transactions of the 31st Annual Meeting of the American Conference of Governmental Industrial Hygienists (1969).

934. Knight, G., and Lichti, E. K., Comparison of Cyclone and Horizontal Elutriator Size-Selectors. Presented at American Industrial Hygiene Conference, Denver 1969.

935. Gloger, J., and Jugel, W., (GE) Influence of Geometrical Parameters and Crude Gas-Dust Loading on Separating Degree and Pressure Loss of Cyclone Separators. Maschin. Tec. 20, 156, 1971.

936. Freudental, P., High Collection Efficiency of Aerotec-3 Cyclone for Submicron Particles, Atmos. Envir. 5, 151, 1971.

937. Dennis, R., Coleman, R., Silverman, L., and Fust, M. W., Particle Size Efficiency Studies on a Design 2 Aerotic Tube NYO-1583, 1952.

938. Dyna Therm Corp. Bulletin 4-65, P.O. Box 66356, Houston, Texas, 77006.

939. Bauer Bros. Corp. Bulletin G-33A, Springfield, Ohio, 45501.

940. Fisher Klosterman, Inc. Bulletin 216, 2909 Magazine Street, Louisville, Ky., 40211.

941. R. P. Adams Bulletin 715, 225 E. Park Drive, Buffalo, 17, N. Y.

942. Dorr Oliver, Inc., Bulletin 2550 and 2500, Stamford, Conn.

943. Equipment Eng., Inc., Bulletin 830, 41 Sutter St., San Francisco, Calif.

944. Buell Eng. Corp., Inc., Bulletin C112, Lebanon, Pa.

945. Technical Bulletin, Alpine America, Natick, Mass.

946. Technical Bulletin, Bauer Bros., Inc., Springfield, Ohio 45501.

947. Technical Bulletin, Dietert, 9330 Roselawn Ave., Detroit 4, Mich.

948. Technical Bulletin, Donaldson Co., Inc., 1400 West 94th St., Minneapolis, Minn. 55431.

949. Technical Bulletin, Geoscience Inst. Corp., Mt. Vernon, N. Y.

950. Technical Bulletin, Micromeritics, Goshen Springs Rd., Norcross, Ga.

951. Technical Bulletin, Neu, 32 Baker St., Weybridge, Surrey, England.

952. Technical Bulletin, Vortec, 13933 Crenshaw Boul., Hawthorne, Calif. 90250.

953. Technical Bulletin, Walther and Cie, Akriengellschaft Köln - Dellbrück, West Germany.

954. Plitt, L. R., Analysis of Solid-Solid Separations in Classifiers, Can Min Met 64 42, 1971.

955. Leschonski, K.,(GE) Principle and Experimental Results of 2 New Crosscurrent Jet Air Separators. Chem-Ing-T 43 317, 1971.

956. Black, H. C., and Williams, P. C., A Laboratory Air-Classifier. Cereal Sci. 14, 358, 1969.

957. Jones, H. W., A Study of Bauer McNett Fibre Classifier. Pulp Paper, 71, 176, 1970.

958. Zverev, N. I., and Ushakov, S. G., Experimental Investigation of Process of Centrifugal Dust Separation. Therm. Eng. R. 17, 34, 1970.

959. Goetz, A., An Instrument for the Quantitative Separation and Size Classification of Air-Borne Particulate Matter down to 0.2 Micron. Rev. Geofisica Pura E. Applicata, Proc. II Internat. Symp. Condensation Nuclei, Basel/Locarno, 36, 46-49, 1957.

960. Goetz, A., and Stevenson, H.J.R., The Aerosol Spectrometer, Its Theory, Construction and Application to the Analysis of Exhaust and Atmospheric Aerosols, Proceedings of the Semi-Annual Technical Conference of the APCA, November 1957, San Francisco, pp. 228-267.

961. Goetz, A., Study of the Properties of Aerosols, with Particular Reference to the Nature of the Air-Particle Interface. Final Report USPHS Research Contract SAph-69557, The R. A. Taft Sanitary Engineering Center Technical Report No. A58-10, 1958.

962. Goetz, A., The Aerosol Spectrometer, a New Instrument for the Analysis of Air-Borne Particles in the Submicron Range, Public Works Magazine, 91-93, February 1959.

963. Goetz, A., Stevenson, H.J.R., and Preining, O., The Design and Performance of the Aerosol Spectrometer, 52nd Annual Meeting of APCA, June 1959, Los Angeles, Preprint No. 59-40.

964. Preining, O., Stevenson, H.J.R., and Goetz, A., Analysis of Aerosol Spectra, 52nd Annual Meeting of APCA, June 1959, Los Angeles, Preprint No. 59-42.

965. Goetz, A., Preining, O., and Kallai, T., The Metastability of Natural and Urban Aerosols, Review Geofisica Pura E Applicata, Milano, Vol. 50 (1961,111), pp. 67-80.

966. Goetz, A., The Physics of Aerosols in the Submicron Range, International Symposium on "Inhaled Particles and Vapours," Oxford, England, Pergamon Press 1961, pp. 295-301.

967. Goetz, A., and Preining, O., Bestimmung der Grossenverteilung eines Aerosols mittels des Goetz' schen Aerosol-Spektrometers, Acta Physica Austriaca, Bd. XlV, Heft 3-4, pp. 292-304, 1961.

968. Goetz, A., Stoeber, W., and Kallai, T., Synergistic Properties of Aerosols, Progress Report USPHS Res. Grant No. RG-6743(C1) and AP-12(c2), formerly RG-6743 (C2), November 15, 1961.

969. Goetz, A., and Kallai, T., Design and Performance of an Aerosol Channel for the Synthesis and Study of Atmospheric Reaction Products, presented at the Air Pollution Instrumentation Symposium at 55th Annual APCA Meeting, Chicago, Illinois, May 20-24, 1962. Preprint No. 62-18.

970. Kallai, T., and Goetz, A., Instrumentation for Determining Size and Mass-Distribution of Submicron Aerosols, presented at Air Pollution Instrumentation Symposium at 55th Annual APCA Meeting, Chicago, Illinois, May 20-24, 1962. Preprint No. 62-19.

971. Technical Bulletin, Zimney Corp., Monrovia, Calif.

972. Stöber, W., Design and Performance of a Size Separating Aerosol Centrifuge Facilitating Particle Size Spectrometry in the Submicron Range. 1st Atomic Energy Agency, Vienna, Austria 1967.

973. Berner, A., and Reichelt, H., Über Einlassspaltsysteme in Konigfugen. Das ROSL System. Staub 29, 92 1969.

974. Hochrainer, D., and Brown, P. M., Sizing of Aerosol Particles by Centrifugation. Env. Sci. Tec. 3 830, 1969.

975. Stöber, W., and Flachsbart, H., Aerosol Size Spectrometry with a Ring Slit Conifuge. Env. Sci. Tec. 3, 641, 1969.

976. Sawyer, K. F., and Walton, W. H., J. Sci. Inst. 27, 272 1956.

977. Stöber, W., and Flachsbart, H., Size-Separating Precipitation of Aerosols in a Spinning Spiral Duct, Env. Sci. Tec. 3, 1280, 1969.

978. Flesch, J. P., Calibration Studies of a New Sub-Micron Aerosol Size Classifier. J. Coll. I. Sc. 29 502,1969.

979. Hochrainer, D., and Zebel, G., Separation of Aerosol Particles According to their Size, Using a Novel Impactor Jet. Aerosol Sci., 1970 (Aug.), 1 (3), 175-183. In German.

980. Zebel, G., and Hochrainer, H.,(GE) New Type Impactor for Separation of Particles According to Size. Chem-Ing-T 43 308, 1971.

981. Stober, W., Boose, C., and Flachsbart, H., Distribution Analysis of Aerodynamic Size and Mass of Aerosol Particles by Means of Spiral Centrifuge in Comparison to other Aerosol Precipitators. ABS Pap ACS 1971 80, 1971.

982. Litvinov, A. T., (RS) Effective Purification of Gas in Apparatuses Using Centrifugal Force to Separate Dust Particles from Flow. ZH Prik KH 44 1221, 1971.

983. Hochrainer, D., A New Centrifuge to Measure Aerodynamic Diameter of Aerosol Particles in Submicron Range - Coll. ABS Pap ACS 1970 20, 1970.

984. Hochrainer, D., New Centrifuge to Measure Aerodynamic Diameter of Aerosol Particles in Submicron Range. J. Coll. Int. Sc. 36, 191, 1971.

985. Technical Bulletin, Casella Ltd.

986. Technical Bulletin, Willson Products.

987. Walton, W. H., and Harris, W. J., (1947). A Modified Thermal Precipitator for the Quantitative Sampling of Aerosols for Electron Microscopy. Technical Paper No. 1. Chemical Defence Research Establishment, Porton, Hants, England.

988. Prewett, W. G., and Walton, W. H., (1948). The Efficiency of the Thermal-Precipitator for Sampling Large Particles of Unit Density. Technical Paper No. 63, Chemical Defence Research Establishment, Porton, Hants, England.

989. Schadt, C. F., and Cadle, R. D., (1961). Thermal Forces on Aerosol Particles. J. Phys. Chem. 65, 1689-1694.

990. Watson, H. H. (1958). The Sampling Efficiency of the Thermal Precipitator. Brit. J. Appl. Phys. 2, 78-79.

991. Watson, H. H., (1936). The Thermal Precipitator. Trans. Inst. Min. Mett. 46, 176-187.

992. Donoghue, J. K., (1953). A Modification to the Hotwire Thermal Precipitator, J. Sci. Instrum. 30, 59.

993. Walkenhorst, W., (1952). Electron-microscope Investigations on Dust, Methods and Results. Beiträge zur Silikoseforschung 18, 29-62.

994. Burdekin, J. T., and Dawes, J. G., (1956). The Use of a Size-Selector for Dust-sampling with the Thermal Precipitator. Brit. J. Industr. Med. 13, 196-201.

995. Beadle, D. G., and Kitto, P. H. (1952). A Modified Form of Thermal Precipitator. J. Chem. Mett. Min. Soc. South Africa 52, 284-311.

996. Cember, H., Hatch, T., and Watson, J. A., (1953). Dust Sampling witn a Rotating Thermal Precipitator. Amer. Ind. Hyg. Assoc.-Quart 14, 191-194.

997. Walton, W. H., (1950). J. R. Micr. Soc. 70, 51.

998. Orr, C., and Martin, R. A. (1958). Thermal Precipitator for Continuous Aerosol Sampling. Rev. Sci. Instrum. 29, 129-130.

999. Hamilton, R. J., (1956). A Portable Instrument for Respirable Dust Sampling. J. Sci. Instrum. 33, 395-399.

1000. Hamilton, R. J., and Phelps, B. A., (1956). The Production of Transparent Profiles of Dust-Particles as an Aid to Automatized Particle Counting. Brit. J. Appl. Phys. 7, 186-189.

1001. Wright, B. M., (1953). Gravimetric Thermal Precipitator. Science 118, 195.

1002. Wright, B. M. (1954). A Reversible Aspirator for the Thermal Precipitator. J. Sci. Instrum. 31, 263-264.

1003. Technical Bulletin, American Inst. Co.; Silver Spring, Md.

1004. Technical Bulletin, Corner House Lab., Johannesburg, S.Africa

1005. Technical Bulletin, Numinco., Apollo, Pennsylvania.

1006. Technical Bulletin, Joseph Ficklen, Inc., Pasadena, Calif.

1007. Technical Bulletin, Konisampler, Ibid.

1008. Technical Bulletin, Continuous Sampler, Ibid.

1009. Technical Bulletin, Oscillating Sampler, Ibid.

1010. Technical Bulletin, Gravitational Sampler, Ibid.

1011. Technical Bulletin, Micro Sampler, Ibid.

1012. Hasenclever, D., (1955). A Comparative Study of Different Dust-measuring Instruments for the Routine Measurement of Mineral Dusts. Staub 41, 388-435.

1013. Ashford, J. R., (1969). Some Statistical Aspects of Dust Counting. Brit. J. Appl. Phys. 11, 13-21.

1014. Dawes, J. G., and Maguire, B. A., (1960). The Thermal Precipitator and the P.R.U. Handpump: A Critical Study. Safety in Mines Research Establishment Report, No. 187.

1015. Hodkinson, J. R., Air Sampling Instruments, Am. Conference of Governmental Industrial Hygienists, 1014 Broadway, Cincinnatti, Ohio, 1962.

1016. Hodkinson, J. R., (1960). Reproducibility and Correlation of Long-period and Short-period Thermal-precipitator Samples of Airborne Dust in Mines. Ann. Occ. Hyg. 2, 235-242.

1017. Hodkinson, J. R., (1962). Dust-measurement by Light Scattering and Absorption. Ph.D. thesis. University of London.

1018. Hodkinson, J. R., Critchow, A., and Stanley, N., (1960). Effect of Ambient Airspeed on Efficiency of Thermal Precipitator. J. Sci. Instrum. 37, 182-183.

1019. Tomany, J. P., A Guide to the Selection of Air Pollution Control Equipment. Form 5-070 Air Correction Div., Tokeneke Road, Darien, Conn.

1020. Liu, B.Y.H., et al., Theory of Charging of Aerosol Particles by Unipolar Ions in the Absence of an Applied Electric Field.

1021. Liu, B.Y.H., et al., Electrical Aerosol Samples for Light and Electron Microscopy. Rev. Sci. Inst. 38, 100 1967.

1022. Whitby, K. T., and Clark, W. E., Electrical Aerosol Particle Counting and Size Distribution Measuring System for the 0-015-1 μ Size Range. Tellus XVIII 2, 1966.

1023. Technical Bulletin, Whitby Aerosol Analyzer Thermo-Systems, St. Paul, Minn.

1024. Niedra, J. M., and Penney, G. W., Orientation and Adhesion of Particles, IEEE Trans Vol. IECI-12, No. 2, pp. 46-50 (Nov. 1965).

1025. Seman, G. W., and Penney, G. W., Photographic Records of Particle Trajectories during Electrostatic Precipitation, IEEE Convention Record Pt. 7, pp. 69-72 (1965).

1026. Seman, G. W., and Penney, G. W., Photographic Studies of Particle Behavior under Varying Precipitating Conditions, IEEE Trans. Vol. PAS86, No. 3, pp. 365-368 (March 1967).

1027. Penney, G. W., and Craig, S. W., Sparkover as Influenced by Surface Conditions in D-C Corona, AIEE Trans. Vol. 79, pt. 1, pp. 112-118 (1960).

1028. Penney, G. W., and Craig, S. E., Pulsed Discharges Preceding Sparkover at Low Voltage Gradients, AIEE Trans. Vol. 80, part I, pp. 156-162 (May 1962).

1029. Schmidt, L. S., and Penney, G. W., Sparkover in Mixtures of Air and Water Vapor. IEEE Trans. Vol. PAS-86, No. 3, pp. 360-364 (March 1967).

1030. Penney, G. W., Electrostatic Precipitation Studies at Carnegie Institute of Technology, J. Air Poll. Cont. Adm. 17, 888 (1967).

1031. Williams, J. C., and Jackson, R., The Motion of Solid Particles in an Electrostatic Precipitator, Proc. Symp. Interaction Fluids Particles, Inst. Chem. Engrs., London, pp. 282-288, 291-293, 297-298 (1962).

1032. Cooperman, P., Boundary Layer Effects in Electrostatic Precipitation, Paper 66-124, Air Pollution Control Assoc., 59th Annual Meeting, San Francisco (1966).

1033. Robinson, M., The Role of Turbulence in Electrostatic Precipitation, Paper 67-34, Air Pollution Control Assn., 60th Annual Meeting, Cleveland, Ohio (1967).

1034. Robinson, M., Movement of Air in the Electric Wind of the Corona Discharge, Trans. Am. Inst. Elec. Engrs., 801, 143-50 (1961).

1035. Robinson, M., Electric Wind Turbulence in Electrostatic Precipitation. J. Air Poll. Control Admin. 17(9), 605, 1967.

1036. Herrick, R. A., A Field Comparison of the Electrostatic Precipitator Sampler and the High Volume Sampler. Preprint, Resources Research, Inc., Reston, Va., 9p., 1968. (Presented at the 61st Annual Meeting, Air Pollution Control Assn., St. Paul, Minn., June 23-27, 1968.

1037. Sickles, R. W., Electrostatic Precipitators, Chem. Eng., 75 (22):156-159, Oct. 14, 1968.

1038. Rimberg, D., and Keafer, D., Evaluation of a Commercial Electrostatic Aerosol Sampler. Atmos. Envir. 5 65 71. N 3R N1 393.

1039. Oglesby, S., Manual of Electrostatic Precipitation Technology, I. Fundamentals, II. Application. Southwest Research Inst. Report, 1971.

1040. Wait, G. R., Terrestrial Magnetism and Atmospheric Electricity, 39, 47 (1934).

1041. Technical Bulletin, Wessex Electric Heater Company, San Francisco, Calif.

1042. Daniel, J. H., J. of Appl. Phys. 22, 542 (1951).

1043. Langer, G., Radnik, J., and Templeton. Development of a Simple High Resolution Mobility Analyzer for Small Charged Particles, Rev. Sci. Inst. 33 (1) 63 (1962).

1044. Teodosic, V., A Highly Sensitive Electrostatic Precipitator with No Moving Parts. Nuclear Ind. and Methods 59 359 (1968).

1045. Strindehag, O. M., Liquid Surface Electrostatic Precipitator, Rev. Sci. Inst. 38 (1) 95 (1967).

1046. Technical Bulletin, Bendix Corp., 3625 Hauck Road, Cincinnatti, Ohio 45241.

1047. Technical Bulletin, Del Electronic Corp., 250 E. Sanford Blvd., Mt. Vernon, N. Y.

1048. Technical Bulletin, M.S.A., 201 N. Braddock, Pittsburgh, Pa.

1049. Technical Bulletin, Environmental Research Corp., 3725 N. Dunlap St., St. Paul, Minn. 55112.

1050. Technical Bulletin, Litton Systems, Inc. 2003 E. Henepin Ave., Minneapolis, Minn. 55413.

1051. Technical Bulletin, Model 3100 Thermo Systems, 2500 Cleveland Avenue, N. St. Paul, Minn. 55113.

1052. Technical Bulletin, Model 3200, Thermo Systems, 2500 Cleveland Avenue, N. St. Paul, Minn. 55113.

1053. Technical Bulletin, Model 3205, Thermo Systems, 2500 Cleveland Avenue, N. St. Paul, Minn. 55113.

1054. Technical Bulletin, Climet Instrument Co., 1240 Birchwood Avenue, Sunnyvale, Calif. 94086.

1055. Technical Bulletin, Dynac, Box 552, Summit, N. J.

1056. Technical Bulletin, Royco, 111 Jefferson Drive, Menlo Park, Pa.

1057. Technical Bulletin 2364, Research Appliance Co., Allison Park, Pa. 15101.

1058 Technical Bulletin, Coulter Electronics, 590 W. 20th Street, Hialeah, Florida 33010.

1059. Technical Bulletin, Bausch & Lomb, Inc., Rochester 2, N. Y.

1060. Technical Bulletin, Environment/One Corporation, 2773 Balltown Road, Schenectady, N. Y. 12309.

1061. Technical Bulletin, General Electric Company, P. O. Box 43, Schenectady, N. Y. 12301.

1062. Technical Bulletin, 2347, Research Appliance Co., Allison Park, Pa. 15101.

1063. Technical Bulletin, Singco, Inc., 11 Cypress Drive, Burlington, Mass. 01813.

1064. Sem, G., et al., State-of-the-Art Instruments for the Measurement of Particle Emissions from Combustion Sources. Thermo System Contract CPA-70-23 Ca E.P.A.

1065. Fawcett, H. H., and Gardner, G., A Small Particle Detector, Industrial and Engineering Chemistry, p. 87A-88A (1958).

1066. Skala, G. F., A New Instrument for the Continuous Measurement of Condensation Nuclei, Analytical Chemistry, V. 35, p. 702 (1963).

1067. Pollak, L. W., Counting of Aitken Nuclei and Applications of Counting Results, Int. J. Air Poll., V. 1, no. 4, p. 293-305.

1068. McGreevy, G., The Evaluation of the Performance of an Electrostatic Precipitator using a Pollak-Nolan Nucleus Counter, Atmospheric Environment, v. 1, no. 2, p. 87-95 (1967).

1069. Peterson, C. M., and Paulus, H. J., Continuous Monitoring of Aerosols over the 0.001- to 10-Micron Spectrum, American Industrial Hygiene Assn. J., p. 111-122 (Mar-Apr 1968).

1070. Pedder, M. A., Measurement of Size and Diffusion Characteristics of Aerosols with Particle Sizes Less than 0.01 Mum Using Pollak Condensation Nucleus Counter. J. Phys. D. 4 531, 1971.

1071. Pircher, F. J., Lerner, S. R., Cooper, P. H., and Eastland, D. K., Aerosol Scans with Particles in Submicronic Range. J. Nucl. Med. 12 385, 1971.

1072. Binek, B., and Dohnalov, B., New Aerosol Particle Analyzer, Coll. Czech. 36 954, 1971.

1073. Trawinski, H., (GE) Centrifuges, Hydrocyclones, and Sludge Thickeners. Chem-Ing-T 42 1445, 1970.

1074. Neesse, T., (GE) Hydrocyclone as a Turbulence Classifier, Chem. Tech. 23 146, 1971.

1075. Kristek, L., Svizela, A., and Hamp., I., Classifier for Liquid Suspensions. Czech Patent No. 134572 Appl 2/26/68 Granted 12/15/69. Int's Class B03B.

1076. Colon, F. J., et al., Centrifugal Elutriation of Particles in Liquid Suspension. Particle Size Anal. Conf. Bradford Univ., England, Sept. 1970.

1077. Treasure, C.R.G., private communication.

1078. Marshall, C. E., Keen, B. A., and Schofield, R. K., (1930), Nature, 126, 94.

1079. Norton, F. H., and Spiel, S. J., (1938), J. Amer. Ceram. Soc. 21, 89.

1080. Jacobson, A. E., and Sullivan, W. F., (1946), Ind. Eng. Chem. Analyt ed., 18, 360.

1081. Menis, O., House, H. P., and Boyd, C. M., (1957), Oak Ridge National Laboratory Report 2345 (22, p. 86), (23, p. 87).

1082. Conner, P., Hardwick, W. M., and Laundy, B. J., (1958), U.K.A.E.A. Report, A.E.R.E., CE/R 2465.

1083. Hildreth, J. D., and Patterson, D., (1964), J. Soc. Dyers and Colourists, 80, 474.

1084. Musgrove, J. R., and Harner, H. R., (1947), Turbimetric Particle Size Analysis, (Cincinnati, Ohio, The Eagle Pilcher Co.).

1085. Irani, R. R., and Callis, C. E., (1963), Particle Size Measurement, Wiley, N. Y.

1086. Orr, C., and Dallavalle, J. M., (1960), Fine Particle Measurement, Macmillan, N. Y.

1087. Gupta, A. K., (1959), J. Appl. Chem., 9,487.

1088. Romwalter, A., and Vendl, M., (1935), Kolloid Z., 72, 1.

1089. Brown, C., (1944), J. Phys. Chem., 48, 246.

1090. Martin, S. W., (1939), Industr. Eng. Chem., Analyt ed., 11, 471.

1091. Martin, S. W., and Robinson, H. E., (1948). J. Phys. Colloid Chem., 42, 854; ibid (1949), 53, 860.

1092. Murley, R. D., (1965)., Nature, 207, 1089.

1093. Donoghue, J. K., and Bostock, W. (1955), Trans. Inst. Chem. Engrs., 33, 72.

1094. Berg, S., (1940), Ingen. Vidensk. Skr. B., No. 2.

1095. Kamak, H. J. (1951)., Analyt. Chem., β3(6), 844.

1096. Slater, C., and Cohen, L, (1962), J. Sci. Instr., 39, 614.

1097. Treasure, C.R.G., (1964), Whiting and Industrial Powiers Res. Council, Welwyn, Tech. Paper No. 50.

1098. Abarbane, Z. I., and Viner, I. Y., (RS) On Sedimentation of Particles in Field of Centrifugal Forces. Ivuz. Fiz. 27, 1969.

1099. Bennert, W., (GE) Use of Separation Function Appearing during Sedimentation in Heavy and Centrifugal Field for Special Purposes of Grain-size Analysis. Chem. Tech. 23 121, 1971.

1100. Marshall, C. E., (1930), Proc. Roy. Soc., A, 126, 427.

1101. Whitby, K. T., (1955), Heating, Piping and Air Conditioning, 61, 449.

1102. Technical Bulletin, MSA., Pittsburgh, Penn.

1103. Whitby, K. T., (1955)., J. Air Pollution Control Assoc., 5, 120.

1104. Whitby, K. T., Algren, A. B., and Annis, J. C., (1958), A.S.T.M. Sp. Publ., No. 234, 117.

1105. Cartwright, L. M., and Gregg, R. Q., Ibid, 127.

1106. Dewell, P., (Sept. 1966)., Soc. for Analytical Chem., Particle Size Analysis Conference, Loughborough.

1107. Irani, R. R., and Fong, W. S., (1961), Cereal Chem., 38, 67.

1108. and 1109. Bradley, D., (1962)., Chem. and Proc. Engng., 43, 591 et seq., 634 et seq.

1110. Atherton, E., and Cooper, A. C., Brit. Patent 983760, Feb. 1962.

1111. Technical Bulletin, Joyce Loebl, Princesway, Team Valley, Gateshead, NE 1100 J, England.

1112. Hauser, E. A., and Reed, C. E., (1936), J. Phys. Chem., 40, 1169.

1113. Hauser, E. A., and Schachman, H. K., (1940), ibid, 44, 584.

1114. Hauser, E. A., and Lynn, J. E., (1940), Ind. Eng. Chem., 32, 660.

1115. Technical Bulletin, Sharples Corp., Philadelphia, 40, Pa.

1116. Saunders, E., (1948), Analyt. Chem., 20, 379.

1117. McCormick, H. W., (1954), J. Colloid. Sci., 19, 173.

1118. Brodnyan, J. G., (1960), J. Colloid Sci., 15, 563.

1119. Svedberg, T., and Pederson, K. O., The Ultracentrifuge Clarendon Press, Oxford, 1940.

1120. Pickels, E. G., Biophysical Methods Interscience, N. Y. 1959.

1121. Svedberg, T., and Nichols, J. B., J. Am. Chem. Soc., 45, 2910, 1923.

1122. MacInnes, D. A., et al., The Ultracentrifuge, Ann. N. Y. Acad. Sci., 43, 173 1942.

1123. Schumaker, V. N., Zone Centrifugation, Advan. Biol. Med. Phys. 11, 245 1957.

1124. Scheeler, P., et al., Biochim. Biophys. Acta 237, 28 1971.

1125. Halsall, H. B., Sedimentation Coefficients in Zonal Ultracentrifuges, Anal. Biochem. 30,(3) 368 1969.

1126. Hsu, H. W., et al., Separation, Science 6, (3) 461 1971.

1127. Kornguth, S. E., et al., J. Biol. Chem. 216, (4)117 1971.

1128. Wilcox, H. G., et al., J. Lipid Res. 12,(2) 160 1971.

1129. Moser, H., and Schmidt, W., Papier 1, (11) 189 1957.

1130. Technical Bulletin, Martin Sweets, 3131 Market St., Louisville, Ky. 40212.

1131. Technical Bulletin, ICI/Jiscoot Yalding, Maidstone, Kent, England.

1132. Technical Bulletin, Norsk Hydro Verksteder A. S. N 3671 Norolden, Norway.

1133. Alterton, E., Cooper, A. C., and Fox, M. R., J. Soc. Dyers Col. 80, 521, 1964.

1134. Kaye, B. H., and Boardman, R. P., Proc. Sym. Interact. Particles and Fluids, Inst. Chem. Eng. London, 1962.

1135. Boardman, R. P., MSc Thesis, London University, 1961.

1136. Scarlett, B., Rippon, M., Lloyd, P. S., Conf. Particle Size Anal., Loughborough, 1966.

1137. Kaye, B. H., and Jackson, M. R., Powder Technology, 1, 81 1967.

1138. Burt, M.W.G., Powder Technology 1, 103 1967.

1139. Beresford, J., J. Oil Col. Chem. Assoc. 50, 594, 1967.

1140. Murley, M., Nature 207, 1089, 5001, 1965.

1141. Karuhn, R., Kaye, B. H., and Jackson, Powder Technology 2 290, 1968/69.

1142. Jones, M. H., SAC Particle Size Anal. Group Lecture 3, 116 1966.

1143. Kaye, B. H., Powder Technology, In Press.

1144. Toyoshima, Y., ICI-Joyce Loebl Disk Centrifuge and Use of It for Pigment Particle Size Measurement, Shikizai Kyokaishi Vol. 43, No. 7, pp. 364-9, 1970.

1145. Toyoshima, Y., Ono, M., and Yauchi, O., Measurement of Particle Size Distribution of Phthalocyanine Blue by the Centrifugal Sedimentation Method. Shikizai Kyokaishi Vol. 43, No. 7, pp. 325-32, 1970.

1146. Haug, R., and Zorll, Ulrich, Pigment Particle Size Determination by Centrifuge Sedimentation. Deut. Farben-Z. 25(2), 59-63, 1971.

1147. Gast, T., (GE) Particle-size Analysis in Small Diameter Range with a New Sedimentation Centrifuge. Chem-Ing.-T, 43 533, 1971.

1148. Anon., (GE) Disk Centrifuge-Classification Particle Sizes Down to 10(-2) Microns. Chem Zeitun, 93 638, 1969.

1149. Burkholz, A., Particle Size Determination in the Range from 0.1 to 10μM with a Centrifugal Sedimentation Balance. Staub, English Edn., 30, (1), 1970.

1150. Schmidt, P. W., Small-angle X-ray Scattering from Suspensions of Particles. Soil Sci. 112 53, 1971.

1151. Elaasser, M. S., and Robertson, A. A., Ultracentrifugation Technique for Study of Latex Coalescence. J. Coll. 1 Sc. 36 86, 1971.

1152. Davidson, J. A., Collins, E. A., and Haller, H. S., Latex Particle-size Analysis III Particle-size Distribution by Flow Ultramicroscopy. Abs. Pap. ACS 1971. 25, 1971.

1153. DeBlois, W. W., and Bean, C. P., Counting and Sizing of Submicron Particles by the Resistive Pulse Technique. Rev. Scient. Instrum., 1970 (July) 41, 909-916.

1154. Muta, A., and Watanabe, S., Particle Size Distribution Analysis of Ultrafine Powders. Shikizai Kyokaishi Vol. 43, No. 7, pp. 357-63, 1970.

1155. Svarovsky, A. T., Particle Size Conf. Bradford, England 1970.

1156. Svarovsky, A. T., J. Physics E. Sci. Inst. 3, 458, 1970.

1157. Smithwick, J., Orr, C., and Hendrix, W., Fine Particle Soc. Ann. Meeting, Chicago, 1970.

1158. Smithwick, J., Orr, C., and Hendrix, W., Particle Size Conf., Bradford, England, 1970.

1159. Technical Bulletin, Quantimet 720, IMANCO, Monsey, N. Y.

1160. Technical Bulletin, Leitz Integrammat. Rockleigh, N. J.

1161. Technical Bulletin, MC. Millipore Corp., Bedford, Mass.

1162. Technical Bulletin, Carl Zeiss, 454 Fifth Avenue, New York, N. Y.

GLOSSARY OF TERMS

A. SYSTEMS

discrete particle	A single unit of matter which can change in size only by the breakdown or fracture of chemical bonds within its structure. It may or may not be of uniform density throughout its mass, and its shape will be dependent on its method of manufacture.
aggregate	A statistical group of discrete particles bound together by strong chemical bonds. This unit of matter cannot be separated into discrete particles without the fracture of chemical bonds. Typical separation techniques include comminution.
agglomerates	A statistical group of similar discrete particles bound together by weak physical bonds. Hence this unit of matter can be separated into discrete particles without the fracture of chemical bonds. Typical separation techniques include shear in the presence of surfactants.
conglomerate	A statistical group of disimilar discrete particles bound together by weak physical bonds. Hence this unit of matter can be separated into discrete particles without the fracture of chemical bonds. Typical separation techniques include shear in the presence of surfactants.
powder	A statistical group of "Particles" which can contain discrete particles, agglomerates and aggregates. The particle size involved is related to the ratio of inertial to surface forces. In a granular solid, e.g., + 100μ inertial

	forces are high compared to surface forces. In a colloidal solid, e.g., 0.1μ, surface forces are high compared to inertial forces. In a powder the forces are of similar magnitude and compete for the control of the properties of the bulk material. The powder phase is static, and particles are at rest relative to their immediate neighbors.
aerosol	A statistical group of solid or liquid particles suspended in a gas or vapor. The particulate phase is dynamic and particles are subject to motion relative to their neighbors. Interaction can take place.
suspension	A statistical group of solid particles suspended in a liquid. The particulate phase is dynamic, and particles are subject to motion relative to their neighbors. Interaction can take place.
emulsion	A statistical group of liquid particles suspended in another immiscible liquid. The particulate phase is dynamic and particles are subject to motion relative to their neighbors. Interaction can take place.
dispersion	The state of particle separation in a particulate system. In size analysis this demands that only discrete particles and aggregates be present, and that each particle be allowed to move in the fluid in accordance with Stokes' Law.
dispersion technique	The mechanism of separating a particulate phase into discrete particles and aggregates by physical work or chemical surface treatment. Agglomerates are separated into discrete particles and aggregates so that subsequent size data reflects the state of subdivision in the particulate phase.

B. MEASUREMENTS MADE ON SYSTEMS

particle size	The parameter quoted to describe the state of subdivision of a particulate system. For smooth, spherical particles, this can be defined as the diameter, surface or volume of the sphere. For particles of different shape, the diameter will vary dependent on the way it is measured. Size alone has no meaning unless it is qualified by the method of measurement. In consequence it is necessary to define the various diameters associated with particulate systems. Size is usually expressed in the units of microns, where 1 micron (μ) = 10^{-4} cm.
average thickness	The average diameter between the upper and lower surfaces of a particle in its most stable position of rest.
average length	The average diameter of the longest chords measured along the upper surface of a particle in the position of rest.
average breadth	The average diameter at right angles to the diameter of average length along the upper surface of a particle in its position of rest.
projected area diameter	The diameter of the sphere having the same projected area as the particle profile in the position of rest.
Feret's diameter	The diameter between the tangents at right angles to the direction of scan, which touch the two extremeties of the particle profile in its position of rest.
Martin's diameter	The diameter which divides the particle profile into two equal halves measured in the direction of scan when the particle is in a position of rest.

antithetic variable — The average of two diameters measured at right angles on a particle profile in a position of rest.

Stokes' diameter — The diameter of the sphere having the same terminal velocity as the particle.

Stokes' Law — A physical law which describes the settling velocity of a dense smooth sphere falling under the action of gravity through an infinite fluid. The sphere accelerates until the frictional drag of the fluid balances the inertial force of the falling sphere at this point. The sphere falls at a uniform or terminal velocity and the following relationship holds.

$$d^2 = \frac{18\ \eta\ u}{(\rho_s - \rho_f)\ g} \times 10^8$$

where

d = Stokes diameter in microns

η = viscosity of fluid in poise

u = terminal velocity cms/sec

ρ_s = density of sphere gms/cc

ρ_f = density of fluid gms/cc

g = acceleration due to gravity cms/sec/sec

This law holds providing that the Reynolds number of the particle is less than 0.2 and the particle is a dense smooth sphere. When many irregular shaped particles are present or the Reynolds numbers exceed the value stated, modification to this law must be applied.

Reynolds number of a particle	A dimensionless number which describes the ratio of inertial forces to viscous forces of the fluid. It is denoted by N_{RE} and is equivalent to $\frac{\rho_f d u}{\eta}$ where ρ_f and η are the density and viscosity of the fluid, respectively, d the diameter of the particle and u is the terminal velocity.
particle sieve diameter	The width of the minimum square aperture through which the particle will pass.
specific surface diameter	The diameter of the sphere having the same ratio of external surface area to volume as the particle.
surface diameter	The diameter of the sphere having the same surface area as the particle.
volume diameter	The diameter of the sphere having the same volume as the particle.
envelope volume diameter	The diameter of the sphere having the same volume as that contained by an envelope or skin around the external particle surface.
particle size distribution	A statistical representation of the distribution of particles of various particle sizes in a particulate system. The distribution of sizes is denoted in terms of frequency or mass, and reported on an incremental or cumulative basis.
particle concentration	The fraction or percentage of a particulate system, occupied by the particulate phase. In the size analysis of suspensions and powders the most meaningful way of expressing concentration is in terms of the volume % occupied by the particles. In the size analysis

	of aerosols it is more customary to relate concentration in terms of the frequency of particules/cc of gas.
void volume or pore volume	The volume fraction or percentage of a particulate system occupied by a fluid phase. This can consist of macrovoids due to spaces between particles in a system or microvoids due to capillaries or cracks in a particle structure. These are also referred to as macro- and micro-pores, respectively.
porosity	The ratio of pore or void volume to the total volume of the particulate system, therefore, % volume concentration of powder + % porosity = 100%.
density	The ratio of the mass of the particle to its volume. This is usually expressed in gms/cc.
shape	Macroshape or form is a term used to describe the geometric nature of the particle by reference to a standard geometric body. It usually encompasses the three-dimensional measurements of length, breadth, and thickness combined with a specific surface to volume ratio. Microshape or rugosity is a term used to describe the nature of the surface of a body. Rough surfaces have high rugosity and smooth surfaces have low rugosity.
surface	Is the interface between a solid body and the surrounding fluid phase.

external surface area	The amount of surface measured on all prominences on the particle plus the area of all indentations which are wider than they are deep. It is usually expressed in meters^2/gm.
internal surface area	The amount of surface measured in all indentations which are deeper than they are wide. Usually expressed in meters^2/gm.
total surface area	The sum of the external and internal surface area values.
surface energy	This is defined as the isothermal reversible work that is required in creating 1 sq cm of new surface.
wettability	The tendency for a liquid to spread on a specific surface.
contact angles	When a surface is not wetted by a liquid, the angle between the interface of the liquid and the surface is known as the contact angle. For complete wettability, the contact angle of a liquid = 0°.
surface tension	This is defined as the isothermal reversible work done to increase the interface of a liquid by unit area.
dispersing agent surface active agent surfactant	A chemical substance used to reduce interfacial or surface tension and surface energy between particles and fluid, so that a particulate system can be dispersed with less physical effort.
flocculating agent	A chemical substance used to agglomerate discrete particles and aggregates in a system.
zeta potential	The potential difference between any point in a bulk solution and the shear plane between the electrical double layer around a particle and the bulk solution.

Tamman temperature	That temperature which is approximately half the value of the solid melting point in °K at which the rate of sintering rapidly increases.

C. PARTICLE INTERACTIONS

adhesion adherence	The process by which particles, films, or liquids stick to surfaces by physical bonding.
cohesion	The general process by which particles stick to each other in a powder or bed.
agglomeration	The process by which chemically similar particles stick together by physical bonding.
conglomeration	The process by which chemically different particles stick together by physical bonding.
flocculation	The mechanism of physically or chemically agglomerating discrete particles and aggregates in a liquid system.
adsorption	The physio-chemical phenomenon involved in the attraction to and retention of gases, vapors, and liquids on the surface of a solid.
physical adsorption	The retention of adsorbed gases, vapors or liquids on a solid surface by physical, e.g., Van der Waals forces. The adsorbate can be completely removed by heat, and the process is therefore reversible.
chemi-sorption	The retention of adsorbed gases, vapors or liquids by chemical bonding. The adsorbate cannot be removed by heat and the process is irreversible.

D. FORCES BETWEEN PARTICLES

force of adhesion	That force applied perpendicular to the center of gravity of the particle necessary to remove the particle from a surface in a fixed period of time.
force of mechanical adhesion	The force that is necessary to remove a particle from a surface in the above manner, when it is held by purely mechanical mechanisms, e.g., interlocking of surface roughnesses or dendrites.
Van der Waals forces	The long-range attractive forces that arise due to molecular interactions within the structure of particles.
electrical forces	The force caused by the contact potential difference between a particle and a surface. This applies only upon contact.
coulombic forces	The force induced when particles are highly charged by an outside electric field before they approach each other. These apply before contact.
capillary forces	The forces that apply due to the negative capillary pressure induced in a neck or meniscus of liquid present between particles and surfaces.
electrical double layer forces	The forces that are present due to the presence of an electrical double layer around a particle. These are usually repulsive in nature and account for particle stability in fluids.
valency forces	The short range chemical forces that bind atoms together in solids. Examples are ionic, metallic, molecular, and homopolar bonds. When these are present between particles an aggregate structure exists.